Investigations of androgenic steroids by liquid chromatography / mass spectrometry.

Yu, Jinglei

Investigations of Androgenic Steroids by Liquid Chromatography / Mass Spectrometry

By

Jinglei Yu

A thesis submitted for the degree of Doctor of Philosophy in the University of Wales

March 2004

DECLARATION

This work has not previously been accepted in substance for any degree, and is not being concurrently submitted in candidature for any degree.

Signed ..... (Candidate)

Date 27/06/04

STATEMEMT 1

This thesis is the result of my own investigations, except where otherwise stated. Other sources are acknowledged by footnotes giving explicit references. A bibliography is appended.

Signed ..... (Candidate)

Date 27/06/04

Signed ..... (Supervisor)

Date .....

STATEMEMT 2

I hereby give consent for my thesis, if accepted, to be available for photocopying and for inter-library loan, and for the title and summary to be made available to outside organizations.

Signed ..... (Candidate)

Date 27/06/04

ACKNOWLEDGEMENT

I would like to thank my supervisor Professor D.E. Games for providing me with the opportunity of entering the field of mass spectrometry and for all his fully support during the time of my study. I would also express my great acknowledgement to Dr. T. J. Walton in the School of Biological Science for directing me into this study and many helpful suggestions.

I would like to thank Dr. Marguerite L. Games for her advices and kindness for daily life, to Mrs. Eileen Jones for her considerable assistance, to Mr. Brian Cooper for his technique support and to all my colleague students and other members in the MSRU for their help and friendship.

Finally, I would like to thank my husband, Siying Shen, and my family for their love and endless support.

Summary

Androgen steroids are an important group in the hormone family. As they play significant roles in the human body, identification and determination of these compounds have been of great interest in many fields. In this thesis, systematic studies of the compounds in the androgen group by liquid chromatography / mass spectrometry have been undertaken.

The first chapter gives a brief introduction to the structure, function and classification of the steroid family, and is followed by a review of different analytical techniques applied in this family. The theory behind the chromatographic and mass spectrometric techniques used has also been introduced.

Structural information about the androgenic steroids and their conjugates has been obtained in chapters 2 and 3 respectively by both ESI and APCI mass spectrometry. The effect of different solvent systems was studied in detail in both the positive and negative ionization modes and the collision induced dissociation of these compounds was also investigated by tandem mass spectrometry.

In chapter 4, LC/MS methods have been optimized in terms of columns, solvent systems, flow rate and mass spectrometer parameters to quantify some of the androgens and their conjugates respectively. The linearity, precision and limits of detection were estimated for these compounds.

A derivatization method was developed to enhance the sensitivities for detection of the androgens and their conjugates by LC/MS in the final chapter. A TMPP reagent was used as a derivatizing reagent, and the spectra of these TMPP-derivatives of androgens were studied by ESI mass spectrometry. A LC/MS method was also set up with the aim of quantitation of five TMPP-derivatives of androgens.

ABBREVIATIONS

α	selectivity factor
5α-Diol G	5α-androstan-3α, 17β-diol glucuronide
5β-Dione G	5β-androstane-11, 17-dione-3α-ol glucuronide
ac	radio frequency
A	androsterone, 5α-androstan-3α-ol-17-one
A G	androsterone glucuronide
ANOVA	analysis of variance
APCI	atmospheric pressure chemical ionization
A S	androsterone sulfate
CI	chemical ionization
CID	collision induced dissociation
C_s	molar concentration in the stationary phase
C_m	molar concentration in the mobile phase
dc	direct current
DHEA	dehydroepiandrosterone
DHEA G	dehydroepiandrosterone glucuronide
DHEA S	dehydroepiandrosterone sulfate
DHT	dihydrotestosterone, 5α-androstan-17β-ol-3-one
ECD	electron capture detector
EO-TMS	ethoxime-trimethylsilyl
ESI	electrospary ionization
ET	epitestosterone
FAB	fast atom bombardment
FID	flame ionization detector
GC	gas chromatography

HETP	theoretical plate
HPLC	high performance liquid chromatography
I.D.	internal diameter
I. S.	internal standard
k'	capacity factor
K	equilibrium constant
kV	kilovolts
L	length of column
LC	liquid chromatography
LOD	limit of detection
LOQ	limit of quantification
MALDI	matrix-assisted laser desorption ionization
MeCN	acetonitrile
MeOH	methanol
MO-TMS	methoxime-trimethylsilyl
MS	mass spectrometry
MS^n	mass spectrometry to power n
ml	milliliter
min	minute
m/z	mass-to-charge ratio
N	plate number
nm	nanometer
ODS	ocatdecylsilane
PGC	phase-porous graphitic carbon
Q1	first quadrupole
q2	second quadrupole
Q3	third quadrupole

RIA	radioimmunoassay
RP	reverse phase
RSD	relative standard deviation
R_s	column resolution
SFC	supercritical fluid
SIM	selected ion monitoring
SPE	solid phase extraction
SRM	selected reaction monitoring
T	testosterone
T G	testosterone glucuronide
TIC	total ion chromatography
TLC	thin layer chromatography
TMS	trimethylsilyl
TMPP	tris (2,4,6-trimethoxyphenyl) phosphonium bromide
TOF	time of flight
T S	testosterone sulfate
t_M	dead time
t_R	retention time
TS	thermospray
µl	microlitre
UV	ultraviolet
V_M	dead volume
W	peak width

Contents

Chapter 1

Introduction

1.1 Introduction to the steroid hormones

1.1.1 Structures of steroids

All the structures of the steroid hormones are related to the cyclopentanoperhydro-phenanthrene nucleus. The numbering of the cyclopentanoperhydrophenanthrene ring system and the lettering of the ring are presented in Figure 1.1 The ring system of steroids is stable and is not catabolized by mammalian cells. Biological activities of steroids vary by alteration of the ring substituents rather than alteration of the ring structure itself.

Figure 1.1 Structure and numbering system of cyclopentanoperhydrophenanthrene

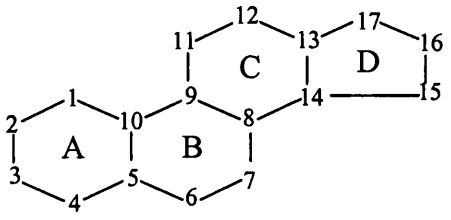

Figure 1.2 Structure of cholesterol

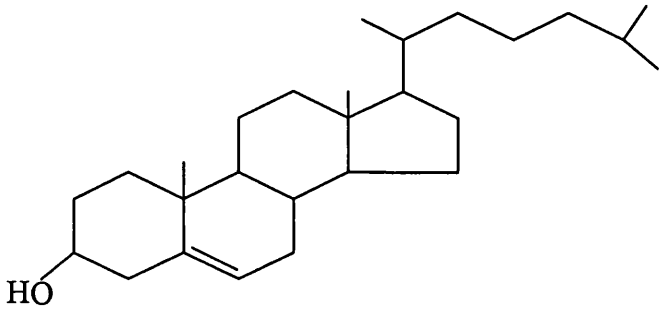

The parental precursor of the steroid is cholesterol (shown in Figure 1.2), which is a white crystaline compound originally isolated from gallstones. Cholesterol is a constituent of every animal tissue and occurs partly as the free alcohol and partly esterified with the higher fatty acids.

1.1.2 Classification and function

Steroid hormones are derived in specific tissues in the body and are more often classified by their biological activities, into adrenal hormones, progestogens, estrogens and androgens.

1.1.2.1 Adrenal hormones

This group of steroids are formed in the adrenal cortex, and usually classified into glucocorticoids and mineralocorticoids according to their different physiological functions. The structures of these two groups are similar, and the difference depends on the presence or absence of a 17-hydroxy group. The 17-hydroxylated compounds are glucocorticoids, while the 17-deoxy compounds are mineralocorticoids. But there is some overlap of function between the two groups.

Glucocorticosteroids promote the deposition of glycogen in the liver, produce glucose from amino acids, retard the oxidation of glucose and kill certain T cells in high doses. They are essential for the maintenance of life and important in resistance to shock and infection. The principal steroid of this group is cortisol.

Mineralocorticosteroids control the balance of salt and water. Their actions retain sodium and prevent the retention of excess potassium. Aldosterone is the most potent adrenal steroid of this type.

1.1.2.2 Progestogens

Progesterone is the most important steroid of this group. It is secreted by the corpus luteum of the ovary and is responsible for preparing the endometrium for pregnancy. It maintains the uterine endometrium for implantation (with estradiol) and is a differentiation factor for mammary glands. Progesterone is an intermediate in the biosyntheses of the corticosteroids, the estrogens and the androgens.

1.1.2.3 Estrogens

Naturally occurring estrogens have a basic C18 structure with an oxygen substituent at C (17) and a characteristic aromatic A ring. The hydroxyl group at C (3) gives them phenolic and therefore weakly acidic properties.

Estrogens are produced in the gonads, the placenta and the andrenal cortex. In combination with other hormones, estrogens are responsible for the development and maintenance of the female sexual organs and characteristics, and are important in the anterior pituitary. Estrogen formed by the placenta gradually increases and in late pregnancy the production may exceed one thousand times that of the ovary. They also have some effects on oral structures, such as influence the growth of the oral epithelium and increase the activity of cells in the buccal epithelium.

1.1.2.4 Androgens

All the androgens comprise a group of C19 steroids, but differences occur in the type and position of the moieties, which are attached to the basic C19 unit. The major naturally occurring androgens are testosterone, 5α-dihydrotestosterone (5α-DHT) and 5α-androstane-3α, 17β-diol, with Δ4-androstenedione and dehydroepiandresterone (DHA) having only weak biological activity (Fig. 1.3).

The androgens are secreted to a large extent by the Leydig cells of the interstitial tissues of the testes and to a lesser extent by the adrenals and ovaries. There is some evidence that the Sertoli cells of the seminiferous tubules can also synthesize and secrete testosterone. Androgens exert numerous diverse effects; they develop and maintain the male reproductive organ's characteristics, involve the normal functioning and structure of the prostate gland and seminal vesicles. Moreover, there is an increase in the size of the testes, scrotum, penis, seminal vesicles, prostate, vas deferens and epididymis at puberty. The anabolic effects of androgens are also noted at this time when there is an increase in muscle protein, reflected urinary creatinine, a decrease in urinary nitrogen excretion without an increase in blood urea. These effects, including those on bone, give rise to the dramatic increases in height and weight noted in boys at puberty. Effects of androgens on non-sexual organs include those on the length of the vocal chords, resulting in deepening of the voice, and on the kidneys. These are larger in men than in women and numerous enzymes are increased in quantity. A further well-known increased activity of the sebaceous glands occasionally leading to the troublesome problem of acne. Sexual,

auxiliary and facial hair-growth is also androgen-dependent. The androgen steroids are chiefly metabolized by the liver and excreted in the urine.

Figure 1.3 Some important metabolic pathways of androgens [127]

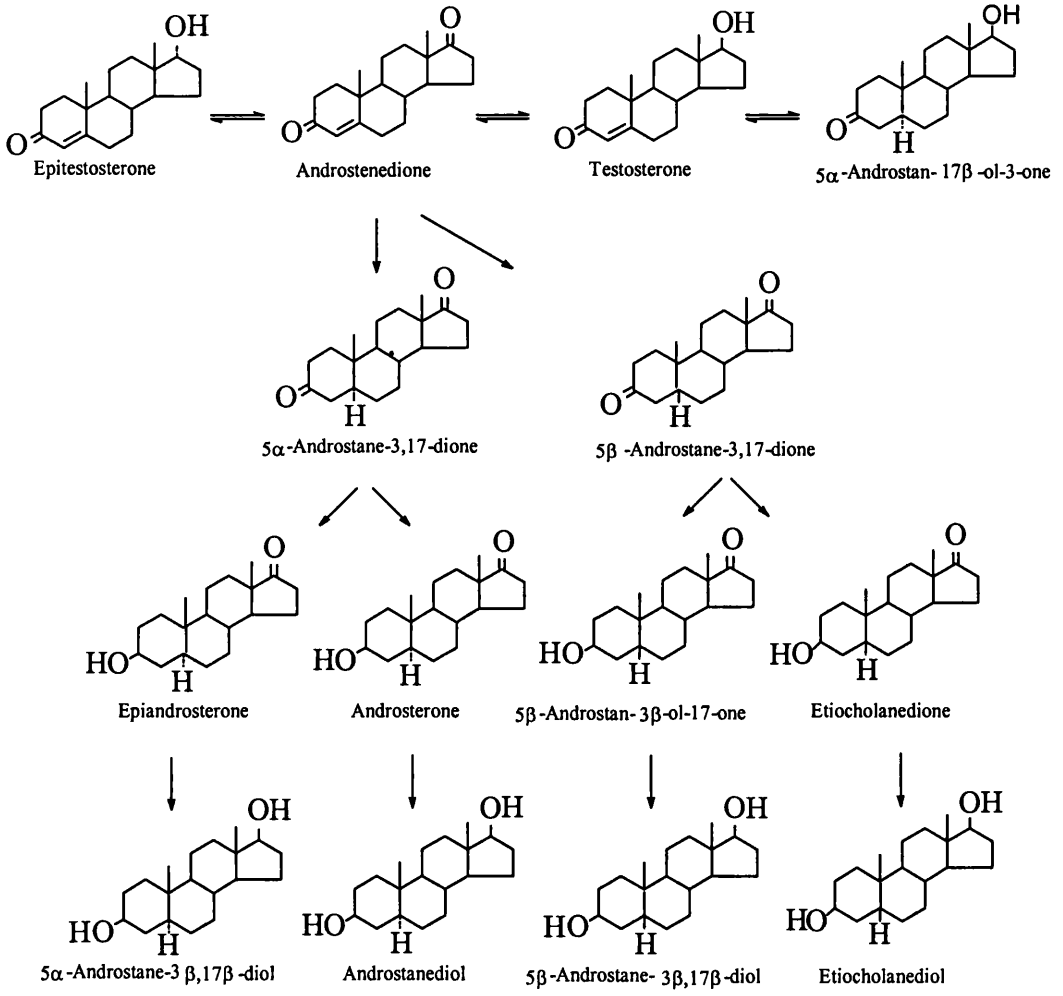

Figure 1.3. Summarizes some of the more important metabolic pathways of the androgens, with the exception of conversion to estrogens. These pathways include: the reduction of the double bond at C4, leading to 5α/5β isomers; the reduction of the 3-oxo group to 3α/3β-hydroxy steroids; the oxidation of the 17β-hydroxy group to 17-carbonyl group if a 17-methyl group is absent; hydroxylation (eg: at C6, C12, C16) and

epimerization (eg: 17β-hydroxy group to 17α-hydroxy group); conjugation, mainly as glucuronide and to a lesser extend as sulphate, occurs at C3 or C17.

1.1.3 Analytical techniques of steroids

There are many different analytical techniques involved in the biological or clinical analysis of steroids, such as traditionally bioassays, colorimetric, fluorimetric, and most widely used immunoassay and chromatographic methods. However, the incidence of bioassays, colorimetric, and fluorimetric methods has declined sharply in recent years whereas commercial assay kits have become available for most important steroids. Several types of immunoassays including radioimmunoassay [1-2], enzyme-immunoassay [3-4] and fluoroimmunoassay [5] are currently used for most of routine determinations and still used in research of the measurements of steroid concentrations. However, immunoassay is restricted to determination of a single steroid whereas the study of broad steroid profile, requiring the simultaneous determination of various steroids not appropriately to be carried out with conventional methodologies.

1.1.3.1 Radioimmunoassay

In radioimmunoassay (RIA), a fixed concentration of labeled tracer antigen is incubated with a constant amount of antiserum, such that the concentration of antigen binding sites on the antibody is limiting; for example, only 50% of the total tracer concentration may be bound by antibody. If unlabeled antigen is added to this system, there is competition between labeled tracer and unlabeled antigen for the limited and

constant number of binding sites on the antibody, and thus the amount of tracer bound to antibody will decrease as the concentration of unlabeled antigen increases. This can be measured after separating antibody-bound from free tracer and count either the bound fraction, the free fraction or both. A calibration curve is set up with known amount of androgen, from which unknown samples can be calculated. Thus the four basic necessities for a RIA system are an antiserum to the compound to be measured, the availability of a radioactively labeled form of the compound, a method whereby antibody-bound tracer can be separated from unbound tracer, and a standard unlabeled material.

RIA has long been established and involved for the analysis of steroids [6-9]. As steroids are typically in very low concentrations in biological extract, it has the added advantage of concentrating the analyte in addition to removing unwanted cross-reactants from the sample. Although selective extraction of the analyte is possible, it is becoming common practice to perform multiple determinations on a single extract requiring the use of less selective extracting media [10-12]. A common problem with RIA techniques is specific and nonspecific interference with the antibody-analyte binding. Antibodies to steroids are usually made by immunizing animals to the steroid, which has been conjugated to an antigenic protein (e.g., bovine serum albumin) as a hapten [13]. Such antisera, typically, have some degree of cross-reactivity with structurally similar steroids which is usually reported as the amount of cross-reacting steroid needed to displace 50% of bound labeled ligand in the absence of the steroid being analyzed. This is often expressed as a percentage of the analyte required achieving the same displacement. Although low cross-reactivities are frequently regarded as insignificant, the concentration of different steroids varies over a wide range. Hence, apparently small cross-reactivities can become significant. Nonspecific interference can be attributed to compounds in the

incubation mixture, which interfere with the antibody-analyte binding. This is a problem with all RIA procedures, but more particularly with those incorporating an extraction step where the analyte and interfering species have both been concentrated.

1.1.3.2 Gas chromatography

Horning and coworkers [14-18] pioneered the gas chromatography (GC) of steroids emphasizing aspects of stationary phase selectivity and the development of non-adsorptive, thermal stable steroid derivatives. Most studies with steroids have relied on the formation of suitable derivatives to enhance the chromatographic separation due to their poor thermal stability. Steroids undergo all of the reactions expected of molecules containing double bonds, keto-groups, and hydroxyl groups. Many of these reactions have been exploited to convert the polar oxo- and hydroxyl functions of steroids to non-polar derivatives for GC. The formation of methoxime-trimethylsilyl (MO-TMS) ethers is one of the most satisfactory procedures. In certain circumstances, other derivatives have been more useful, as in the determination of isomeric urinary estrogens where resolution of the ethoxime (EO)-TMS derivatives was superior to that of the corresponding MO-TMS ethers [19]. Related derivatives include n-butyloxime-TMS ethers [20], trimethylsilyloxime (TMSO)-TMS ethers [21-22], benzyloxime-TMS ethers [23], and persilyloxime-TMS ethers [24]. In addition to improve chromatographic behavior, halogenated derivatives significantly increase sensitivity when used with electron capture detector (ECD) [25]. Fluorinated derivatives have been used with mass spectrometric detection presumably because of intense ions of high mass in the mass spectrum and enhanced volatility allowing lower column temperatures or reduced analysis times [26].

There are generally two categories of stationary phases used for the GC of steroids: non-selective phases in which separation is based on volatility effects; and selective phases in which the separation based on volatility is modified by the presence or absence of characteristic groups in the steroid molecule. Before 1965, Horning *et al.* [14] relied on selectivity effects based on the use of selective phases and derivatization to effect separations. However, a fundamental change occurred in their approach, in which they emphasized column efficiency rather than selectivity to obtain a urinary metabolic profile in 1971 [16]. One of the most important developments for improving the separation of steroids was the application of fused silica columns to steroid analysis [27-29]. Excellent separations of the free underivatized steroids have been achieved on these columns, which have been used successfully to establish comprehensive urinary steroid profiles [30]. However, adsorption-related problems were reported for steroids with underivatized oxo-functions [19].

Three major detectors have been used in the GC analysis of steroids. Flame ionization detector (FID) has been used particularly in combination with TMS ethers permitting detection down to the nanogram level in relatively impure biological extracts. The ECD has been less used compared to the others because of its extreme sensitivity to nonspecific background substances. The most popular and widely used detection system is a mass spectrometer (MS) coupled with GC. Determinations of steroids in biological samples such as urine, plasma and cell cultures have been intensively studied with this system and its applications have been reviewed by Gaskel in 1983 [31], Wolthers and Kraan [32] in 1999 and Shimada et al. [33] in 2001.

1.1.3.3 Thin layer chromatography

Thin layer chromatography (TLC) has been widely used in routine clinical analysis for steroids. Many types of phases [34-37] have been studied including silica gel, alumina, celite, and cellulose. The reversed phase generated by silanizing silica gel was described by Corti *et al.* [38]. Furthermore, silica gel is also well suited as a support for partition chromatography with various mobile phases but is more commonly used as an adsorbent. Indeed, most TLC work with steroids has been carried out on silica gel or alumina [39-43]. The mobile phases were chosen based on the nature of stationary phase and the polarity of steroid. For example, an ether, ester or ketone in the mobile phase often effects useful modification in relative retentions [44]. Many separations are achieved by simple development on more or less activated layers [45]. For difficult separations, multiple developments in the same or different mobile phases or 2-dimensional development can be used [46]. Detection methods for steroids in TLC include UV absorption, fluorescence, iodine vapour and enzymatic detection [47-48].

1.1.3.4 High performance liquid chromatography

The investigation of steroids by high performance liquid chromatography (HPLC) began in the early 1970's with the evaluation of several coated phases for steroid separation by Siggia and Dishman [49]. Since then, it has become one of the most important techniques in steroid research because of its advantages, which include: (i) offering a simple and effective technique for rapidly separating and quantitating small concentrations in the presence of large contaminants; (ii) not normally requiring a complicated sampling procedure, such as preparing antisera or labeling the antigen in immunoassay methods; (iii) being suitable for nonvolatile- and thermally labile steroids, [50-51] which are not possible to analyze by GC without derivatization. The application of

HPLC to steroids has been reviewed by Heftmann and Hunter in 1979 [52] and Kautsky in 1981 [53].

The most widely used stationary phases for steroids are C18 or C8 ligands bonded to the silica support [56-59]. This silica-based reversed-phase possess the desirable characteristics of well-controlled particle size, pore structure and mechanical strength as well as a rich repertoire of bonding chemistry. Many successful separations of steroids have been reported by these kinds of columns. Purdon et al. reported the separation of 15 different testosterone metabolites on a Supelcosil LC-18 column with a one-step linear gradient of methanol in water (10%-60% methanol) [60]. Navajas et al. described an alternative HPLC method for the determination of testosterone and epitestosterone on a Hypersil BDS-C18 reversed-phase column with gradient elution and UV absorbance detection [61]. Some urinary glucuronide conjugates were separated on a C18 column and were detected spectrofluorimetrically at 445nm with excitation at 367nm by Iwata et al [62]. Reversed phase chromatography on Partisil 10 ODS was recommended for the simultaneous determination of estriol, estradiol and estrone [63]. Similarly, reversed phase chromatography was preferred for the determination of corticosteroids [64] in plasma. Radial compression columns containing C18 and C8 reversed phases (10 μm) have been utilized [65] as complementary packing to effect the separation of up to 21 progesterone and pregneonlone metabolites in 20-40min using high flow rates of 2-3 ml/min. However, the silica-based reversed phase becomes undesirable because of the pH stability and residual chemical activity of the unprotected silica support, although manufacturers use various methods to reduce the unreacted-silanol content. Apart from the reversed phase materials with alkyl or phenyl functionality, bonded phase silica with 1, 2-dehydroxypropyl ether (DIOL) has been popular for the HPLC of steroids. The advantage of DIOL phases is the reversal in elution pattern relative to reversed phase packing [66-67]. Most routine analyses

can be performed on a reversed phase column such as Lichrosorb PR-18 with a DIOL column being used for more difficult separations [66].

A novel reversed phase-porous graphitic carbon (PGC) provided unique selectivities in addition to improve chemical stability and surface homogeneity [68]. PGC is produced by the graphitization of a phenol-formaldehyde resin-impregnated silica gel and exhibits the inherent pH stability and the chemical homogeneity that a bonded silica phase does not. Wade and Haegele [69] described an HPLC-UV method for simultaneous measurement of cortisone and cortisol in human saliva with sample preparation by solid-phase extraction on cyclodextrin (CD) media. However, compared to silica particles, PGC is limited by its lower efficiency and higher fragility. Moreover column of this material are available only in short lengths and are expensive. A variety of pore sizes are not available at this time.

A few optimization procedures have been described, such as solvent triangle [70], window diagram [71], factorial design techniques [72] and multi-criteria decision-making methods [73]. Valko and Slegel [74] used molecular modeling for mobile-phase optimization in RP-HPLC. Chong et al. [75] achieved the optimization of the solvent composition by making use of the overlapping resolution.

The correct combination of stationary and mobile phase is essential. This is demonstrated by the reversed-phase chromatography of adrenal steroids on various ODS materials differing in the number of free silanol groups [76]. Many useful steroid separations have been achieved using isocratic elution with a binary solvent as mobile phase. In some cases, phosphate buffer is incorporated in the mobile phase. With these systems, the buffer anion and pH exert a significant effect on the separation. For a complex biological sample containing many hormones, the use of a ternary mobile phase

has permitted high selectivity [77]. In the case of normal-phase HPLC, the elution of highly polar steroids takes a long time, and therefore, a gradient system needs to be employed as the mobile phase. The success of a separation, particularly for late eluting steroids, often depends on the gradient shape. Non-linear, linear and stepped gradients have been used.

Shalahy and Shahjahan [59] tested the selectivity of different organic solvents: methanol, acetonitrile and tetrahydrofuran separately after mixing with phosphate buffer at different pH and with different ratios. All the tested analytes (dexamethasone, hydrocortisone, hydrocortisone acetate, prednisolone and prednisolone acetate) gave highly resolved, sharp peaks with acetonitrile-phosphate buffer (6:4) at pH 8 as mobile phases. Saisho et al. [78] separated several adrenal steroids without the use of any gradient system by using a mixture of methanol-acetonitrile-water (55:3:42, v/v/v). While separation of androstenedione and its stereospecific hydroxyandromatic derivatives were achieved by using a linear gradient of acetonitrile and water in increasing amounts from 30%-60% of the first solvent [79]. Elisabetta Venturelli et al. [80] measured urinary testosterone with a mobile phase of acetonitrile-water (1:9 v:v), and acetonitrile content was increased to 100% in 25min and maintained at 100% for 5min.

HPLC has proved a versatile technique for the quantitative determination of steroids by using ultraviolet (UV) [66, 81, 82], fluorescence [83-85], electrochemical [86-88] and mass spectrometry (MS) as detectors.

The choice of detection system is governed largely by the expected concentration range of steroids and sample type. The low levels of steroids normally encountered in biological samples required a detector of maximal sensitivity. UV and fluorescence detection are usually part of HPLC analyses for steroid hormones. However, the limit of a

quantitative determination of these methods is thought to be 0.5-1.0ng. Simultaneous measurement with two complementary detectors offers considerable potential for the quantification of a steroid. For example, UV and fluorescence make a powerful combination. Further developments in coupled HPLC-mass spectrometric systems will undoubtedly enhance the role of HPLC in the determination of steroids.

Historically, UV absorption has occupied a pre-eminent position as a detection system in HPLC. Whereas isolated carbonyl groups absorb UV with a maximum around 275-285nm, the 1,3-unsaturated ketones in the A-ring of steroids absorbs with a maximum around 240 nm. Thus, steroid metabolites of progesterone and testosterone [89] have been quantified at 240 nm [90-91]. Measurements in the 210-220nm region required highest purity solvents to avoid excessive baseline noise [92]. For those steroids absorbing in the UV below 200nm, it is difficult to obtain a signal free from noise, particularly when gradient elution is used. Whilst baseline correction is also necessary at higher wavelength with some gradients.

Mass spectrometry (MS) affords specificity and sensitivity for steroid detection. Since the mass spectrometer only detects ionizable components in the mass range selected, much interference could be avoided by choosing a mass range or "window" applicable to the compounds of interest but still above the majority of ionizable endogenous material. The greatest disadvantage to HPLC is the difficulty of interfacing with MS. However, the development of interface techniques including thermospray (TS) [93], atmospheric pressure chemical ionization (APCI) [113] and electrospray (ESI) [118] make the combination of HPLC separations with specific MS identification a practical technique. With the improvement of techniques, LC-MS has increasingly been applied to the analysis of steroids, giving molecular mass information and limited fragmentation.

Prough *et al.* have studied the metabolism of DHEA in rat and human liver microsomal fractions using LC-APCI-MS. Metabolites identified in both species included 16α-hydroxy-DHEA, 7α-hydroxy-DHEA and 7-oxo-DHEA [55]. The use of the isotope-labeled internal standards has proved to be useful in LC-MS to compensate for the substantial variations in ionization conditions [84]. The technique developed by Esteban and Yeergey [94] for measurement of plasma cortisol using stable isotope dilution MS is accurate and reliable. A thermospray-HPLC/MS method for determination of serum dehydroepiandrosterone sulfate has been described by Shackleton *et al.* [95], using [7,7-$^2H_2$] dehydroepiandrosterone (DHEA) sulfate as internal standard. Chung et al. [96] synthesized deuterium labeled 5α-androstane-3α, 17β-diol and its 17β-glucuronide, and the products were identified by TS-MS and ESI-MS. The analysis of natural steroids using LC-MS has been reviewed by Shimada *et al.* [54] in 2001.

1.2. Introduction to high performance liquid chromatography/mass spectrometry

1.2.1 Introduction to chromatography

The Russian botanist Mikhail Tswett [97] first introduced chromatography in 1906. He used a column of powdered calcium carbonate to separate green leaf pigments into a series of colored bands by allowing a solvent to percolate through the column bed. He

described this technique as chromatography, from the Greek words of " chroma " meaning color and " graphein " meaning writing. The generic terminology now encompasses a wide range of separation sciences.

Essentially, chromatography is a physical method of separation in which the components to be separated are distributed between two phases, one is held static which is termed as the stationary phase, the other travels past the stationary phase under gravity, pressure or by capillary action which is termed as the mobile phase. The stationary phase is a dispersed medium with a large surface area and it can be either a solid or a liquid spread over an inert support or spread as a thin film on the walls of the column. The mobile phase can be a gas (GC), a liquid (LC) or a supercritical fluid (SFC). Based on the nature of the mobile phase, chromatography can be categorized as gas chromatography, liquid chromatography and supercritical fluid chromatography. In this thesis, liquid chromatography coupled with mass spectrometry was applied for the study of androgenic steroids.

1.2.1.1 Terms used in chromatography

The chromatographic theory was first proposed by Nobel Prize winners Martin and Synge [98] and developed by Craig [99] and Glueckauf [100] as the plate theory. Later, van Deemter [101] and Giddings [102] established the rate theory. The terms introduced here can be used for all chromatographic techniques not only for liquid chromatography.

Partition coefficients

The equilibrium constant K of an analyte for the equilibrium between mobile phase and stationary phase is defined as

$$K = C_s / C_m \qquad (1.2.1)$$

Where C_s is the molar concentration of analyte in the stationary phase and C_m is its molar concentration in the mobile phase. Components with a high distribution in the stationary phase will move slowly through the column and hence be separated from components with a lower distribution in the stationary phase. A separation can't be achieved without a difference in distribution between the components.

Retention time

The time it takes after sample injection for the analyte peak to reach the detector is called the retention time (t_R). The time for the unretained components to reach the detector is called the dead time (t_M).

Capacity factor

Capacity factor (k') is used to describe the migration rates of analytes on the column. The relation between capacity factor and retention time is:

$$k' = (t_R - t_M) / t_M \qquad (1.2.2)$$

When k' is much less than unity, the analytes are eluted so rapidly that accurate determination of the retention times is difficult. When the capacity is more than 20, elution time is too long and peak is very wide. The ideal separations are performed under the conditions, which the capacity factor of the components in a mixture is 1 to 5.

Selectivity factor

The selectivity factor (α) of a column for the two components A and B is defined as:

$$\alpha = K_B / K_A \qquad (1.2.3)$$

Where K_B is the partition ratio for the more strongly retained components B and K_A is the partition ratio for the less strongly held components A.

Resolution

The resolution (R_S) is the ability of the chromatographic column to separate two components and is derived from the separation of the peak maxima, Δ_t, and the baseline peak widths W_1 and W_2 (see figure 1.4) where:

$$R_S = 2\Delta_t / (W_1 + W_2) \qquad (1.2.4)$$

Base line resolution corresponds to $R_S > 1.5$ is desirable for peaks of similar size.

Figure 1.4 Resolution of the chromatographic separation of two components

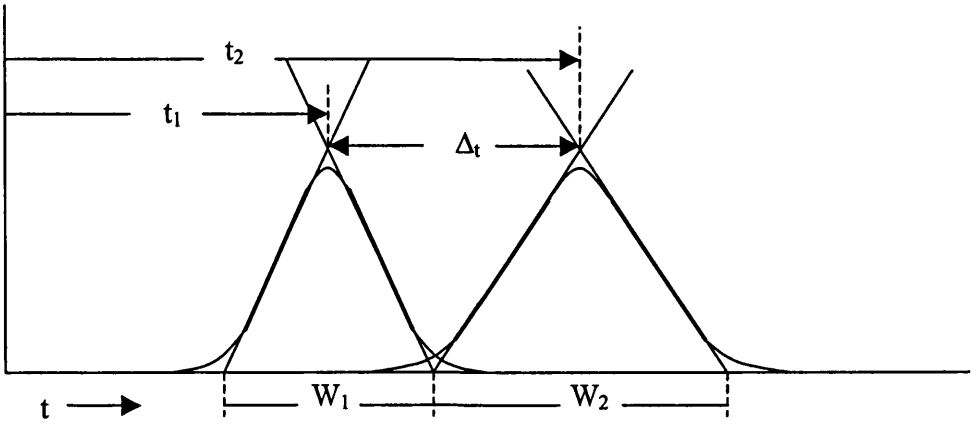

Column efficiency

Column efficiency is described in terms of a plate number, originating from distillation theory and first applied to chromatography by Martin and Synge [98]. At each plate, equilibrium of the solute between the stationary and mobile phase is assumed to take place. The efficiency of a chromatographic system improves as the number of equilibrations increases, that is, the number of theoretical plates increases. The plate number, N, of a chromatographic system is given by:

$$N = 16 (t_R / W_b)^2 \qquad (1.2.5)$$

Where t_R is the retention time of peak and the W_b is the baseline peak width.

The efficiency of a column is, however, usually determined as the height equivalent to a theoretical plate (HETP), defined as the number of theoretical plates per unit length of column (L):

$$HETP = L / N \qquad (1.2.6)$$

1.2.1.2 High performance liquid chromatography

Classical liquid chromatography (LC) employed wide bore glass tubes (10-50mm) ranging from 50-500 mm in length containing large diameter (150-200 μm) particles of stationary phase. However, column efficiencies using these systems were poor but they are still used considerably for preparative purpose, this context technique has since been superseded. Early in the history of LC, it was realized that large increases in column efficiency could be achieved by decreasing particle-packing sizes. In the late 1960s, a number of workers effectively produced the technology to create and utilize small particle diameters of 10 μm with impressive speed and resolution [103]. The term high

performance liquid chromatography (HPLC) has since been coined to differentiate the newer procedures incorporating small diameter packing in stainless steel tubes, necessitating sophisticated instrumentation, from the classical techniques.

1.2.1.2.1 HPLC instrument

An HPLC instrument has at least the elements which are shown in Figure 1.5: solvent reservoir, transfer line with frit, high-pressure pump, sample injection device, column, detector and data recorder, usually together with data evaluation. For temperature-controlled separations, a thermostat is enclosed around the column, and it is also quite common to work with more than one solvent, thus a mixer and controller are needed. If data acquisition is done by a computer, it can also be used for the control of the whole system.

Figure 1.5 Schematic diagram of an HPLC system

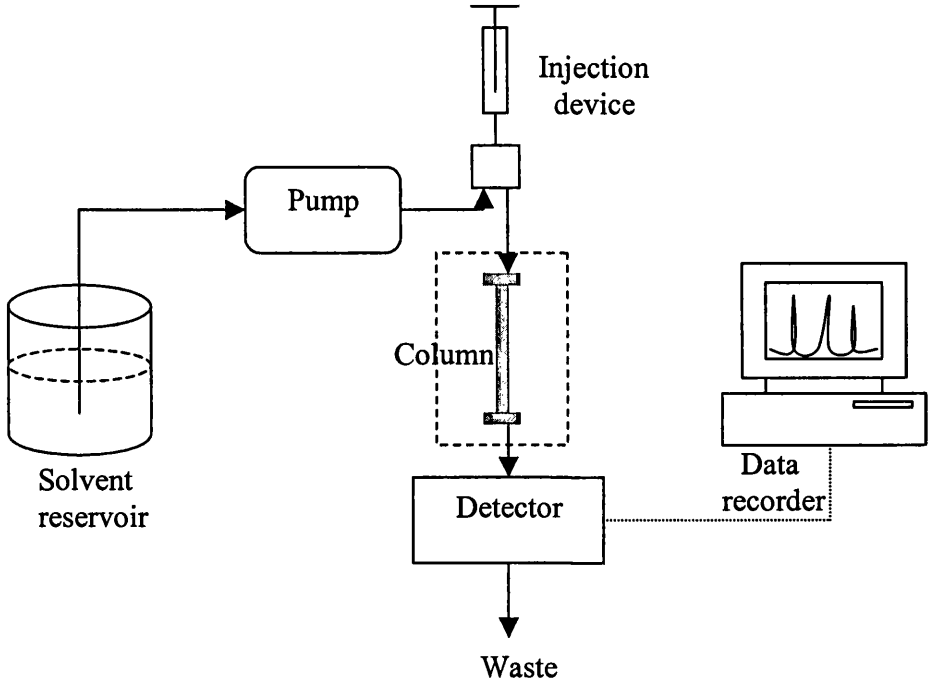

Mobile phase

The mobile phase is chosen for its chromatographic properties: it interacts with a suitable stationary phase to separate a mixture as fast and as efficiently as possible. Generally, a range of solvents is potentially able to solve any particular problem based on different criteria, such as viscosity, boiling point, purity and detector character.

For separation of a complex mixture, several solvents are normally used. In this case, solvent miscibility must be considered. It is always best to use solvents which are fully miscible with each other; acetone, glacial acetic acid, absolute ethanol, isopropanol and tetrahydrofuran are normally miscible with almost all other solvents. The usual eluents for reversed phase chromatography (RPC) are mixtures of an aqueous buffer or water, as the weaker component, and an organic solvent, either methanol, acetonitrile or tetrahydrofuran (THF) as the stronger component. Buffered solutions are usually used if the analyte can ionize and pH control is required.

Stationary phases and columns

Several different materials are usually used to synthesize stationary phases for different purpose, including silica, chemically modified silica, styrene-divinylbenzene, alumina and porous graphitic carbon.

Silica is an adsorbent with outstanding properties. It consists of silicon atoms bridged three-dimensionally by oxygen atoms and the lattice is saturated at the surface with OH groups, the so-called silanol groups. All these functional groups at the surface

could act as adsorptive centers, and the different properties of these functional groups could be used for the separation of different compounds.

The silanol groups on the surface of silica usually are chemically modified to give stationary phases with specific properties. The silanol group can be derivatised with an alcohol, ROH, where R may be an alkyl or an other functional group. Octadecylsilane (ODS), in which R = $-(CH_2)_{17}CH_3$, is the most widely used in this way. It is extremely non-polar and is the preferred choice for use in reversed-phase chromatography.

Cross-linked polystyrene is a versatile stationary phase resulting from copolymerization of styrene and divinylbenzene. Styrene-divinylbenzene can be used as a reversed-phase material in combination with aqueous mobile phase, and is stable in the pH range 1 to 13, as opposed to pH 2 to 8 for bonded silicas. The excellent pH resistance allows a good deal of scope for selecting the best eluent composition, this being a distinct advantage over stationary phases derived from silica.

Most HPLC columns are made of 316-grade stainless steel, which is austenitic chromium-nickel-molybdenum steel, resistant to the usual HPLC pressure and also relative inert to chemical corrosion. The inside of the column should have no rough surfaces, grooves or microporous structures, so the steel tubes must be either precision drilled or polished or electropolished after common manufacturing.

Columns of i.d. 2-5 mm are generally used for analytical purposes. Wider columns of i.d. between 10 mm and 25.4 mm may be used for preparative work. Columns 5, 10, 15 or 25 cm long are common if microparticulate stationary phases of 10 μm or less are used. If higher plate numbers are needed it is usually better to use a packing with smaller particles than to lengthen the column. A longer column increases the retention volume, thus decreasing the concentration of the peak in the eluate and impairing the detection limit.

Detectors

Several detectors can be coupled to HPLC, e.g. ultraviolet (UV) detectors, refractive index detectors, fluorescence detectors, electrochemical detectors as well as the very powerful mass spectrometer.

UV is the most commonly used type of detector as it can be rather sensitive, has a wide linear range, is relatively unaffected by temperature fluctuations and is also suitable for gradient elution. The principal of a UV detector is shown in Figure 1.6 Light travels in a longitudinal direction through the cells, and the same lamp transmits light through the measurement and reference cells. Two photodiodes measure the light intensity in both cells; the electronic system compares these signals and fluctuations in illumination intensity are balanced accordingly. Low-pressure mercury vapor lamps or cadmium, zinc, deuterium and tungsten lamps are suitable light sources.

Figure 1.6 Principle of UV detector used in HPLC

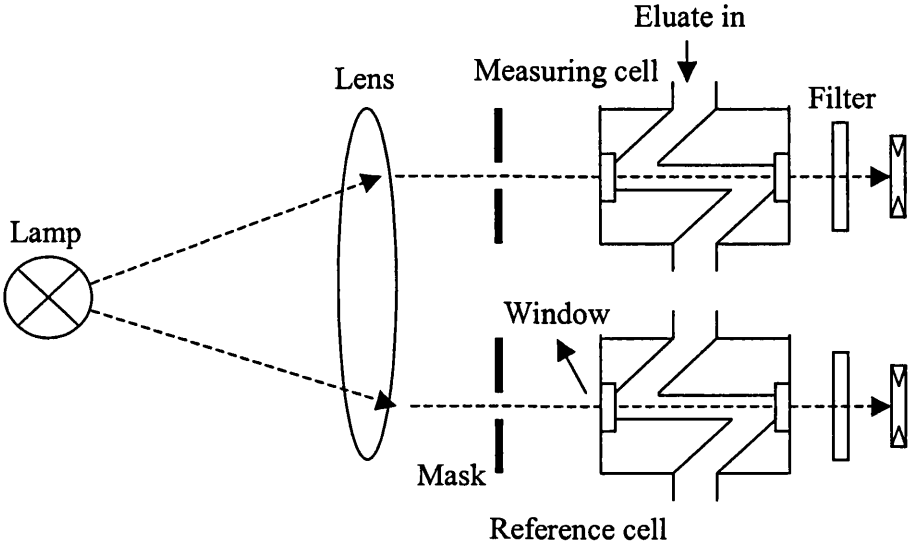

1.2.2 Introduction of mass spectrometry

The history of mass spectrometry can be traced back to 1897, when Nobel Prize winner J.J. Thompson [104] measured the ratio of charge-to-mass of the electron using magnetic and electric deflection. He later constructed the first mass spectrometer (then called a parabola spectrograph) and obtained mass spectra of O_2, N_2, CO, CO_2 and $COCl_2$. He also observed negative and multiple charged ions and discovered the isotopes 20 and 22 of neon [105]. After that, Dempster [106] developed the electron ionization source and the first spectrometer with a sector shaped magnet (180°) and direction focusing. A year later, Aston [107] developed the first mass spectrometer with velocity focusing and won Nobel Prize in 1922. Since then, mass spectrometry has undergone tremendous improvements. In 1948, Cameron and Eggers [108] published a design for a linear time-of-flight (TOF) mass spectrometer after the concept of this analyzer first proposed by Stephens [109]. In 1950's, the quadrupole analyzer and the ion trap or quistor was described in a patent by Paul and Steinwedel [110], and then the quadrupole mass spectrometer was developed by Paul and other cooperators [111]. At the same period, the first spectrometer coupled with a gas chromatograph was developed by McLafferty *et al* [112]. In the 1970's, the most important advances in mass spectrometry were the discovery of atmospheric pressure chemical ionization (APCI) by Horning *et al* [113] and the coupling of HPLC to MS by Arpino *et al* [114]. Many other important techniques have been invented in recently years, which include the fast atom bombardment (FAB) source[115], thermospray (TI) [116], matrix-assisted laser desorption ionization (MALDI) [117], electrospray (ESI) [118-120], and nanoelectrospray source[121].

1.2.2.1 Diagram of a mass spectrometer

A mass spectrometer always contains the five components as shown in Figure 1.7, namely (i) an inlet device to introduce the compound that is analyzed, e.g. a gas or liquid chromatograph or a direct syringe pump, (ii) a source to produce ions from the sample, (iii) one or several analyzers to separate the various ions according to their mass-to-charge ratios, (iv) a detector to count ions emerging from the last analyzer and to measure their abundance, (v) a computer to process the data, which produces the mass spectrum in a suitable form and controls the instrument feedback.

Figure 1.7 Schematic diagram of a mass spectrometer

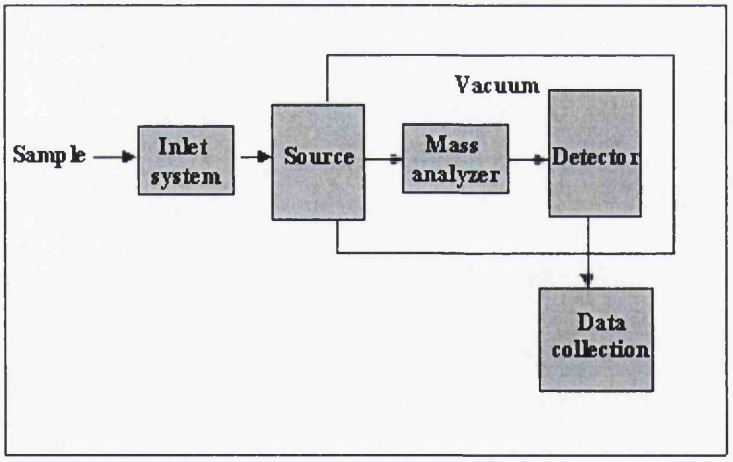

1.2.2.2 Ion sources

In the ion source, the analyzed samples are ionized for analysis in the mass spectrometer. A variety of ionization techniques are used for mass spectrometry such as:

electron ionization (EI) and chemical ionization (CI) for gas-phase ionizations; electrospray, thermospray and APCI for liquid-phase ion sources; MALDI, secondary ion mass spectrometry, field desorption and plasma desorption for solid-phase ion sources. The ion sources produce ions mainly by ionizing a neutral molecule through electron ejection, electron capture, protonation, deprotonation, adduct formation or transfer of a charged species from a condensed phase to the gas phase. Ion production often implies gas-phase ion-molecule reactions. A brief description of the most commonly used ESI and APCI sources is given below.

Electrospray

Electrospray ionization (ESI) is a soft ionization method that proceeds at atmospheric pressure and then transfers the ions into the mass spectrometer. ESI is the most unique interface in LC/MS because the ion generation process imparts very little internal energy into the analyte. The energy driving the thermodynamic change-of-state is electrostatic potential energy from a high voltage applied between the electrospray needle and collector (Figure 1.8). When the analyte solution flows constantly through a capillary with small diameter or a needle tip to which is applied a high voltage (3~5 kV), ions in solution migrate from the bulk to the surface of the liquid under the influence of the high field strength near the tip of the needle. Counter-ions are depleted from the surface of the liquid leaving a net charge. The characteristic " Taylor cone" is the result of the liquid accelerating toward the collection electrode. When the electrostatic forces exceed the inward forces from the surface tension a cone-jet is created. The highly charged surface of the liquid jet immediately disrupts into droplets toward the collector electrode.

Figure 1.8 Taylor cone formed at the capillary tip in ESI

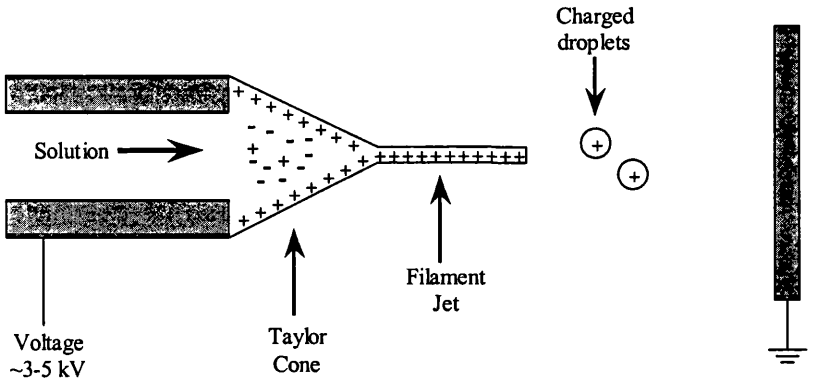

Figure 1.9 The mechanism of the formations of ions in ESI; (a) representation of the process of the shrinkage of the charged droplets; (b) representation of the process of the generation of gas phase ions.

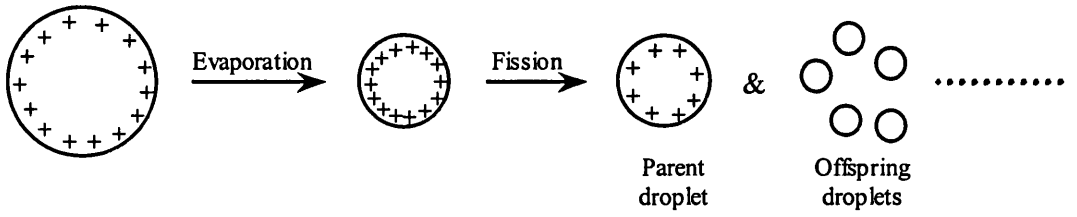

a. Shrinkage of Charged Droplets

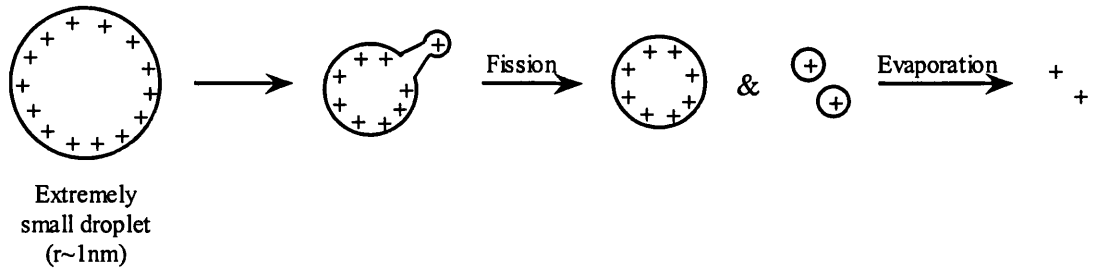

b. Generation of Gas Phase Ions

At a sufficiently high electric field, liquid filament is emitted from the Taylor cone tip. At some distance downstream, the liquid filament becomes unstable and forms separate charged droplets [122]. While in flight, the charged droplets release organic solvents and modifiers and are reduced in size. This reduction in the volume of the droplets results in the generation of excess charged droplets. As the coulombic forces prevail over the surface-tension forces, the droplets are broken into smaller droplets (Figure 1.9 (a)). The charged droplets become progressively smaller by a serial repetition of this process, and finally the charge is transferred to analyte molecules in the gas-phase (Figure 1.9 (b)) [123].

Unlike most ionization processes in mass spectrometry which occur in the gas phase, ESI involves the transfer of ions present in a liquid phase into the gas phase. If a species exists in solution with more than one ionizable site, then ESI will also produce more than one charge in the gas phase. In this way we can observe multiple-charged species in the mass spectrum. This effectively folds the mass spectrum of a high molecular weight species into the mass range of a typical mass analyzer.

Atmospheric pressure chemical ionization

APCI is an ionization technique analogous to chemical ionization (CI) that uses gas-phase ion-molecule reactions at atmospheric pressure, and in which primary ions are produced by corona discharges on a solvent spray. The principle governing APCI is shown in Figure 1.10.

The analyte in solution from a direct inlet probe or a liquid chromatography eluting at a flow rate of between 0.2 and 2 ml/min is introduced directly into a pneumatic

nebulizer where it is converted into a thin fog by a high-speed nitrogen beam. Droplets then are displaced by the gas flow through a heated quartz tube called a desolvation/vaporizer chamber. The heat transferred to the spray droplets allows vaporization of the mobile phase and of the sample in the gas flow. The temperature of chamber is controlled, which makes the vaporization conditions independent of the flow and the nature of the mobile phase. The hot gas and the compounds leave this tube. After desolvation, they are carried to a corona discharge electrode where ionization occurs. In the positive ion mode, either proton transfer or adduction of reactant gas ion can occur to produce ions of the molecular species, depending on the relative proton affinities of the reactant ions and the gaseous analyte molecules. In the negative mode, the ions of the molecular species are produced either by proton abstraction or adduct formation.

Figure 1.10 Principle of APCI

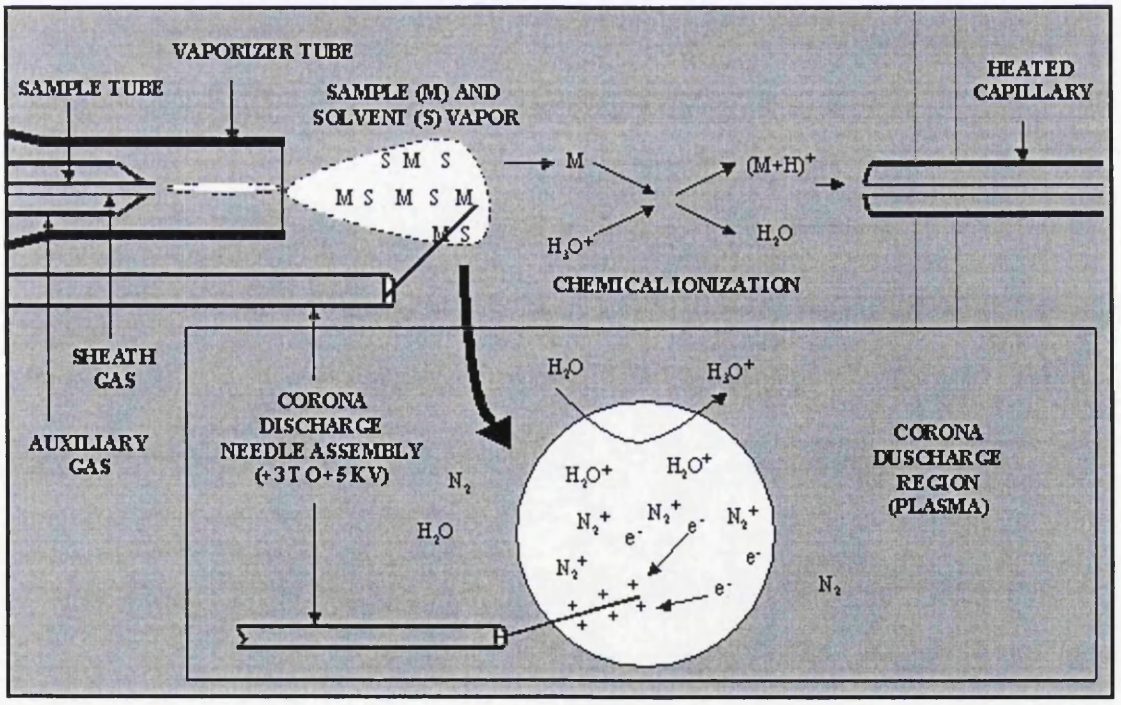

Generally, the evaporated mobile phase acts as the ionizing gas and reactant ions are produced from the effect of a corona discharge on the nebulized solvent. Typically, the corona discharge forms primary ions such as $N_2^{\bullet+}$ or $O_2^{\bullet+}$ by electron ionization. These ions then collide with vaporized solvent molecules to form secondary reactant gas ions. Because the ionization of the substrate occurs at atmospheric pressure and thus with a high collision frequency, it is very efficient. Furthermore, the high frequency of the collisions serves to thermalize the reactant species. In the same way, the rapid desolvation and vaporization of the droplets reduces considerably the thermal decomposition of the analyte. The result is ionization producing predominantly ions of molecular species with few fragmentations.

1.2.2.3 Mass analyzer

Once the ions have been produced, they need to be separated according to their masses, which must be determined. There are many different analyzers, such as the magnetic or electromagnetic analyzer, the time-of –flight mass analyzer, the quadrupole or ion trap, and the Fourier transform ion cyclotron resonance mass spectrometry.

The time-of-flight mass analyzer requires the ions to be produced in bundles and thus is especially well suited for pulsed laser sources. The ion trap, previously used as a gas chromatography/mass spectrometry (GC/MS) analyzer, is now also used as a high-performance mass spectrometer. Ion cyclotron resonance mass spectrometers using Fourier transform have shown impressive possibilities particularly for high resolution and collision-induced dissociation.

Instruments combing several analyzers in sequence, known as tandem mass spectrometry (MS/MS), are becoming increasingly common. They allow one to obtain a

mass spectrum resulting from the decomposition of an ion selected in the first analyzer. The time-dependent decomposition of a selected ion can also be observed in cyclotron or ion trap instruments.

Quadrupole mass analyzer

The principle of the quadrupole was described by Paul and Steinwegen [110] at the Bonn University in 1953. The quadrupole has since been developed for commercially available instruments by the work of Shoulders, Finnigan and Story [124].

As the name implies, the quadrupole consists of four precisely engineered parallel rods equally spaced around a central axis. Ions are introduced along the axis of the poles. There are four electrodes applied onto the quadrupole, with either a circular or hyperbolic cross section. Opposing sets of rods have both a direct current (dc) and an alternating current or a radio frequency (ac) voltage component; one set positive, one set negative as shown in Figure 1.11.

Figure 1.11 Schematic of quadrupole mass analyzer

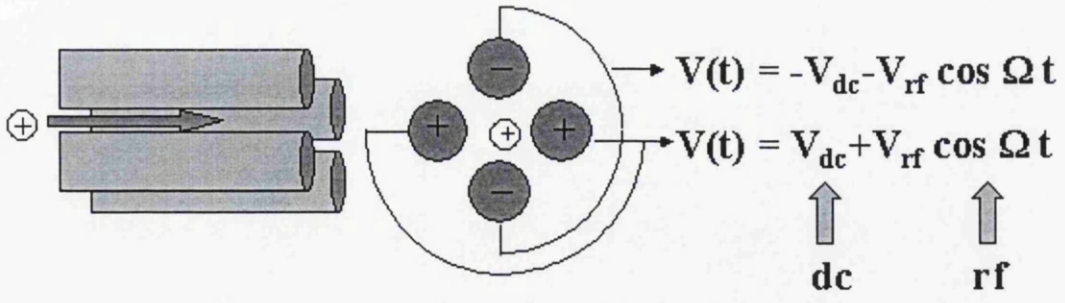

For mass analysis, a continuous beam of ions enters one end of this assembly from the ion source, and exits the opposite end to be detected by a high voltage detector. Ions are filtered on the basis of their mass-to-charge ratio. Ions below and above a certain m/z value will be filtered out of the beam depending on the ratio of the dc and ac voltage. The motion of an ion through a quadrupole analyzer is described by the following two equations:

$$\frac{d^2x}{d^2t}+\left(\frac{z}{m}\right)\frac{2x(V_{dc}+V_{ac}\cos\Omega t)}{r^2}=0 \qquad \textbf{(1.2.7)}$$

$$\frac{d^2y}{d^2t}+\left(\frac{z}{m}\right)\frac{2x(V_{dc}+V_{ac}\cos\Omega t)}{r^2}=0 \qquad \textbf{(1.2.8)}$$

Where x and y represent x-axis and y-axis respectively, V_{dc} and V_{ac} are dc voltage and ac voltage, r is the distance between the inner edge of the rod and the center of the space between rods and Ω is the frequency of the applied alternating voltage.

In practice, the highest detectable m/z ratio of quadrupole is about 4000 Th and the resolution hovers at around 3000 (resolving power). Thus, beyond 3000 u the isotope clusters are no longer clearly resolved. The resolution normally obtained is not sufficient to deduce the elementary analysis. Usually, quadrupole mass spectrometers are operated at " unit resolution", i.e. a resolution that is sufficient to separate two peaks one mass unit apart. Quadrupoles are low-resolution instruments.

Tandem mass spectrometry in quadrupoles

Figure 1.12 shows the general diagram of an instrument with three quadrupoles. A collision gas can be introduced into the central quadrupole at a pressure such that an ion entering the quadrupole undergoes one or several collisions.

Figure 1.12 Diagram of a triple quadrupole instrument. The first and last (Q1 and Q3) are mass spectrometers. The center quadrupole q2 is a collision cell made up of a quadrupole using RF only

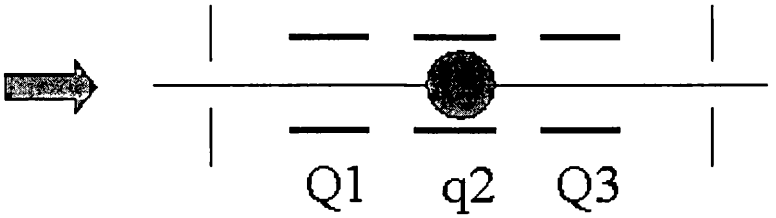

When a gas is inert, internal energy is transferred to the ion by converting a fraction of the kinetic energy into internal energy. The ion then fragments and the products are analyzed by quadrupole Q3. The collisions in these instruments occur at low energy. When the gas is reactive, ion-molecule reactions can be induced. The reaction products then are analyzed by Q3. These instruments with several analyzers in series can be scanned in several ways, such as product ion scan, precursor ion scan and neutral loss scan.

The product ion scan mode consists of selecting an ion with a chosen mass-to-charge ratio using the first Q1. This ion collides inside the central quadrupole and reacts or fragments. The reaction products are analyzer by Q3.

The precursor ion scan mode consists of focusing the Q3 on a selected ion while scanning the masses using Q1. All of the ions that produce the ion with the selected mass through reaction or fragmentation are thus detected.

In the neutral loss scan mode both Q1 and Q3 are scanned together, but with a constant mass offset between the two. Thus for a mass difference a, when an ion of mass m goes through the Q1, detection occurs if this ion has yielded a fragment ion of mass (m-a) when it leaves the collision cell.

Ion trap mass analyzer

The ion trap has been modified to a useful mass analyzer by Stafford *et al* [125] of the Finnigan Company. Conceptually, an ion trap can be imagined as a quadrupole bent on itself in order to form a closed loop. The inner rod is reduced to a point at the center of the trap, the outer rod is the circular electrode and the top and bottom rods make up the caps. The principle of the ion-trap mass analyzer is introduced below.

Figure 1.13 Section of a quadruple ion trap and the potentials applied.

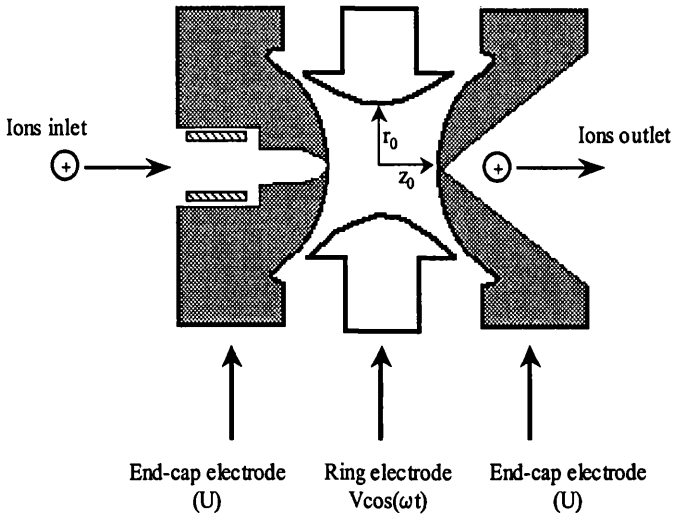

The ion trap mass analyzer consists of three electrodes: two end-cap electrodes and one ring electrode. The end-caps are applied with a DC potential (U) and the ring electrode is applied with a RF potential (Vcos (ωt)) as shown in Figure 1.13. If

$$a_z = -\frac{8zU}{mr_0^2\omega^2} \tag{1.2.9}$$

$$q_z = \frac{4zV}{mr_0^2\omega^2} \tag{1.2.10}$$

where:

m = the mass of ion detected,

z = the charges that the ion is carrying,

r_0 = internal radius of the ring electrode,

U = DC potential applied to the end-cap electrodes,

V = the amplitude of the RF potential applied to the ring electrode,

ω = angular frequency of the applied RF waveform,

the ion motion in the trap could be described by an a-q stability diagram (Figure 1.14). Ions with different masses can be trapped at different points in the stability zone when U and V are adjusted properly. When U and ω are fixed, the RF amplitude (V) increases gradually, some ions will move out of the stable zone and have unstable motions and get out of the trap to the detector, through which mass-selective instability scan is achieved. From equation (1.2.9) and (1.2.10), we can obtain an equation of

$$m/z = \frac{4V}{r_0^2 \omega^2 q_z} \qquad (1.2.11)$$

For a given ion trap instrument, there is an instability boundary that is defined by the value of q_z (equation (1.2.10)). In a commercial Finnigan ion trap, $q_z = 0.908$ is the point of instability boundary. Depending upon the amplitude of RF voltage (V) placed on the ring electrode, an ion of a given m/z will have a q_z value that will fall within the boundaries of the stability diagram, and the ion will be trapped. If the q_z value at the voltage falls outside of the boundaries of the stability diagram, the ion will move out of the trap.

Figure 1.14 a-q stability diagram of a quadruple ion-trap mass spectrometer.

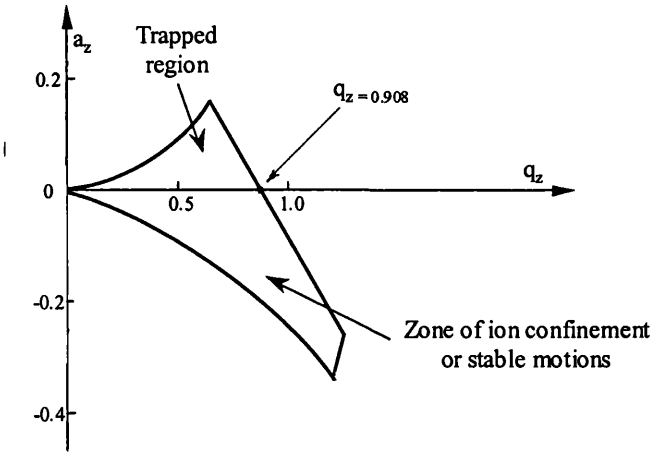

Resonance ejection

As the voltage (V) is increased, the q_z value for the ion also increases. When V is high enough and the q_z value falls out of the stability boundary, the ion will be ejected out of the trap. However, The amplitude of the RF cannot be increased too high due to practical difficulties encountered when interfacing high voltages to electronic circuits.

Ions oscillate with a frequency, known as the secular frequency, that is determined by the values for a_z and q_z and by the frequency of the RF potential. An applied oscillating signal, an AC voltage, may be applied across the end-cap electrodes to increase ion kinetic energies and excite ion trajectories [126]. If the amplitude of the signal is large enough, ions will be ejected from the trap rather than undergo fragmentation. This technique, termed resonance ejection, allows ejection to occur at voltages lower than those required for ejection at q_z of 0.908, extending the nominal mass range of the ion trap.

Tandem mass spectrometry in ion trap

For the performance of tandem MS, parent ions are selected by choosing DC voltage (U) and the amplitude of RF voltage (V). An AC voltage is applied to match the secular frequency of parent ion, from which the parent ions gain kinetic energy. Since ion traps are operated in a helium gas bath (1mTorr), parent ions will collide with the gas molecules and gain internal energy, resulting in fragmentation. The fragment ions then can be analyzed as described above. There are several ways to perform tandem mass spectrometry in an ion trap. Time-dependent rather than space-dependent tandem mass spectrometry occurs in the trap. The general sequence of operations is as follows:

1. Select ions of given mass-to-charge ratio by expelling all the others from the ion trap. This can be performed either by selecting the precursor ion at the apex of the stability diagram or by resonant expulsion of all ions except for the selected precursor.

2. Let these ions fragment. Energy is provided by collisions with the helium gas, which is always present. This fragmentation can be improved by excitation of the selected ions by irradiation at secular frequency.

3. Analysis of the ions by the scanning methods using stability or resonant ejection.

4. Alternatively, select a fragment in the trap and let it fragment further. This step can be repeated to provide MS^n spectra.

1.2.2.4 Ion Detectors

The ion beam passes through the mass analyzer and then can be detected by two kinds of detectors: one is like a photographic plate or Faraday cage which allows a direct measurement of the charges; the other is an electron or photon multiplier which increases the intensity of the signal.

Electron multiplier

The electron multiplier is the most commonly used detector in mass spectrometers because of its low cost and good linear dynamic response range. When a positive or negative ion reaches the conversion dynode, it causes the emission of several secondary particles. These secondary particles can include positive ions, negative ions, electrons and neutrals. When positive ions strike the negative high-voltage conversion dynode, the secondary particles of interest are negative ions and electrons. When negative ions strike the positive high-voltage conversion dynode, the secondary particles of interest are positive ions. These secondary particles are accelerated into the continuous-dynode

electron multiplier. They strike the cathode with sufficient energy to dislodge electrons as they collide with its curving inner walls. These electrons pass further into the electron multiplier, again striking the walls, causing the emission of more and more electrons as they travel towards the ground potential. Thus a cascade of electrons is created that finally results in a measurable current at the end of the electron multiplier. The amplifying power is the product of the conversion factor (number of secondary particles emitted by the conversion dynode for one incoming ion) and the multiplying factor of the continuous-dynode electron multiplier. It may reach 10^7. Their lifetime is limited to 1 or 2 years because of surface contamination from the ions or from a relatively poor vacuum. The conversion factor depends on the nature (mass, charge and structure) and on the energy of the detected ions, so these detectors are not as precise as Faraday cylinders. However, their sensitivity is such that they allow rapid scanning. The principle of electron multiplier is shown in Figure 1.15.

Figure 1.15 Diagram of the principle of electron multiplier

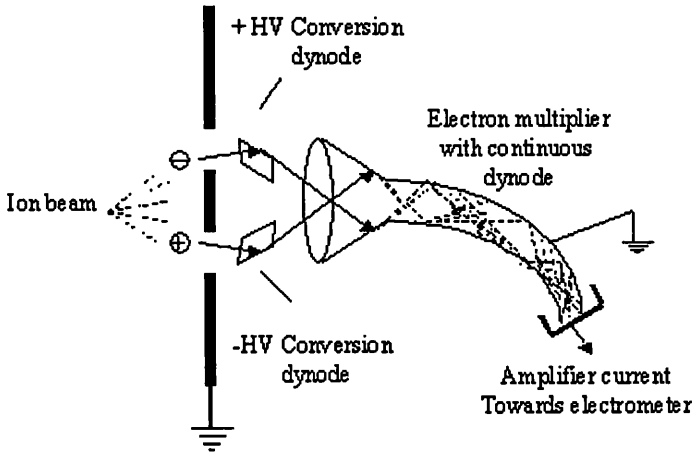

References

1. G. E. Abraham, R. S. Swerdloff, D. Tulchinsky, K. Hopper and W. Odell, *J. Clin. Endocrinol Metab.*, 33 (1971) 42
2. G. E. Abraham, R. S. Swerdloff, D. Tulchinsky and W. Odell, J. Clin. *Endocrinol Metab.*, 32 (1971) 619
3. T. M. Osterman, K.O. Juntunen and G. D. Gothoni, *Steroids,* 34 (1979) 575
4. H. Arajawa, M. Maeda and A. Tsuji, *Chem. Pharm. Bull.*, 30 (1982) 3036
5. B. A. El-Gamal, S. A. Eremin, D. S. Smith and J. Landon, *Ann. Clin. Biochem.*, 25 (1988) 35
6. C. Hanquez, P. Urios, B. Desfosses, H. Samake, E. Lince, K. Rajkowski and N. Cittanova, *Clin. Chim. Acta.*, 164 (1987) 71
7. S. Kono, G. R. Merrian, D. D. Brandon, D. L. Loriaux and M. B. Lipsett, J. *Clin. Endocrinol Metab.*, 54 (1982) 150
8. T. Liu, *Dingwuxue Zazhi.*, 3 (1982) 42
9. H. J. Makin, *Biochemistry of Steroid hormones, Ed H. L. J. Markin, Blackwell Scientific, London, UK*
10. S. T. Chan and W. S. Yeung, *J. Steroid Biochem.*, 25 (1986) 1013
11. E. Hamalainen, Scand. *J. Clin. Lab. Invest.*, 42 (1982) 493
12. Seki, M. Seki and K. Kato, *Acta Endocrinol (Copenhagen),* 110 (1985) 130
13. T. Chard, *An Introduction to Radioimmunoassay and Related Techniques, 3 rd Ed. 6 (1987) Pt. 2 of Laboratory Techniques in Biochemistry and Molecular Biology, Ed R. H. Bardon and P. H. van Knippenberg, Elsevier, Amsterdam.*

14. E. C. Horning, W.J. Vandenheuvel and E. O. Haahti, *Gas Chromatogrphy, Ed N. Brenner, J. E. Callen and M. D. Weiss, Academic Press, New York, USA (1962) 507*

15. E. C. Horning and W.J. Vandenheuvel, *Advances in chromatogaraphy, Ed J. C. Giddings and R. A. Keller, Dekker, New York, USA (1965) 153*

16. E. C. Horning and M. G. Horning, *Recent advances in chromatography Ed I. J. Domsky, Dekker, New York, USA (1971) 341*

17. L. German and E. C. Horning, L. *Chromatogr. Sci.* 11 (1973) 76

18. L. German, C. D. Pfaffenburger, J. P. Thenot, M. G. Horning and E. C. Horning, *Anal. Chem.,* 45 (1973) 930

19. T. Fotsis and H. Adlercreutz, *J. Steroid Biochem.,* 28 (1987) 203

20. T. A. Baillie, C. J. Brooks and E. C. Horning, *Anal. Lett.,* 5 (1972) 351

21. J. Brooks and D. J. Harvey, *Steroids* 15 (1970) 283

22. A. Reiffsteck, L. Dehennin and R. Scholler, *J. Steroid Biochem.*, 17 (1982) 567

23. P. G. Devaux, M. J. Horning and E. C. Horning, *Anal. Lett.* 4 (1971) 151

24. E. M. Chambaz and Ch. Madani, *International Congress Series,* 210 (1970) 97

25. T. Feher, L. Bodrogi, K. G. Feher and E. Poteczin, *Chromatographia,* 10 (1977) 86

26. Y. Shinohara, S. Baba and Y. Kasuya, *J. Clin. Endocrinol. Metab.,* 51 (1980)1459

27. T. Fotsis, *J. Steroid Biochem.,* 28 (1987) 215

28. M. Matsuguchi, L. Dehennin, G. Habrioux, L. Matsuguchi-Moreau and H. Degrelle, *J. Steroid Biochem.,* 28 (1987) 311

29. G. Moneti, M. G. Giovanni, A. Guarna, G. Forti, R. Salerno, A. Margini and M. Serio, *J. Steroid Biochem.,* 27 (1987) 53

30. C. H. L. Shackleton and J. O. Whitney, *Clin. Chim. Acta., 107 (1980) 231*

31. S. J. Gaskell, *In Methods of Biochemical Analysis, Ed D. Glick, John Wiley & Sons, New York, USA, 29 (1983) 385*

32. G. Wolthers and G. P. B. Kraan, *J. Chromatogr. A 843 (1999) 247*

33. K. Shimada, K. Mitamura and T. Higashi, *J. Chromatogr. A 935 (1999) 141*

34. V. Schwarz, *Pharmazie* 18 (1963) 22

35. R. Neher, *Steroid chromatography., Elsevier, Amsterdam*

36. J. Vaedtke, A. Gajewska, *J. Chromatogr.*, 9 (1962) 345

37. M. Yawara, E. M. Gold, *Steroids,* 3 (1964) 435

38. P. Corti, E. Lencioni, C. Murratzu, A. Cenni, Boll. Chim. Farm., 123 (1984) 565

39. L. M. Thienpont, P. G. Verhaeghe, K. A. Van Brussel, A. P. De Leenheer, *Clin. Chem.,* 34 (1988) 2066

40. L. Dehennin, *Clin. Chem.,* 35 (1989) 532

41. M. S. Shapiro, S. Zelefsky, R. Chayen, M. M. Werber, *J. Clin. Chem. Clin. Biochem.,* 27 (1989) 27

42. E. Vanluchene, D. Vandekerckhove, *J. Chromatogr.* 546 (1988) 175

43. M. Axelson, B. L. Sahlberg, J. Sjovall, *J. Chromatogr.* 224 (1981) 355

44. R. Neher, *Thin Layer Chromatography, Ed. E. Stahl, George Allan & Unwin, London UK (1969) 323*

45. M. Risk, O. B. Holland, H. Brown, *J. Chromatogr.* 317 (1984) 367

46. D.B. Gower, *J. Chromatogr.* 14 (1964) 424

47. M. A. Heindorf, V. L. McGuffin, *J. Chromatogr.* 464 (1989) 186

48. Y. Yamaguchi, *J. Chromatogr.* 228 (1982) 317

49. S. Siggia, R. A. Dishman, *Anal. Chem.,* 42 (1970) 1233

50. R. A. Henry, J. A. Schmit, J. F. Dieckman, *J. Chromatogr. Sci.* 9 (1989) 513

51. M. Lafosse, G. Keravis, M. H. Durand, *J. Chromatogr.* 118 (1976) 283

52. Heftman, I. R. Hunter, *J. Chromatogr.*, 165 (1979) 283

53. M. P. Kautsky, Ed. *Steroid Analysis by HPLC: Recent Applications. Dekker, New York, USA (1981)*

54. K. Shimada, K. Mitamura, T. Higashi, *J. Chromatogr.* A, 935 (2001) 141

55. J. L. Fitzpatrick, S. L. Ripp, N. B. Smith, W. M. Pierce Jr., R. A. Prough, *Arch. Biophys.* 389 (2001) 278

56. J.A.Shan and D.J.Weber, *J. Chromatogr.*, 496 (1989) 245.

57. R.S.Gardner, M.Walker and D.A.Hollingsbee, *J. Pharm. Biomed. Anal.*, 8 (1990) 1083.

58. J. H. McBride, D. O. Rodgerson, S. S. Park and A. F. Reyes, *Clin.Chem.*, 37 (1991) 643.

59. A. Shalaby and M. Shahjahan, *J. Liq. Chromatogr.*, 14 (1991) 1267.

60. M. P. Purdon and L. D. Lehman-Mckeeman, *J. Pharmacological and Toxicological Methods,* 37 (1997) 67

61. R. Navajas, C. Imaz, D. Carreras, M. Garcia, M. Perez, C. Rodriguez, A. F. Rodriguez and R. Cortes, *J. Chromatogr. B,* 673 (1995) 195.

62. T. Iwata, T. Hirose, M. Nakamura and M. Yamaguehi, *J. Chromatogr. B,* 654 (1994) 171.

63. R. J. Dolphin and P. J. Pergande, *J. Chromatogr.*, 143 (1977) 267.

64. J. C. Touchstone and W. Wortman, *J. Chromatogr.*, 76 (1973)244.

65. M. J. Kessler, *Steroids,* 39 (1982) 21.

66. G. P. Cartoni and F. Coccioli, *J. Chromatogr.*, 278 1983) 144.

67. M. Schoneshofer and H. J. Doulce, *J. Chromatogr.*, 164 (1979) 17.

68. B. J. Bassler and R. A. Hartwick, *J. Chromatogr.Sci.*, 27 (1989) 162.

69. S. E. Wade and A. D. Haegele, *J. Liq. Chromatogr.*, 14 (1991) 1257.

70. L. R. Snyder, *J. Chromatogr. Sci.*, 16 (1978)223.

71. M. Otto and W. Wegscheider, *J. Liq. Chromatogr.*, 6 (1983) 685.

72. P. Wester, J. Gotteries and K. Johansson, *J. Chromatogr.*, 415 (1987) 261.

73. A. K. Smilde, C. H. P. Bruins and D.A. Doombos, *J. Chromatogr.*, 410 (1987) 1.

74. K. Valko and P. Slegel, *J. Liq. Chromatogr.*, 14 (1991) 3167.

75. K. Y. Chong, T. H. Khoo, F. S. Koo, C. P. Org, S. F. Li, H. K. Lee, B. Venkatesh and C. H. Tan, *J. Liq. Chromatogr.*, 14 (1991) 2445.

76. M. W. Capp and M. H. Simonian, *Anal. Biochem.*, 147 (1985)374.

77. J. Q. Wei, J. L. Wei, C. Lucarelli, X. T. Zhou, D. Q. Wang, W. J. Dai, S. Li, S. M. Li and R. T. Liu, *Clin. Chem.*, 38 (1992) 76.

78. S. Saisho, K. Shimozawa and J. I. Yata, *Horm. Res.*, 33 (1990) 27.

79. A. W. Meikle, *Clin. Endocrinol.*, 16 (1982) 401.

80. E. Venturelli, A. Manzari, A. Cavalleri, M. Benzo, G. Secreto and E. Marubini, *J. Chromatogr.*, 582 (1992) 7.

81. M. Risk, O. B. Holland and H. Brown, *J. Cgr.*, 317 (1984) 367.

82. Beussac, M. C. Maotini and J. Cotte, Int. *J.Cosmet. Sci.*, 8 (1986) 175.

83. F. Andreolini, C. Borra, A. DiCorcia, R. Samperi and G. Graponi, *Clin. Chem.*, 31 (1985) 124.

84. G. J. Schmidt, *Chromatogr. Newslett.*, 7 (1079) 6.

85. T. Seki. and Y. Yamaguchi, *J. Chromatogr.*, 305 (1984) 188.

86. M. Numazawa, R. Osada, M. Tsuji and Y. Osawa, *Anal. Biochem.*, 146 (1985)75.

87. K. Sxhimada, T. Tanaka and T. Nambara, *J. Chromatogr.*, 307 (1984) 23.

88. K. Watanabe, *J. Chromatogr.*, 337 (1985) 126.

89. M. P. Purdon and L. D. Lehman-Mckeeman, *J. Pharmacological and Toxicological Methods,* 37 (1997) 67.

90. K. J. Darney, T. Y. Wing and L. L. Ewing, *J. Chromatogr.*, 257 (1983)81.

91. G. Walters, P. M. Foster and R. C. Cottrell, *J. Chromatogr.*, 219 (1981) 152.

92. S. Allenmark, A. A. Berg, M. Hammar and E. Lindstroem, *J. Chromatgr.*, 224 (1981) 399.

93. R. Blakley and M. L. Vestal, *Anal. Chem.*, 55 (1983) 750.

94. Nv. Esteban and A. L. Yeergey, *Steroids,* 55 (1990) 152.

95. C. H. L. Shackleton, C. Kletke, S. Wudy and J. H. Pratt, *Steroids,* 55 (1990) 472.

96. B. C. Chung, J. P. Mallamo, p. E. Juniewicz and C. H. C. Shackleton, *Steroids,* 57 (1992) 530.

97. M. Tsweet, Ber. Deutsch, *Botan. Ges.*, 24 (1906) 384

98. J. P. Martin, R. L. M. Synge, *Biochem.*, 35 (1941) 1358

99. L. C. Craig, *Anal. Chem.* 22 (1950) 1346

100. E. Gluekauf, *Trans. Faraday Soc.* 22 (1955) 1346

101. J. *van* Deemter, F. J. zuiderweg, A. Klinkenberg, *Chem. Eng. Sci.* 5 (1956) 271

102. J. C. Giddings, *J. Chem. Phys.*, 31 (1959) 1462

103. J. F. K. Huber, *Anal. Chim. Acta.*, 38 (1967) 305

104. J. J. Thomson, *Philos. Mag.*, V 44 (1897) 293.

105. J. J. Thomson, *Rays of Positive Electricity and Their Application to Chemical Analysis, Longmans Green, London, 1913*

106. J. Dempster, *Phys. Rev.*, 11 (1918) 316

107. W. Aston, *Philos. Mag.*, 38 (1919) 707

108. A. E. Cameron and D. F. Eggers, *Rev. Sci. Instrum.,* 19 (1948) 605

109. W. Stephens, *Phys. Rev.,* 69 (1946) 691

110. W. Paul and H. S. Steinwedel, *Z. Naturforsch.,* 8a, (1953) 448

111. W. Paul, H. P. Reinhard, U. von Zahn, *Z. Phys.,* 152 (1958) 143

112. W. MacLafferty, *Appl. Spectrosc.,* 11 (1957) 148.

113. E. C. Horning, D. I. Carroll, I. Dzidic, *J. Chromatogr. Sci.,* 412 (1974) 725

114. P. J. Arpino, M. A. Baldwin, F. W. MacLafferty, *Biomed. Mass Spectrom.,* 1 (1974) 80

115. M. Barber, R. S. Bardoli, R. D. Sedgwick et al., *J. Chem. Soc., Chem. Commun.,* 15 (1981) 325

116. R. Blakney and M. L. Vestal, *Anal. Chem.,* 55 (1983) 750

117. M. Karas, D. Bachman, U. Bahr et al., *Int. J. Mass Spectrom. Ion Processes,* 78 (1987) 53

118. J. B. Fenn, M. Mann, C. K. Meng, et al., *Science,* 246 (1989) 64

119. M. Yamashita and J. B. Fenn, *J. Chem. Phys.,* 80 (1984) 4451

120. M. Dole, L. L. Mach, R. L. Hines et al., *J. Chem. Phys.,* 49 (1968) 2240

121. M. Wilm and M. Mann, *Proc. 42nd ASMS Conference, Chicago, IL (1994) 770*

122. P. Kebarle and L. Tang, *Anal. Chem.*, 972A (1993) *65*

123. N. Mano and J. Goto, *Anal. Sci.*, *19* (2003) 3

124. R. E. Finnigan, *Anal. Chem.,* 66 (1994) 969A

125. C. Stafford, P. E. Kelley, J. E. Syka, *et al., Int. J. Mass Spectrom. Ion Processes, 60 (1984) 85*

126. R.E. Kaiser, R. G. Cooks Jr., G. C. Stafford, J. E. P. Syka Jr., and P. H. Hemberger, *Int. J. Mass Spectrom. Ion Processes*, 106 (1991) 79

127. R.Heftman, *Steroid Biochemistry, Academic Press, London*, 1970, p97-140

Chapter 2

Tandem Mass Spectrometry of Free Androgenic Steroids

2.1 Introduction

To help identification and determination of androgen steroids in biological samples, the mass spectrometric (MS) properties for the free androgens shown in Figure 2.1 are described in this chapter. The effect of different solvent system on the spectra of these compounds using electrospray (ESI) and atmospheric pressure chemical ionization (APCI) were studied in details, and their collision induced dissociation (CID) spectra were also investigated by tandem mass spectrometry.

2.2 Experimental

2.2.1 Materials

Testosterone, epitestosterone, androstendione, adrenosterone, androsterone, epiandrosteone, 5α-dihydrotestosteone, 5β-dihydrotestosterone, etiocholan-3β-ol-17-one, eticholan-3α-ol-17-one, 5α-androstan-3β-ol-17-one, 5α-androstane-3, 17-dione, dehydroepiandrosteone, 5-androstane-3β, 17β-diol, androstanediol, 11-ketoandrosterone, 11β-hydroxyandrosterone were purchased from Sigma-Aldrich Ltd (Poole, Dorset, UK). The standards were dissolved in methanol, and further diluted to the concentrations ranging from 1-10ng/μl with methanol/water (1:1) for the experiments. The structures of the investigated androgens are present in Figure 2.1.

The HPLC grade methanol, acetonitrile and water were purchased from Fisher Scientific (Loughborough, Leicester, UK).

Figure 2.1 Structures of 17 free androgenic steroids

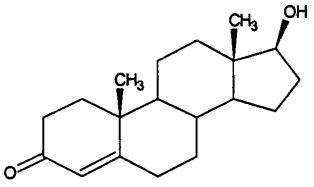

Testosterone

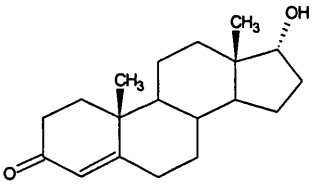

Epitestosterone

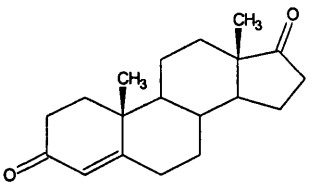

Androstendione

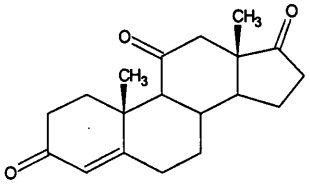

Adrenosterone

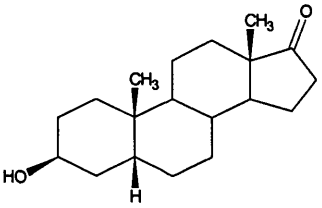

Etiocholan-3β-ol-17-one

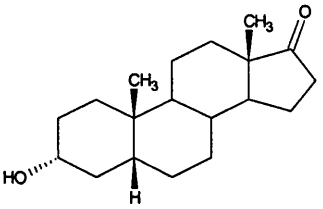

Etiocholan-3α-ol-17-one

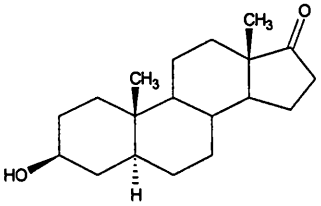

Epiandrosterone

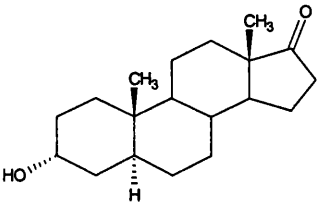

Androsterone

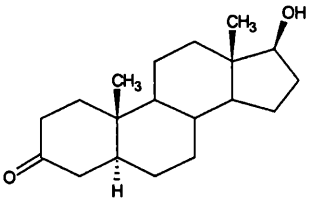

5α-Dihydrotestosterone

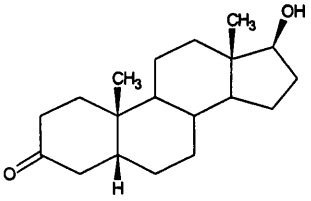

5β-Dihydrotestosterone

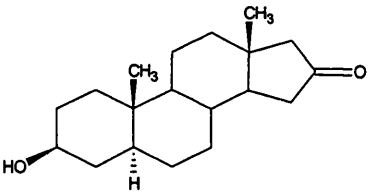

5α-Androstan-3β-ol-16-one

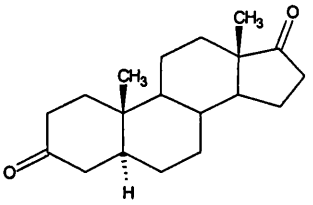

5a-Androstane-3, 17-dione

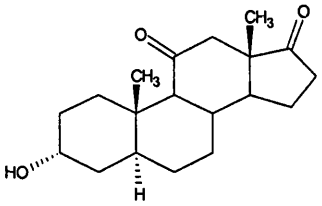

11-Keto-androsterone

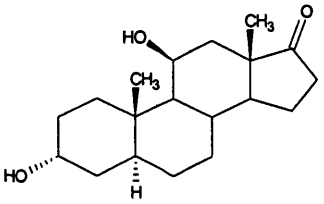

11β-Hydroxyandrosterone

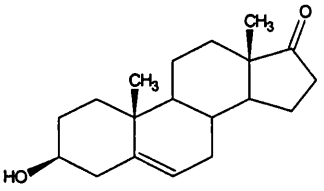

Dehydroepinadrosterone

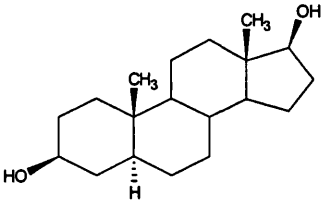

5α-Androstane-3β, 17β-diol

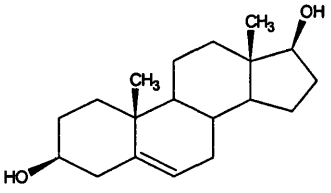

5-Androstene-3α, 17β-diol

2.2.2 HPLC

The chromatographic system consisted of a Hewlett-Packard 1100 HPLC system comprised of a binary gradient pump, auto sampler, column oven, and diode-array detector (Hewlett-Packard, Waldborn, Germany). Sample introduction into the mass spectrometer with methanol/ water (1:1, v/v) was delivered by HPLC system. The flow rate was 200μl/min for ESI-MS, and 400μl/min for APCI-MS.

2.2.3 Mass spectrometry

2.2.3.1 ESI-MS

The ESI-MS and ESI-CID experiments were performed on a LCQ ion trap mass spectrometer (Finnigan, Hemel Hempstead, UK) equipped with an ESI source. Standard solutions were loop (5μl) injected into the mass spectrometer by the HPLC system. Typical ESI-MS conditions were:

Parameter	Positive-ion mode
Sheath gas flow (arbitrary units)	80
Auxiliary gas flow (arbitrary units)	20
Spray voltage	4.5 kV
Capillary temperature	250°C
Capillary voltage	20 V
Tube lens offset	10 V

2.2.3.2 APCI-MS

The APCI-MS and APCI-CID experiments were also performed on a LCQ ion trap mass spectrometer using an APCI source. The APCI-MS conditions were:

Parameter	Positive-ion mode
Vaporizer temperature	550°C
Sheath gas flow (arbitrary units)	70
Auxiliary gas flow (arbitrary units)	20
Discharge current	5 μA
Capillary temperature	175°C
Capillary voltage	10 V
Tube lens offset	30 V

Methanol / water (1:1) and acetonitrile / water (1:1) were used as carrier solvent.

2.3 ESI-MS of androgenic steroids

2.3.1 Solvent effect for the spectra of representative androgenic steroids

In order to optimize the best solvent system for determining the spectra of androgens by ESI-MS, standards were prepared by dilution in either methanol/water (1:1) or acetonitrile/water (1:1) respectively, and loop injected into the flow of acetonitrile/water (1:1) delivered into the mass spectrometer by the HPLC system. The comparison between this two dilution solvents is shown in Figure 2.2.

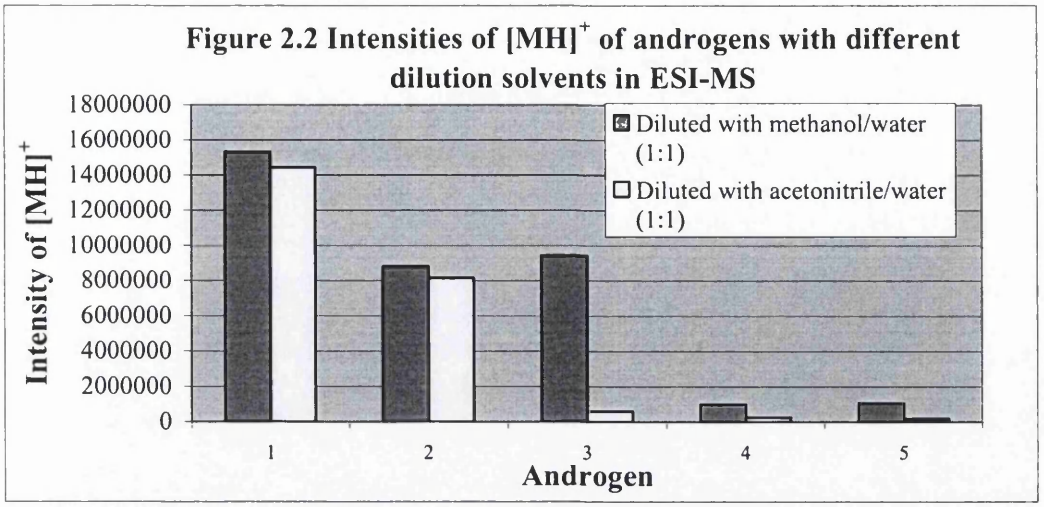

1. Testosterone (m/z 289), 2. Androstenedione (m/z 287), 3. 5α-dihydrotestosterone (m/z 291), 4. 5α-androstane-3, 17-dione (m/z 289), 5. Androsterone (m/z 273).

Similarly, samples were diluted in methanol/water (1:1), and injected into the different flow of methanol/water (1:1) or acetonitrile/water (1:1). The results are shown in Figure 2.3.

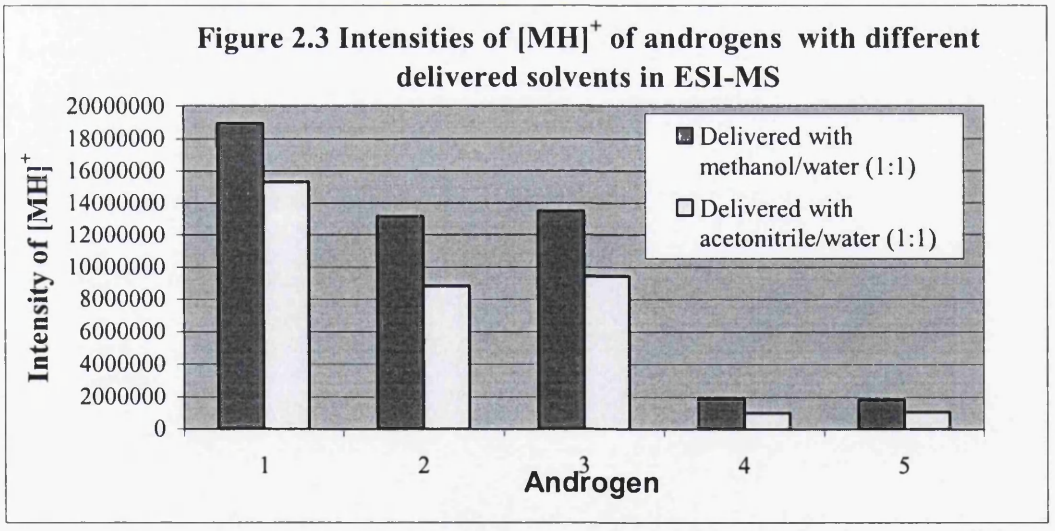

1. Testosterone (m/z 289), 2. Androstenedione (m/z 287), 3. 5α-dihydrotestosterone (m/z 291), 4. 5α-androstane-3, 17-dione (m/z 289), 5. Androsterone (m/z 273).

The two figures (2.2 and 2.3) show that the intensity of the androgens is optimal when samples are diluted in methanol/water and also delivered to the mass spectrometer with a methanol/water solvent system.

2.3.2 ESI-MS spectra of androgenic steroids

Both positive and negative ionization models were evaluated for investigation of the androgenic steroids, but no significant ions were observed in the negative ion mode, and therefore only positive ion mode spectra with ESI-MS are reported in Table 2.1.

The protonated molecular ion $[MH]^+$ was dominant in the elecrospray mass spectra of all of the investigated steroids with the single exception of 11β-hydroxyandrosterone, for which the ion ($[MNa]^+ + H_2O$) was most abundant. Relatively weak ions corresponding to adducts of the molecular ion with sodium were observed in all the spectra of the steroids. The orientation (α or β) of 17-OH or 3-OH group influenced the abundance of ($[MNa]^+ + H_2O$) rather than $[MNa]^+$, and the abundances of $[MNa+ H_2O]^+$ were apparently higher for the α-OH than for β-OH groups. The presence of a ketone or hydroxy group on the 11 position of the steroids resulted in a significant increase of $[MNa]^+$ and ($[MNa]^+ + H_2O$), and a large decrease of $[MH]^+$ for 11β-hydroxyandrosterone (Table 2.1). Adducts with methanol and water were not present in the spectra of 4-ene-3-one steroids, 11-keto-androsterone, and 11β-hydroxyandrosterone, but were observed for the rest of steroids investigated. The intensities of ($[MH]^+ + H_2O$) and ($[MH]^+$ +MeOH) ions seemed slightly higher for 17-OH groups than for those of 3-OH groups, but their orientation did not make any difference.

Table 2.1 ESI-MS of androgen steroids: m/z and relative abundances (%) of major ions

Androgenic steroid	$[MH]^+$	$[MNa]^+$	$[MNa]^+ + H_2O$	$[MH]^+ + H_2O$	$[MH]^+ + MeOH$	$[MH]^+ - H_2$	$[MH]^+ - H_2O$	$[MH]^+ - 2H_2O$
Testosterone	289 (100)	311 (5)	329 (20)	–	–	–	–	–
Epitestosterone	289 (100)	311 (8)	329 (34)	–	–	–	–	–
Androstendione	287 (100)	309 (<5)	327 (8)	–	–	–	–	–
Adrenosterone	301 (100)	323 (6)	341 (44)	–	–	–	–	–
Etiocholan-3β-ol-17-one	291 (100)	313 (<5)	331 (<5)	309 (<5)	323 (12)	289 (40)	273 (96)	255 (27)
Etiocholan-3α-ol-17one	291 (100)	313 (<5)	331 (32)	309 (<5)	323 (15)	289 (43)	273 (65)	255 (28)
Epiandrosterone	291 (100)	313 (<5)	331 (5)	309 (<5)	323 (14)	289 (17)	273 (74)	255 (22)
Androsterone	291 (100)	313 (<5)	331 (16)	309 (10)	323 (9)	289 (<5)	273 (82)	255 (10)
5α-Dihydrotestosterone	291 (100)	313 (<5)	331 (5)	309 (14)	323 (23)	289 (8)	273 (5)	255 (7)
5β-Dihydrotestosterone	291 (100)	313 (<5)	331 (<5)	309 (16)	323 (20)	289 (5)	273 (17)	255 (13)
*5α-Androstan-3β-ol-16-one	–	–	–	–	–	–	–	–
5α-Androstane-3, 17-dione	289 (100)	311 (<5)	329 (9)	307 (13)	321 (42)	–	271 (16)	253 (<5)
11-Ketoandrosterone	305 (100)	327 (21)	345 (32)	–	–	–	287 (21)	269 (8)
11β-hydroxyandrosterone	307 (10)	329 (21)	347 (100)	–	–	–	289 (25)	271 (54)
Dehydroepiandrosterone	289 (100)	311 (12)	329 (11)	307 (26)	321 (9)	–	271 (62)	253 (23)
*5α-Androstane-3β,17β-diol	–	–	–	–	–	–	–	–
*Androstanediol	–	–	–	–	–	–	–	–

* Spectra not available with ESI-MS.

There were no fragment ions for dehydration observed for the steroids with 4-ene-3-one in the A ring. However, for those steroids without a Δ4-double bound in the A ring, the spectra showed a peak of high relative intensity corresponding to water loss from their protonated molecular ions. It was suggested by Williams' group[1] and Bouchoux's group[2] that the protonation may probably start at the 3-one functional group for 4-ene-3-one steroids, due to the strong proton affinity of the conjugated double bonds in the structure of 4-ene-3-one steroids, and this structure makes the protonated ions very stable for these compounds. However, protonation may be initialed at the C-17 or the C-3 hydroxy group for those steroids without a Δ4-double bond in the A ring, and their protonated ions easily lose of water due to the unstable structures of these compounds. ($[MH]^+$ $-H_2O$) and ($[MH]^+$ $-2H_2O$) were present at quite high intensities in the mass spectra of these compounds. This result is in a good agreement with the previous studies[1-2]. In addition, ratios of $[MH-H_2O]^+$ /$[MH]^+$ were much lower of C-17 hydroxy steroids (5-17%) than those of C-3 hydroxy steroids (65-96%). Introduction of ketone or hydroxy group on the 11-position also decreased these ratios.

2.4 APCI-MS of androgenic steroids

2.4.1 Solvent effect of androgenic steroids for APCI-MS

The effects of the solvent system used for sample prepare from and HPLC were also studied for APCI-MS. As was the case in ESI-MS, methanol/water gave

substantially stronger signals for the androgens in APCI-MS than acetonitrile as shown in Figure 2.4 and 2.5.

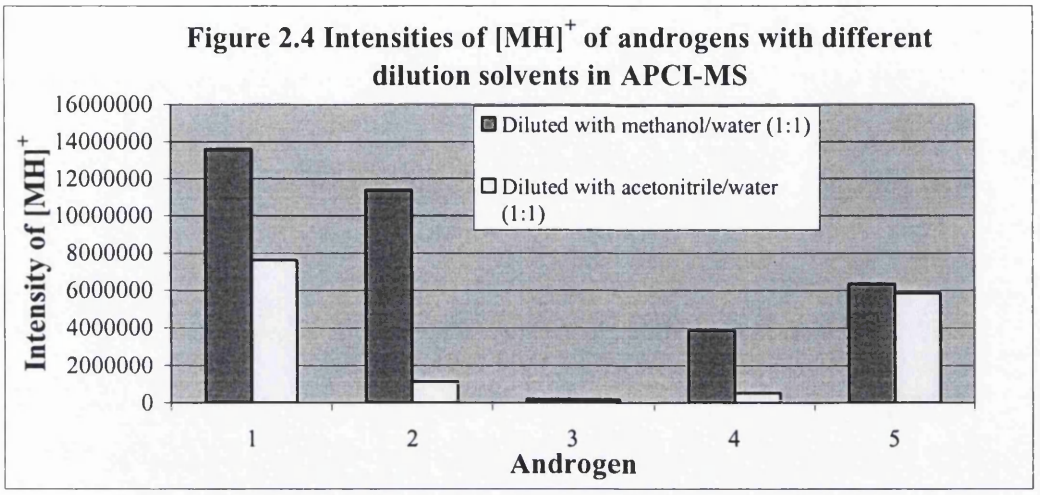

1. Testosterone (m/z 289), 2. Androstenedione (m/z 287), 3. 5α-dihydrotestosteone (m/z 291), 4. 5α-androstane-3, 17-dione (m/z 289), 5. Androsterone (m/z 273).

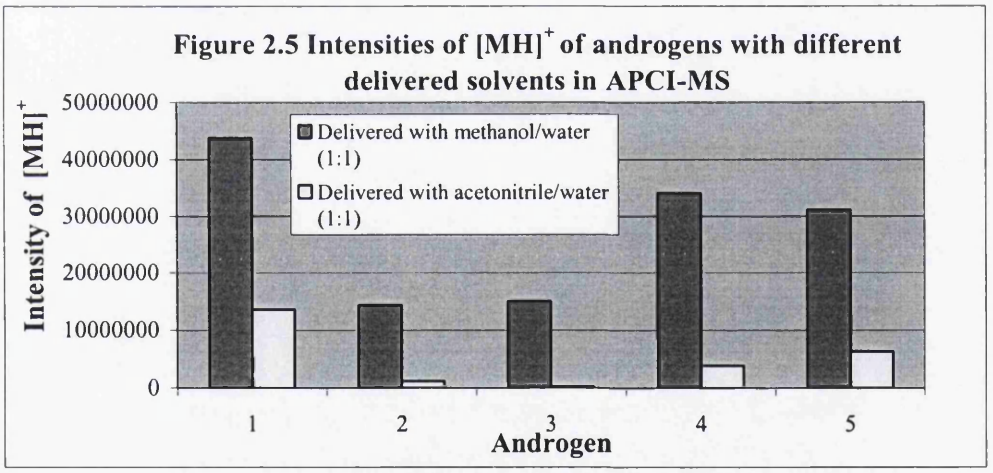

1. Testosterone (m/z 289), 2. Androstenedione (m/z 287), 3. 5α-dihydrotestosteone (m/z 291), 4. 5α-androstane-3, 17-dione (m/z 289), 5. Androsterone (m/z 273).

2.4.2 APCI-MS of androgenic steroids

2.4.2.1 Positive ion mode

As shown in Table 2.2, the protonated ion $[M+H]^+$ was the most intense peak for the androgenic steroids with 4-ene-3-one structures, e.g. 5α-dihydrotestosterone, 5β-dihydrotestosterone and 5α-androstane-3, 17-dione. In contrast, the dehydration ion of $[M+H]^+$ was dominant in the spectra of steroids without Δ_4 bond in the A ring. For steroids with 4-ene-3-one structure, there was either absent or of very low abundance the ion corresponding to ($[MH]^+$-H_2O) or ($[MH]^+$ -$2H_2O$), whilst, high intensity ions of ($[MH]^+$ -H_2O) or ($[MH]^+$ -$2H_2O$) were present in the spectra of the steroids without 4-ene-3-one structure. Similar spectra were also obtained by a Japanese research group[7] for 11β-hydroxyandrostenedione (m/z 303), Δ_4-androstenedione (m/z 287) and dehydroepiandrosterone (m/z 271). There were no sodium adducts observed for the APCI spectra in contrast to the ESI-spectra. Some methanol adduct ions were also observed for these kinds of steroids. A peak corresponding to ($[MH]^+$-H_2) was found in all the spectra of the steroids. Honing's research group[6] investigated adduct formation by three groups of steroids using an APCI source, and they also found that the group of 4-ene-3-one steroids showed a very good response for the protonated molecule in the positive mode, but no significant signals in the negative mode; however, the group of 3-OH aliphatic A ring steroids did not generate any abundant ions in either mode. Steroids lacking keto-groups show a low tendency to the formation of protonated molecules. Our observations were consistent with these fundings.

As in the ESI-MS spectra, the orientation of 17-OH group (α or β) did not result in any significant difference between the spectrum of testosterone and epitestosterone. For those steroids without a Δ4-double bond in the A the ring, the spectra showed

Table 2.2 APCI-MS of androgen steroids: m/z and relative abundances of major ions (positive mode)

Androgen steroid	$[MH]^+$	$[MH]^+ -H_2$	$[MH]^+ -2H_2$	$[MH]^+ -H_2O$	$[MH]^+ -2H_2O$	$[MH]^+$+MeOH	$[MH]^+ -H_2O$+MeOH
Testosterone	289 (100)	287 (12)	285 (7)	271 (5)	_	_	_
Epitestosterone	289 (100)	287 (17)	285 (5)	271 (6)	_	_	_
Androstendione	287 (100)	285 (18)	283 (<5)	_	_	_	_
Adrenosterone	301 (100)	299 (<5)	_	283 (10)	_	_	_
Etiocholan-3β-ol-17-one	291 (45)	289 (18)	287 (8)	273 (100)	255 (56)	323 (<5)	305 (<5)
Etiocholan-3α-ol-17one	291 (41)	289 (9)	287 (5)	273 (100)	255 (35)	323 (<5)	305 (<5)
Epiandrosterone	291 (49)	289 (6)	287 (18)	273 (100)	255 (65)	323 (<5)	305 (6)
Androsterone	291 (42)	289 (<5)	287 (<5)	273 (100)	255 (36)	323 (<5)	305 (<5)
5α-Dihydrotestosterone	291 (100)	289 (12)	287 (17)	273 (35)	255 (10)	323 (18)	305 (<5)
5β-Dihydrotestosterone	291 (100)	289 (23)	287 (14)	273 (40)	255 (14)	323 (22)	305 (6)
5α-Androstan-3β-ol-16-one	291 (6)	289 (<5)	287 (17)	273 (100)	255 (9)	323 (9)	305 (<5)
5α-Androstane-3,17-dione	289 (100)	287 (41)	285 (8)	271 (87)	253 (10)	321 (39)	305 (15)
11-Ketoandrosterone	305 (8)	303 (<5)	301 (<5)	287 (100)	269 (13)	_	_
11β-hydroxyandrosterone	307 (11)	305 (<5)	303 (<5)	289 (62)	271 (100)	_	_
Dehydroepiandrosterone	289 (22)	287 (23)	285 (37)	271 (100)	253 (40)	321 (<5))	303 (6)
5α-Androstane-3β,17β-diol	_	289 (14)	287 (25)	273 (100)	255 (63)	_	305 (<5)
Androstanediol	_	291 (25)	289 (10)	275 (76)	257 (100)	_	307 (13)

apparent differences between 3-OH group and 17-OH group; whereas, ($[MH]^+$ -H_2O) was dominant for the former, $[MH]^+$ was the most abundant for the latter. In addition, the ratio of ($[MH]^+$-H_2O) / $[MH]^+$ or ($[MH]^+$-$2H_2O$) / $[MH]^+$ was increased by the 16-one group compared to 17-one group. An increased ratio of adduct ions was observed with 11-one or 11-OH steroids, and moreover, the 11-OH androgens showed the most intensive peak of ($[MH]^+$-$2H_2O$). There was also higher ratio of ($[MH]^+$-H_2O) / $[MH]^+$ or ($[MH]^+$-$2H_2O$) / $[MH]^+$ present in the spectrum of dehydroepiandrosterone, assigned to the presence of the Δ5-double bond in the B ring. There was no $[MH]^+$ observed for the spectra of androstanediol and 5α-androstane-3β, 17β-diol, with ($[MH]^+$-$2H_2O$) was most abundant in the spectrum of the former and ($[MH]^+$-H_2O) was dominant for the latter. The major ions and their relative abundances were summarized in Table 2.2.

2.4.2.2 Negative ion mode

Whereas no significant ions were observed for most of androgen steroids in negative ion mode. Androgen steroids containing a 4-ene-3-one system and 11-ketoandrosterone were found to yield significant ions in negative ion mode APCI, as shown in Table 2.3.

The deprotonated molecular ion $[M-H]^-$ dominated in the mass spectra of the steroids in Table 2.3 except for adrenosterone. An ion corresponding to loss of water from the deprotonated molecule, ($[M-H]^-$ -H_2O), was also observed in the spectra of adrenosterone and 11-ketoandrosterone, and an ion corresponding to further loss of water was observed in the spectrum of 11-ketoandrosterone. The loss of hydrogen from the pseudo-molecular ions was observed in all the spectra of the above steroids and strong

tandem loss of hydrogen were observed in the spectra of androstendione, adrenosterone and 11-ketoandrosterone which has more than one keto-group on their structures

Table 2.3 APCI-MS of androgen steroids: m/z and relative abundances of major ions (negative mode)

Androgen steroid	T*	ET*	Androstendione	Adrenosterone	11-Ketoandrosterone
$[M-H]^-$	287 (100)	287 (100)	285 (100)	299 (98)	303 (100)
$[M-H]^- -H_2$	285 (14)	285 (15)	283 (61)	297 (100)	–
$[M-H]^- -2H_2$	–	–	281 (32)	295 (12)	–
$[M-H]^- -3H_2$	–	–	279 (9)	–	–
$[M-H]^- -4H_2$	–	–	277 (8)	–	–
$[M-H]^- -H_2O$	–	–	–	281 (29)	285 (13)
$[M-H]^- -H_2O-H_2$	–	–	–	279 (14)	283 (53)
$[M-H]^- -H_2O-2H_2$	–	–	–	277 (5)	281 (35)
$[M-H]^- -H_2O-3H_2$	–	–	–	275 (5)	279 (20)
$[M-H]^- -H_2O-4H_2$	–	–	–	–	277 (30)
$[M-H]^- -2H_2O$	–	–	–	–	267 (5)
$[M-H]^- -2H_2O-H_2$	–	–	–	–	265 (15)
$[M-H]^- -2H_2O-2H_2$	–	–	–	–	263 (19)

*T, testosterone; ET, epitestosterone.

2.5 Comparison of the sensitivity between ESI and APCI

The same concentration (10μg/ml) of each steroid was injected into the ESI source and the APCI source respectively, and the different intensities of their extracted base peak were compared in Figure 2.6.

The extracted peak intensities of most steroids were more than twenty times higher using the APCI source than using the ESI source, except for 11β-hydroxyandrosterone which was only two times higher using the APCI source than using the ESI source. The APCI source has showed the much better sensitivity than the ESI source for the detection of the investigated androgen steroids, due to the low polarity of the group compounds, and was selected for the subsequent collision induced dissociation (CID) studies.

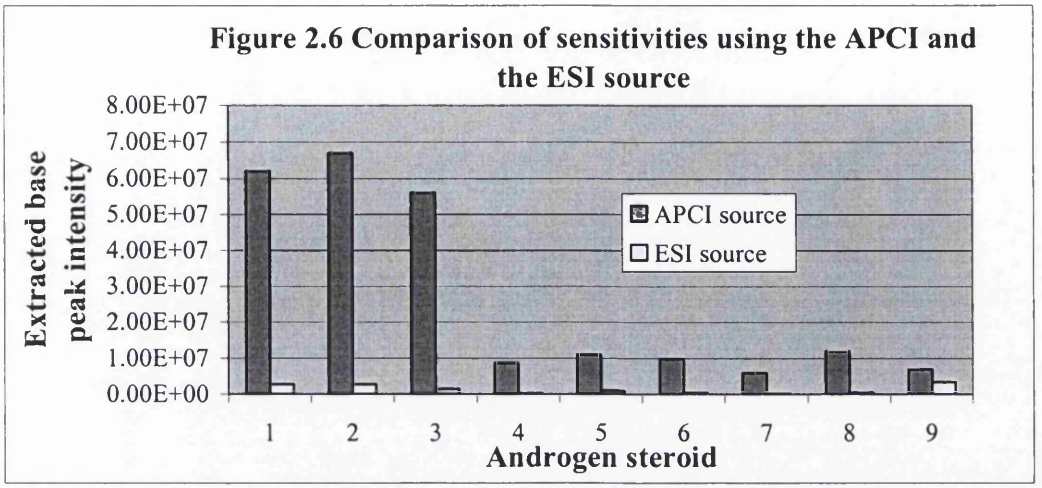

1. Testosterone (m/z 289), 2. Epitestosterone (m/z 289), 3. Androstenedione (m/z 287), 4. Epiandrosterone (m/z 273), 5. Dehydroepiandrosterone (m/z 271), 6. 5α-Dihydrotestosteone (m/z 291), 7. 5α-Androstane-3, 17-dione (m/z 289), 8. 11-Ketoandrosterone (m/z 287), 9. 11β-Hydroxyandrosterone (m/z 271).

2.6 Collision induced dissociation (CID) of APCI-MS

2.6.1 CID of 4-ene-3-one steroids

2.6.1.1 MS^2 of 4-ene-3-one steroids

There were two fragments ($[MH]^+ -H_2O$) and ($[MH]^+ -2H_2O$) observed in the high mass range of the MS^2 spectra yielded by the protonated molecule of all 4-ene-3one steroids, whilist major fragment ions at m/z 97, 109, 121, 123 were characteristically present in the low mass ions. Draisci and his co workers [9] observed similar fragment ions of m/z 97 and 109 in the spectra of testosterone and epitestosterone using APCI-MS. Other researchers [3, 4] have obtained similar CID spectra using ESI-MS. Curcuruto et. al [5]

observed fragment ions of m/z 97, 109 and 123 of testosterone by thermospray tandem mass spectrometry. The fragment ion of m/z 97 was clearly presented in all the 4-ene-3-one steroids except adrenosterone, which had oxygen substitution in the C-11 position. It has been proposed that this fragment was related to the A ring fission by T.M. Williams et. al [1], but the mechanism is still unclear.

Figure 2.7 Possible mechanism for the formation of the m/z 109 ion in the CID mass spectrum of testosterone by Williams et al.

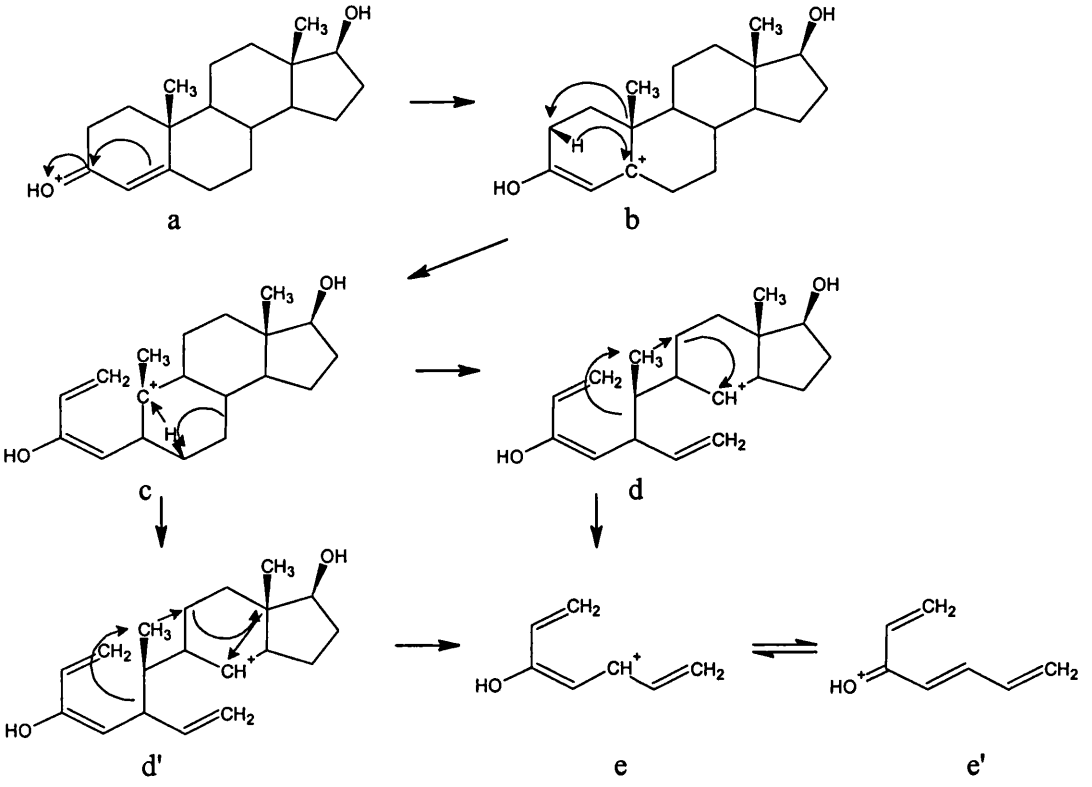

The fragment ion at m/z 109 were observed in all the spectra for this group steroids, and it has been suggested by Zaretskii [6] and Shackleton [3] that the formation of this fragment was due to the fission of the C9-C10 and C5-C6 bonds. However, Williams and his co-workers [1] examined the ^{13}C- and deuterium-labeled testosterone analogs, and

they suggested that the formation of the m/z 109 was related the cleavages of C1-C10, C7-C8 and C5-C10 bonds. They also proposed a possible mechanism for formation of m/z 109 (Figure 2.7). Our studies were consistent with Williams' proposal, because a keto-group at the C-11 position would inhibit the reactions of structure c to structure d and d', so there would be much reduction of m/z 109 ion expected for adrenosterone., as observed in the CID spectrum of adrenosterone in the present sudy.

It has been proposed by previous investigators [1, 3, 5] that the ion at m/z 123 was generated by the cleavage of the C6-C7 and C9-C10 bonds. Our studies however showed no significant peak at m/z 123 in the spectra of epitestosterone and adrenosterone, but these CID spectra did contain a significant peak at m/z 121. It seemed that the formation of this ion was somehow related to substitution at C-11 and C-17, but further study is still needed to investigate its mechanism. The MS^2 spectra of 4-ene-3-one steroids are shown in Figure 2.8.1-4.

Figure 2.8.1 MS^2 of testosterone from parent ion of m/z 289; collision energy 23%

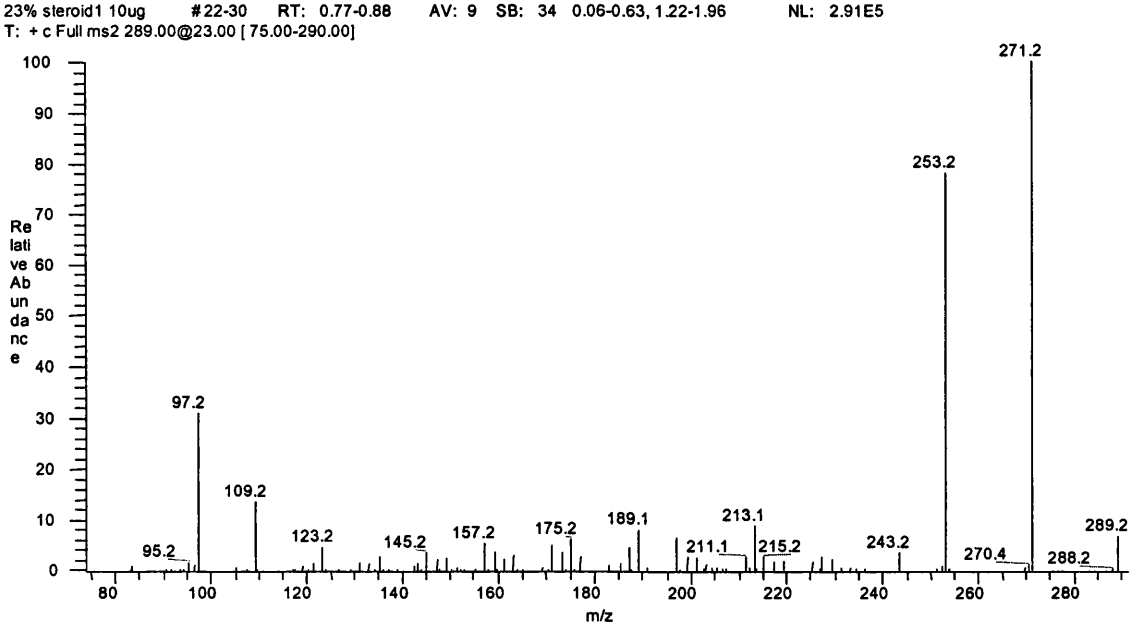

Figure 2.8.2 MS^2 of epitestosterone from parent ion of m/z 289; collision energy 23%

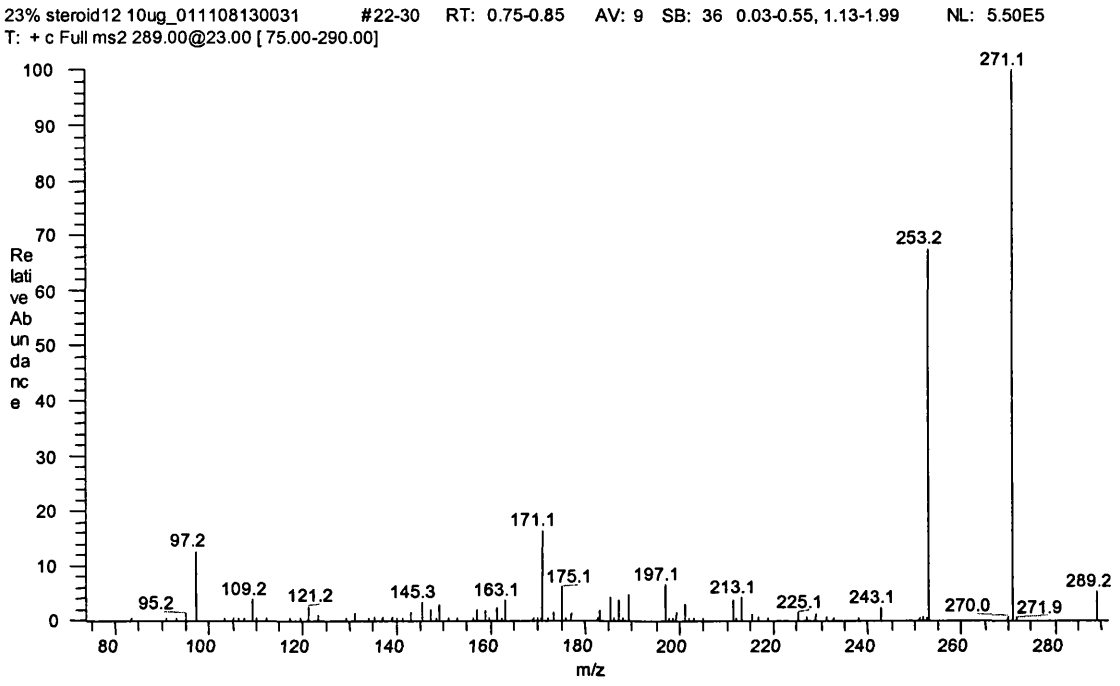

Figure 2.8.3 MS^2 of androstendione from parent ion of m/z 287; collision energy 25%

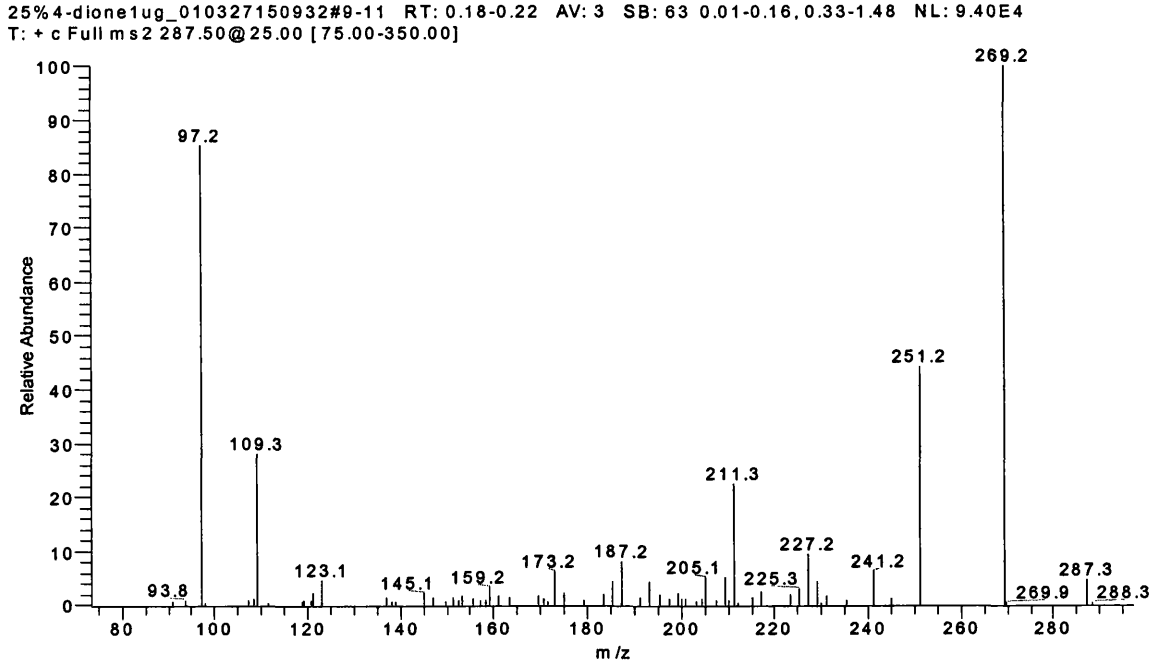

Figure 2.8.4 MS^2 of adrenosterone from parent ion of m/z 301; collision energy 25%

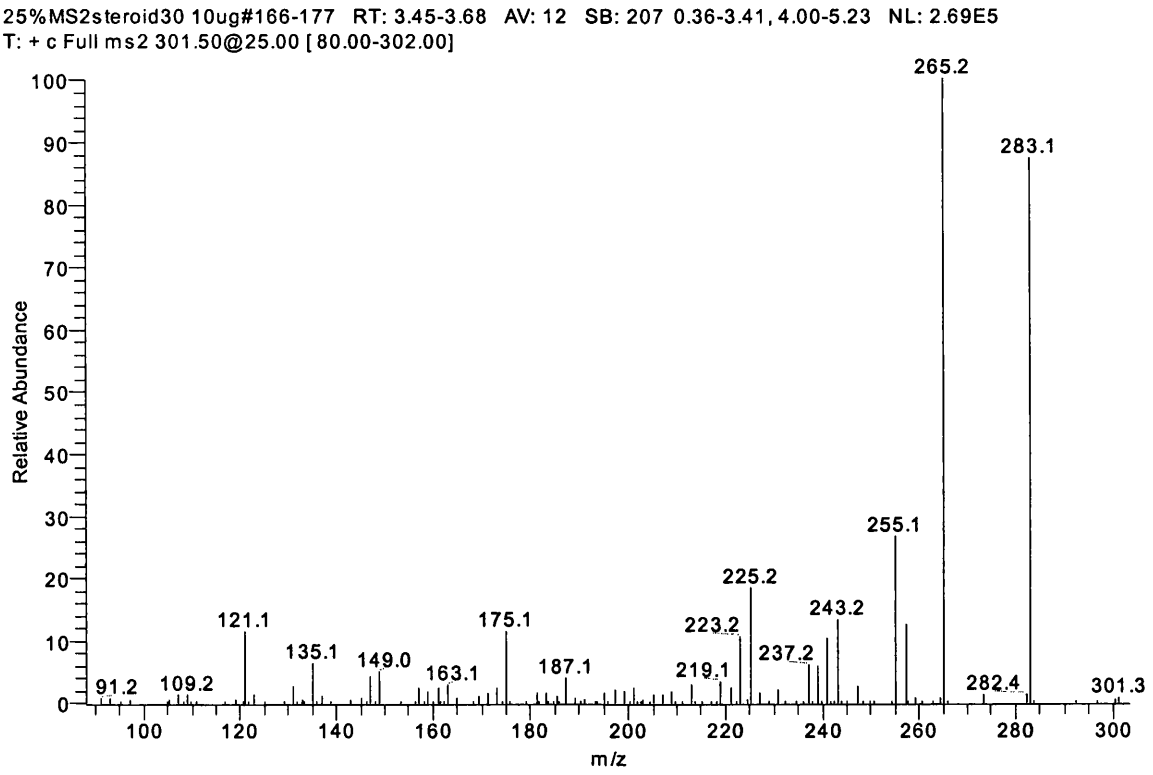

2.6.1.2 MS^3 of 4-ene-3-one steroids

Ions of m/z 253, 251 and 265 corresponding to further loss of water from their precursor ions ($[MH]^+ -H_2O$) derived from 4-ene-3one steroids, were observed in the MS^3 spectrum of any of these compounds but no ions of m/z 97 and 109 were present. There was an abundant ion of m/z 105 present in the MS^3 spectrum of testosterone, but not in the spectrum of epitestosterone. This apparent difference may be useful for the distinguishing the two isomers, compared to the strong similarity of their MS^2 spectra. The MS^3 spectra of 4-ene-3one steroids were shown in Figure 2.9.1-4.

Figure 2.9.1 MS^3 of testosterone from ion of m/z 289-271; collision energy 23%-30%

$[MH]^+$ (m/z 289) → ($[MH]^+$ - H_2O) (m/z 271)

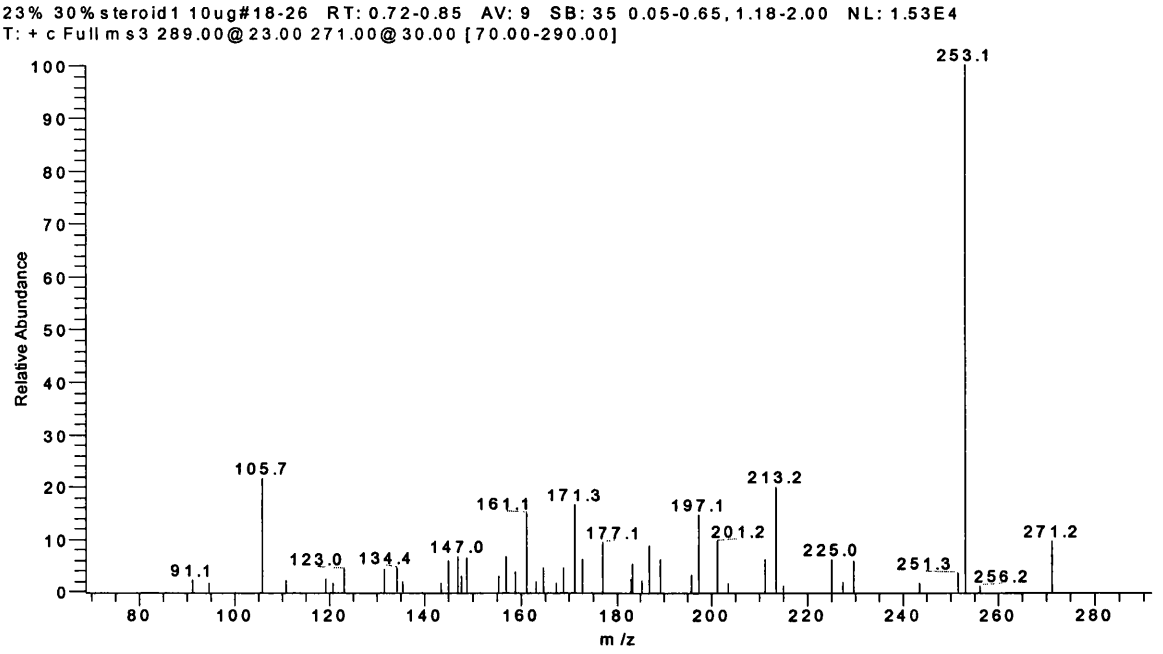

Figure 2.9.2 MS^3 of epitestosterone from ion of m/z 289-271; collision energy 23%-30%

$[MH]^+$ (m/z 289) → ($[MH]^+$ - H_2O) (m/z 271)

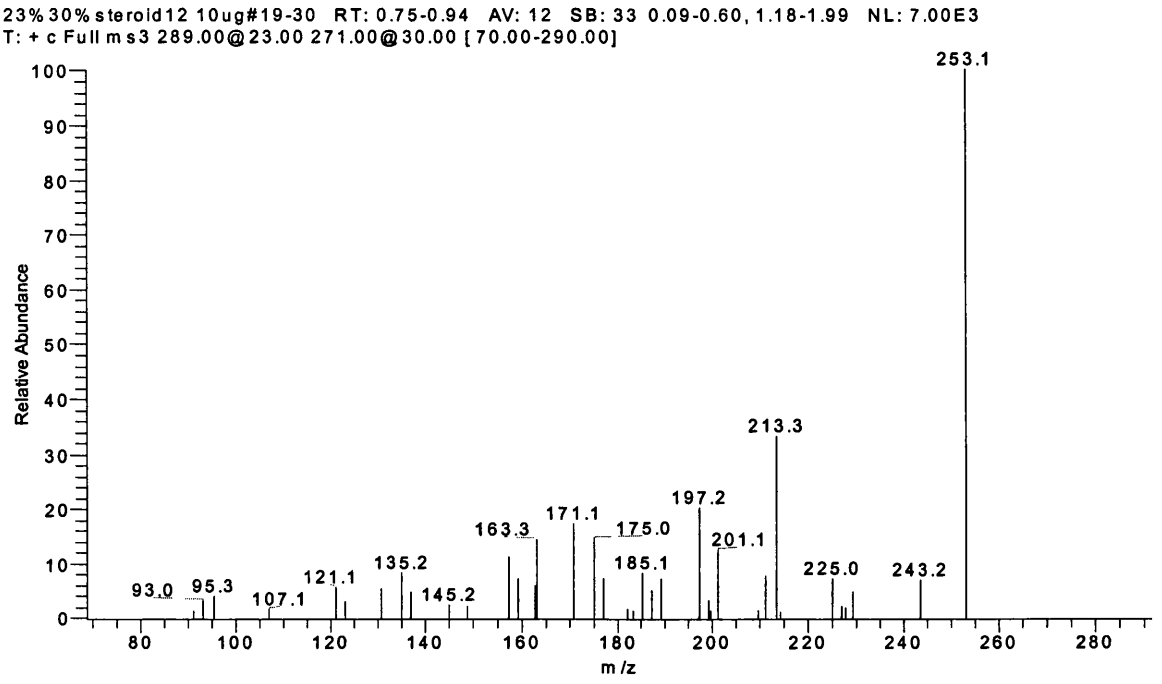

Figure 2.9.3 MS^3 of androstendione from ion of m/z 287-269; collision energy 25%-30%

$[MH]^+$ (m/z 287) → ($[MH]^+$ - H_2O) (m/z 269)

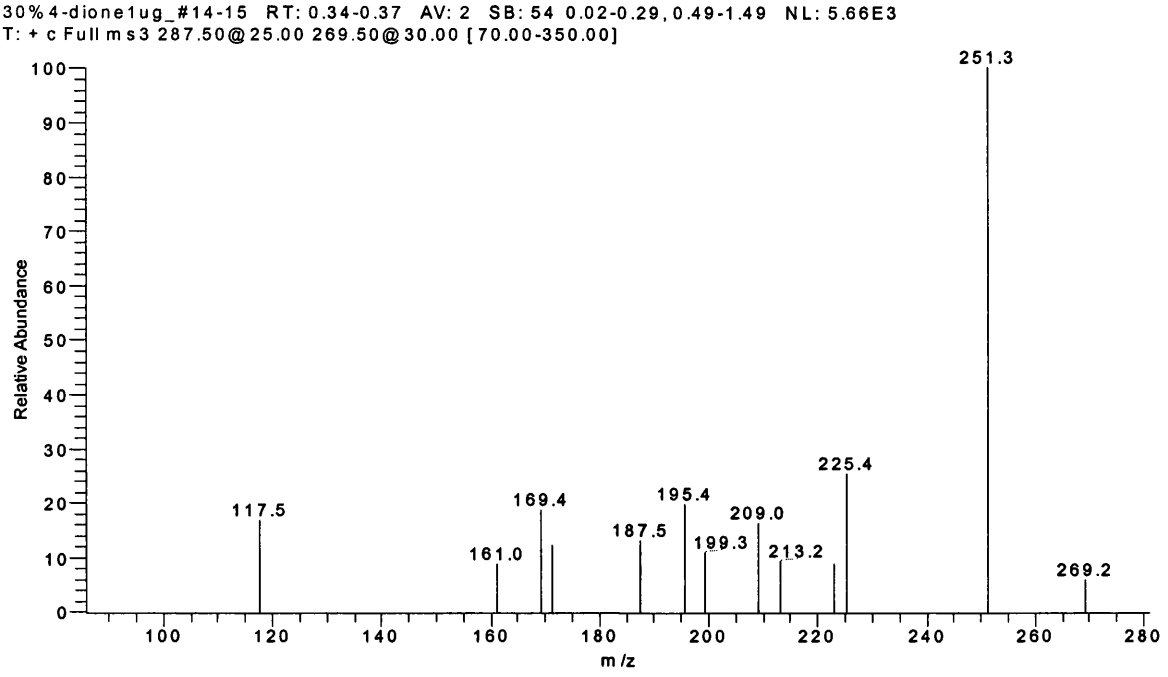

Figure 2.9.4 MS^3 of androstendione from ion of m/z 301-283; collision energy 25%-30%

$[MH]^+$ (m/z 301) → ($[MH]^+$ - H_2O) (m/z 283)

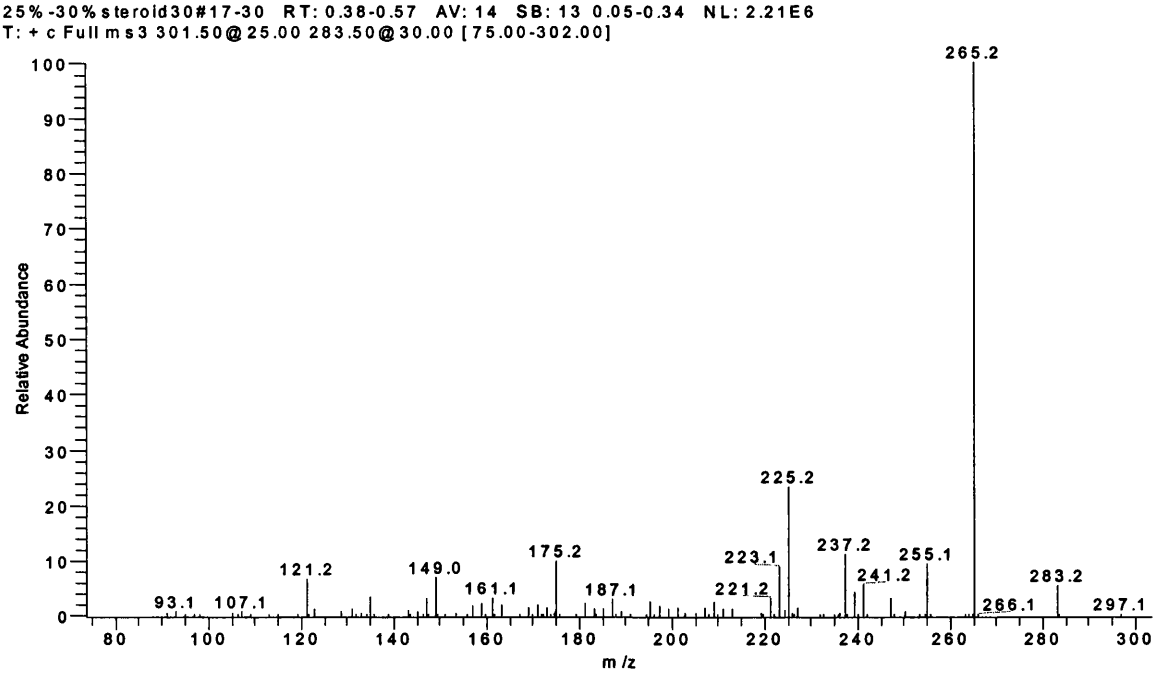

2.6.2 CID spectra of 5α-dihydrotestosterone and its isomers

2.6.2.1 CID spectra of 5α-dihydrotesterone and its isomers from parent ion of m/z 291

The CID spectrum from the ion of m/z 291 in the APCI-MS was only available for 5α-dihydrotestosterone due to the poor sensitivity for its other isomers. Two fragment ions, m/z 273 and 255 were dominant in the CID spectrum, corresponding to consecutive loss of water from $[MH]^+$. Relative to their abundance in the CID spectra of 4-ene-3-one steroids, there were significant reductions in the intensity of the ions at m/z 97, 109 and 123, so it appears that the presence of Δ4-double bond at the A-ring of the steroid is very important to generate these fragments. The MS^2 spectrum of 5α-dihydrotestosterone from parent ion of m/z 291 was shown in Figure 2.10.

Figure 2.10 MS^2 of 5α-dihydrotestosterone from parent ion of m/z 291; collision energy 30%

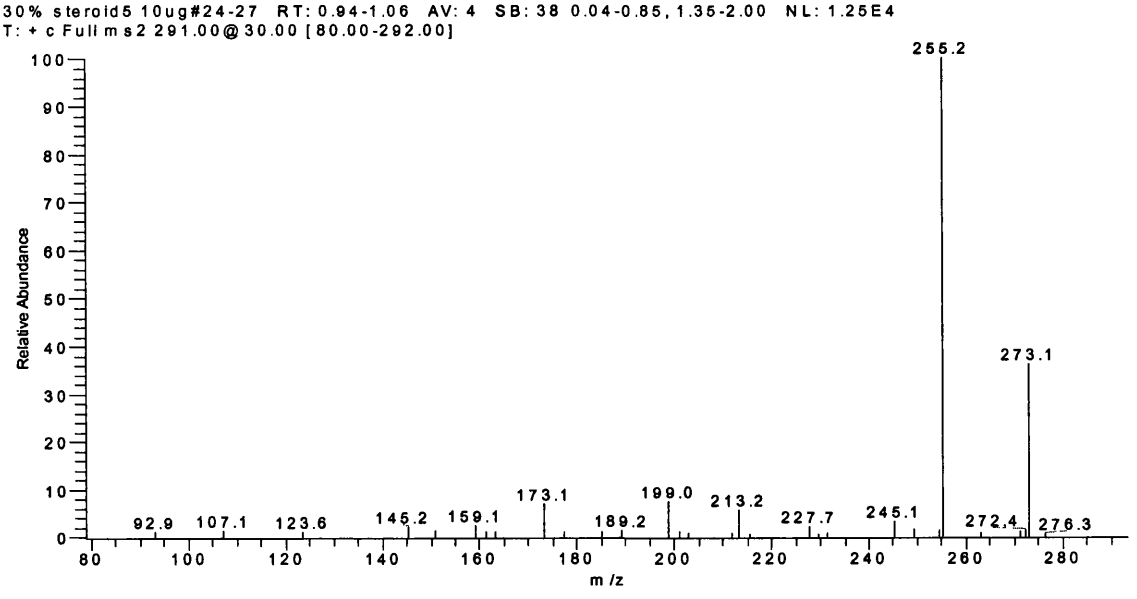

2.6.2.2 CID spectra of 5α-dihydrotesterone and its isomers from fragment ion of m/z 273

A fragment ion at m/z 255 was dominant in the CID spectra of 5α-dihydrotestosterone and its isomers generated from parent ion of m/z 273 in the APCI-MS. Fragment ions at m/z 97, 109 and 123 ions were present in a very low relative abundance for 5α- and 5β- dihydrotestosterone, but no fragment ions of m/z 97 and 109 were observed for the other isomers. The MS^2 spectrum of 5α-dihydrotestosterone from ion of m/z 273 was present in Figure 2.11, and the spectra of its other isomers were present in Appendix 1-5.

Figure 2.11: MS^2 of 5α-dihydrotestosterone from fragment ion of m/z 273; collision energy 28%

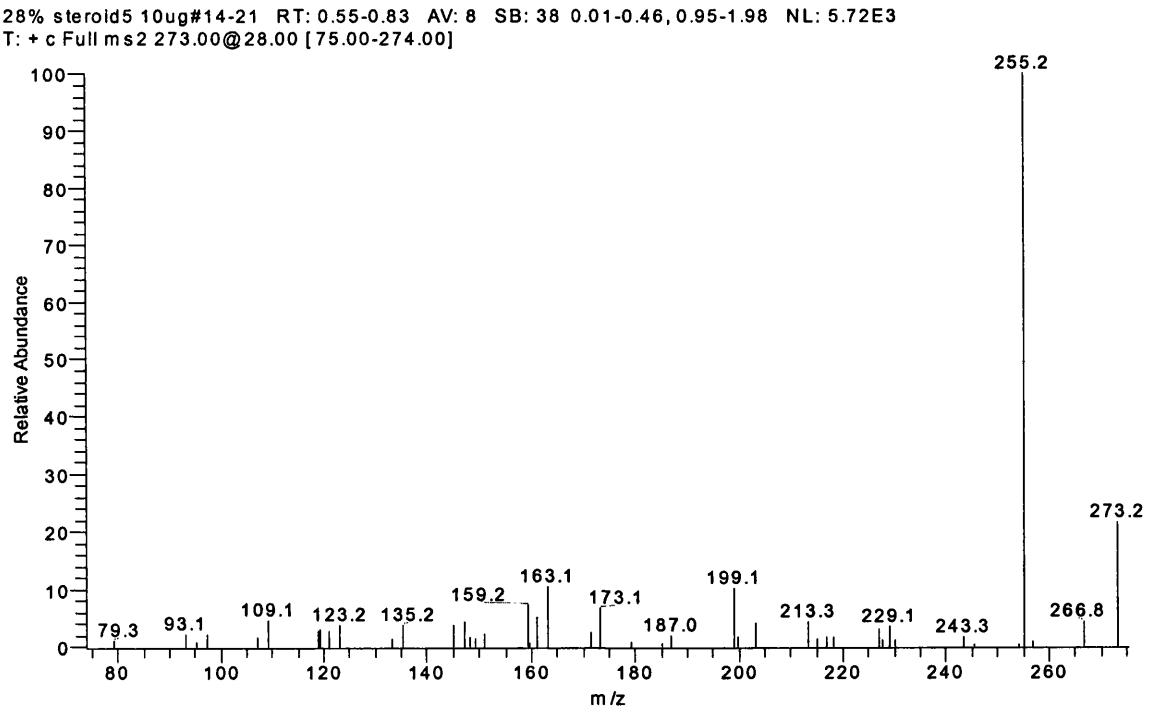

2.6.2.3 CID spectra of dihydrotesterone and its isomers from fragment ion of m/z 255

There were very similar CID spectra from m/z 255 for 5α-dihydrotestosterone and its isomers, and no m/z 97, 109 and 123 ions could be detected for these compounds. The MS^2 spectrum of 5α-Dihydrotestosterone from ion of m/z 255 was shown in Figure 2.12 and the spectra of its other isomers were present in Appendix 6-10.

Figure 2.12: MS^2 of 5α-dihydrotestosterone from fragment ion of m/z 255; collision energy 30%

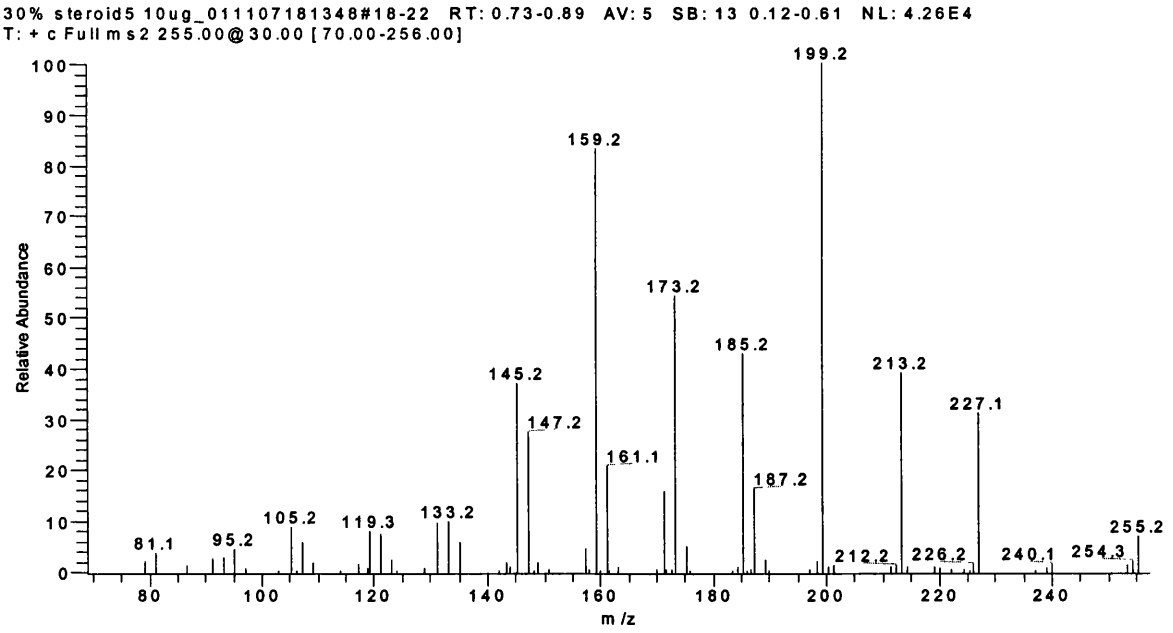

2.6.3 CID spectra for the other steroids

2.6.3.1 MS^2 of 5α-androstan-3β-ol-16-one

In a similar manner to the 17-one steroid, no MS^2 spectrum could be obtained from the parent ion of m/z 291 for 5α-androstan-3β-ol-16-one, but CID spectra from m/z 273 and 255 were observed. The spectra generated from m/z 255 for the 17-one and 16-one steroid were very similar. However, there was apparent fragment ion of m/z 109 that were absent from the spectra for 17-one steroids observed in the spectra of the 16-one steroids from the parent ion at m/z 273. The MS^2 spectra from ion of m/z 273 and 255 were shown in Figure 2.13.1-2.

Figure 2.13.1 MS^2 of 5α-androstan-3β-ol-16-one from ion of m/z 273; collision energy 30%

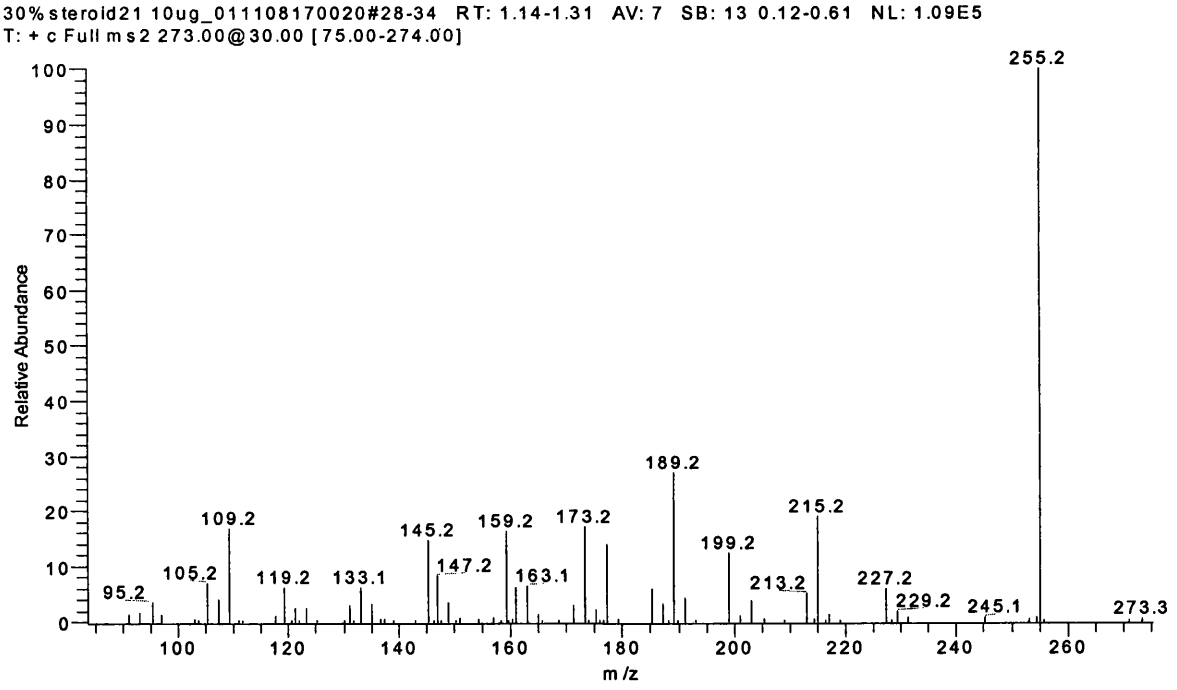

Figure 2.13.2 MS^2 of 5α-androstan-3β-ol-16-one from ion of m/z 255; collision energy 30%

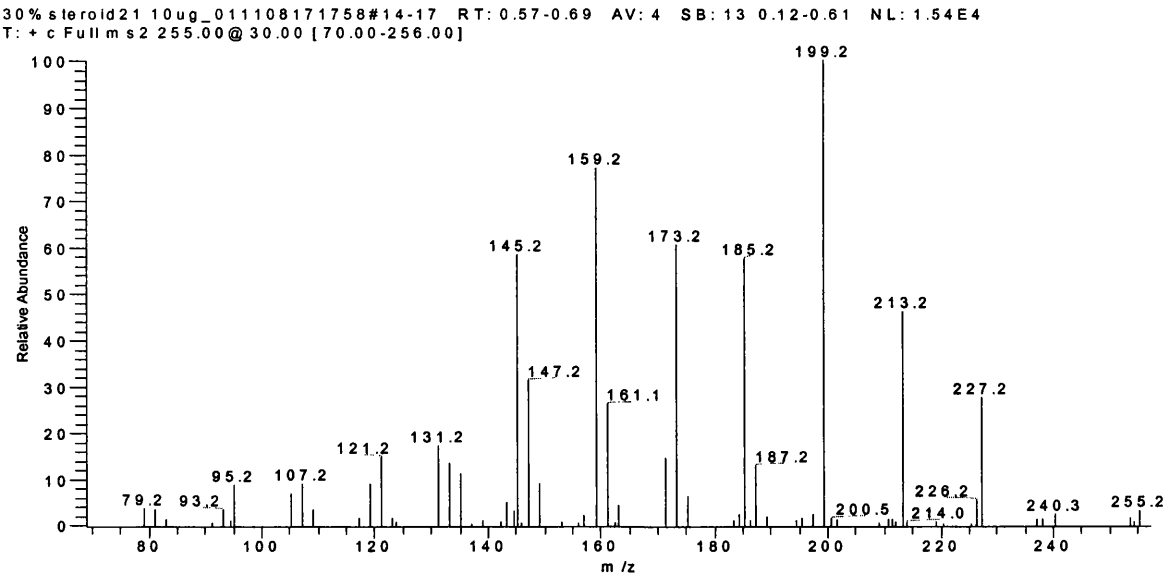

2.6.3.2 MS^2 of dehydroepiandrosterone

Fragment ions at m/z 97, 109 and 123 were observed in the low mass range of the spectrum for dehydroepiandrosterone generated from the parent ion at m/z 289, but no such ions were observed in the CID spectrum from the parent ion at m/z 271. In addition, the fragment ion at m/z 97 was quite abundant in the spectrum. Compared with the fragmentation pattern proposal to account for the CID spectra of 4-ene-3-one steroids and dihydrotestosterone, the mechanism to generate the fragment ion at m/z 97 may be the result of the fission at both A-ring and B-ring. For the spectrum from the ion at m/z 253, the fragment at m/z 197 was the most abundant ion presented, corresponding to loss of the fragment of butene (C_4H_8). The MS^2 spectra of dehydroepiandrosterone from ion of m/z 289, 271 and 253 were present in Figure 2.14.1-3.

Figure 2.14.1 MS^2 of dehydroepiandrosterone from parent ion of m/z 289; collision energy 25%

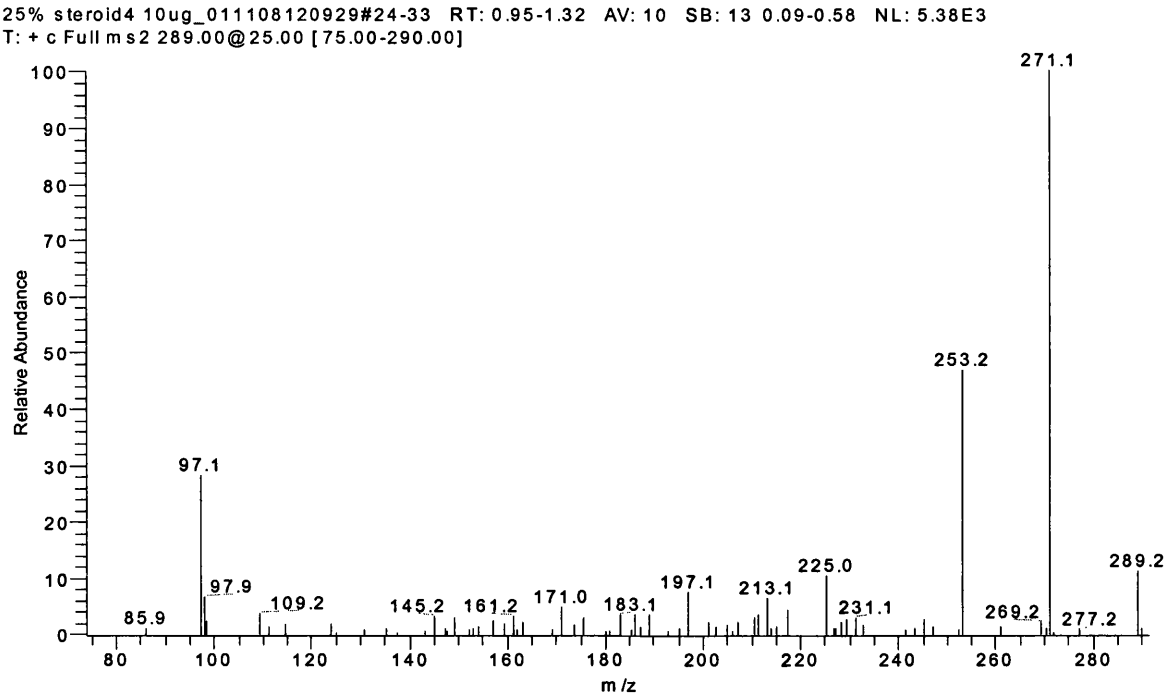

Figure 2.14.2 MS^2 of dehydroepiandrosterone from ion of m/z 271; collision energy 30%

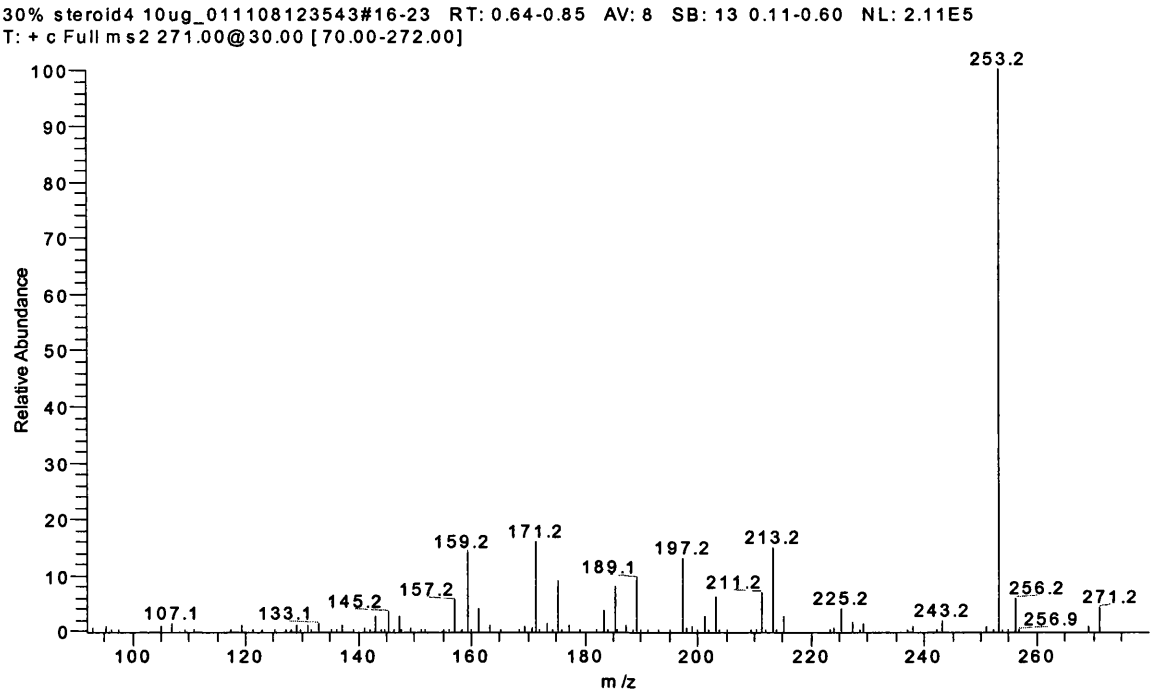

Figure 2.14.3 MS^2 of dehydroepiandrosterone from ion of m/z 253; collision energy 32%

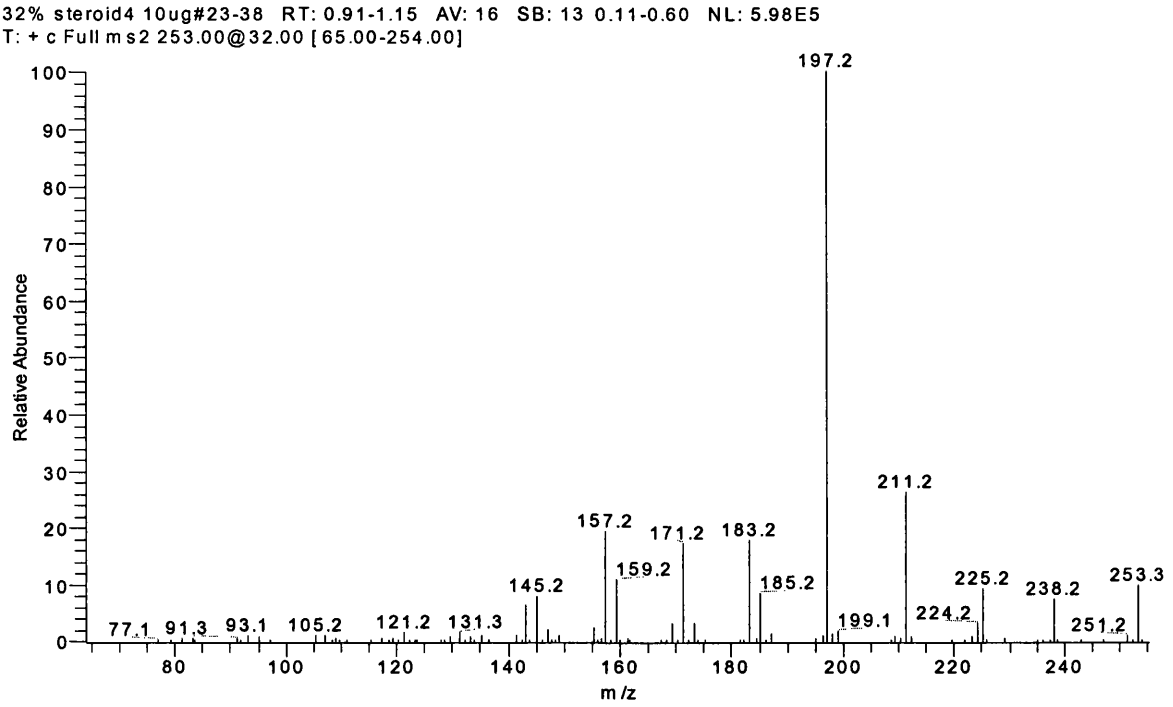

2.6.3.3 MS^2 spectra of 11-ketoandrosterone

The m/z 287, 269 and 251 ions were presented the spectrum of 11-ketoandrosterone from parent ion of m/z 305, and were assigned to loss of water involving the oxygen atoms at the position of C3, C11 and C17. Compared to adrenosterone, loss the keto-group at the position of C11 appeared to occur more readily. A fragment of m/z 247 was also present, corresponding to further loss of hydrogen. There were no fragment ions observed at m/z 97, 109 and 123 in this spectrum. The spectrum of 11-ketoandrosterone from ion of m/z 305 was shown in Figure 2.15, and other spectra from ion of m/z 287 and 269 are shown in Appendix 11-12.

Figure 2.15 MS^2 of 11-ketoandrosterone from parent ion of m/z 305; collision energy 25%

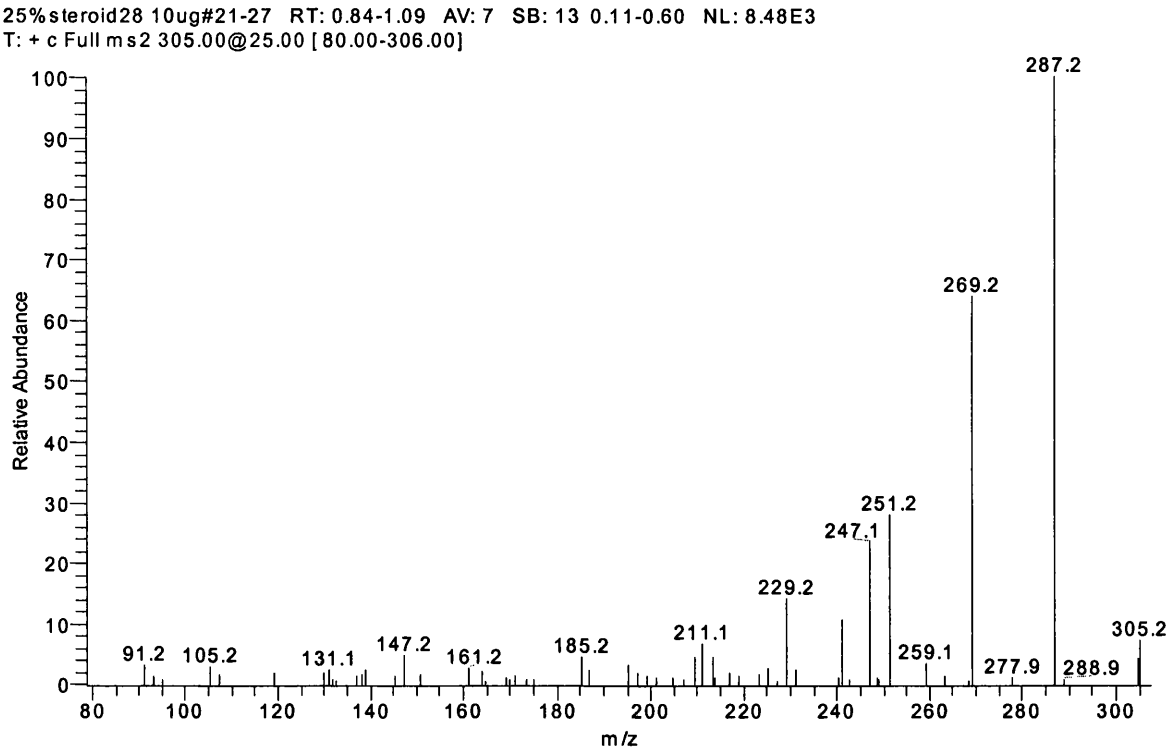

2.6.3.4 MS^2 spectrum of 11β-hydroxyandrosterone

There was no protonated molecular ion of m/z 307 observed in the MS spectrum for 11β-hydroxyandrosterone. Consequently dehydration ions of m/z 271 and 253 were observed in the spectrum from the parent ion at m/z 289. The MS^2 spectrum of 11β-hydroxyandrosterone from ion of m/z 289 was shown in Figure 2.16, and other spectra from ion of m/z 271 and 253 were present in Appendix 13-14.

Figure 2.16 MS^2 of 11β-hydroxyandrosterone from ion of m/z 289; collision energy 30%

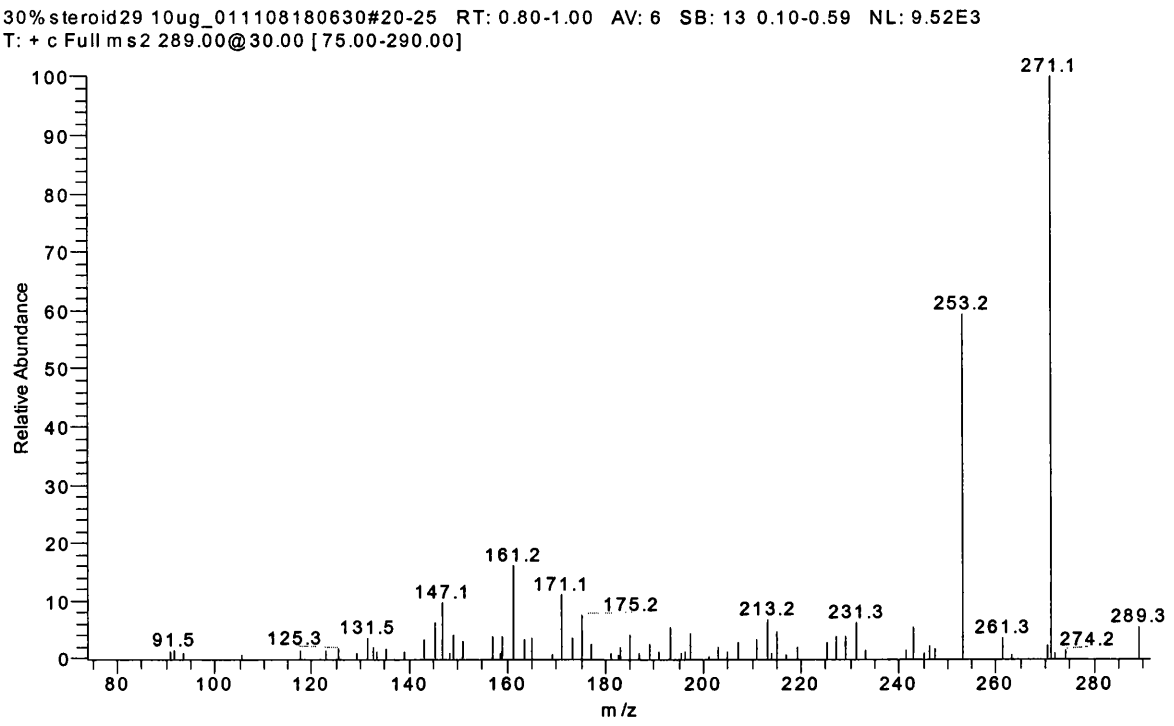

2.6.3.5 MS^2 of 5α-Androstan-3, 17-dione

There were no ions of m/z 97, 109 or 123 observed in the CID spectrum of 5α-androstane-3, 17-dione, in contrast to its biological precursor androstendione, again demonstrating the importance of the Δ_4-double bond for the formation of these ions. The MS^2 spectrum of 5α-androstan-3, 17-dione from ion of m/z 289 was shown in Figure 2.17, and other spectra from ion of m/z 271 and 253 were present in Appendix 15-16.

Figure 2.17 MS^2 of 5α-Androstan-3, 17-dione from ion of m/z 289; collision energy 25%

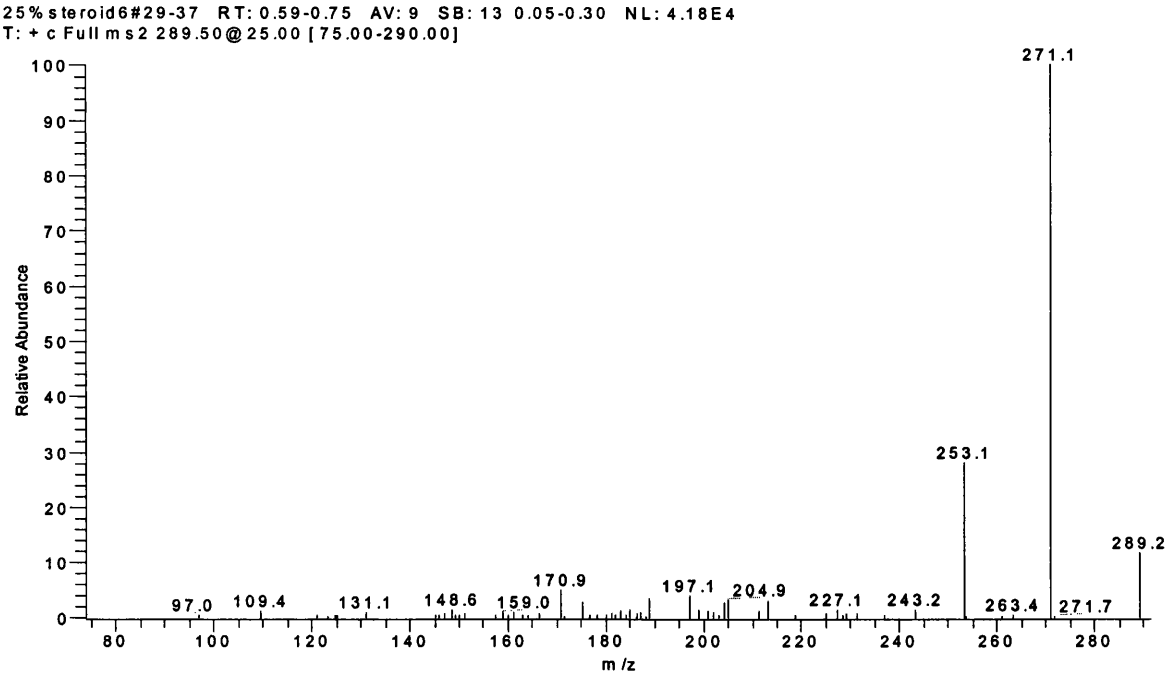

2.6.3.6 MS^2 of two diol-steroids

No CID spectra are obtained from the protonated parent ions of m/z 293 for androstanediol and of m/z 291 for Δ_5-androstene-3β, 17β-diol, but there were CID spectra from ion of m/z 257 for androstanediol, ion of m/z 273 and 255 for Δ_5-androstene-3β, 17β-diol present in Appendix 17-19.

2.7 Conclusions

Androgenic steroids were ionized with both ESI and APCI source, and two solvent systems (methanol/water and acetonitrile/water) were also studied for the effects of the two ionization methods. Solvent system of methanol/water proved better than

acetonitrile/water as a dilution and injection solvent for the ionization efficiency of both sources, therefore, methanol/water was adopted as the solvent system in the development of LC-MS on-line analysis.

Androgenic steroids were studied in both positive and negative mode, and significant spectra were obtained in positive mode for both ESI and APCI source. However, no significant ions were obtained in the negative mode using the ESI source, and only spectra of 11-ketoandrosterone and 4-ene-3-one steroids were obtained in negative mode using the APCI source. In positive mode, similar ions of $[MH]^+$, $([MH-]^+$-$H_2O)$ and $([MH]^+$-$2H_2O)$ were present in quite high abundances; $([MH]^+$-$H_2)$ and $([MH]^+$ +MeOH) were present in relative low abundances in the spectra of both ESI-MS and APCI-MS. However, sodium adduct ions $[M+Na]^+$ were observed in only ESI-MS spectra. In negative mode of APCI-MS, very abundant deprotonated molecular ion of $[M-H]^-$ was observed in the spectra of 11-ketoandrosterone and 4-ene-3-one steroids, and also ion of $([M-H]^-$-$H_2)$ or $([M-H]^-$-$H_2O)$ was presented in low abundances.

The collision induced dissociation of androgenic steroids was performed using positive APCI-MS, because the APCI source showed much better sensitivities and less chemical noise than using the ESI source. The CID spectra showed product ions formed by loss of water for all the investigated androgenic steroids, and structural specific ions of m/z 97, 109, 121 and 123 were characteristic for the 4-ene-3-one steroids and DHEA, but there were either much reduced in relative abundance or absent these ions in the CID spectra of the other steroids.

As a conclusion, positive CID of precursor ions generated by APCI provides good sensitivities and abundant diagnostic product ions and is therefore the preferred choice of

identification of androgenic steroids, as well as the possible efficient screening method in the future analysis in LC-MS.

References

1. T.M. Williams, A.J. Kind, E.Houghton, D.W. Hill, *J. Mass Spectrom.* 34 (1999) 206.
2. G.Bouchoux, D. Leblanc, O. Mo and M. Yanez, *J. Org. Chem.* 62 (1997) 8439.
3. C.H.L. Shackleton, H. Chuang, J. Kim, X. Torre and J. Segura, *Steroids* 62 (1997) 523.
4. J. Antignac, B.L. Bizec, F. Monteau, F. Poulain and F. Andre, *Rapid Commun. Mass Spectrom.* 14 (2000) 33.
5. O.Curcuruto, D. Franchi and M. Hamdan, *Rapid Commun. Mass Spectrom.*, 7 (1993) 673.
6. Z.V. Zaretskii, *Mass Spectrometry of Steroids*. Wiley, New York (1996) 28.
7. M. Honing, E.van Bockxmeer and D. Beekman, *Analusis* 28 (2000) 921.
8. Fumito Komatsu, Masaaki Morioka and Yukitoshi Fujita, *J. Mass Spectrom.* 30 (1995) 698.
9. R. Draisci, L. Palleschi, E. Ferretti, L. Lucentini and P. Cammarata, *J Chromatogr. A* 870 1-2 (2000) 54.

Chapter 3

Tandem Mass Spectrometry of Androgenic Steroid Conjugates

3.1 Introduction

Conjugated androgenic steroids mainly as glucuronides or sulfates are phase II metabolites of androgens [1]. Usually these conjugates are hydrolyzed, yielding the free androgens which are derivatized and then identified by means of gas chromatography / mass spectrometry (GC/MS) [2]. The improvements in interfacing liquid chromatography (LC) with mass spectrometry (MS) allow the direct detection of these compounds without hydrolysis [3, 4]. To help to identify and determine the steroid conjugates shown in Figure 3.1 by LC/MS, a series of studies of electrospray ionization (ESI), atmospheric pressure chemical ionization (APCI) together with tandem mass spectrometry of these compounds were described in this chapter.

3.2 Experimental

3.2.1 Materials

Testosterone glucuronide, testosterone sulfate sodium salt and androstanediol glucuronide sodium salt were purchased from Steraloids (USA). All the other steroid conjugates presented in Figure 3.1 were from Sigma-Aldrich Ltd (Poole, Dorset, UK). The standards were dissolved in methanol, and further diluted to concentrations ranging from 1-10ng/μl with methanol/water (1:1) for the experiments.

HPLC grade methanol, acetonitrile and water were purchased from Fisher Scientific (Loughborough, Leicester, UK).

Figure 3.1 Structures of the ten androgenic steroid conjugates included in the current study

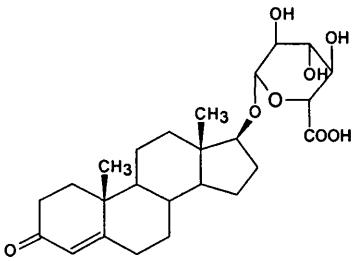

Testosterone glucuronide

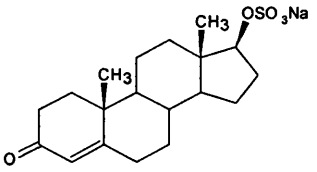

Testosterone sulfate sodium salt

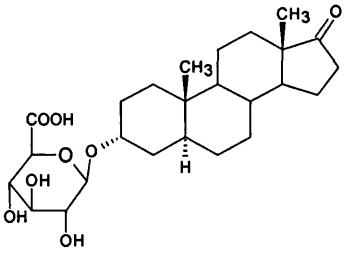

Androsterone glucuronide

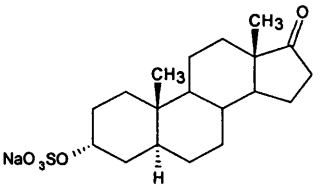

Androsterone sulfate sodium salt

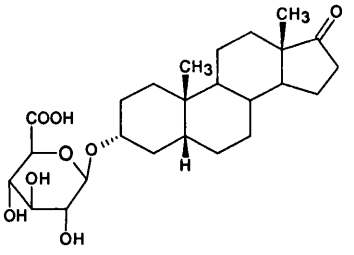

Etiocholan-3α-ol-17-one glucuronide

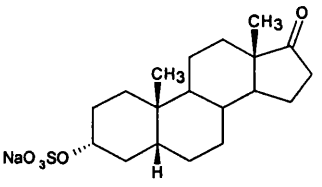

Etiocholan-3α-ol-17-one sulfate sodium salt

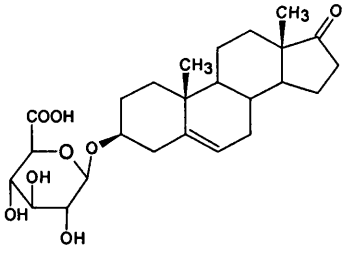

Dehydroepiandrosterone glucuronide

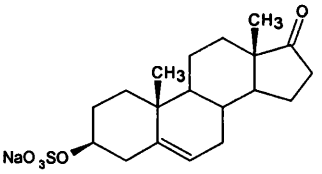

Dehydroepiandrosterone sulfate sodium salt

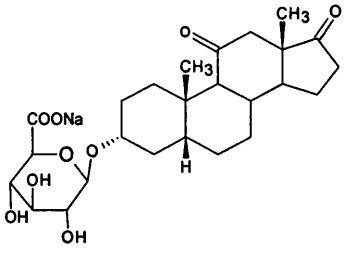

5β-Androstane-11, 17-dione-3α-ol glucuronide sodium salt

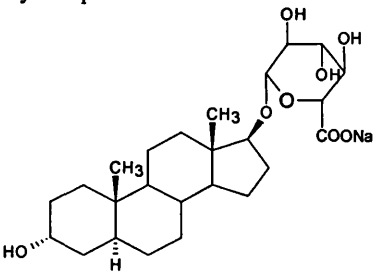

5α-Androstan-3α, 17β-diol glucuronide sodium salt

3.2.2 HPLC and mass spectrometry

The HPLC instrument and conditions were the same as those described in Chapter 2.

The same LCQ ion trap mass spectrometer (Finnigan, Hemel Hempstead, UK) was used for the experiments of steroid conjugates; the conditions for ESI-MS and APCI-MS were summarized as follow:

ESI-MS

Parameter	Positive-ion mode	Negative-ion mode
Sheath gas flow (arbitrary units)	80	70
Auxiliary gas flow (arbitrary units)	20	20
Spray voltage	4.5 kV	4.5kV
Capillary temperature	220 °C	220 °C
Capillary voltage	+20 V	-45 V
Tube lens offset	+5 V	-40 V

APCI-MS

Parameter	Positive-ion mode	Negative-ion mode
Vaporizer temperature	500°C	500°C
Sheath gas flow (arbitrary units)	70	70
Auxiliary gas flow (arbitrary units)	20	20
Discharge current	5 μA	5 μA
Capillary temperature	175°C	175°C
Capillary voltage	+12 V	-30 V
Tube lens offset	+30 V	-50 V

3.3 ESI-MS of androgenic steroid conjugates

3.3.1 ESI-MS of androgenic steroid conjugates in positive mode

The solvent system was also studied for conjugated steroids. Unlike free steroids, there was little difference in the peak intensity whether the sample was diluted in methanol/water (1:1) or acetonitrile /water (1:1), however, the mass spectra of conjugated steroids were very different when they were eluted with these two different solvent systems (Table 3.1 and 3.2). M is corresponding to the molecular weight of each compound.

3.3.1.1 ESI-MS of androgenic steroid conjugates eluted with acetonitrile/water

Peaks corresponding to the sodium ion adduct of the conjugated dimer $[2M+Na]^+$ were dominant for steroid glucuronides in the spectra of positive ESI/MS, and also consecutive sodium adducts of M, 2M or 3M were presented in the spectra of these compounds (Table 3.1). Only testosterone glucuronide was observed to yield a protonated molecule, whilst 5β-androstane-11, 17-dione-3α-ol glucuronide yield a protonated dimer $[2M+H]^+$ in the ESI/MS spectra. The ions of $[2M+Na]^+$ were dominant, and also the ions of $[3M+Na]^+$ and $[4M+Na]^+$ were observed in the spectra of steroid sulfates.

3.3.1.2 ESI-MS of androgenic steroid conjugates eluted with methanol/water

The protonated ion $[M+H]^+$ was dominant for testosterone glucuronide, 5β-Androstane-11, 17-dione-3α-ol glucuronide sodium salt and 5α-Androstan-3α, 17β-diol glucuronide sodium salt (Table 3.2), whilst the sodium adduct ion $[M+Na]^+$ was dominant for the other 3-O-conjugated steroid glucuronides, for which no $[M+H]^+$ was observed. These results were in good agreement with the earlier studies [5-8], and have been

Table 3.1 ESI-MS of steroid conjugates eluted with acetonitrile/water (1:1) m/z and relative abundances of major ions (positive mode)

Steroid conjugates	T G	T S	A G	A S	E G	E S	DHEA G	DHEA S	5β-Dione G	5α-Diol G
$[M+H]^+$	465 (10)	_	_	_	_	_	_	_	_	_
$[M+Na]^+$	_	_	_	_	489 (16)	_	_	_	525 (49)	513 (56)
$[M-H+2Na]^+$	509 (24)	_	511 (40)	_	511 (33)	_	509 (20)	_	547 (22)	535 (48)
$[M-H+2Na]^+ +H_2O$	_	454 (59)	_	456 (65)	_	456 (18)	_	454 (49)	_	553 (75)
$[M-2H+3Na]^+$	531 (19)	_	533 (27)	_	533 (15)	_	531 (21)	_	_	_
$[M-2H+3Na]^+ +H_2O$	549 (99)	_	551 (25)	_	551 (17)	_	549 (78)	_	_	_
$[M-2H+3Na]^+ +2H_2O$	_	495 (38)	_	497 (31)	_	497 (35)	_	495 (26)	_	_
$[2M+H]^+$	_	_	_	_	_	_	_	_	1005 (40)	_
$[2M+Na]^+$	_	803 (100)	_	807 (100)	_	807 (100)	_	803 (100)	1027 (100)	1003 (100)
$[2M-H+2Na]^+$	973 (30)	_	977 (100)	_	977 (100)	_	_	_	1049 (39)	1025 (40)
$[2M-H+2Na]^+ +H_2O$	_	843 (25)	_	847 (42)	_	847 (21)	_	843 (47)	_	_
$[2M-2H+3Na]^+$	995 (100)	_	999 (89)	_	999 (65)	_	995 (100)	_	_	_
$[2M-3H+4Na]^+$	1017 (33)	_	1021 (20)	_	1021 (15)	_	1017 (30)	_	_	_
$[3M+H]^+$	_	_	_	1178 (28)	_	1178 (49)	_	_	_	_
$[3M+Na]^+$	_	1193 (59)	_	1199 (33)	_	1199 (64)	_	1193 (30)	1530 (32)	1495 (24)
$[3M-2H+3Na]^+$	1461 (9)	_	1466 (28)	_	1466 (19)	_	_	_	_	_
$[3M-3H+4Na]^+$	1483 (29)	_	1488 (19)	_	1488 (20)	_	1482 (29)	_	_	_
$[4M+H]^+$	_	_	_	_	_	1570 (12)	_	_	_	_
$[4M+Na]^+$	_	1584 (24)	_	1592 (15)	_	1592 (16)	_	1584 (14)	_	_

T G, Testosterone glucuronide; T S, Testosterone sulfate sodium salt; A G, Androsterone glucuronide; A S, Androsterone sulfate sodium salt; E G, Etiocholan-3α-ol-17-one glucuronide; E S, Etiocholan-3α-ol-17-one sulfate sodium salt; DHEA G, Dehydroisoandrosterone glucuronide; DHEA S, Dehydroisoandrosterone sulfate sodium salt; 5β-Dione G, 5β-Androstane-11,17-dione-3α-ol glucuronide sodium salt; 5α-Diol G, 5α-Androstan-3α,17β-diol glucuronide sodium salt.

Table 3.2 ESI-MS of steroid conjugates eluted with methanol/water (1:1) m/z and relative abundances of major ions (positive mode)

Steroid conjugates	T G	T S	A G	A S	E G	E S	DHEA G	DHEA S	5β-Dione G	5α-Diol G
$[M+H-Glu]^+$	289 (12)	_	_	_	_	_	_	_	_	_
$[M+H-Glu-H_2O]^+$	_	_	273 (20)	_	273 (17)	_	271 (18)	_	287 (49)	275 (<5)
$[M+H-Glu-2H_2O]^+$	_	_	255 (18)	_	255 (18)	_	253 (8)	_	269 (5)	257 (14)
$[M+2H-Na]^+$	_	369 (78)	_	_	_	_	_	_	_	_
$[M+H-SO_3]^+$	_	311 (12)	_	313.6 (22)	_	313 (26)	_	_	_	_
$[M+H-SO_3-Na-H_2O]^+$		_	_	_	_	273 (5)	_	271 (12)	_	_
$[M+H-SO_3-Na-2H_2O]^+$		_	_	_	_	255 (11)	_	253 (16)	_	_
$[M+H]^+$	465 (100)	_	_	_	_	_	_	_	503 (100)	491 (100)
$[M+Na]^+$	487 (63)	413 (53)	489 (100)	415 (54)	489 (100)	415 (26)	487 (100)	413 (50)	525 (26)	513 (28)
$[M-H+2Na]^+$	509 (14)	_	511 (15)	_	511 (11)	_	509 (8)	_	_	535 (8)
$[M-2H+2Na+H_2O]^+$	_	_	_	_	_	_	_	_	_	553 (25)
$[M-2H+3Na+H_2O]^+$	549 (14)	_	551 (13)	_	_	_	549 (27)	_	_	_
$[2M+H-SO_3]^+$	_	701 (40)	_	705 (33)	_	705 (26)	_	701 (14)	_	_
$[2M+2H-Na]^+$	_	_	_	_	_	_	_	_	983 (34)	959 (34)
$[2M+H]^+$	929 (10)	781 (100)	_	785 (58)	_	785 (23)	_	781 (8)	1005 (28)	981 (14)
$[2M+Na]^+$	951 (13)	803 (84)	955 (64)	807 (100)	955 (49)	807 (100)	951 (21)	803 (100)	1027 (14)	1003 (11)
$[2M-H+2Na]^+$	973 (16)	_	977 (28)	_	977 (29)	_	973 (13)	_	_	_
$[2M-2H+3Na]^+$	995 (7)	_	999 (13)	_	999 (15)	_	995 (19)	_	_	_
$[3M+H]^+$	_	_	_	1178 (14)	_	1178 (34)	_	1172 (6)	_	_
$[3M+Na]^+$	_	1193 (12)	_	1199 (9)	_	1199 (47)	_	1193 (9)	_	_

T G, Testosterone glucuronide; T S, Testosterone sulfate sodium salt; A G, Androsterone glucuronide; A S, Androsterone sulfate sodium salt; E G, Etiocholan-3α-ol-17-one glucuronide; E S, Etiocholan-3α-ol-17-one sulfate sodium salt; DHEA G, Dehydroisoandrosterone glucuronide; DHEA S, Dehydroisoandrosterone sulfate sodium salt; 5β-Dione G, 5β-Androstane-11,17-dione-3α-ol glucuronide sodium salt; 5α-Diol G, 5α-Androstan-3α,17β-diol glucuronide sodium salt.

explained by Harrison [9] in terms of the differences in proton affinities: proton affinity of the 4-ene-3-one in the steroid ring structure is significantly higher than that of a hydroxy or carbonyl group not in conjugation with a double bond.

There were also ions containing dimers observed for steroid glucuronides. Fragmentation of steroid glucuronides by loss of the glucuronide moiety and further loss of water were observed. The ion corresponding to $[2M+Na]^+$ was dominant for most steroid sulfates but for testosterone sulfate spectrum, which was dominant by the ion corresponding to $[2M+H]^+$. Quite intensive peaks of $[M+Na]^+$ and $[3M+Na]^+$ were also observed for steroid sulfates, similar to steroid glucuronides; ions corresponding to fragmentation of steroid sulfates involving loss of the sulfate moiety or further loss of water were also present in the ESI/MS spectra.

3.3.1.3 Comparison of the sensitivities obtained using the two eluting solvent systems

The most abundant peak in the spectra of each steroid conjugate using acetonitrile/water and methanol/water as HPLC eluting solvent was compared by its absolute intensity of the most abundant peak in the spectrum of each compound (Figure 3.2). When methanol/water was used, peak intensity was about 2 to 4 times higher than that using acetonitrile/water.

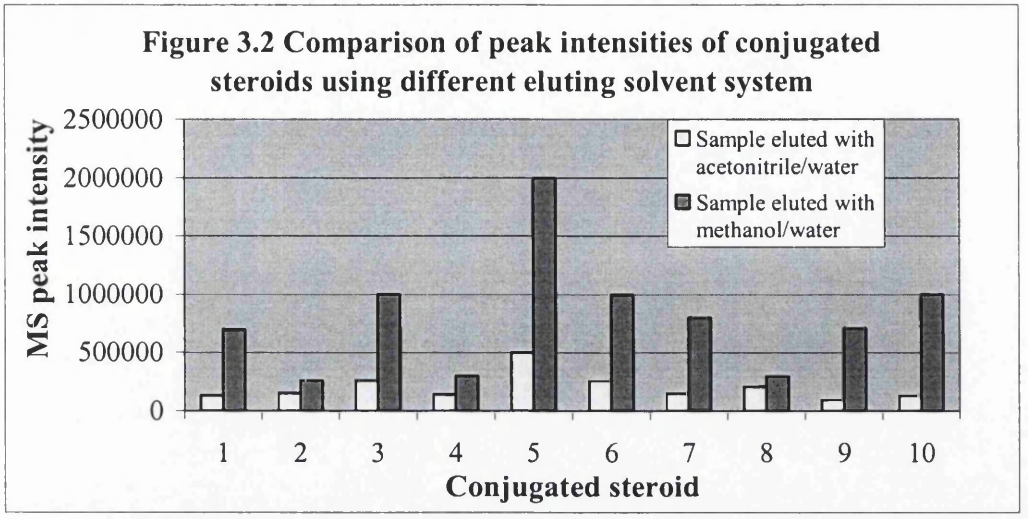

* Concentration of each sample was 10 ng/μl.

1. Testosterone glucuronide (m/z 995, 465) 2. Testosterone sulfate (m/z 803, 781)
2. Androsterone glucuronide (m/z 977, 489) 4. Androsterone sulfate (m/z 807, 807)
5. Etiocholan-3α-ol-17-one glucuronide (m/z 977, 489) 6. Etiocholan-3α-ol-17-one sulfate (m/z 807, 807) 7. DHEA glucuronide (m/z 995, 487) 8. DHEA sulfate (m/z 803, 803)
9. 5β-Androstane-11,17-dione-3α-ol glucuronide (m/z 1027, 503)
10. 5α-Androstan-3α,17β-diol glucuronide (m/z 1003, 491)

3.3.2 ESI-MS of androgenic steroid conjugates in negative mode

The effect of the solvent system on ESI-MS was also studied in negative mode, but unlike positive mode, there were much smaller differences between the resulting spectra for the acetonitrile/water and methanol/water systems in negative mode (Table 3.3 and 3.4).

3.3.2.1 ESI-MS of androgenic steroid conjugates eluted with acetonitrile/water

For the negative ESI-MS spectra using acetonitrile/water elution (Table 3.3), $[M-H]^-$ was dominant for most of steroid glucuronides except 5β-androstane-11, 17-dione-

3α-ol glucuronide sodium salt and 5α-androstan-3α, 17β-diol glucuronide sodium salt, which were dominanted by $[M-Na]^-$. There was also a series of sodium adduct peaks formed by consecutive addition of sodium to dimers and trimers of steroid glucuronides in low intensities. Compared to the spectra of steroid glucuronides, the spectra of steroid sulfates were quite simple, as only ions of $[M-Na]^-$ and $[2M-Na]^-$ were observed.

3.3.2.2 ESI-MS of androgenic steroid conjugates eluted with methanol/water

Similar spectra were observed in negative ion mode for the steroid conjugates eluted with methanol/water. The deprotonated molecule of $[M-H]^-$ was the base peak for testosterone glucuronide, androsterone glucuronide and etiocholan-3α-ol-17-one glucuronide; whereas, the de-sodiated ion $[M-Na]^-$, was dominant for the 5β-androstane-11, 17-dione-3α-ol glucuronide sodium salt, 5α-androstan-3α, 17β-diol glucuronide sodium salt and the steroid conjugate sulfates. It seemed that the methanol/water solvent system inhibits the formation of the dimers or trimers, because only relative low abundance ions corresponding to $[2M-Na]^-$ or $[2M-2H+Na]^-$ were observed in their spectra. The major ions and their abundance were present in Table 3.4.

3.3.2.3 Comparison of sensitivities obtained using the two eluting solvent system

The same base peak either $[M-H]^-$ or $[M-Na]^-$, was chosen for the comparison between the above solvent systems, due to the very similar spectra of the androgenic steroid conjugates using both solvents. Unlike positive mode, the sensitivities of these steroids were not greatly affected by the different solvent systems. There were however

Table 3.3 ESI-MS of steroid conjugates m/z and relative abundances of major ions eluted with acetonitrile/water (negative mode)

Ion	T G	T S	A G	A S	E G	E S	DHEA G	DHEA S	5β-Dione G	5α-Diol G
$[M-Na-]^-$ Glu	–	–	–	–	–	–	–	–	303 (10)	–
$[M-H]^-$	463 (100)	–	465 (100)	–	465 (100)	–	463 (100)	–	501 (19)	–
$[M-H]^-+H_2O$	–	–	–	–	–	–	–	–	–	507 (20)
$[M-2H+Na]+H_2O$	–	–	–	–	–	–	–	–	–	529 (9)
$[M-Na]^-$	–	367 (100)	–	369 (100)	–	369 (100)	–	367 (100)	479 (100)	467 (100)
$[2M-H]^-$	–	–	–	–	–	–	–	–	1003 (13)	–
$[2M-Na]^-$	–	757 (5)	–	761 (16)	–	761 (23)	–	757 (5)	981 (49)	957 (37)
$[2M-2H+Na]^-$	949 (43)	–	953 (58)	–	953 (86)	–	949 (5)	–	1025 (11)	979 (16)
$[2M-3H+2Na]^-$	971 (12)	–	975 (16)	–	975 (11)	–	971 (24)	–	1047 (8)	1001 (9)
$[2M-4H+3Na]^-$	993 (13)	–	997 (14)	–	997 (7)	–	993 (15)	–	–	1023 (<5)
$[2M-5H+4Na]^-$	1015 (7)	–	1019 (7)	–	1019 (<5)	–	1015 (10)	–	–	–
$[3M-H]^-$	–	–	–	–	–	–	–	–	1506 (6)	–
$[3M-Na]^-$	–	–	–	–	–	1154 (8)	–	–	1484 (15)	1448 (10)
$[3M-2H+Na]^-$	–	–	–	–	–	–	–	–	1528 (5)	1470 (<5)
$[3M-3H+2Na]^-$	1436 (19)	–	1442 (20)	–	1442 (28)	–	1436 (13)	–	–	1492 (<5)
$[3M-4H+3Na]^-$	1458 (8)	–	1464 (5)	–	1464 (9)	–	1458 (8)	–	–	–
$[3M-5H+4Na]^-$	1480 (5)	–	1486 (6)	–	1486 (<5)	–	1480 (6)	–	–	–

T G, Testosterone glucuronide; T S, Testosterone sulfate sodium salt; A G, Androsterone glucuronide; A S, Androsterone sulfate sodium salt; E G, Etiocholan-3α-ol-17-one glucuronide; E S, Etiocholan-3α-ol-17-one sulfate sodium salt; DHEA G, Dehydroisoandrosterone glucuronide; DHEA S, Dehydroisoandrosterone sulfate sodium salt; 5β-Dione G, 5β-Androstane-11, 17-dione-3α-ol glucuronide sodium salt; 5α-Diol G, 5α-Androstan-3α, 17β-diol glucuronide sodium salt

Table 3.4 ESI-MS of steroid conjugates' m/z and relative abundances of major ions eluted with methanol/water (negative mode)

Ion	T G	T S	A G	A S	E G	E S	DHEA G	DHEA S	5β-Dione G	5α-Diol G
$[M-H]^-$	463 (100)	_	465 (100)	_	465 (100)	_	463 (100)	_	501 (4)	_
$[M-H]^- + H_2O$	_	_	_	_	_	_	_	_	_	_
$[M-2H+Na]^- + H_2O$	_	_	_	_	_	_	_	_	_	_
$[M-Na]^-$	_	367 (100)	_	369 (100)	_	369 (100)	_	367 (100)	479 (100)	467 (100)
$[2M-H]^-$	_	_	_	_	931 (8)	_	_	_	_	_
$[2M-Na]^-$	_	757 (3)	_	761 (14)	_	761 (28)	_	757 (11)	981 (39)	957 (11)
$[2M-2H+Na]^-$	949 (10)	_	953 (27)	_	953 (47)	_	949 (16)	_	_	_
$[3M-Na]^-$	_	_	_	_	_	1154 (4)	_	_	_	_
$[3M-2H+Na]^-$	_	_	_	_	_	_	_	_	_	_
$[3M-3H+2Na]^-$	_	_	_	_	1442 (6)	_	1436 (4)	_	_	_

T G, Testosterone glucuronide; T S, Testosterone sulfate sodium salt; A G, Androsterone glucuronide; A S, Androsterone sulfate sodium salt; E G, Etiocholan-3α-ol-17-one glucuronide; E S, Etiocholan-3α-ol-17-one sulfate sodium salt; DHEA G, Dehydroisoandrosterone glucuronide; DHEA S, Dehydroisoandrosterone sulfate sodium salt; 5β-Dione G, 5β-Androstane-11, 17-dione-3α-ol glucuronide sodium salt; 5α-Diol G, 5α-Androstan-3α, 17β-diol glucuronide sodium salt

slightly higher intensities consequent on elution with methanol/water compared with acetonitrile/water for most of steroid conjugates (Figure 3.3).

Figure 3.3 Comparison of the peak intensities of androgenic streroid conjugates using different eluted solvents

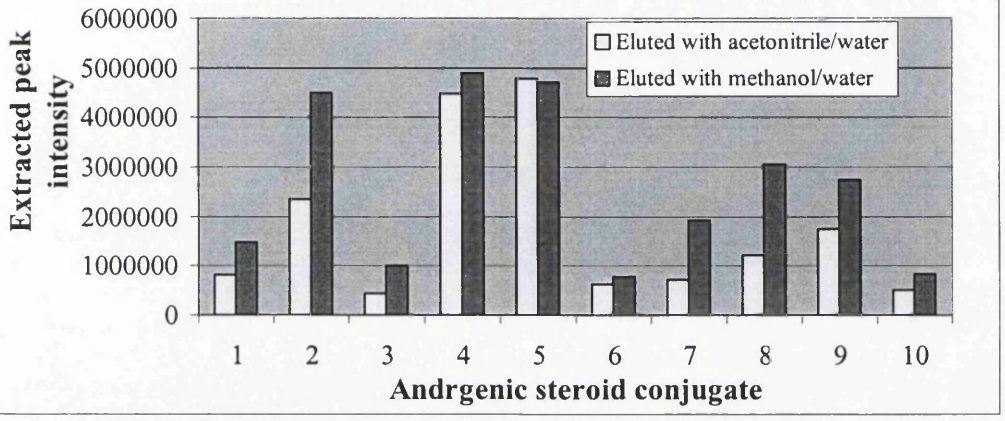

* Concentration of each sample was 10ng/μl.

1.Testosterone glucuronide (m/z 463) 2. Testosterone sulfate (m/z 367) 3.Androsterone glucuronide (m/z 465) 4. Androsterone sulfate (m/z 369) 5. Etiocholan-3α-ol-17-one glucuronide (m/z 465) 6. Etiocholan-3α-ol-17-one sulfate (m/z 369) 7. DHEA glucuronide (m/z 463) 8. DHEA sulfate (m/z 367) 9. 5β-Androstane-11,17-dione-3α-ol glucuronid (m/z 479) 10. 5α-Androstan-3α,17β-diol glucuronide (m/z 467).

3.3.3 Comparison of sensitivity between positive and negative mode

For the steroid sulfates, peak intensities were apparently higher in negative mode than in positive mode, but similar intensities in the spectra of steroid glucuronides were observed in positive mode and negative mode. The spectra in negative mode were quite simple, and this may benefit the quantitative analysis, however, the spectra in positive mode gave more structural information and would benefit the compound identification.

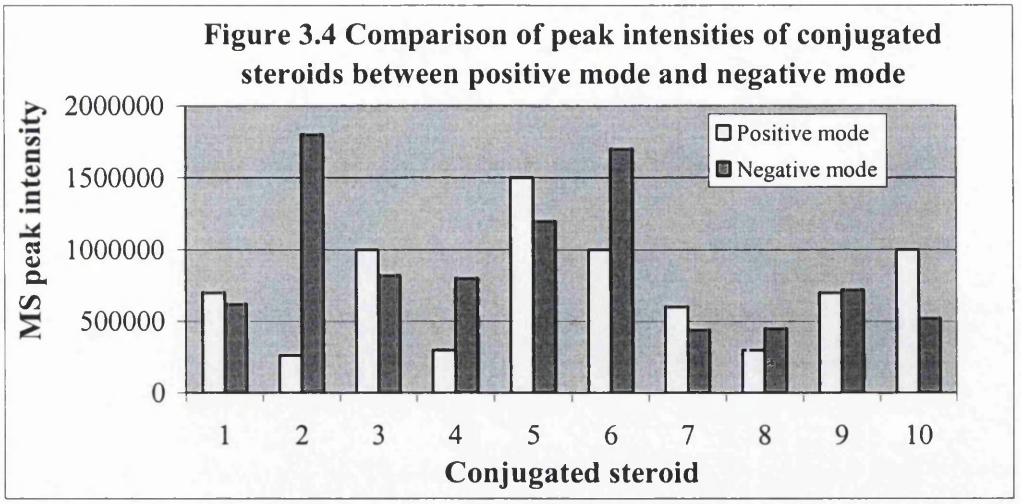

Concentration of each sample was 10ng/μl.

1. Testosterone glucuronide (m/z 489, 463) 2. Testosterone sulfate (m/z 781, 367) 3.Androsterone glucuronide (m/z 489, 465) 4. Androsterone sulfate (m/z 807, 369) 5. Etiocholan-3α-ol-17-one glucuronide (m/z 489, 465) 6. Etiocholan-3α-ol-17-one sulfate (m/z 807, 369) 7. DHEA glucuronide (m/z 487, 463) 8. DHEA sulfate (m/z 803, 367) 9. 5β-Androstane-11,17-dione-3α-ol glucuronide (m/z 503, 479) 10. 5α-Androstan-3α,17β-diol glucuronide (m/z 491, 467).

3.4 APCI-MS of androgenic steroid conjugates

3.4.1 APCI-MS spectra in positive mode

3.4.1.1 APCI-MS of androgenic steroid conjugates eluted with acetonitrile/water

Unlike ESI-MS spectra of androgenic steroid conjugates, there was no protonated molecule $[MH]^+$ or sodium adduct $[M+Na]^+$ observed in the APCI-MS spectra except testosterone glucuronide, for which the protonated molecule $[MH]^+$ was observed in a very low abundance. For steroid glucuronides, the most abundant ion either

corresponding to ($[MH]^+$-Glu) or ($[MH]^+$-Glu-H_2O) was present in the spectra by loss of their glucuronide moiety or further loss of water from their protonated molecules. In the case of steroid sulfates, peak corresponding to ($[MH\text{-}Na]^+$-SO_3-H_2O) or ($[MH\text{-}Na]^+$-SO_3-H_2O) was dominant in the spectra. Similar to the ESI-MS spectra, there were still some dimerions observed in the spectra of several of the conjugates eluted with acetoniltrile/water. The major ions and the abundances were present in Table 3.5.

3.4.1.2 APCI-MS of androgenic steroid conjugates eluted with methanol/water

APCI-MS spectra (Table 3.6) of conjugated steroids eluted with methanol/water were very similar to the spectra of their free steroids. It seemed that the conjugated steroids readily lost their glucuronide or sulfate moieties in the APCI source under the conditions. The similar spectra were also observed by the research group of Kuuranne [8] for testosterone glucuronide and epitestosterone glucuronide. Moreover, they observed the protonated ion of $[MH]^+$ for these two compounds, but we did not observe this ion in our spectra. Most significant difference between the spectra of steroid glucuronides and steroid sulfates is that the fragmentations of steroid glucuronides corresponding to loss of the glucuronide moiety ($[MH]^+$-Glu) were observed in the former spectra, but no fragmentations of steroid sulfates corresponding to loss of sulfate moiety ($[MH]^+$-Sulf) were observed in the latter spectra.

Table 3.5 APCI-MS of steroid conjugates eluted with acetonitrile/water (1:1) m/z and relative abundances of major ions (positive mode)

Ion	T G	T S	A G	A S	E G	E S	DHEA G	DHEA S	5β-Dione G	5α-Diol
$[MH]^+$	465 (5)	_	_	_	_	_	_	_	_	_
$[M+Na]^+$	479 (11)	_	_	_	_	_	_	_	_	513 (23)
$[M+2Na-H]^+$	_	_	_	_	_	_	509 (6)	_	_	_
$[MH]^+$ -Glu	289 (100)	_	291 (25)	_	291 (9)	_	289 (21)	_	287 (100)	_
$[MH]^+$ -Glu-H_2	287 (64)	_	289 (<5)	_	_	_	287 (7)	_	285 (28)	291 (27)
$[MH]^+$ -Glu-$2H_2$	285 (28)	_	287 (15)	_	_	_	285 (25)	_	283 (11)	289 (14)
$[MH]^+$ -Glu-H_2O	271 (47)	_	273 (100)	_	273 (100)	_	271 (100)	_	269 (23)	_
$[MH]^+$ -Glu-H_2O- H_2	269 (24)	_	271 (7)	_	_	_	_	_	267 (14)	273 (42)
$[MH]^+$ -Glu-H_2O- $2H_2$	267 (6)	_	_	_	_	_	_	_	265 (8)	271 (8)
$[MH]^+$ -Glu-$2H_2O$	253 (6)	_	255 (59)	_	255 (60)	_	253 (52)	_	_	257 (100)
$[MH]^+$ -Glu-$2H_2O$- H_2	_	_	_	_	_	_	_	_	_	255 (37)
$[MH-Na]^+$ -SO_3	_	289 (6)	_	_	_	_	_	_	_	_
$[MH -Na]^+$ -SO_3- H_2O	_	271 (100)	_	273 (94)	_	273 (100)	_	271 (100)	_	_
$[MH-Na]^+$ -SO_3- H_2O- H_2	_	269 (42)	_	_	_	_	_	_	_	_
$[MH-Na]^+$ SO_3- H_2O-2 H_2	_	267 (8)	_	_	_	_	_	_	_	_
$[MH -Na]^+$ -SO_3- $2H_2O$	_	_	_	255 (100)	_	255 (87)	_	253 (76)	_	_
$[2M+Na]^+$	_	_	_	807 (5)	_	_	_	_	1027 (9)	1004 (32)
$[2M+3Na]^+$ -H_2	995 (4)	_	999 (5)	_	999 (5)	_	995 (11)	_	_	_

T G, Testosterone glucuronide; T S, Testosterone sulfate sodium salt; A G, Androsterone glucuronide; A S, Androsterone sulfate sodium salt; E G, Etiocholan-3α-ol-17-one glucuronide; E S, Etiocholan-3α-ol-17-one sulfate sodium salt; DHEA G, Dehydroisoandrosterone glucuronide; DHEA S, Dehydroisoandrosterone sulfate sodium salt; 5β-Dione G, 5β-Androstane-11,17-dione-3α-ol glucuronide sodium salt; 5α-Diol G, 5α-Androstan-3α,17β-diol glucuronide sodium salt.

Table 3.6 APCI-MS of steroid conjugates eluted with methanol/water (1:1) m/z and relative abundances of major ions (positive mode)

Ion	T G	T S	A G	A S	E G	E S	DHEA G	DHEA S	5β-Dione G	5α-Diol
$[MH]^+$ -Glu	289 (99)	_	291 (20)	_	291 (8)	_	289 (15)	_	287 (100)	293 (<5)
$[MH]^+$ -Glu-H_2	287 (79)	_	289 (<5)	_	289 (18)	_	287 (28)	_	285 (25)	291 (14)
$[MH]^+$ -Glu-$2H_2$	285 (62)	_	287 (7)	_	287 (7)	_	285 (62)	_	283 (10)	289 (9)
$[MH]^+$ -Glu-H_2O	271 (100)	_	273 (100)	_	273 (100)	_	271 (100)	_	269 (31)	275 (10)
$[MH]^+$ -Glu-H_2O- H_2	_	_	_	_	_	_	_	_	267 (21)	273 (60)
$[MH]^+$ -Glu-H_2O- $2H_2$	_	_	_	_	_	_	_	_	265 (17)	271 (8)
$[MH]^+$ -Glu-$2H_2O$	253 (6)	_	255 (51)	_	255 (46)	_	253 (38)	_	_	257 (100)
$[MH]^+$ -Glu-$2H_2O$- H_2	_	_	_	_	_	_	_	_	_	255 (25)
$[MH]^+$ -Glu-$2H_2O$- $2H_2$	_	_	_	_	_	_	_	_	_	253 (<5)
$[MH-Na]^+$ -SO_3- H_2O	_	271 (100)	_	273 (100)	_	273 (100)	_	271 (100)	_	_
$[MH-Na]^+$ -SO_3- H_2O- H_2	_	269 (27)	_	_	_	_	_	_	_	_
$[MH-Na]^+$-SO_3- H_2O- $2H_2$	_	267 (5)	_	_	_	_	_	_	_	_
$[MH-Na]^+$ -SO_3- $2H_2O$	_	_	_	255 (83)	_	255 (74)	_	253 (61)	_	_

T G, Testosterone glucuronide; T S, Testosterone sulfate sodium salt; A G, Androsterone glucuronide; A S, Androsterone sulfate sodium salt; E G, Etiocholan-3α-ol-17-one glucuronide; E S, Etiocholan-3α-ol-17-one sulfate sodium salt; DHEA G, Dehydroisoandrosterone glucuronide; DHEA S, Dehydroisoandrosterone sulfate sodium salt; 5β-Dione G, 5β-Androstane-11,17-dione-3α-ol glucuronide sodium salt; 5α-Diol G, 5α-Androstan-3α,17β-diol glucuronide sodium salt.

3.4.2 APCI-MS of androgenic steroid conjugates in negative mode

Negative mode APCI was also studied using both two solvent systems (Table 3.7 and 3.8), and very similar spectra between each other were obtained. In the spectra eluted with methanol/water, ions of $[M-Na]^-$ were dominant for steroid sulfates and 5β-Androstane-11, 17-dione-3α-ol glucuronide, and ions of $[M-H]^-$ were dominant for the other steroid glucuronides. In contrast in the spectra of acetonitrile/water eluted conjugates, deprotonated molecular ions of $[M-H]^-$ or de-sodiated ions of $[M-Na]^-$ were dominant most of investigated steroid conjugates, and very abundant ions of $[2M-2H+Na]^-$ or $[2M-Na]^-$ were also observed. Compared with the two solvent systems, it was easier to get the multi-conjugates when the investigated steroids were injected with acetonitrile/water.

3.4.3 Sensitivities of androgenic steroid conjugate by APCI-MS

The polarity of the analyte increases when the free steroid is conjugated with a glucuronide or sulfate moiety, the sensitivity should be better by ESI-MS than by APCI-MS, as the ESI source is designed for more polar compounds. This was found to be the case in these experiments. The peak intensities in the ESI-MS spectra were more than thirty times higher than those in the APCI-MS spectra for steroid glucuronides in the negative mode, and more than a hundred times higher for steroid sulfates. The comparison of the sensitivities by ESI-MS and APCI-MS in negative mode is presented in Figure 3.5.

Table 3.7 APCI-MS of steroid conjugates' m/z and relative abundances of major ions eluted with methanol/water (negative mode)

Ion	TG	T S	A G	A S	E G	E S	DHEA G	DHEA S	5β-Dione G	5α-Diol G
$[M-H]^-$	463 (100)	_	465 (100)	_	465 (100)	_	463 (100)	_	_	_
$[M-Na]^-$	_	367 (100)	_	369 (100)	_	369 (100)	_	367 (100)	479 (100)	467 (100)
$[2M-H]^-$	_	_	_	_	_	_	927 (11)	_	_	935 (24)
$[2M-Na]^-$	_	757 (25)	_	761 (15)	_	_	_	757 (<5)	981 (8)	_
$[2M-2H+Na]^-$	_	_	_	_	_	_	949 (10)	_	_	_

Table 3.8 APCI-MS of steroid conjugates' m/z and relative abundances of major ions eluted with acetonitrile/water (negative mode)

Ion	T G	T S	A G	A S	E G	E S	DHEA G	DHEA S	5β-Dione G	5α-Diol G
$[M-H]^-$	463 (100)	_	465 (77)	_	465 (100)	_	463 (100)	_	_	_
$[M-Na]^-$	_	367 (100)	_	369 (100)	_	369 (57)	_	367 (100)	479 (99)	467 (100)
$[2M-H]^-$	927 (48)	_	931 (43)	_	931 (17)	_	927 (65)	_	_	_
$[2M-Na]^-$	_	757 (5)	_	761 (90)	_	761 (100)	_	757 (83)	981 (100)	958 (31)
$[2M-2H+Na]^-$	949 (66)	_	953 (100)	_	953 (93)	_	949 (43)	_	_	_
$[3M-H]^-$	_	_	_	_	_	_	_	_	_	_
$[3M-Na]^-$	_	1148 (13)	_	1154 (64)	_	1154 (76)	_	1148 (80)	1484 (11)	1448 (46)
$[3M-3H+2Na]^-$	_	_	1442 (37)	_	1442 (40)	_	1436 (21)	_	_	_
$[4M-Na]^-$	_	1538 (13)	_	1546 (66)	_	1546 (76)	_	1538 (94)	_	_

T G, Testosterone glucuronide; T S, Testosterone sulfate sodium salt; A G, Androsterone glucuronide; A S, Androsterone sulfate sodium salt; E G, Etiocholan-3α-ol-17-one glucuronide; E S, Etiocholan-3α-ol-17-one sulfate sodium salt; DHEA G, Dehydroisoandrosterone glucuronide; DHEA S, Dehydroisoandrosterone sulfate sodium salt; 5β-Dione G, 5β-Androstane-11,17-dione-3α-ol glucuronide sodium salt; 5α-Diol G, 5α-Androstan-3α,17β-diol glucuronide sodium salt.

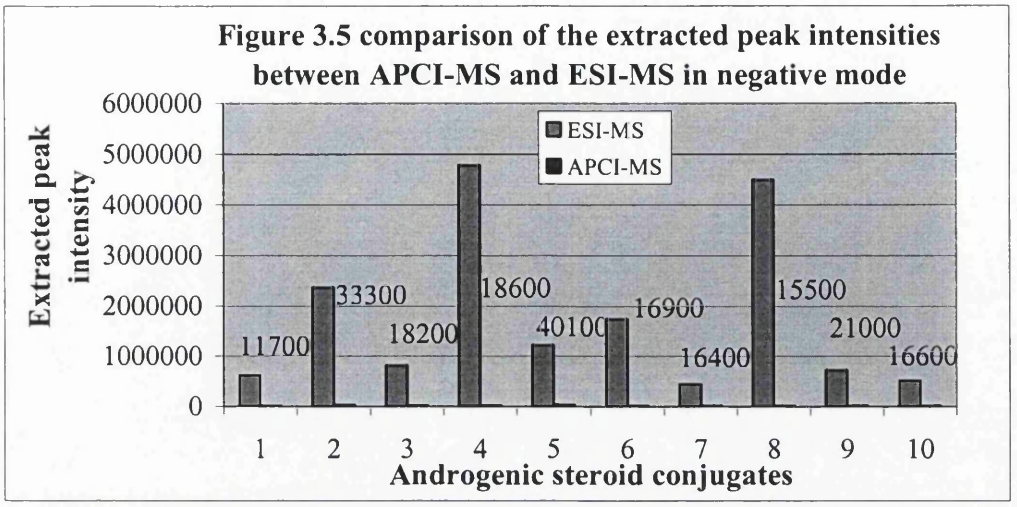

Note: Samples (10ng/μl) were injected with acetonitrile/water. The labeled value is for APCI-MS.

1. Testosterone glucuronide (m/z 463) 2. Testosterone sulfate (m/z 367) 3. Androsterone glucuronide (m/z 465) 4. Androsterone sulfate (m/z 369) 5. Etiocholan-3α-ol-17-one glucuronide (m/z 465) 6. Etiocholan-3α-ol-17-one sulfate (m/z 369) 7. DHEA glucuronide (m/z 463) 8. DHEA sulfate (m/z 367) 9. 5β-Androstane-11,17-dione-3α-ol glucuronide (m/z 479) 10. 5α-Androstan-3α,17β-diol glucuronide (m/z 467).

3.5 Collision induced dissociation of steroid conjugates by ESI-MS

The ESI source was chosen for collision induced dissociation (CID) studies for the androgenic steroid conjugates due to its good sensitivity.

3.5.1 CID of steroid conjugates in positive mode

The CID spectra of the selected androgenic steroid conjugates were studied using both acetonitrile/water and methanol/water as delivered solvent for loop injection.

3.5.1.1 Injected with acetonitrile/water

Many abundant ions were studied for generation of MS^2 spectra, such as $[M-H+2Na]^+$, $[M-2H+3Na]^+$, ($[M-2H+3Na]^+ + H_2O$), $[2M-H+2Na]^+$ and $[2M-2H+3Na]^+$. However, significant CID spectra were obtained only from the parent ions $[M-H+2Na]^+$ and $[2M-2H+3Na]^+$ for steroid glucuronides. No significant CID spectra were obtained for steroid sulfates in the positive mode.

CID spectra from parent ion of $[2M-2H+3Na]^+$

Fragment ions of m/z 509, 531 and 549 were present in the CID spectra of testosterone glucuronide and DHEA glucuronide from parent ion $[2M-2H+3Na]^+$ (m/z 995), which corresponded to loss of [M-H+Na], M and $[M-H_2O]$. Fragment ions of m/z 511, 551 and 981were observed in the CID spectra of androsterone glucuronide and etiocholan-3α-ol-17-one glucuronide, corresponding to loss of [M-H+Na], $[M-H_2O]$ and H_2O. Fragment ion of m/z 525 were observed in the spectrum of 5β-androstane-11, 17-dione-3α-ol glucuronide, corresponding to loss of M. For the CID spectrum of 5α-androstan-3α, 17β-diol glucuronide, m/z 513, 553 and 985 were present in corresponding to loss of M, $[M-H_2O-Na+H]$ and H_2O. The CID spectra from ion of $[2M-2H+3Na]^+$ were shown in Figure 3.6.1-4 for testosterone, androsterone, 5β-androstane-11, 17-dione-3α-ol, and 5α-androstan-3α, 17β-diol glucuronide; Appendix 20-21 for DHEA and etiocholan-3α-ol-17-one glucuronide.

Figure 3.6.1 CID of testosterone glucuronide from ion of m/z 995; collision energy 31%

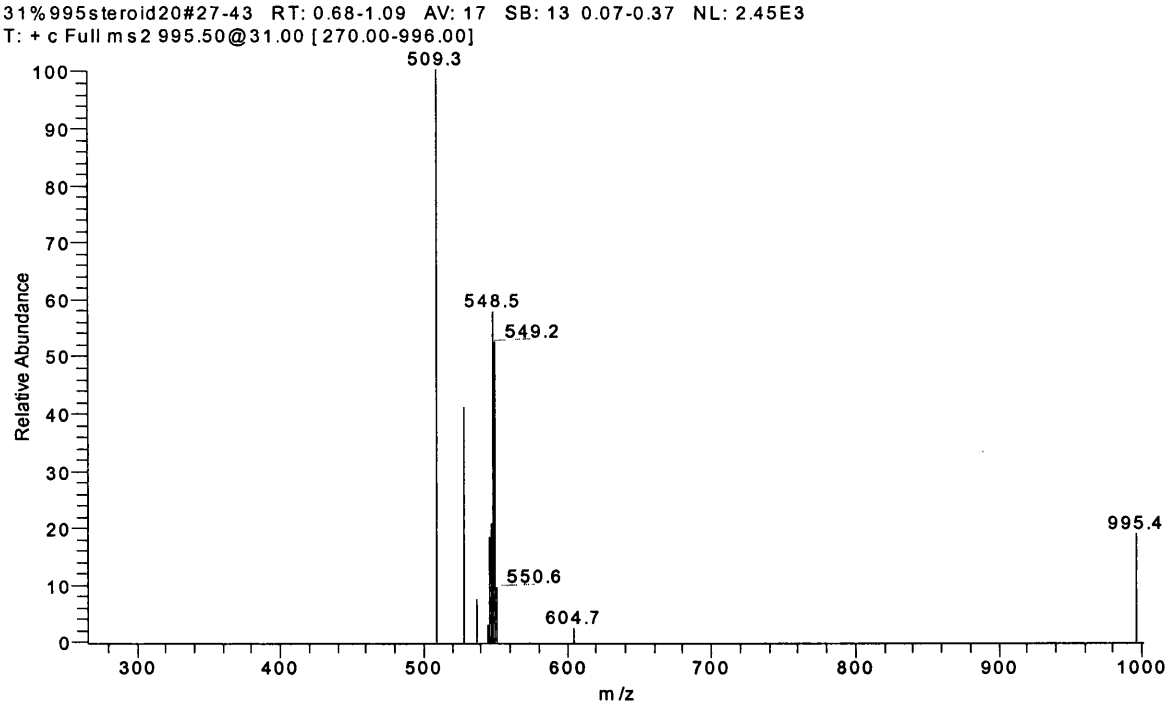

Figure 3.6.2 CID of androsterone glucuronide from ion of m/z 999; collision energy 31%

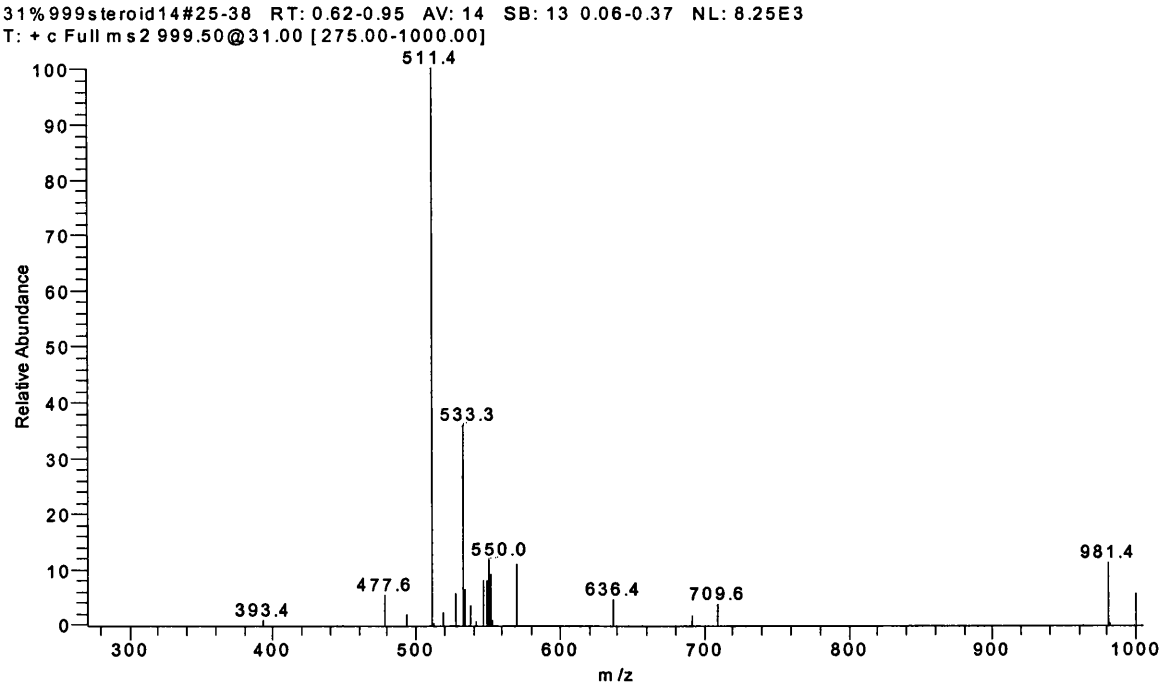

Figure 3.6.3 CID of 5β-Androstane-11, 17-dione-3α-ol glucuronide from ion of m/z 1027; collision energy 32%

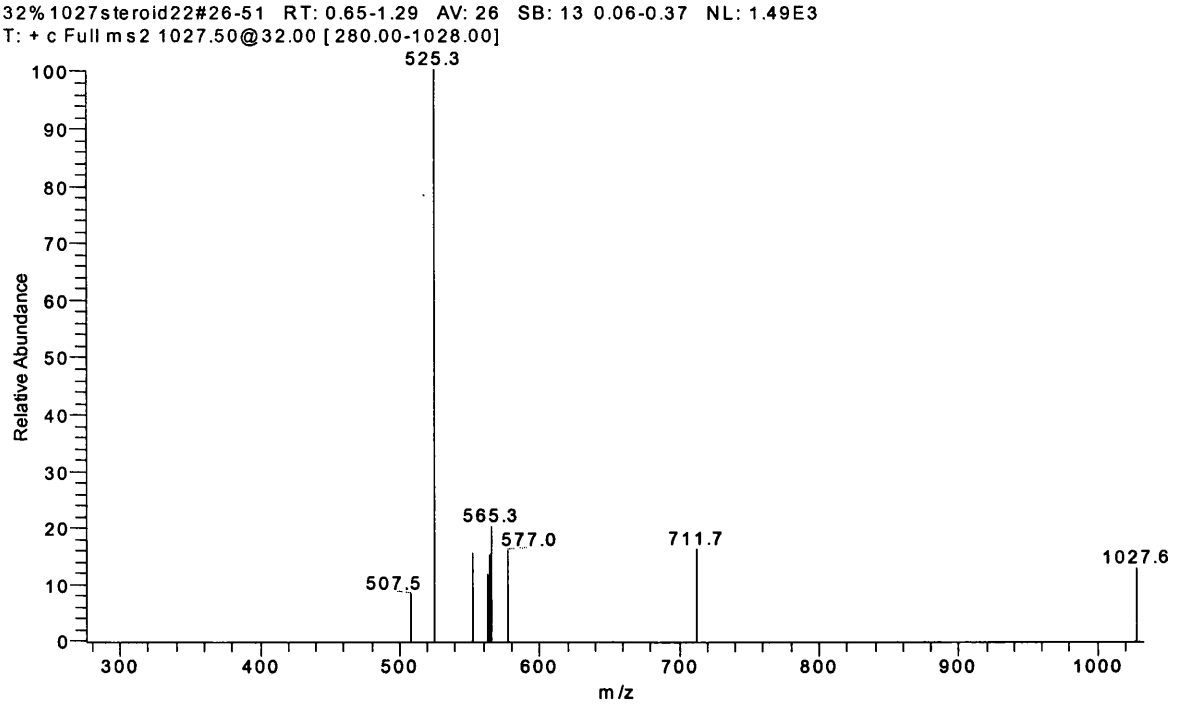

Figure 3.6.4 CID of 5α-Androstan-3α, 17β-diol glucuronide from ion of m/z 1003; collision energy 32%

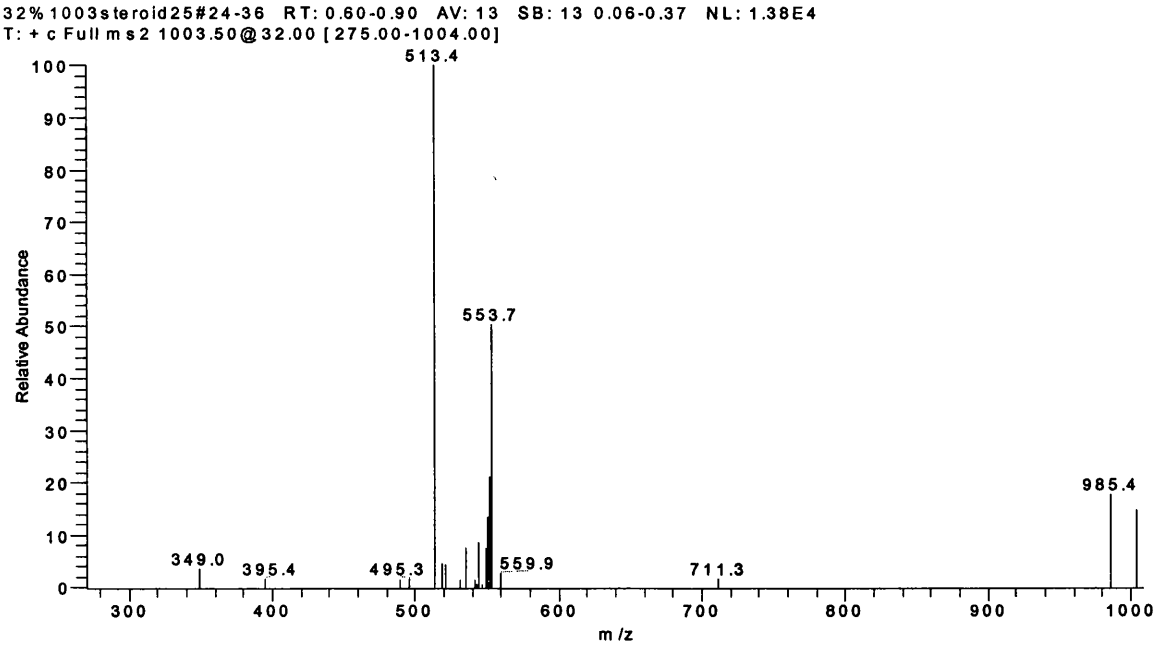

CID spectra from parent ion of $[M-H+2Na]^+$

Similar CID spectra were observed for testosterone glucuronide, DHEA glucuronide, androsterone glucuronide and etiocholan-3α-ol-17-one glucuronide from their respective parent ion $[M-H+2Na]^+$. Fragment ions at m/z 491 or 493 corresponding to the loss of water from parent ion, together with fragment ions at m/z 449 or 451 were observed, corresponding to the loss of CH_3COOH. There was also a fragment ion at m/z 179 observed in the low mass range of all the spectra, corresponding to the protonated glucuronic acid. The CID spectrum of testosterone glucuronide was shown in Figure 3.7.1, and the spectra of DHEA, androsterone, and etiocholan-3α-ol-17-one glucuronide were present in Appendix 22-24.

A fragment ion at m/z 366 was most abundant in the CID spectrum of 5β-androstane-11, 17-dione-3α-ol glucuronide, but its origin was not clear. There were also fragment ions of m/z 507 and 179 observed in its spectrum. The spectrum was shown in Figure 3.7.2.

The most abundant fragment ion m/z 495 was present in the CID spectrum of 5α-androstan-3α, 17β-diol glucuronide, corresponded to loss of water from the parent ion $[M+Na]^+$, the fragment ion at m/z 453 was again observed, corresponding to loss of CH_3COOH from the parent. There was also an ion observed at m/z 354 (m/z 513-159), that could arise in the same way as the ion at m/z 366 formed from 5β-androstane-11, 17-dione-3α-ol glucuronide, but the mechanism is not clear. The spectrum was shown in Figure 3.7.3.

Figure 3.7.1 CID of testosterone glucuronide from ion of m/z 509; collision energy 35%

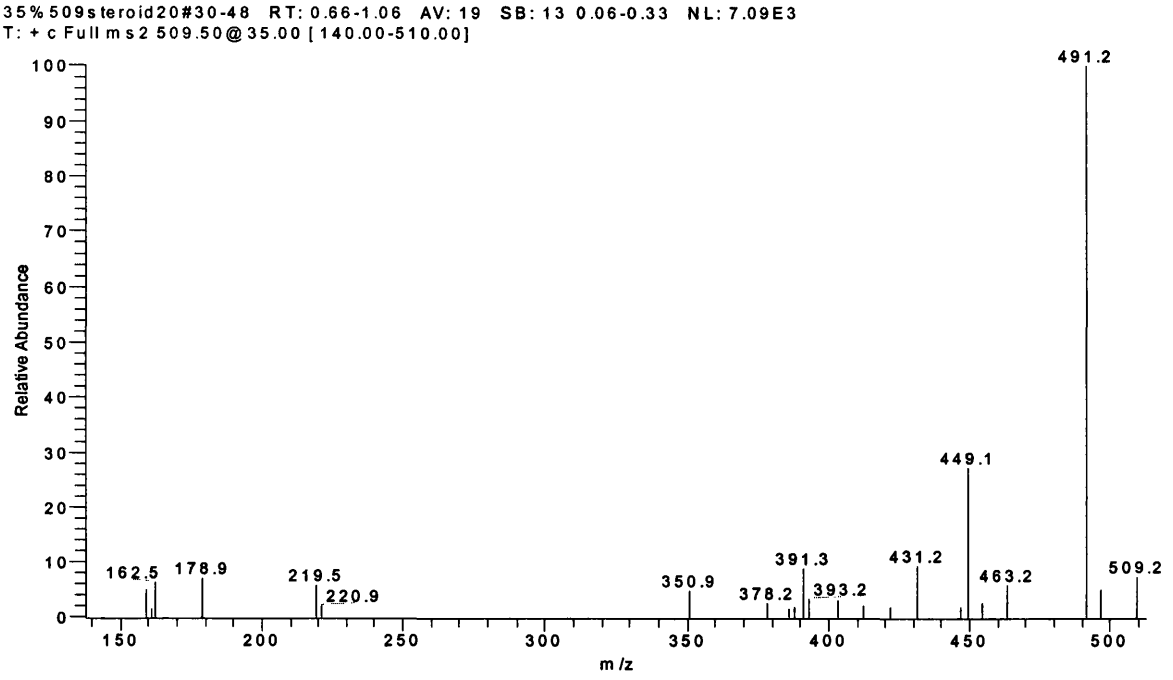

Figure 3.7.2. CID of 5β-androstane-11, 17-dione-3α-ol glucuronide from ion of m/z 525; collision energy 35%

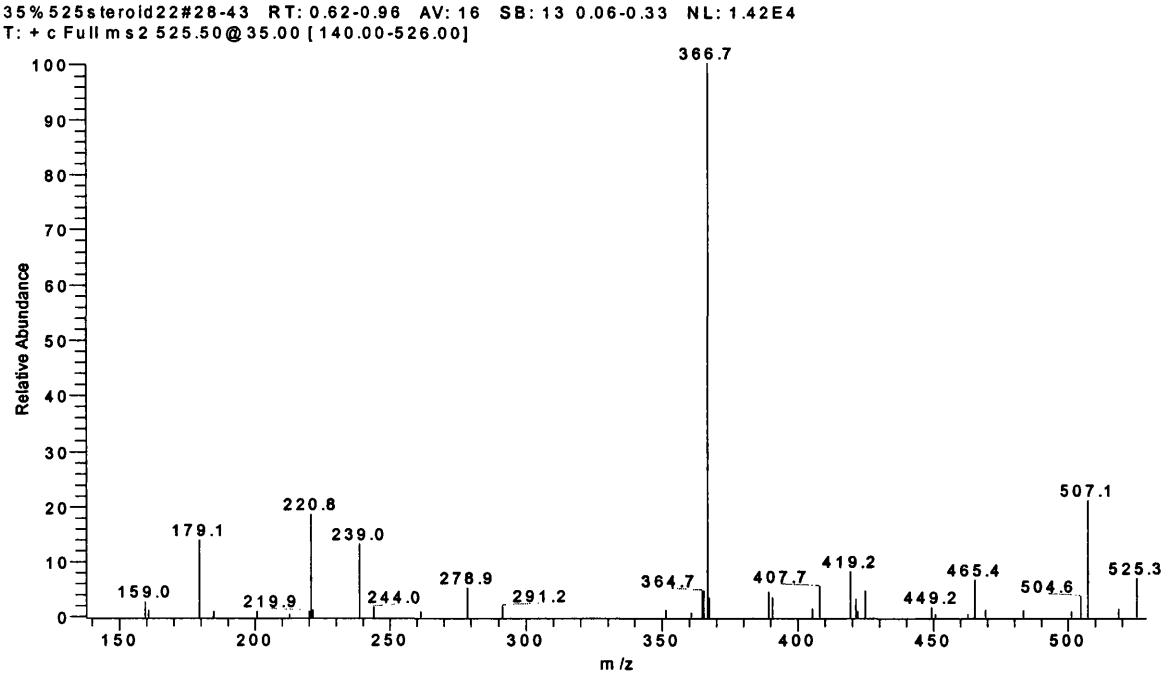

Figure 3.7.3. CID of 5α-androstan-3α, 17β-diol glucuronide from ion of m/z 513; collision energy 35%

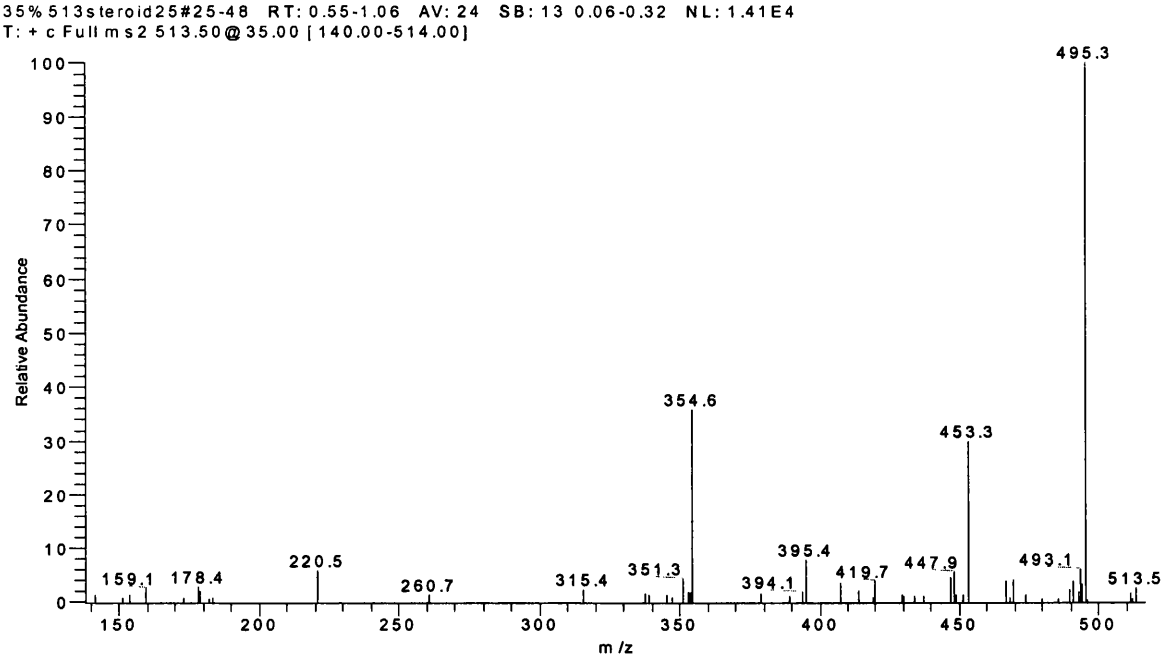

3.5.1.2 Injected with methanol/water

The base peak of $[M+Na]^+$ or $[M+H]^+$ was chosen as the parent ion for generation of CID spectra of the steroid glucuronides using methanol/water. As the case in the spectra using acetonitrile/water, no significant spectra obtained for the steroid sulfates.

CID spectra from the parent ion $[M+Na]^+$

The fragment ions corresponding to the sodium adduct of glucuronic acid ($[Glu+Na]^+$) and $[Glu+Na+H_2O]^+$ derived from glucuronide moiety at m/z 199 and 217 repectively, were presented in all the CID spectra generated from the parent ion of

$[M+Na]^+$. The CID spectra for testosterone, androsterone, etiocholan-3α-ol-17-one, and DHEA glucuronide were present in Appendix 25-28.

CID spectra from the parent ion $[M+H]^+$

A fragment ion of m/z 289 was the base peak in this CID spectrum of testosterone glucuronide, corresponding to the loss of glucuronide moiety. Fragment ions of m/z 271 and 253 were also observed for the further loss of water. Borts and his co-workers [10] using a methanol, NH_4OAc and glacial HOAc buffer, also observed a fragment ion at m/z 289 from parent ion m/z 465 for testosterone and epitestosterone glucuronide. However, they also observed a fragment ion at m/z 271 from parent ion m/z 369 for testosterone sulfate, could not be obtained under the conditions used in the present study. The CID spectrum of testosterone was shown in Figure 3.8.1.

Figure 3.8.1. CID of testosterone glucuronide from ion of m/z 465; collision energy 26%

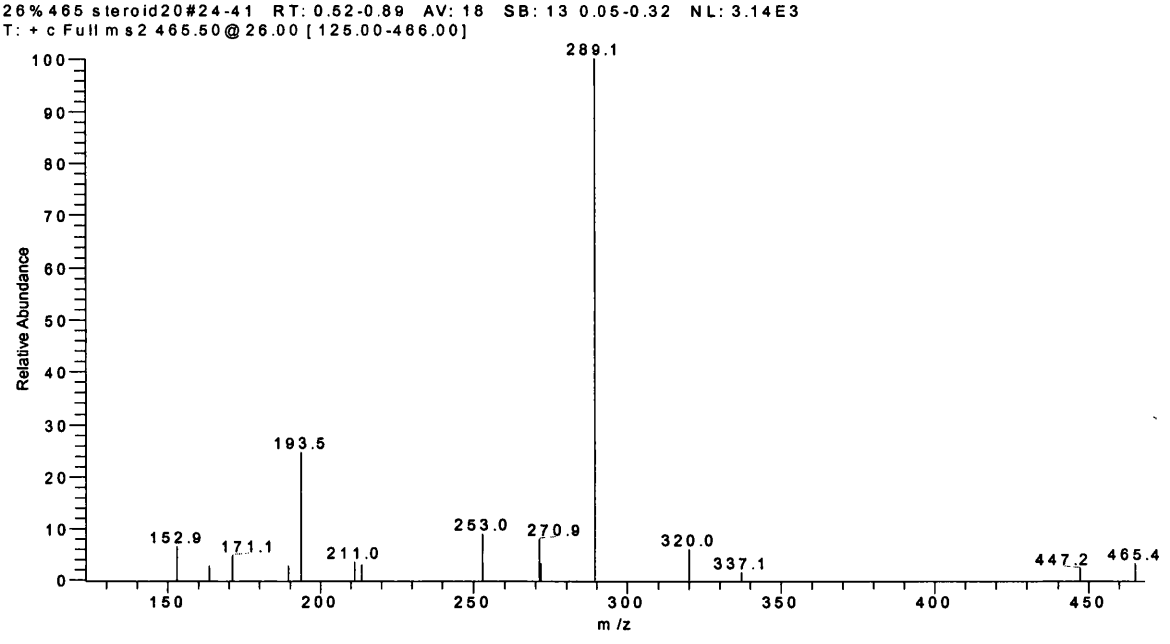

3.5.2 CID of androgenic steroid conjugates in negative mode

3.5.2.1 Androgenic steroid glucuronides

There were style peaks of $[2M+Na-2H]^-$, $[2M-Na]^-$, $[M-H]^-$ and $[M-Na]^-$ present in the ESI spectra of the androgenic steroid glucuronides, and the fragmentation of these ions were studied by the CID-MS.

CID spectra from parent ion of $[2M+Na-2H]^-$

There was very abundant fragment ion of $[M-H]^-$ present in all the CID spectra produced from the parent ion $[2M+Na-2H]^-$, and a peak at m/z 935 was also observed in the spectra of androsterone glucuronide and etiocholan-3α-ol-17-one glucuronide, corresponding to an ion formed by loss of water from the parent, but this ion was absent from the spectra of testosterone glucuronide and DHEA glucuronide. Whilst a fragment ion at m/z 601 was the base peak in the spectrum of etiocholan-3α-ol-17-one glucuronide, no such an ion was observed in the spectrum of its isomer androsterone glucuronide. The CID spectra of these compounds were present in Appendix 31-34.

CID spectra from parent ion of $[2M-Na]^-$

A fragment ion at m/z 501 was the base peak in the CID spectrum of 5β-androstane-11, 17-dione-3α-ol glucuronide sodium salt, corresponding to $[M+Na-2H]^-$, and there was also fragment ion of high abundance at m/z 963, formed by loss of water from the parent, together with a fragment ion at m/z 479, corresponding to $[M-Na]^-$ of

low abundance. In contrast, a fragment ion at m/z 467 was dominant in the CID spectrum of 5β-androstane-11, 17-dione-3α-ol glucuronide sodium salt, but no fragment ions corresponding to $[M+Na-2H]^-$ and $([2M-Na]^- -H_2O)$ were present. The CID spectra of 5β-androstane-11,17-dione-3α-ol and 5β-androstane-11, 17-dione-3α-ol glucuronide sodium salt were present in Appendix 35-36.

CID spectra from the parent ion $[M-H]^-$

The CID spectra showed a very intense peak corresponding to $([M-H]^- -H_2O)$, and weak peaks assigned to $([M-H]^- -CH_3COOH)$, $[M-H-80]^-$ and $[M-H-118]^-$, which are probably due to charge induced fragmentation of the glucuronide moiety. Peaks corresponding to loss of glucuronide moiety ($[M-H]^-$-Glu) and further loss of two hydrogens ($[M-H]^-$-Glu-H_2) were observed in relative high abundance in the CID spectrum of testosterone glucuronide, but in very low abundance in the spectra of the other glucuronides. Glucuronide fragment ion (m/z 175) and $[Glu-H-H_2O]^-$ (m/z 157) were observed in all the CID spectra of steroid glucuronides. Similar spectra were also observed by Kuuranne and M. Vahermo[8], and they suggested that the fragment ion ($[M-H]^-$-Glu-H_2) was formed by the loss of glucuronide group, with the transfer of two hydrogens from the aglycone to the glucuronide group resulting in the α, β-unsaturated structure of the aglycone fragment ion and allowing delocalization of the negative charge at the glucuronide group. Our result is consistent with this suggestion.

Although the CID spectra of the 5α/5β-iomeric steroid glucuronides (androsteorne glucuronide and etiocholan-3α-ol-17-one glucuronide) are quite similar, there is however, an ion of m/z 307 present in the spectrum of androsterone glucuronide;

whereas, no such ion is observed in the spectrum of etiocholan-3α-ol-17-one glucuronide. The CID spectra of these compounds were shown in Figure 3.9.1-4.

Figure 3.9.1 CID of testosterone glucuronide from ion of m/z 463; collision energy 32%

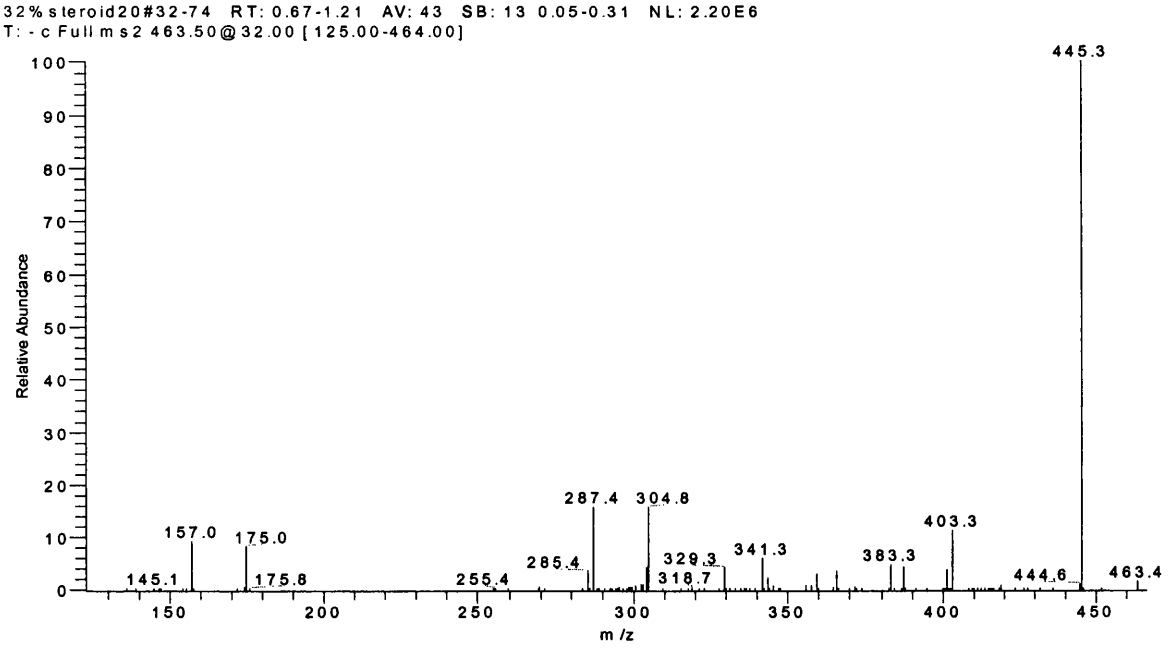

Figure 3.9.2. CID of androsterone glucuronide from ion of m/z 465; collision energy 32%

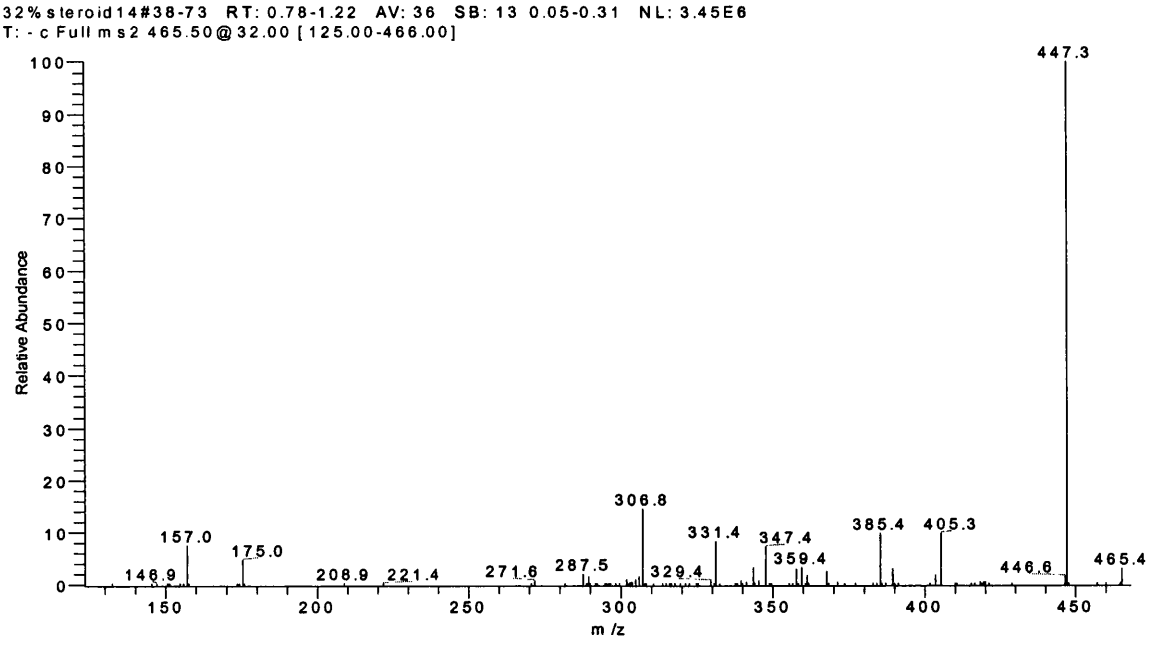

Figure 3.9.3 CID of etiocholan-3α-ol-17-one glucuronide from ion of m/z 465; collision energy 32%

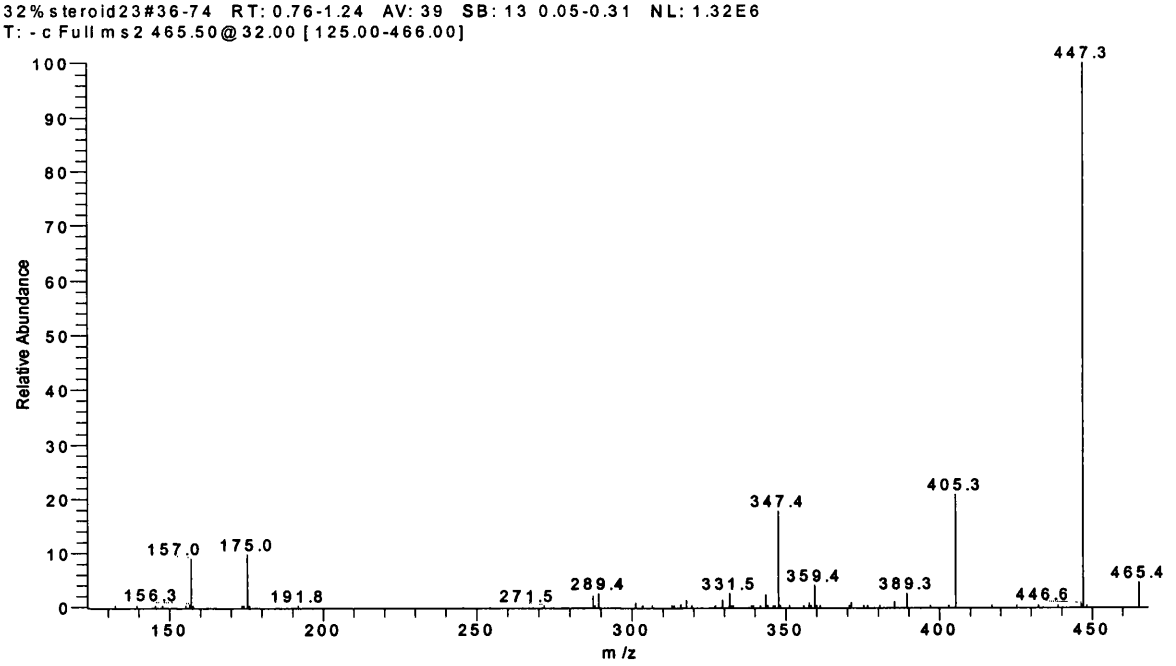

Figure 3.9.4 CID of DHEA glucuronide from ion of m/z 463; collision energy 32%

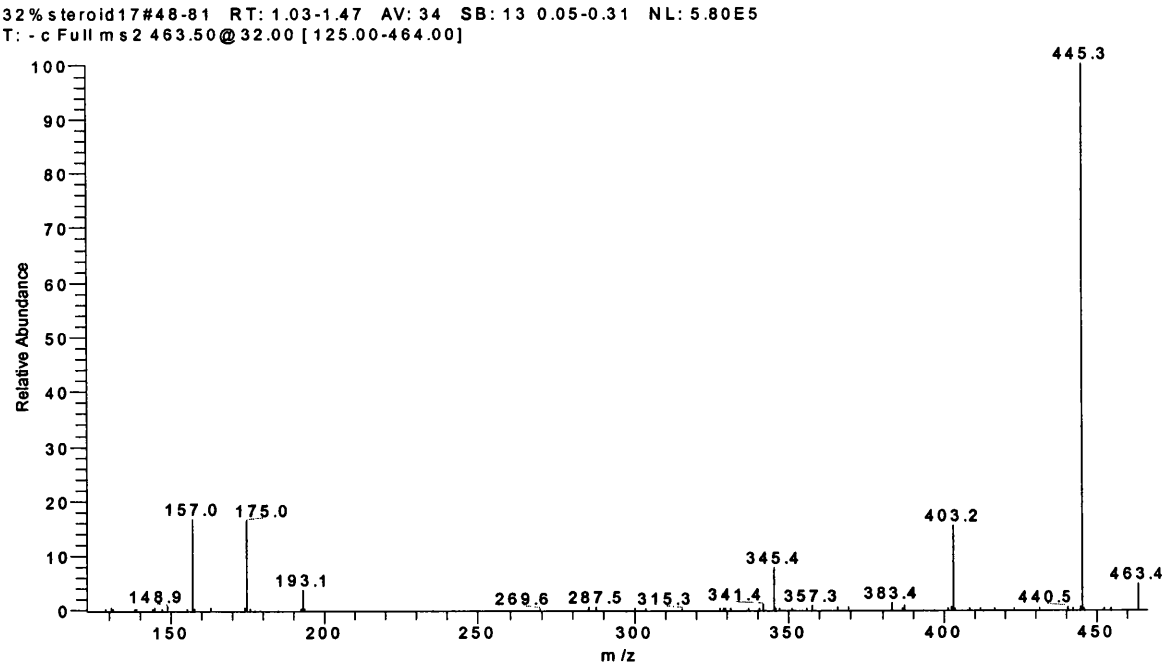

CID spectra from parent ion of $[M-Na]^-$

The CID spectra of 5β-androstane-11, 17-dione-3α-ol glucuronide and 5α-androstan-3α, 17β-diol glucuronide generated from the parent ion $[M-Na]^-$ show the same types of fragment ions as from parent ion of $[M-H]^-$, that is ions formed by the losses of water and acetic acid ($[M-Na]^- - H_2O$) and ($[M-Na]^- - CH_3COOH$), ions formed by the loss of the glucuronide moiety ($[M-Na]^-$-Glu) and ($[M-Na]^-$-Glu-H_2O), and ions for the glucuronide moiety (m/z 175) and ($[Glu-H]^- - H_2O$) (m/z 157). The CID spectra were present in Appendix 37-38.

3.5.2.2 Androgenic steroid sulfates

The de-sodiated molecular ion $[M-Na]^-$ of steroid sulfates is much more stable than $[M-H]^-$ or $[M-Na]^-$ of steroid glucuronides. The more collision energy is used, the greater the sensitivity required for determination of CID spectra. A CID spectrum was obtained only with testosterone sulfate, spectra of none of the other steroid sulfates could be determined due to insufficient sensitivity of the mass spectrometer.

The CID spectrum of testosterone sulfate (Figure 3.10.1) only shows the consecutive losses of methyl groups, which are most likely arise from the cleavage of C18 and C19 bonds.

Figure 3.10.1 CID of testosterone sulfate from ion of m/z 367; collision energy 48%

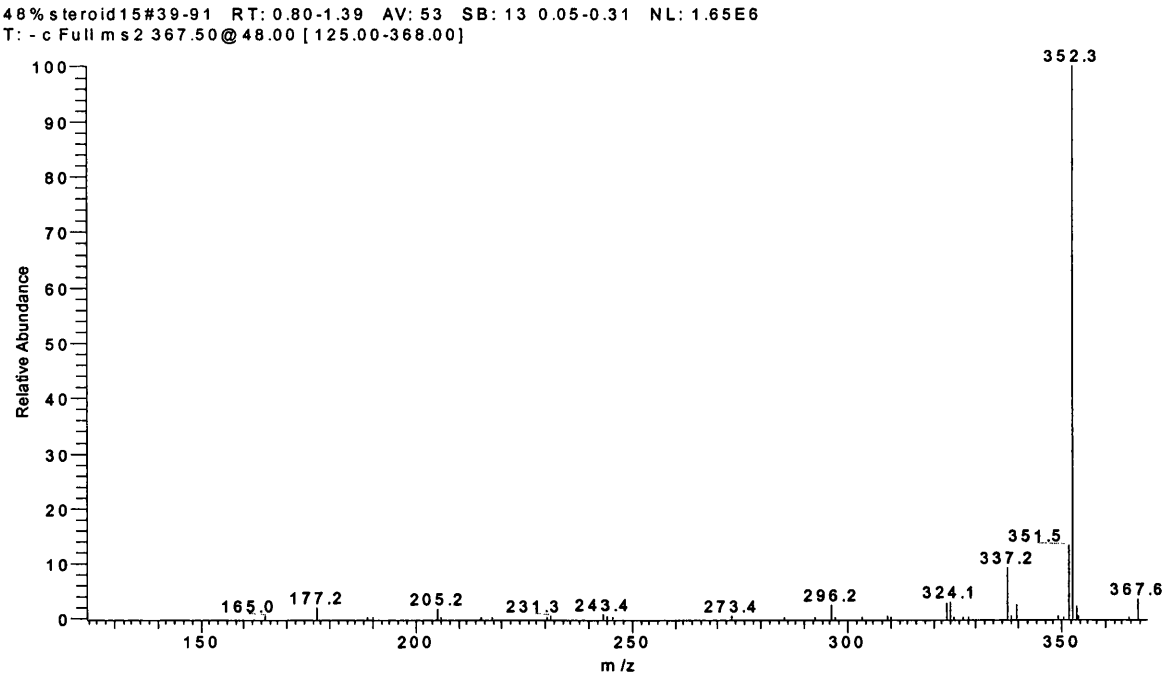

3.6 Conclusions

The steroid conjugates can be ionized with all four ionization techniques: positive and negative ESI and APCI. However, there were very different spectra observed when using different delivering solvents. It seemed formation of dimers or trimers is favored for the investigated steroid glucuronides and sulfates delivered by acetonitrile/water in both ESI and APCI source.

Compared with the APCI source, the ESI source has lower chemical noise and higher sensitivity, so low flow rate ESI was adopted as the method of choice for subsequent on-line analysis for steroid glucuronides and sulfates using micro- or packed capillary-LC.

Positive ion CID using ESI provides more abundant and diagnostic product ions and therefore preferable for the identification of androgenic steroid conjugates, whilst negative mode, despite of the lack of specific structure information, provides simpler spectra and relative better sensitivities and would be useful for quantification of these compounds.

References

1. W. Schänzer *Clin.Chem.* 42 (1996) 1001.
2. G. Messeri, G. Cugnetto, G. Moneti, M. Serio, *J. steroid Biochem.* 20 (1984) 793.
3. L. D. Bowers, Sanaullah, *J. steroid Biochem. Mol. Biol.* 58 (1996) 225.
4. L. D. Bowers, D. J. Bort, *J. Mass Spectrom.* 35 (2000) 50.
5. I. Dzidic and J. A. McCloskey, *Org. Mass Spectrom.* 6 (1972) 939-940.
6. L. D. Bowers and Sanaullah, *J. Chromatogr. Sect. B* 687 (1996) 61-68.
7. T. M. Williams, A. J. Kind, E. Houghton and D. W. Hill, J. *Mass Spectrom.* 13 (1986) 65-69.
8. T. Kuuranne and M. Vahermo, *J. Am SocMass Spectrom.* 11 (2000) 722-730.
9. A.G. Harrison, *Chemical Ionisation Mass Spectrometry, CRC: Boca Raton,* FL (1982) 117.
10. D. J. Borts and L. D. Bowers, *J. Mass Spectrom.* 35 (1999) 50-61.

Chapter 4

HPLC/MS of Free Androgenic Steroids and their Conjugates

4.1 Introduction

As a consequence of the significant way of androgenic steroids and their conjugates in clinical diagnoses [1-6], determination of these compounds has been an important field of analytical chemistry for the biological, clinical and pharmaceutical sciences [7-11]. In addition to analysis by traditional radioimmunoassay (RIA) and gas chromatography (GC), high performance liquid chromatography (HPLC) has become a very useful technique for steroid analysis in recent years. Many determination methods for androgens using HPLC with ultraviolet (UV) detection have been reported. An HPLC optimization method for the separation of a mixture of urinary androgens and synthetic anabolic steroids was described by Gonzalo-Lumbreras and Izquierdo-Hornillos[12-13]. The effect of several variables such as mobile phase, column packing material and temperature on the separation was studied. The detection limits obtained by UV detection were in the range of around 0.01-0.1 μg/ml (S/N = 3) in human urinesamples spiked with steroids. Baltes et al.[14] reported the separation of testosterone (T) and six of its hydroxylated metabolites in the incubation mixture with cell microsomes. Marwah et al.[15] developed a method using HPLC with UV detection at 240 nm for the determination of 7- oxodehydroepiandrosterone sulfate in human plasma after a single dose of 7-oxo-dehydroepiandrosterone 3β-acetate. Using 1 ml of plasma for extraction, the detection limit of the assay was 3 ng/ml (S/N = 3). T and epiT in urine were determined using an HPLC method with UV detection (240 nm) after enzymic hydrolysis and liquid –liquid extraction by Navajas et al.[16].

However, difficulty in measurement of many androgenic steroids by HPLC-UV results essentially from lack of a UV Chromophore in the molecule combined with their low concentration in biological fluid, especially in plasma. Mass spectrometry (MS) is a powerful and specific technique coupled with HPLC for the determination of androgens. Komatsu et al.[17] measured various steroids including Δ_4-androstenedione and DHEA in normal adrenal glands and adrenocortical tumors by HPLC- atmospheric pressure chemical ionization (APCI)-MS, whlist the characteristic peaks observed in positive mode mass spectra. The ratio of glucocorticoid to mineralocorticoid content was measured and compared for Cushing's adenomas and for normal adrenals. Draisci et al.[18] reported a method based on tandem MS with on-line micro-HPLC using ion spray (IS) interface for the direct detection of natural and synthetic hormone residues in bovine serum. Linearity of response to the quantity of each analyte between 10 and 300pg was reported in the selected reaction monitoring (SRM) mode, and the limit of detection was 6-7 pg for the hormones (S/N =3).

Originally, hydrolysis was the first step in their assay [19-23] of conjugated steroids, but hydrolysis invariably results in the loss of valuable information concerning type or site of conjugation. Therefore many researchers tried to separate conjugated steroids without hydrolysis. Nakajima et al.[24] applied HPLC-APCI-MS combined with a column switching technique to the determination of serum DHEAS. Human serum samples were directly injected into the sample preparation column, DHEAS was separated with an analytical column and analyzed by HPLC-APCI-MS in negative mode. The detection limit was 10ng on-column at a S/N of 3. The same group also showed an application for the determination of DHEAS in other tissues including brain, liver, kidney, adrenal and testis [25]. Direct determination of glucuronide and sulfate of T and epiT in urine has been studied by LC-MS-MS. Bean and Henion [26] presented a method using micro-bore HPLC

combined on-line with IS-MS in positive mode with SRM. In contrast, Borts and Bowers[27] used LC-electrospray ionization (ESI)- MS in negative mode. In both methods, the detection limits of analytes were in the low nM range in urine. Jia et al. [28] quantified urinary 17-ketosteroid sulfates and glucuronides by LC- ion trap MS with sonic spray ionization technology. With direct injection of 17-ketosteroid in 100 mM buffer solution, sonic spray generated a signal about 20 times stronger than that obtained using ESI, thereby enabling use of high buffer concentration without any apparent loss of sensitivity; 17-ketosteroids could be quantified down to 3 pg/μl using this technique.

In this chapter, two HPLC/MS methods were optimized and established in the aim of quantifications of eight androgen steroids and five steroid conjugates respectively. The limits of detection, accuracy, precision and linearity of the methods were described.

4.2 Experimental

4.2.1 Materials

Testosterone glucuronide, testosterone sulfate sodium salt and androstanediol glucuronide sodium salt were purchased from Steraloids (USA). The other steroid conjugates and free steroids were from Sigma-Aldrich Ltd (Poole, Dorset, UK). The standards were dissolved in methanol, and further diluted to different concentrations with methanol/water (1:1) for the experiments.

The HPLC grade methanol, acetonitrile and water were purchased from Fisher Scientific (Loughborough, Leicester, UK). Ammonium acetate was purchased from

Sigma-Aldrich Ltd (Poole, UK). Solvents were filtered using a 0.45μm membrane filter and constantly degassed during analysis.

Hypersil C_{18} (150 × 4.6 mm, 5 μm), C_8 (150 × 4.6, 5 μm), LUNA $C_{18\ (2)}$ (100 × 2.0 mm, 3 μm), LUNA Phenyl-hexyl (100 × 2.0 mm, 3 μm) columns were purchased from Phenomenex (Cheshire, UK).

Human plasma from males and females was obtained from the Welsh Blood Service (Ely Valley Road, Talbot Green, Port-y-Clun, CF72 9WB).

4.2.2 UV-visible spectrophotometry and HPLC

UV-visible spectrophotometer (Unicam UV-300, Cambridge, UK) was used to determine the UV-visible spectrum of solution of the scan of the steroids of interest in the region from 190 nm to 400 nm, using methanol as the reference solution.

Hewlett-Packard 1100 and 1050 models (Waldborn, Germany) were used for HPLC experiments, and the temperature was controlled at 40°C. A Hypersil C_{18} (150×4.6 mm, 5 μm) column was used for the separation for free androgenic steroids with isocratic elution (65% methanol / 35% water) at a flow rate of 1ml/min after UV detection to the APCI interface of mass spectrometer.

A micro-bore column (LUNA $C_{18\ (2)}$, 100×2.0 mm, 3 μm) was used for method development for free steroids at a flow rate of 300 μl/min to APCI-MS. The gradient elution program was shown below:

Time (min)	MeOH (v/v %)	H_2O (v/v %)
0	55	45
5	55	45
25	70	30
27	100	0
35	100	0
36	55	45
45	55	45

A LUNA Phenyl-hexyl (100×2.0 mm, 3 μm) column was used for the separation of steroid conjugates at a flow rate of 200 μl/min to the ESI interface of mass spectrometer. The gradient elution program was below:

Time (min)	MeCN (v/v %)	10mM NH_4OAc (v/v %)
0	25	75
7	25	75
12	50	50
20	50	50
21	25	75
35	25	75

4.2.3 Mass spectrometry parameters

Mass spectrometric experiments were performed on a Finnigan LCQ ion trap mass spectrometer (San Jose, CA) equipped with X-callubar software. The APCI interface parameters employed for free steroids in positive mode were as follow:

MS parameter	Flow rate of 1ml/min	Flow rate of 0.3ml/min
Vaporizer temperature	550°C	550°C
Sheath gas flow (arbitrary units)	90 arb	40 arb
Auxiliary gas flow (arbitrary units)	30 arb	10 arb
Discharge current	4.5 μA	3.5 μA
Capillary temperature	175 °C	150 °C
Capillary voltage	10 V	10 V
Tube lens offset	30 V	30 V

The ESI interface parameters used for steroid conjugates in negative mode were as:

MS parameter	Flow rate at 0.2ml/min
Sheath gas flow (arbitrary units)	100
Auxiliary gas flow (arbitrary units)	20
Spray voltage	4.5 KV
Capillary temperature	200°C
Capillary voltage	-45 V
Tube lens offset	-40 V

4.2.4 Steroid extraction

Plasma samples (2 ml) were diluted with of distilled water (3 ml) in a test tube and of diethyl ether (9 ml) added; the contents were vortex mixed thoroughly (30 s). The tubes were centrifuged for 5 min at 1000g, and then the diethyl ether layer was separated by freezing the aqueous layer in a carbon dioxide-dry ice bath. The aqueous layer was thawed and the above procedure repeated. Finally, the combined diethyl ether extracts were evaporated to dryness under a slow stream of oxygen-free nitrogen at room temperature. The residue was dissolved in 200 µl of methanol and was injected directly into chromatograph.

4.2.5 Assay validation

The repeated measurements were evaluated by an ANOVA method with one-tailed F-test.

The intra-day precision of the method was evaluated by injecting four replicates of samples at three different concentrations. The inter-day precision was assessed by analyzing standard samples at three different concentrations on three days against calibration curves. Precision was given by intra-day, inter-day and total coefficient of variation.

The linearity was evaluated using results of calibration curves run on three different days over the different concentration ranges of standards. Calibration curves were constructed by plotting the peak area against the concentration of sample. An unweighted least-squares linear regression analysis was used to obtain standard calibration curves.

4.3 Free androgenic steroids

4.3.1 UV-visible spectrophotometry

Methanol solutions of some major androgenic steroids were scanned using the UV-visible spectrophotomer between the wavelength 190.0 nm to 400.0nm, and their wavelength of maximum absorbance are summarized in Table 4.1.

Table 4.1 UV-visible scan of some androgenic steroids

Compound	Wavelength of maximum absorbance (nm)
Testosterone	238
Δ_4-Androsten-3, 17 -dione	238
Dihydrotestosterone	201
DHEA	211
5α-Androstan-3, 17-dione	203
Adrenosterone	238
Androsterone	201
5α-Androstan-3α, 17β-diol	199

4.3.2 HPLC-UV

4.3.2.1. Column

A literature search indicated that reverse-phase separation is the most popular method for resolution of many androgenic steroids. C_{18} and C_8 column were chosen to test the HPLC separation of a mixture of seven androgens interest. Column efficiency was compared between these two columns in Table 4.2.

Table 4.2 Comparison of HPLC parameters between C18 Column and C8 Column

Steroid	C18 column (150*4.6mm)			C8 column (150*4.6mm)		
	RT	Rs	N	RT	Rs	N
Δ_5-Androstene-3β, 17β-diol	5.45	_	26886	5.29	_	26051
Testosterone*	6.45	7.00	28462	6.16	6.29	27754
Δ_4-Androsten-3, 17 -dione *	8.72	12.72	29261	7.75	9.58	28975
5α-Androstan-3α, 17β-diol	10.32	8.72	64186	8.81	5.90	38346
Dihydrotestosterone	11.19	4.30	34788	9.39	2.78	25969
5α-Androstan-3, 17-dione	15.61	8.24	29651	12.29	8.37	28362
Androsterone	16.43	2.38	37574	13.06	2.76	40352

* detected at 240nm. Acetonitile/water (40:60) was used for both columns.

RT, retention time; Rs, resolution; N, plate number.

4.3.2.2. Elution solvent

Both acetonitrile/water and methanol/water solvent systems were applied to C_{18} column for the separation of the seven steroids studied. Lin and Heftmann[29] studied retention behavior of 69 androstane derivatives on normal- and reversed-phase HPLC. They found that the total number of hydroxyl- and keto groups on the androstane molecule was observed to be the most important factor in determining their

chromatographic behavior. In general, hydroxyl groups contributed more to the polarity of the steroid molecules than keto groups, but an α, β-unsaturated keto group makes the steroids about as polar as does a hydroxyl group. We observed similar behaviour when test steroids were eluted with acetonitrile/water (Figure 4.1). However, when eluted with

Figure 4.1 HPLC separation of seven free steroids with acetonitile/water (40:60) and detection by UV

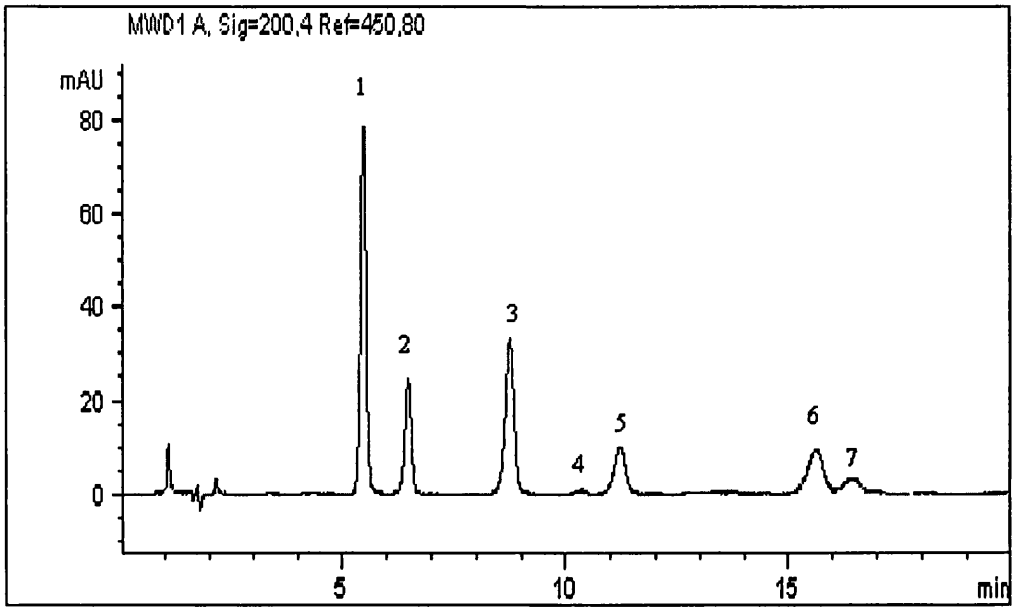

Sample was injected at 20 μl and 100μg/ml for each compound.

1. Δ_5-Androstene-3β, 17β-diol, 2. Testosterone, 3. Δ_4-Androsten-3, 17 –dione,
4. 5α-Androstan-3α, 17β-diol, 5. Dihydrotestosterone, 6. 5α-Androstan-3, 17-dione,
7. Androsterone.

methanol/water, a different order of elution was observed. Δ_4-Androsten-3, 17 –dione was eluted faster than testosterone and 5α-androstan-3, 17-dione was faster than dihydrotestosterone and androsterone (Figure 4.2).

Acetonitrile/water was found to be much better than methanol/water for the UV-detection at 200 nm, due to the lack of UV absorbance at 200 nm which occurs in methanol/water, and the absence of a significant signal attenuation observed at 210 nm

for steroids without Δ_4-bond at A ring when eluted with methanol/water (see Figure 4.1 and 4.2). Moreover, 5α-Androstan-3α, 17β-diol could not be separated from testosterone with methanol/water no matter how the ratio of methanol to water was varied.

Figure 4.2 HPLC separation of seven free steroids with methanol/water (65:35) and detection by UV

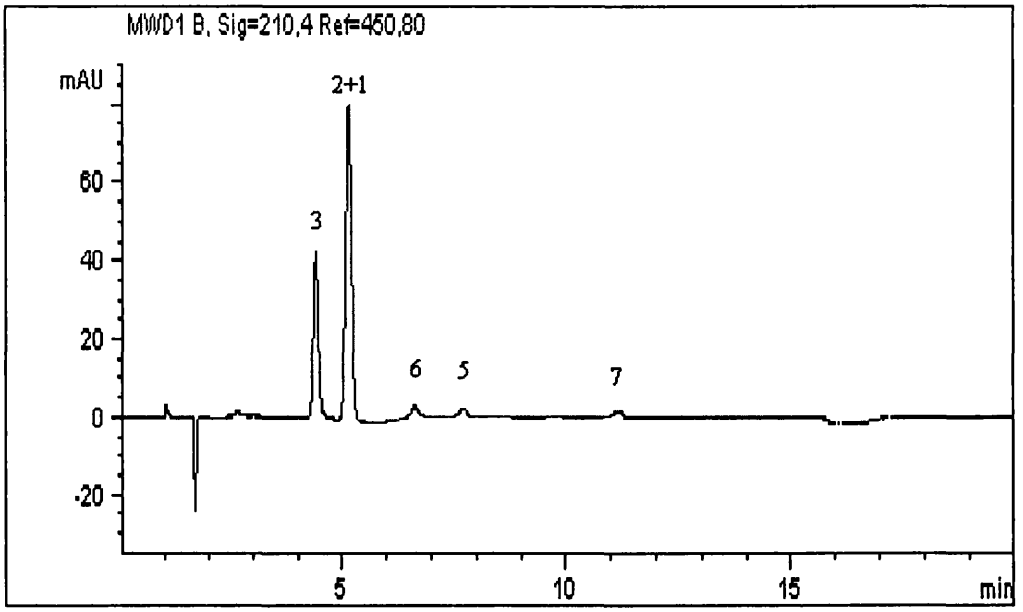

Sample was injected at 20 μl and 100μg/ml for each compound.

1. Δ_5-Androstene-3β, 17β-diol, 2. Testosterone, 3. Δ_4-Androsten-3, 17-dione,
5. Dihydrotestosterone, 6. 5α-Androstan-3, 17-dione, 7. Androsterone.

4.3.3 HPLC-MS

4.3.3.1 HPLC-MS for standard androgen mixture

For many of the steroids investigated, the mass spectrometry proved much more sensitive and specific than UV spectrophotometry as a detector. As reported in Chapter 2, positive APCI/MS was the most sensitive method for the free steroid determinations eluted with methanol/water. Figure 4.3 shows a chromatogram of the m/z values which

relate to the molecular ions or major fragment ions obtained on analysis of a mixture containing eight free androgens. The chromatogram shows the presence of the molecular or major fragment ions at the retention times relating to their elution from the HPLC column. The steroids in the mixture are identified by running each individual standard to determine its retention time and characteristic peak. The ion distribution of the total ion current over a protonated molecule and its fragment ion and adduct ion for each free androgen is presented in Table 4.3.

Figure 4.3 Reconstructed extracted ion current chromatogram of eight steroid mixture by HPLC-APCI/MS

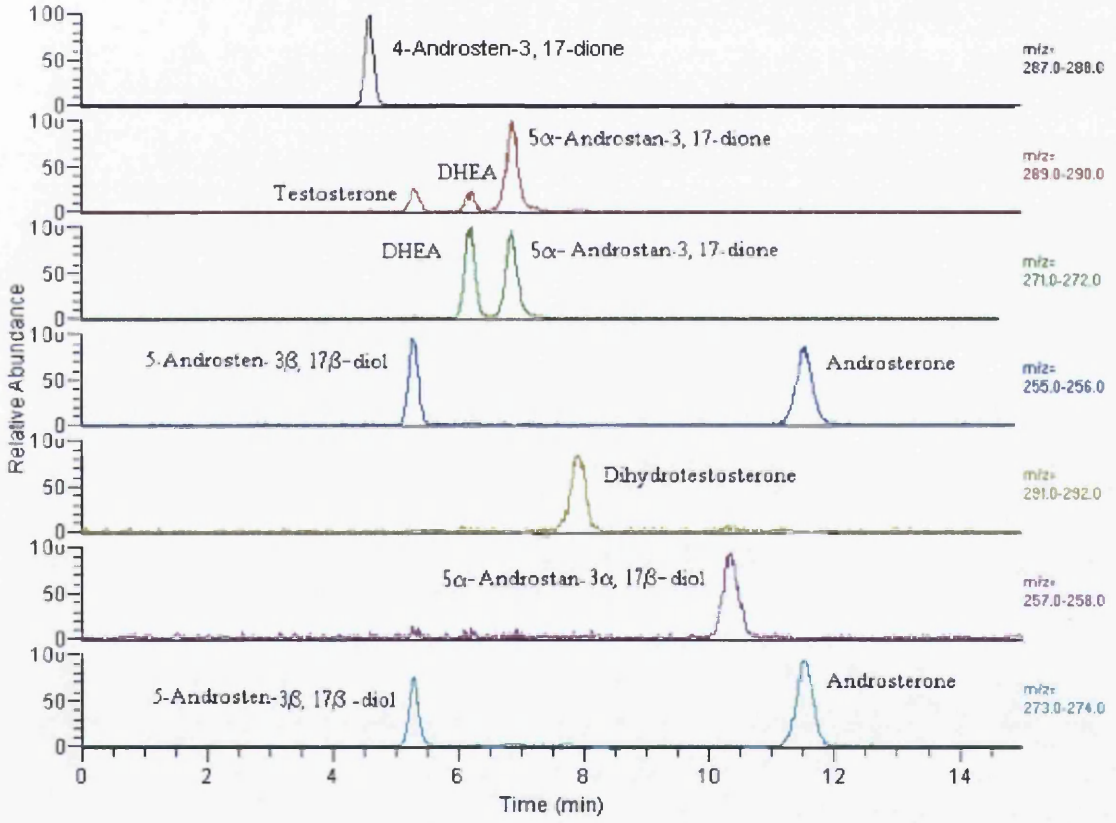

Δ_4-Androsten-3, 17 –dione (100pg/μl); 2. Testosterone (100pg/μl); 3. DHEA (1ng/μl); 4. 5α-Androstan-3, 17-dione (1ng/μl); 5. Dihydrotestosterone (1ng/μl); 6. 5α-Androstan-3α, 17β-diol (1ng/μl); 7. Androsterone (1ng/μl); 8. Δ_5-Androstan-3β, 17β-diol (1ng/μl).
Mobile phase, methanol/water (65:35 v/v), 20 μl injection.

Table 4.3 Distribution of the major ions of eight free androgen steroids (%TIC)

Ion	I	II	III	IV	V	VI	VII	VIII
$[MH]^+$	67	68	_	4	18	5	_	7
$[MH+1]^+$	13	12	_	_	3	_	_	_
$[MH-H_2]^+$	7	5	_	3	4	6	_	_
$[MH-H_2O]^+$	_	_	41	43	27	28	6	49
$[MH-H_2O+1]^+$	_	_	7	7	6	5	_	9
$[MH-2H_2O]^+$	_	_	30	22	4	14	55	21
$[MH-2H_2O+1]^+$	_	_	6	3	_	_	18	3
$[MH+MeOH]^+$	_	_	_	_	5	18	_	_
$[MH-H_2O+MeOH]^+$	_	_	_	_	19	_	_	_

I. Δ_4-Androsten-3, 17-dione, II. Testosterone, III. Δ_5-Andtosten-3β, 17β-diol, IV. Dehydroisoandrosterone (DHEA), V. 5α-Androstan-3, 17-dione, VI. Dihyrotestosterone (DHT), VII. 5α-Androstan-3α, 17β-diol, VIII. Androsterone.

Table 4.3 shows that, for testosterone and Δ_4-androsten-3, 17 –dione, the intensities of the protonated molecules far exceed that of any other ions, but that in the majority of cases, the ions formed by loss of water ($[MH]^+$-H_2O) and ($[MH]^+$-$2H_2O$), contribute more to the %TIC (total ion chromatograph), with the exception of 5α-androstan-3, 17-dione and dihydrotestosterone, for which the adduct ions ($[MH]^+$+MeOH) or ($[MH]^+$-H_2O+MeOH) make a significant contribution. The carbon isotope ions are generally present at no more than 13% for all the test free androgens, and fragment ions ($[MH]^+$-H_2) were present below 7%. In conclusion, the majority of the TIC represents protonated molecules or dehydration fragments, so these ions are the most convenient and most quantitatively sensitive ions to monitor.

4.3.3.2 Application of serum samples to the HPLC-MS method

After extraction and cleaning up procedure, sample from human plasma were analysed by the HPLC-MS method described above. The identifications of the androgens

of interest were based on their retention time and characteristic m/z values, compared with those of standard androgens. Under this conditions, only testosterone could be detected as shown in the reconstructed ion chromatogram (RIC) for the testosterone protonated molecule (m/z 289) obtained from the extracts of male and female plasmas (Figure 4.4), indicating that the present method lacked sufficient sensitivity for routine clinical analysis of androgens other than testosterone.

Figure 4.4 Extracted ion current chromatogram for standard testosterone and extract from male and female plasma sample

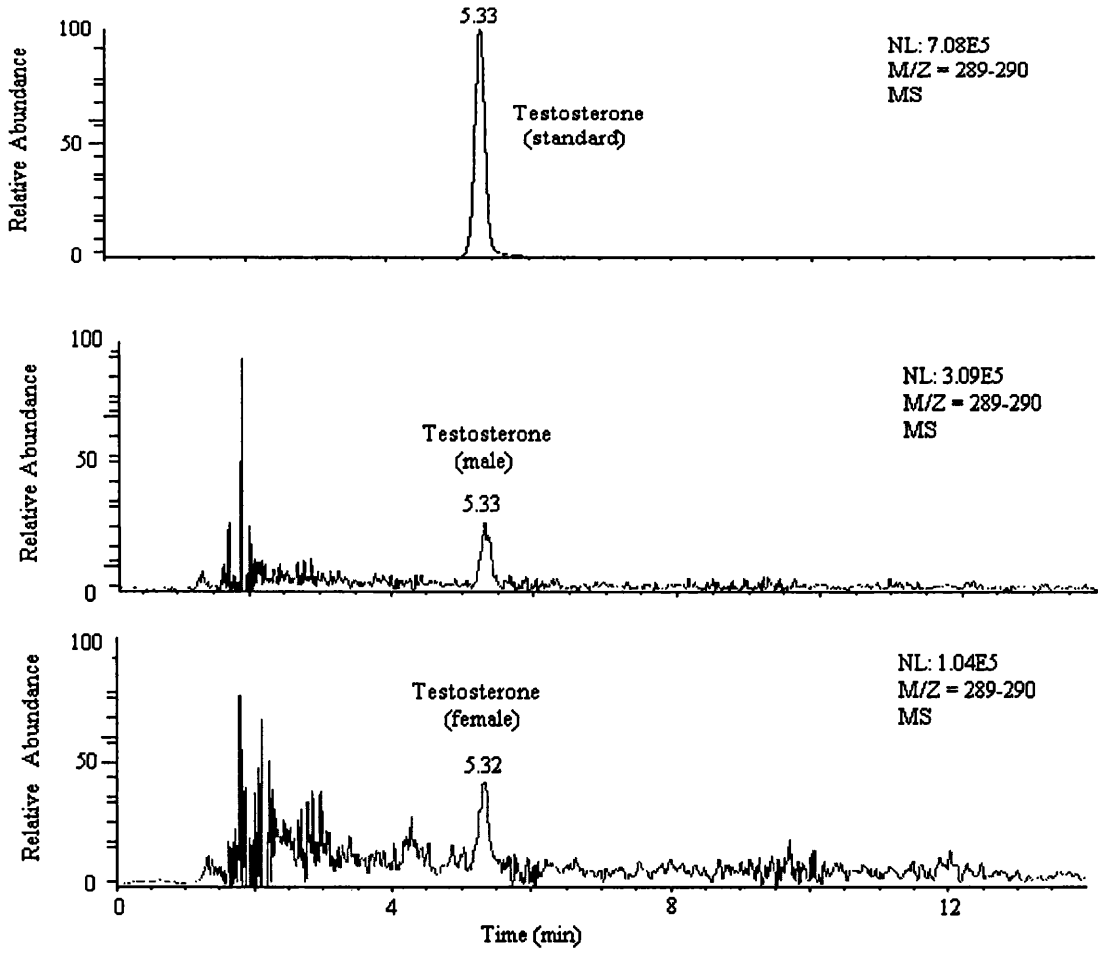

Note, sample was injected at 20 µl, and testosterone standard was at 10 pg/µl.

4.3.4 Micro-bore LC-MS

As an approach to improve sensitivity sufficiently to determine other androgens of interest in bio-samples, the normal LC-MS method was developed to a micro-bore LC-MS method with the optimization of the flow rate and MS parameters.

4.3.4.1 Comparison of the flow rates

To compare the sensitivities between the high flow rate and low flow rate for APCI source, eight test androgen steroids were injected into the mass spectrometer by HPLC pump with methanol/water (50:50). The detection limits were compared at flow rate of 1ml/min and 0.3ml/min (Table 4.4).

Table 4.4 Comparison of the detection limits between high flow rate and low flow rate (S/N ≥ 3).

Steroids	High flow rate (1ml/min)	Low flow rate (0.3ml/min)
Δ_4-Androsten-3, 17 –dione	25 pg	10 pg
Testosterone	20 pg	10 pg
DHEA	150 pg	25 pg
5α-Androstan-3, 17-dione	150 pg	25 pg
Dihydrotestosterone	1 ng	200 pg
5α-Androstan-3α, 17β-diol	750 pg	250 pg
Androsterone	200 pg	50 pg
Δ_5-Androstan-3β, 17β-diol	500 pg	100 pg

As shown in Table 4.4, the detection limits are about 2 to 6 times lower at low flow rate (0.3 ml/min) than at high flow rate (1 ml/min) for the test androgen steroids,

therefore, the micro-bore HPLC column was used to develop a more sensitive micro-bore LC-MS method at low flow rate (0.3 ml/min).

4.3.4.2 Micro-bore LC separation for ten-androgen mixture

A micro-bore column was used for LC separation to meet the requirement for the low flow rate needed to obtain higher sensitivity from the APCI source, for which gradient elution was required (described in 4.2.2) to improve the separation. Figure 4.5 shows the TIC of ten androgens studied in the standard mixture (10 pg/μl for each compound) at flow rate at 0.3 ml/min. While the testosterone and Δ_5-androstan-3β, 17β-diol were better separated compared with the normal size column, they were still not totally resolved. However, these two steroids differ in their characteristic ions in positive mode APCI-MS (m/z values of 289 and 273, respectively), thus their separate mass spectrometric analysis should not cause problems.

Figure 4.5 Total current chromatogram of ten androgen mixture

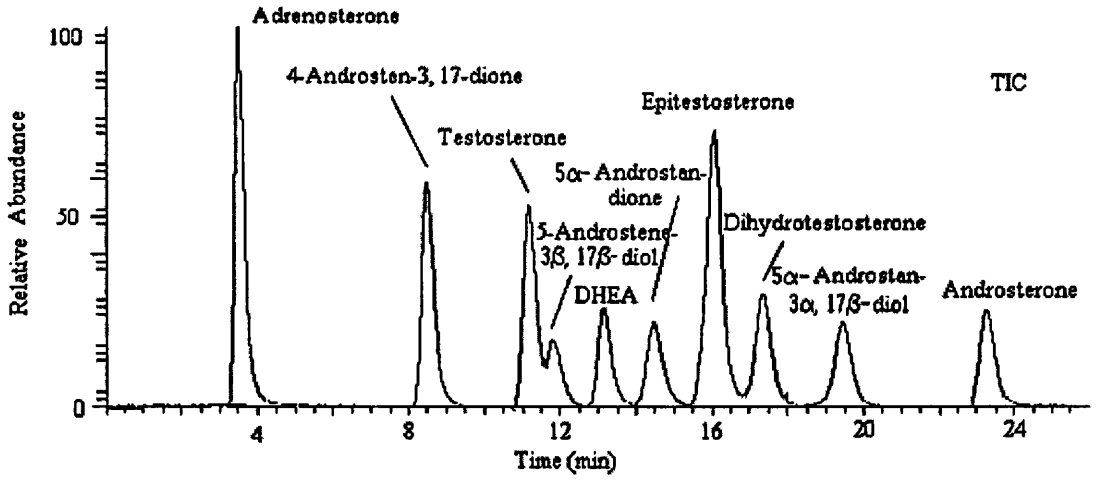

4.3.4.3 Optimization of MS parameters

In order to get the best sensitivity for the androgenic steroids studied, some important mass spectrometric parameters were optimized for an LC flow rate of 0.3 ml/min. The sheath gas levels were tested between 20 and 60 arb (arbitrary units), keeping all other parameters constant. Figure 4.6 (a and b) shows increases in intensities as the sheath gas levels are increased to 30 or 40 arb, and then the intensities drop off as

Figure 4.6 The optimization of some important MS parameters for eight androgenic steroids

(a)

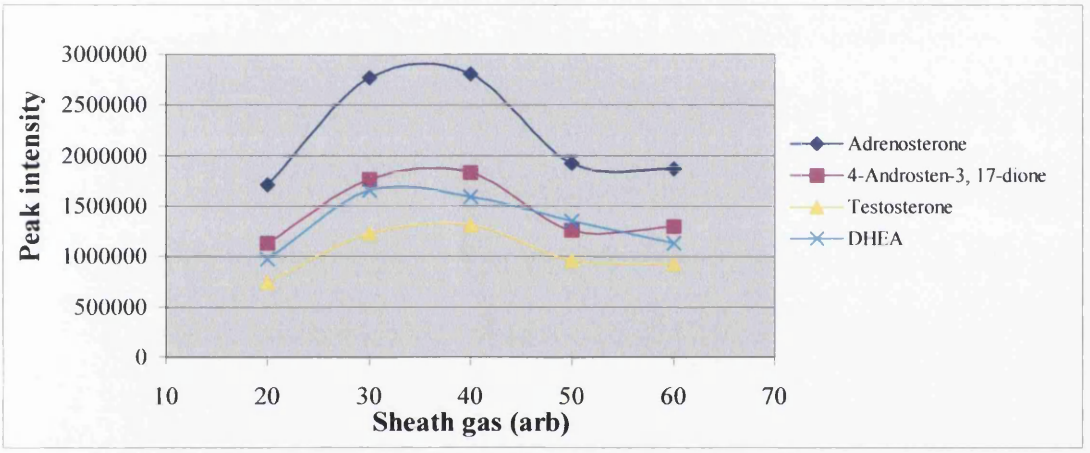

(b)

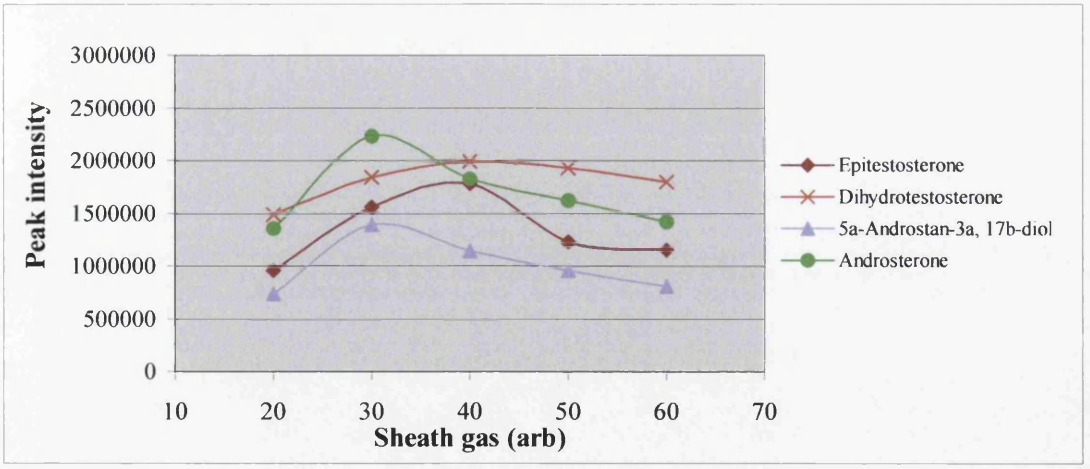

the sheath gas was increased; the sheath gas level therefore was set to 40 arb, because the maximum intensities were observed when the sheath gas was between 30 and 40 arb.

The effect of varying the auxiliary gas levels between 10 and 50 arb as the sheath gas levels were constant at 40 arb was investigated. Figure 4.6 (c and d) shows that as the auxiliary gas level increased abve 10 arb, the signal intensity decreased for most of steroids except dihydrotestosterone, which showed the maximum value as the auxiliary gas increases to 20 arb, and then decreased as the auxiliary gas level increases further. In the majority cases of the investigated steroids, the signals get to the maximum values when the auxiliary gas levels were set to10 arb.

(c)

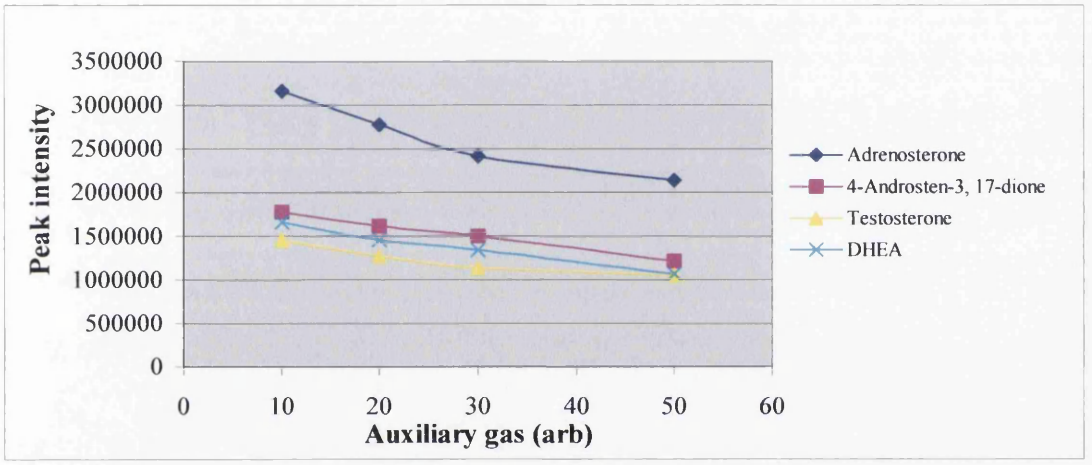

(d)

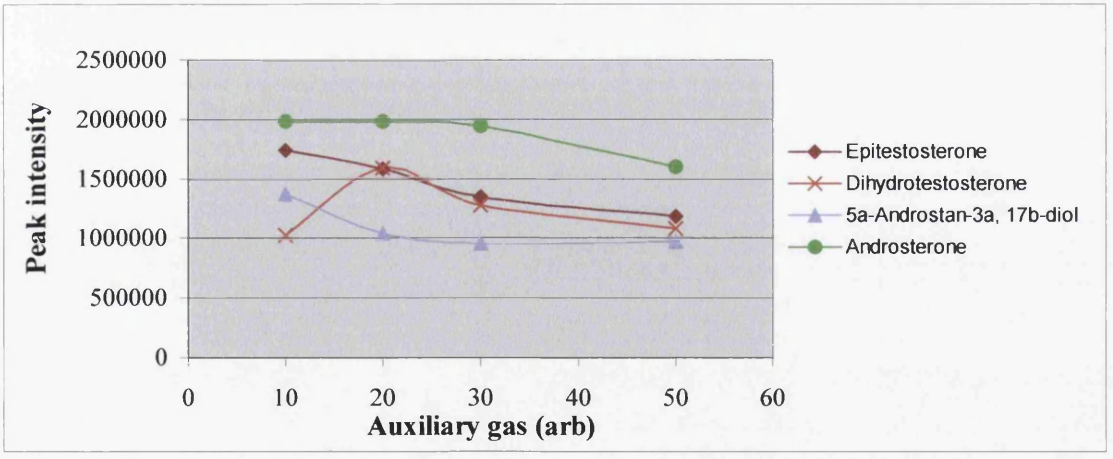

Varying the discharge current between 3 and 5.5 μA (Figure 4.6, e and f) was found, however, to have no significant effects on peak intensity. For most of the steroids,

the signals reached a maximum value when the discharge current was set to 3 μA; however, androsterone and dihydrotestosterone show the maximum values as the discharge current is at 4.5 μA. So the value of 3 μA was used for the future experiments.

(e)

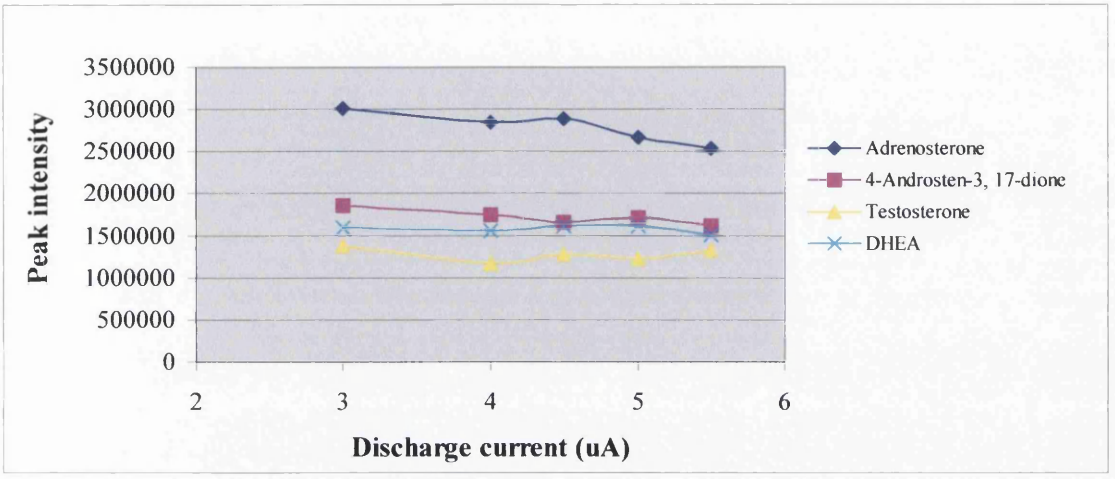

(f)

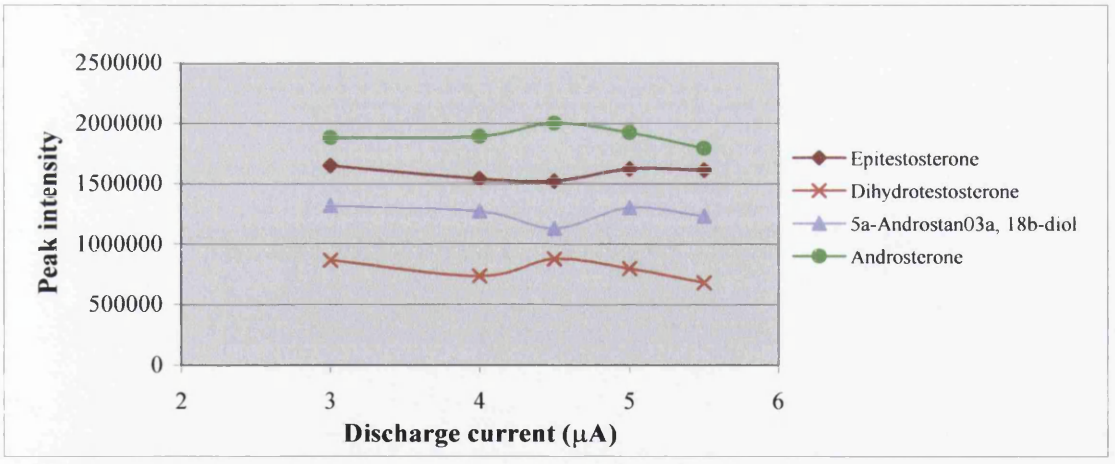

The vaporizer temperature was optimized between 350 °C and 550 °C. Testosterone was the only steroid almost unaffected by this change in vaporizer temperature. The effects upon the other androgenic steroids are shown in Figure 4.6 (g and h). Epitestosterone and androsterone gave the best signals as the temperature

increased to 450 °C and then dropped off if the temperature was further increase; whereas the other steroids, adrenosterone, DHEA, 5α-androstan-3α, 17β-diol and androsterone showed the sharp increasing signals as the temperature increased from 350 °C to 450 °C

(g)

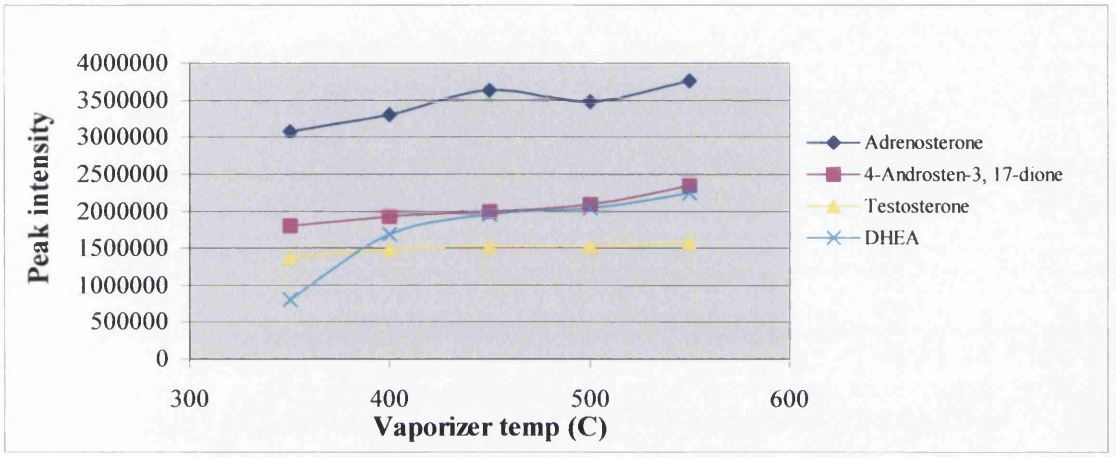

(h)

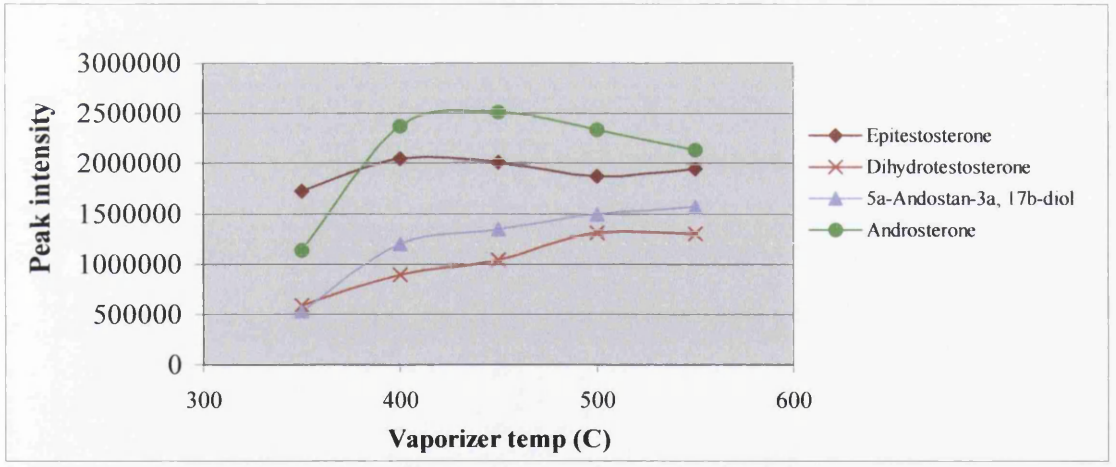

and then slowly increased to their maximum values as the temperature further increased to 550 °C. Δ_4-Androten-3, 17-dione gave the slightly increasing signal over the whole range from 350 °C to 550 °C. The vaporizer temperature was therefore set to 550 °C,

considering the maximum signal for most steroids and this temperature, whlist there was only a 5% drop off for epitestosterone and 15% for androsterone.

Finally the capillary temperature was optimized between 150 °C and 220 °C. Figure 4.6 (i and j) shows that significant decreases in intensities for Δ_4-androten-3, 17-dione, DHEA, 5α-androstan-3α, 17β-diol and androsterone were observed as the

(i)

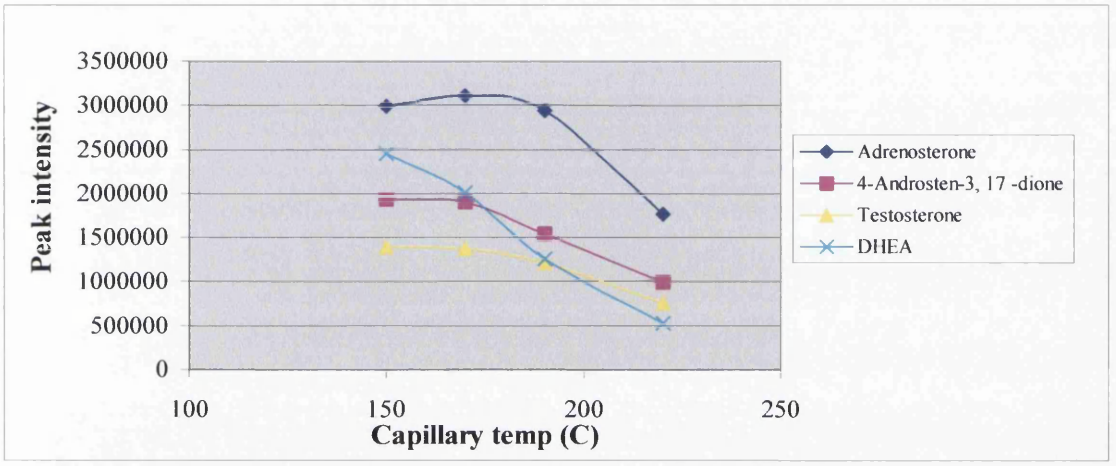

(j)

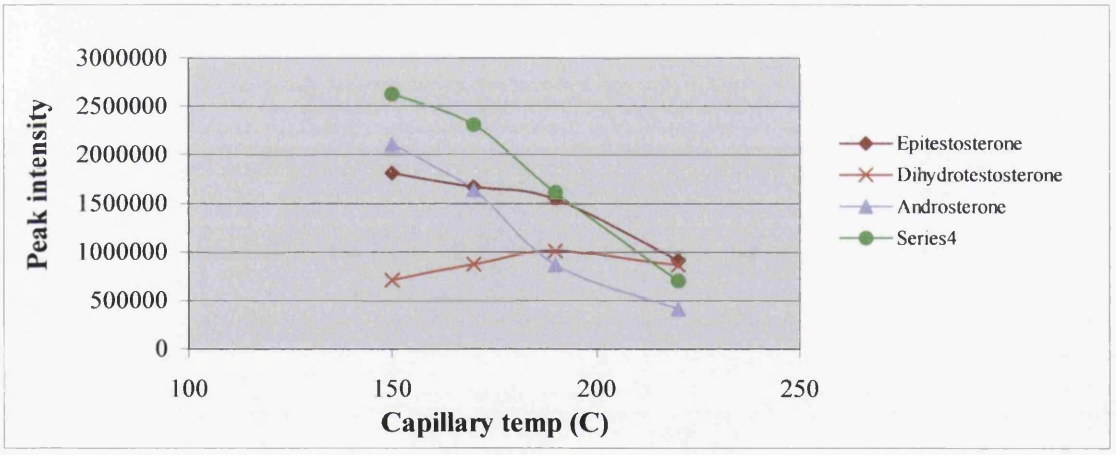

temperature increased from 175 °C and 220 °C, whilst, for adrenosterone, testosterone and epitestosterone much smaller decreases occurred. However, dihydrotestosterone exhibited an increase between 150 °C to 190 °C, after which the intensity decreases gradually as the temperature increases further. It was considered that at 150 °C in general

the steroids gave the best intensities, so this temperature was used for future analysis, although there was 30% drop in signal for dihydrotestosterone.

4.3.5 Limits of detection

To screen for the most sensitive scan mode for the mass spectrometer, five representative free androgenic steroids were chosen to test the limit of detections in full scan, SIM and SRM mode, and the signal to noise ratio was more than three (S/N > 3). Known weights of each steroid in the range of 0.5 to 1000 pg were injected in a volumn of 10 μl into the HPLC-MS system.

Table 4.5 shows that the sensitivities are about 5 to 25 times greater in SIM mode than in full scan mode, and there is similar sensitivity between full scan and SRM mode. The SIM mode was therefore chosen for future quantitative LC-MS experiments, although this approach was compromised by reduced specificity.

Table 4.5 Limits of detection of five androgenic steroids in different scan mode

Steroid	Full scan (pg)	SIM (pg)	SRM (pg)
Adrenosterone	10 (m/z 301)	0.5 (m/z 301)	10 (m/z 301→265)
Testosterone	25 (m/z 289)	1.0 (m/z 289)	50 (m/z 289→271)
DHEA	500 (m/z 271)	50 (m/z 271)	1000 (m/z 271→253)
Dihydrotestosterone	500 (m/z 291)	100 (m/z 291)	500 (m/z 291→255)
5α-Androstan-3α, 17β-diol	1000(m/z 257)	100 (m/z 257)	1000 (m/z 257→161)

4.3.6 Quantitative LC-MS for androgenic steroids

4.3.6.1 Analysis of variance of free androgenic steroids

In order to evaluate the replicate measurements of the experiment results within day and between days, a one-tailed F-test was used to compare the different mean of peak area. Analysis of variance (ANOVA) is a powerful statistical technique which can be used to separate and estimate the different causes of variation. ANOVA is used to test whether the difference between sample means is too great to be explained by the random error.

Table 4.6 Daily and overall mean (peak area) of the investigated steroids at three concentrations by repeated MS-SIM measurements

Steroid	Concentration (pg/μl)	Mean (xE+6)	Concentration (pg/μl)	Mean (xE+6)	Concentration (pg/μl)	Mean (xE+7)
Adrenosterone (m/z 301)	10	Day1 1.44	50	Day1 4.51	250	Day1 2.10
		Day2 1.35		Day2 4.84		Day2 1.98
		Day3 1.30		Day3 4.41		Day3 2.15
		Total 1.36		Total 4.58		Total 2.08
Δ_4-Androsten-3, 17-dione (m/z 287)	20	Day1 1.60	100	Day1 5.06	500	Day1 2.22
		Day2 1.27		Day2 5.03		Day2 2.13
		Day3 1.54		Day3 5.28		Day3 2.40
		Total 1.47		Total 5.12		Total 2.25
Testosterone (m/z 289)	20	Day1 1.47	100	Day1 4.96	500	Day1 2.17
		Day2 1.32		Day2 5.15		Day2 2.26
		Day3 1.40		Day3 4.65		Day3 2.37
		Total 1.40		Total 4.92		Total 2.27
Epitestosterone (m/z 289)	20	Day1 1.71	100	Day1 6.62	500	Day1 3.02
		Day2 1.53		Day2 6.15		Day2 3.07
		Day3 1.84		Day3 6.44		Day3 3.29
		Total 1.69		Total 6.40		Total 3.13
DHEA (m/z 271)	100	Day1 1.29	500	Day1 5.23	2500	Day1 2.20
		Day2 1.16		Day2 5.59		Day2 2.33
		Day3 1.31		Day3 5.54		Day3 2.46
		Total 1.25		Total 5.45		Total 2.33
DHT (m/z 291)	200	Day1 1.66	1000	Day1 8.46	5000	Day1 3.31
		Day2 1.64		Day2 8.85		Day2 3.55
		Day3 1.94		Day3 9.28		Day3 3.73
		Total 1.75		Total 8.86		Total 3.53
Androsterone (m/z 273)	100	Day1 1.74	500	Day1 5.63	2500	Day1 2.82
		Day2 1.59		Day2 6.22		Day2 2.82
		Day3 1.57		Day3 6.16		Day3 3.10
		Total 1.63		Total 6.00		Total 2.91
5α-Androstan-3α,17β-diol (m/z 257)	200	Day1 1.47	1000	Day1 5.54	5000	Day1 2.39
		Day2 1.65		Day2 5.72		Day2 2.48
		Day3 1.45		Day3 5.97		Day3 2.71
		Total 1.52		Total 5.74		Total 2.53

Table 4.7 Summary of ANOVA results for eight free androgenic steroids by repeated MS-SIM measurements

Steroid	Concentration (pg/μl)	Source of variation	Sum of squares	Degree of freedom	Mean square	F
Adrenosterone (m/z 301)	10	Intra-day	1.40 E+11	9	1.55 E+10	1.30
		Inter-day	1.80 E+11	2	2.01 E+10	
	50	Intra-day	1.56 E+12	9	1.73 E+11	2.42
		Inter-day	8.37 E+11	2	4.19 E+11	
	250	Intra-day	5.87 E+12	9	6.52 E+11	2.42
		Inter-day	3.16 E+12	2	1.58 E+12	
Δ_4-Androsten-3, 17-dione (m/z 287)	20	Intra-day	2.69 E+11	9	2.99 E+10	4.09
		Inter-day	2.44 E+11	2	1.22 E+11	
	100	Intra-day	3.25 E+11	9	3.61 E+10	2.03
		Inter-day	1.47 E+11	2	7.33 E+10	
	500	Intra-day	2.37 E+13	9	2.63 E+12	2.86
		Inter-day	1.51 E+13	2	7.53 E+12	
Testosterone (m/z 289)	20	Intra-day	1.61 E+11	9	1.79 E+10	1.39
		Inter-day	4.97 E+10	2	2.48 E+10	
	100	Intra-day	8.15 E+11	9	9.05 E+10	1.78
		Inter-day	5.24 E+11	2	2.62 E+11	
	500	Intra-day	1.17 E+13	9	1.30 E+12	2.08
		Inter-day	8.03 E+12	2	4.01 E+12	
Epitestosterone (m/z 289)	20	Intra-day	4.42 E+11	9	4.91 E+10	1.97
		Inter-day	1.94 E+11	2	9.69 E+10	
	100	Intra-day	8.82 E+11	9	9.80 E+10	2.25
		Inter-day	4.41 E+11	2	2.20 E+11	
	500	Intra-day	3.57 E+13	9	3.97 E+12	2.04
		Inter-day	1.62 E+13	2	8.09 E+12	
DHEA (m/z 271)	100	Intra-day	1.41 E+11	9	1.56 E+10	1.88
		Inter-day	5.88 E+10	2	2.94 E+10	
	500	Intra-day	8.85 E+11	9	9.84 E+10	1.60
		Inter-day	3.14 E+11	2	1.57 E+11	
	2500	Intra-day	2.13 E+13	9	2.37 E+12	2.75
		Inter-day	1.30 E+13	2	6.50 E+12	
DHT (m/z 291)	200	Intra-day	4.46 E+11	9	4.95 E+10	2.33
		Inter-day	2.31 E+11	2	1.16 E+11	
	1000	Intra-day	1.98 E+12	9	2.20 E+11	3.12
		Inter-day	1.37 E+12	2	6.86 E+11	
	5000	Intra-day	7.4 E+13	9	8.23 E+12	2.19
		Inter-day	3.61 E+13	2	1.80 E+13	
Androsterone (m/z 273)	100	Intra-day	2.41 E+11	9	2.68 E+10	1.34
		Inter-day	7.17 E+10	2	3.58 E+10	
	500	Intra-day	1.90 E+12	9	2.11 E+11	2.02
		Inter-day	8.55 E+11	2	4.28 E+11	
	2500	Intra-day	6.34 E+13	9	7.05 E+12	1.54
		Inter-day	2.17 E+13	2	1.08 E+13	
5α-Androstan-3α, 17β-diol (m/z 257)	200	Intra-day	2.81 E+11	9	3.12 E+10	1.53
		Inter-day	9.56 E+10	2	4.78 E+10	
	1000	Intra-day	5.97 E+11	9	6.64 E+10	2.82
		Inter-day	3.74 E+11	2	1.87 E+11	
	5000	Intra-day	6.43 E+13	9	7.14 E+12	1.58
		Inter-day	2.25 E+13	2	1.13 E+13	

To estimate the intra-day and inter-day precision, four repeated injections were made on three days at three different concentrations for each of the steroids. An ANOVA method was used to test for the difference between these means, and the results are summarized in Table 4.6 and 4.7. As shown in Table 4.7, the calculated values of F for each steroid at all concentrations are smaller than the critical value ($F_{critical}$ = 4.26, P = 0.05), so the inter-day variance of the SIM measurements does not significantly differ from the intra-day variance.

4.3.6.2 Precision and linearity

The reproducibility of the LC-MS method is described by the coefficient of variation (CV), and the corresponding values for each of the selected androgens are summarized in Table 4.8 (a to h). The % CV ranges from approximately 4% to 15% for total injection precisions, 4% to 13% for intra-day precisions and 5% to 24% for inter-day precisions. The variations from the inter-day injections are much bigger than from the intra-day injections, and adding an internal standard may decrease this variance.

The response of the base peak area in the mass spectra against various concentrations were studied for each of the steroids, and found to be linear in the relative low range of concentrations for adrenosterone, Δ_4-androsten-3, 17-dione, testosterone and epitestosterone (10 to 1000 pg/μl); and in the high range concentrations for the other steroids (100 pg/μl to 10 ng/μl). Correlation coefficients of the linear regression of these steroids are from 0.9991 up to 0.9998. Calibration curves and corresponding equations of each steroid are presented in Figure 4.7 (a to h).

Table 4.8 (a) Precision in the measurements of adrenosterone

Concentration (pg/μl)	Intra-day (% CV)	Inter-day (% CV)	Total (% CV)
10	9.1	10.4	9.4
50	9.0	14.1	10.1
250	4.0	6.3	4.5

Figure 4.7 (a) Calibration curve of adrenosterone

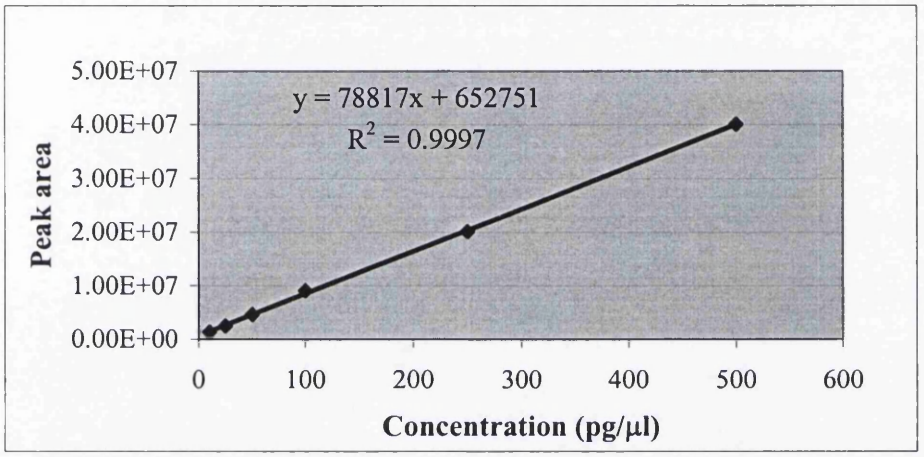

Table 4.8 (b) Precision in the measurements of Δ_4-androsten-3, 17-dione

Concentration (pg/μl)	Intra-day (%CV)	Inter-day (%CV)	Total (%CV)
20	11.8	23.8	14.7
100	3.7	5.3	4.0
500	7.2	12.2	8.4

Figure 4.7 (b) Calibration curve of Δ_4-androsten-3, 17-dione

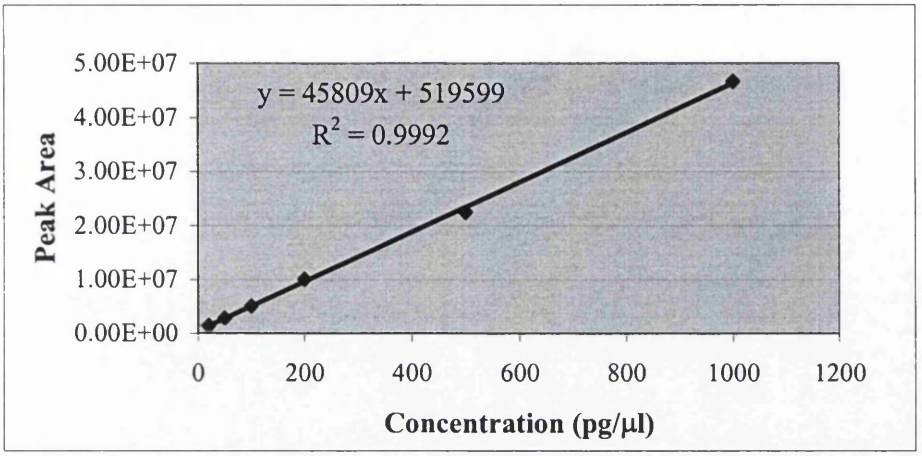

Table 4.8 (c) Precision in the measurements of testosterone

Concentration (pg/µl)	Intra-day (%CV)	Inter-day (%CV)	Total (%CV)
20	9.6	11.3	9.9
100	6.1	10.4	7.1
500	5.0	8.8	5.9

Figure 4.7 (c) Calibration curve of testosterone

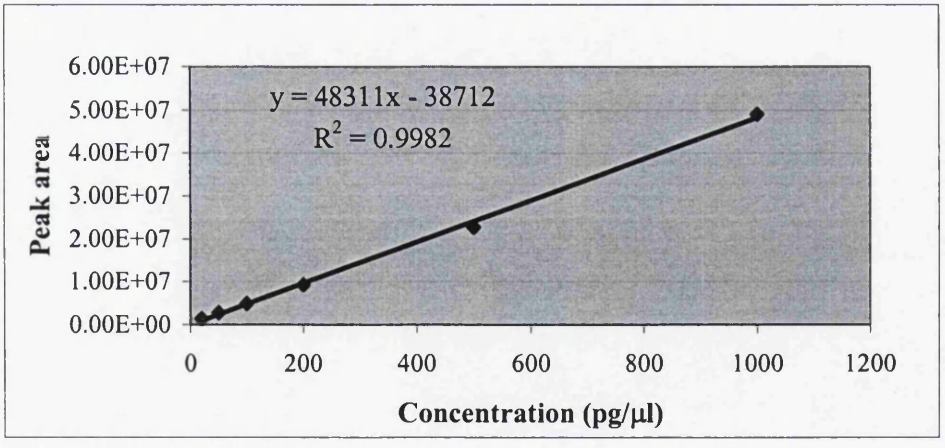

Table 4.8 (d) Precision in the measurements of epitestosterone

Concentration (pg/µl)	Intra-day (%CV)	Inter-day (%CV)	Total (%CV)
20	13.1	18.4	14.2
100	4.9	7.3	5.4
500	6.4	9.1	7.0

Figure 4.7 (d) Calibration curve of epitestosterone

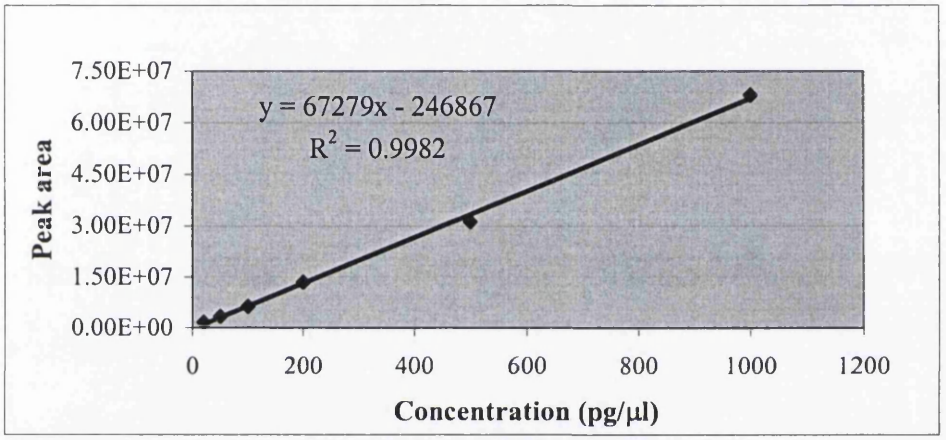

Table 4.8 (e) Precision in the measurements of DHEA

Concentration (pg/µl)	Intra-day (%CV)	Inter-day (%CV)	Total (%CV)
100	10.0	13.7	10.7
500	5.8	7.3	6.1
2500	6.6	11.0	7.6

Figure 4.7 (e) Calibration curve of DHEA

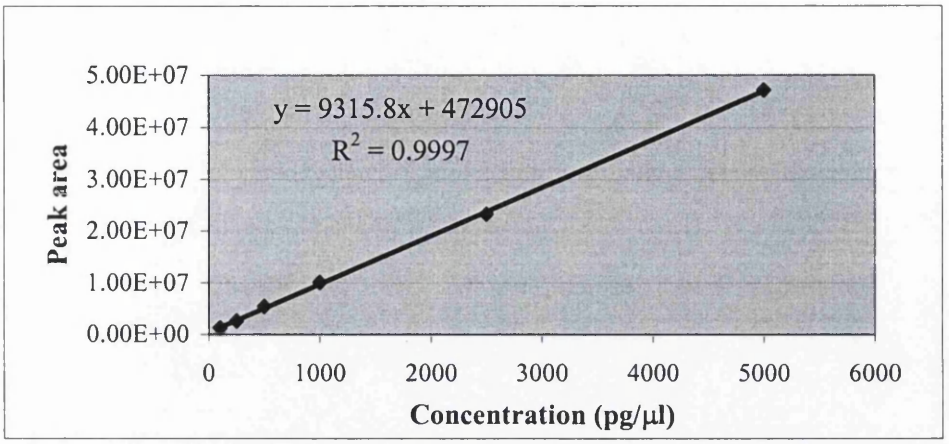

Table 4.8 (f) Precision in the measurements of dihydrotestosterone

Concentration (pg/µl)	Intra-day (%CV)	Inter-day (%CV)	Total (%CV)
200	12.7	19.5	14.2
1000	5.3	9.3	6.2
5000	8.1	12.0	9.0

Figure 4.7 (f) Calibration curve of dihydrotestosterone

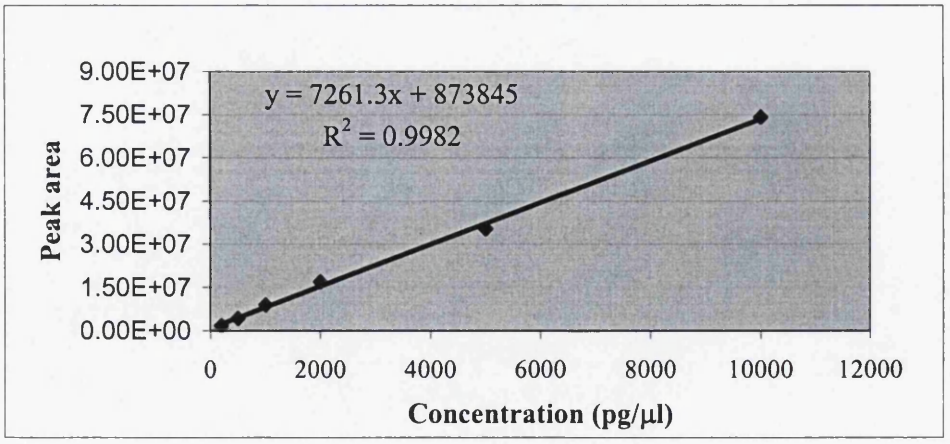

Table 4.8 (g) Precision in the measurements of androsterone

Concentration (pg/μl)	Intra-day (%CV)	Inter-day (%CV)	Total (%CV)
100	10.0	11.6	10.3
500	7.7	10.9	8.3
2500	9.1	11.3	9.6

Figure 4.7 (g) Calibration curve of androsterone

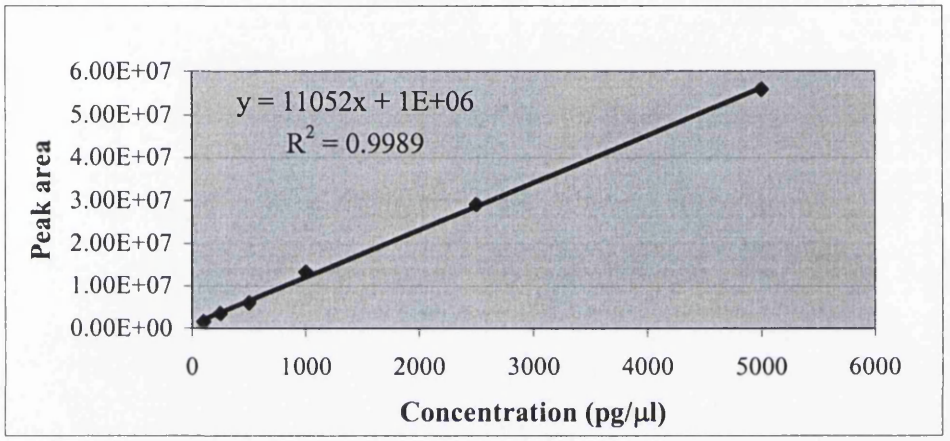

Table 4.8 (h) Precision in the measurements of androstan-3α, 17β-diol

Concentration (pg/μl)	Intra-day (%CV)	Inter-day (%CV)	Total (%CV)
200	11.6	14.4	12.2
1000	4.5	7.5	5.2
5000	10.6	13.3	11.1

Figure 4.7 (h) Calibration curve of androstan-3α, 17β-diol

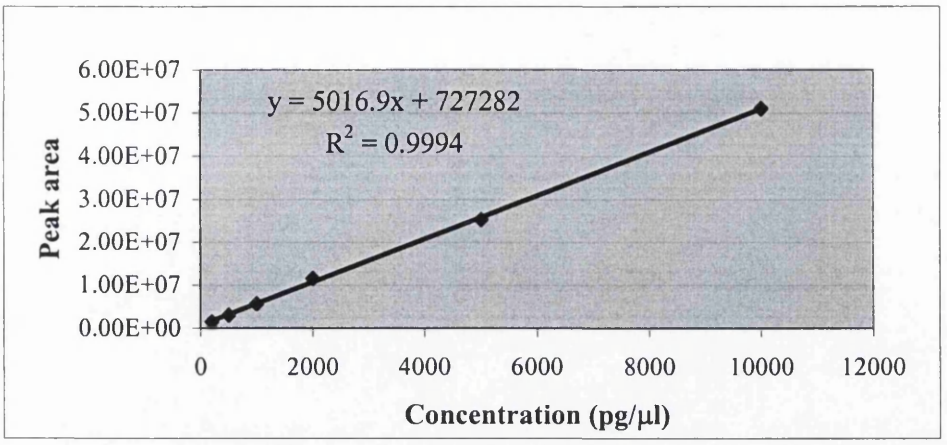

4.3.6.3 Limits of quantitation

The limit of quantitation is defined as $Y_{Blank} + 10S_{Blank}$ [30], and the values of each steroid were calculated using regression lines of y on x from the appropriate calibration curve above. The results were shown in Table 4.9. The steroids with 4-ene-3-one structures had relatively low limits of quantitation between 2.5 and 4.2 pg, but the androgens without this structure had much higher limits of quantitation, the values ranging from 17.5 to 38.6 pg (Table 4.9).

Table 4.9 Limits of quantitation of the free androgenic steroids

Steroid	Limit of quantitation (pg)
Adrenosterone	2.5
Δ_4-Androsten-3, 17-dione	4.2
Testosterone	4.0
Epitestosterone	2.9
DHEA	20.8
Dihydrotestosterone	26.7
Androsterone	17.5
5α-Androstan-3α, 17β-diol	38.6

4.4 Androgenic steroid conjugates

4.4.1 HPLC-UV

Compared to the free steroids, the polarities of steroid conjugates are much increased due to introduction of the glucuronide or sulfate group. Therefore, most of the steroid conjugates were not retained in the C18 or C8 column, so a more polar phenyl-hexyl column was chosen for the separation of the steroid conjugates of interest.

The gradient acetonitrile/ ammonium formate system (section 4.2.2) was used for the separation of seven selected steroid conjugates. However, there is UV absorbance for the buffer system at 200 nm, which is the maximum absorbance for most of steroid conjugates, therefore UV detection is not suitable for quantitative analysis for most of steroid conjugates.

Figure 4.8 HPLC separation of seven steroid conjugates and detected by UV at 210 nm

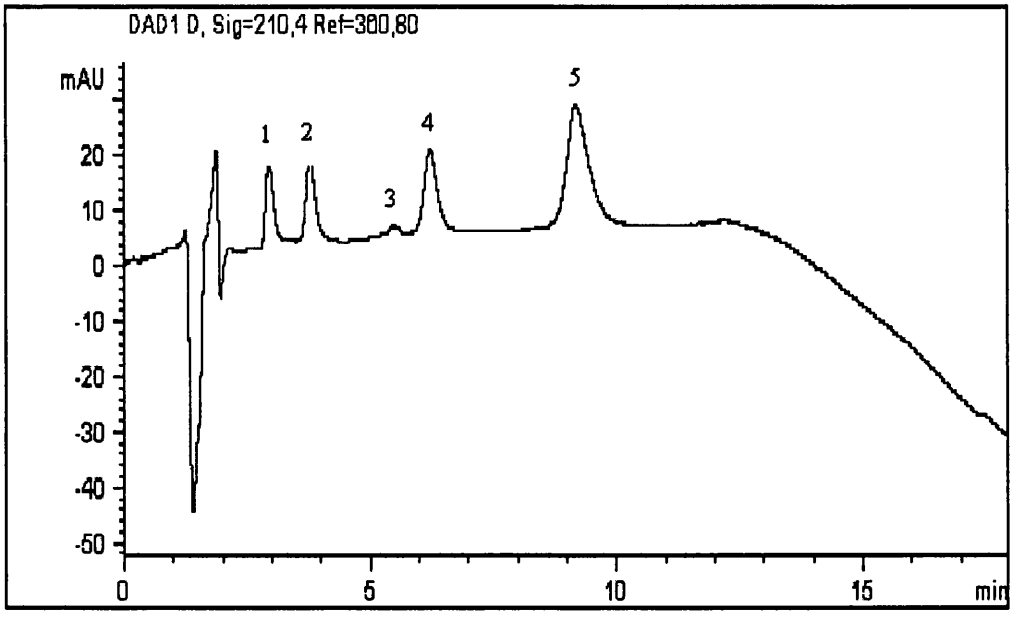

Sample was injected at 20 µl and 100µg/ml for each compound.
* 5α-Androstan-3α, 17β-diol glucuronide and androsterone sulfate are not detectable by UV.
1. Testosterone glucuronide, 2. DHEA glucuronide, 3. Androsterone glucuronide,
4. Testosterone sulfate, 5. DHEA sulfate

4.4.2 HPLC-MS

4.4.2.1 Separation of seven steroid conjugates by HPLC-MS

The same acetonitrile/ammonium formated gradient system was applied for the separation of the steroid conjugates for HPLC-MS, and based on the results described in Chapter 3, negative ESI mode was chosen for quantitative analysis of the steroid conjugates. For compatibility with ESI/MS, micro-bore a phenyl-hexyl column was used with a flow rate of 0.2 ml/min. Figure 4.9 shows the extracted ion chromatograms for the separation of seven steroid conjugates.

Figure 4.9 Extracted ion current chromatograms of seven steroid conjugates by HPLC-MS

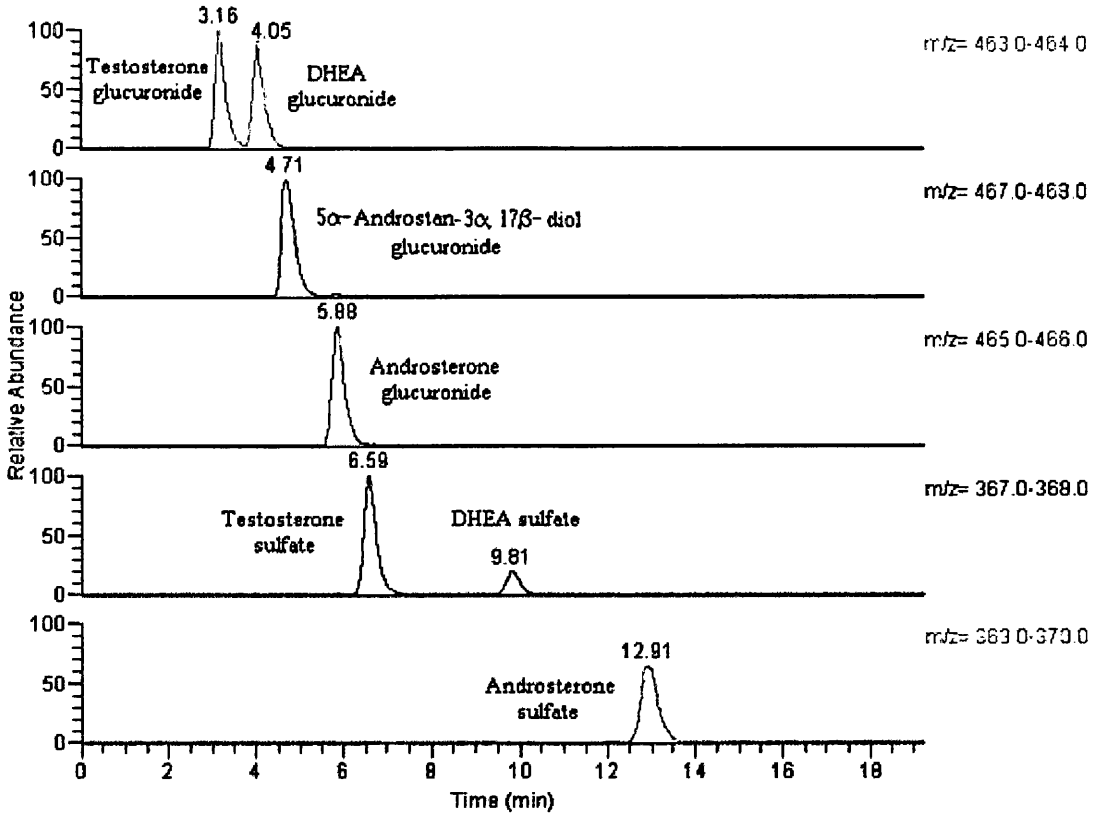

Note: sample was injected at 20 μl and 10pg/μl for each compound.

4.4.2.2 Optimization of buffer concentration for HPLC-MS

To optimize the buffer concentration of ammonium formate, the mixture of seven steroid conjugates was injected into the HPLC-ESIMS system with 10, 20, 30, 50 and 100 mM buffer respectively. With the buffer concentration increasing, the response signal decreased avove 20 mM, decreasing sharply after 50 mM, and showing a 65% drop at 100 mM (Figure 4.10). Figure 4.11 shows the total ion chromatograph at 10, 30 and 100 mM buffer concentrations. It was observed that as the buffer concentration increased, the retention times became longer and the background noisier. Therefore, the buffer concentration of 10 mM was chosen for steroid conjugate separation, as it offered the best detector response, low contamination of the mass spectrometer source and lower retention times.

Figure 4.10 Optimization of buffer concentration for steroid conjugate separation by HPLC-MS

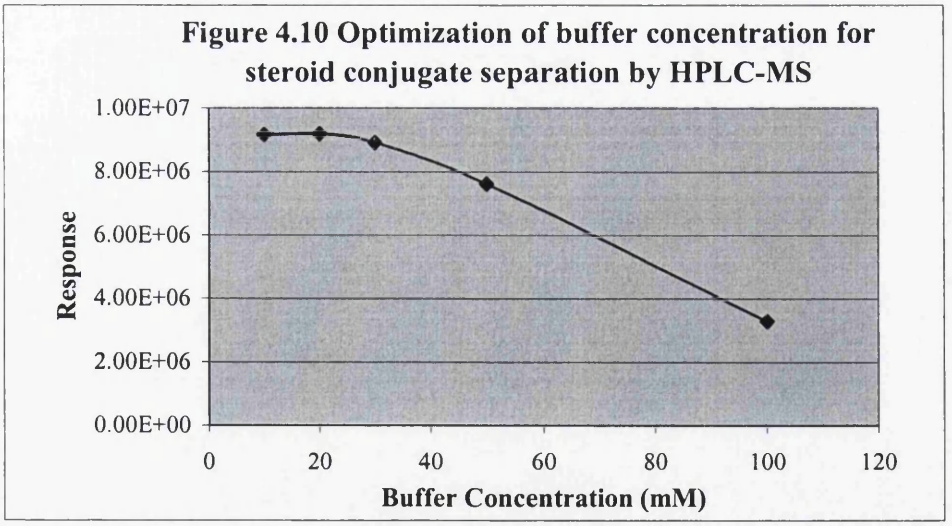

Figure 4.11 Total ion chromatographs of seven steroid conjugates separated with different buffer concentrations

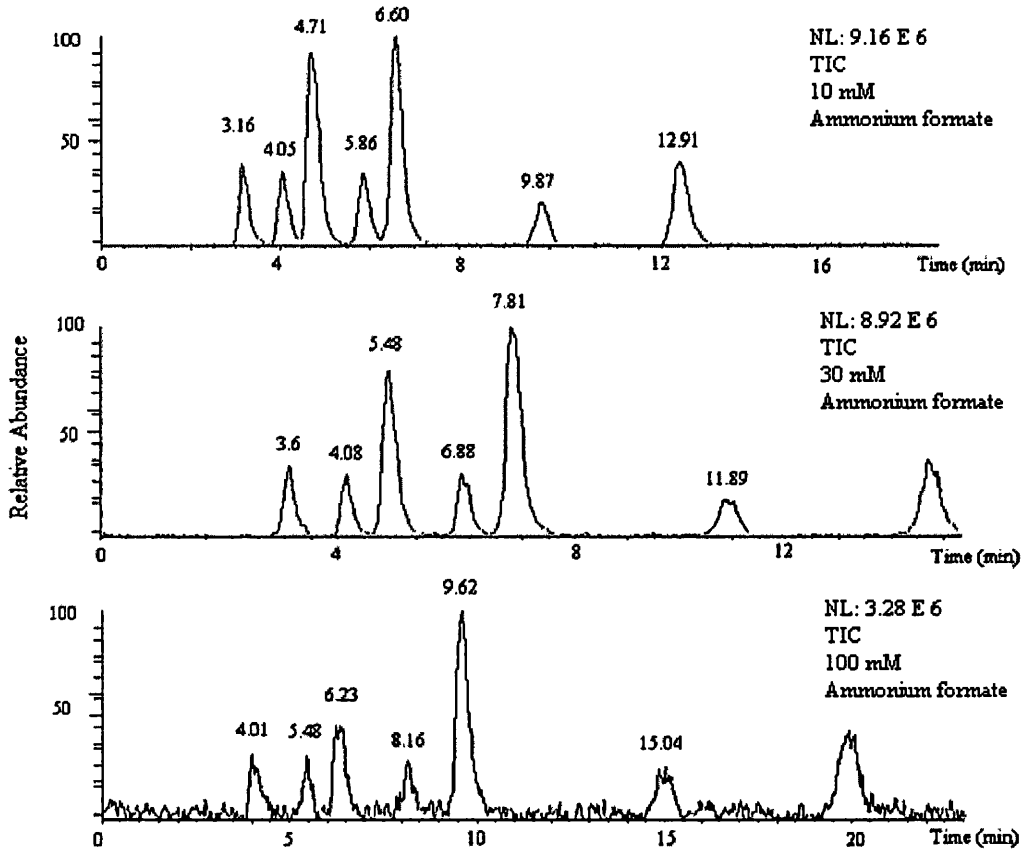

Note: sample was injected at 20 µl and 10pg/µl for each compound.

4.4.2.3 Optimization LC-ESI-MS

The mass spectrometer parameters were also optimized for LC-ESI-MS of the conjugated androgens at a flow rate of 0.2 ml/min. First, the sheath gas levels were tested between 60 and 100 arb. As figure 4.12 (a and b) shows intensities increased as the sheath gas levels were increased to 100 arb for testosterone glucuronide (T G), 5α-androstan-3α, 17β-diol (Diol G), androsterone glucuronide (A G) and androsterone sulfate (A S), with dehydroisoandrosterone sulfate (DHEA S) showing an increase to

optimum intensity at between 70 and 100 arb, whereas, dehydroisoandrosterone glucuronide (DHEA G) and testosterone sulfate (T S) exhibit maximum intensities at 90 arb and then show a small decline as the sheath gas levels are further increased to 100 arb. The sheath gas level was therefore set to100 arb, as this provided the best overall ionization for the majority of the steroid conjugates.

Figure 4.12 Optimization of some important MS parameters for eight androgenic steroids

(a)

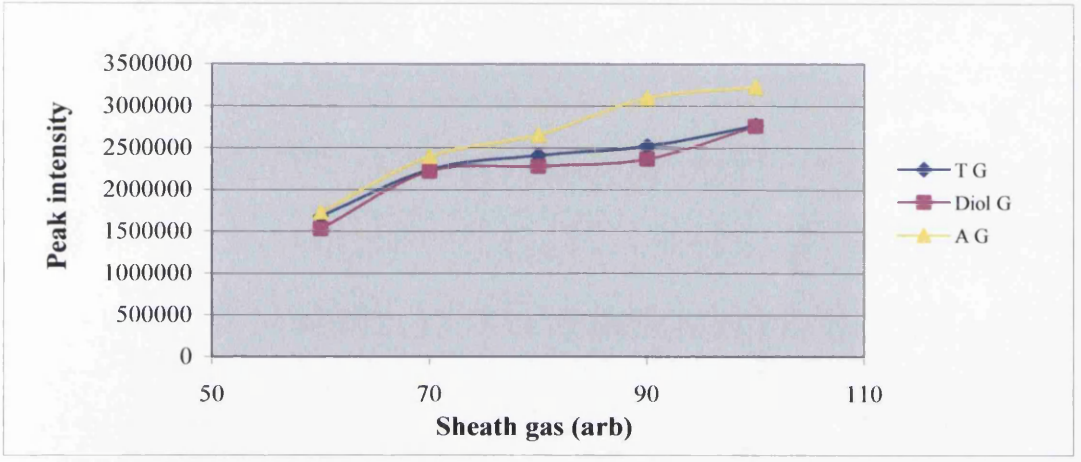

(b)

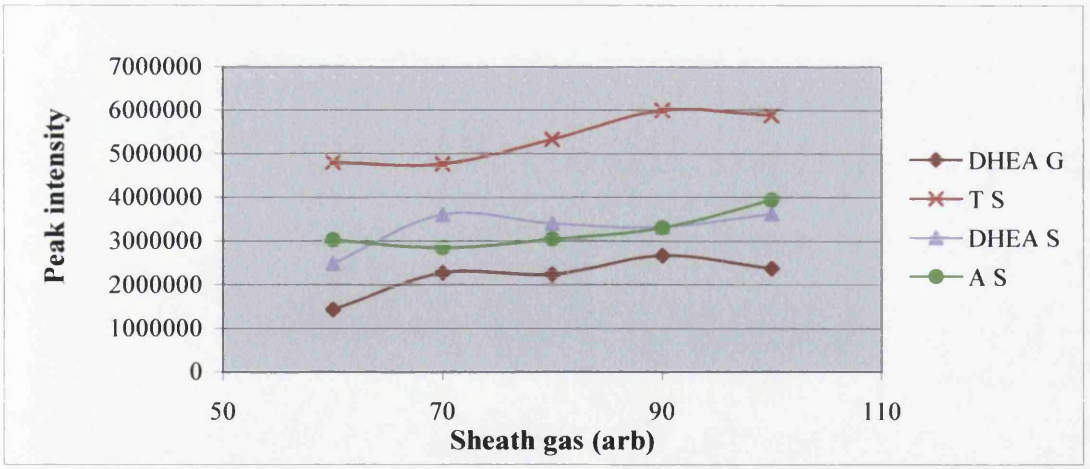

The auxiliary gas levels were altered between 10 and 60 arb, and the resulting intensities of the steroid conjugates against this variation are presented in Figure 4.12 (c

and d). Except for A G, which showed no significant change in signal as the sheath gas level was varied in this range, most of the investigated steroid conjugates showed increases to optimum ionization as the auxiliary gas levels were increased to 20 arb, which then decreased to minimum values as the gas levels were increased to 30 to 60 arb. Sheath gas level were therefore set to 20 arb for further experiments.

(c)

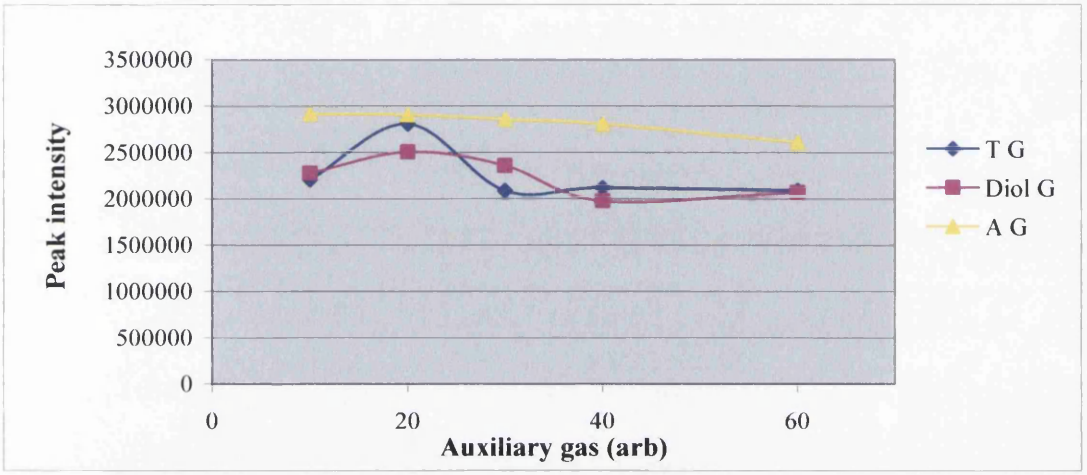

(d)

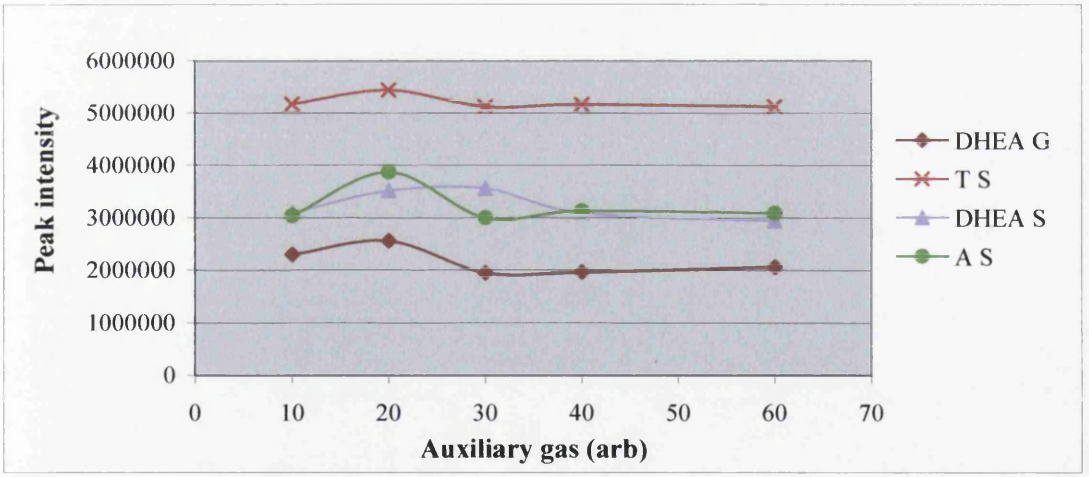

The spray voltage was optimized between 2.5 and 4.5 kV. Figure 4.12 (e and f) show that base peak intensities were significantly affected by spray voltage variation. Of the steroid conjugates, DHEA G and T G exhibit increases in signals from 2.5 to 3 kV,

little further change between 3 and 4 kV, and then a sharp decrease from 4 to 4.5 kV. The other steroid conjugates showed parabolic curves between 2.5 and 4.5 kV (Figure 4.12 e and f) with maximum intensities at 3.5 kV. There was only an approximate 5% drop in signal for T G if the spray voltage was set to 3.5 kV, thus this value was selected for later experiments because it was the best value for the majority of the steroid conjugates.

(e)

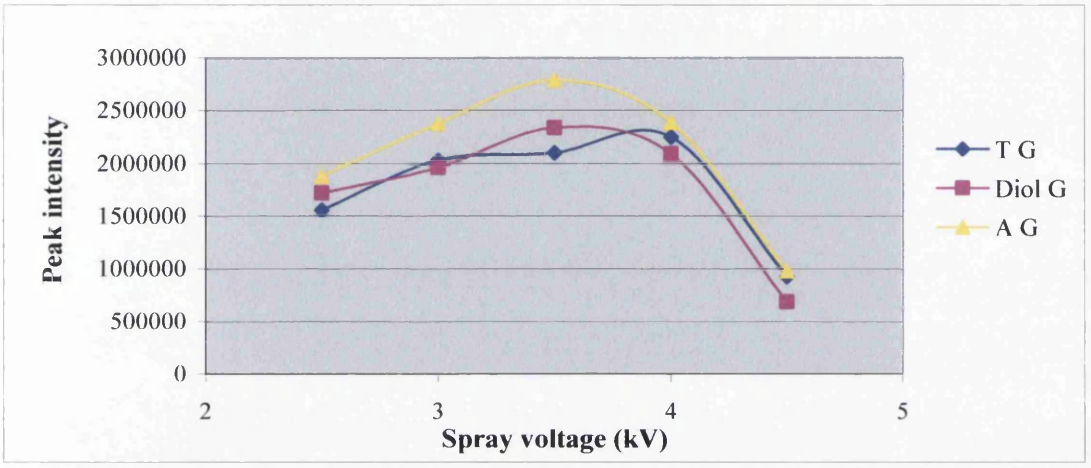

(f)

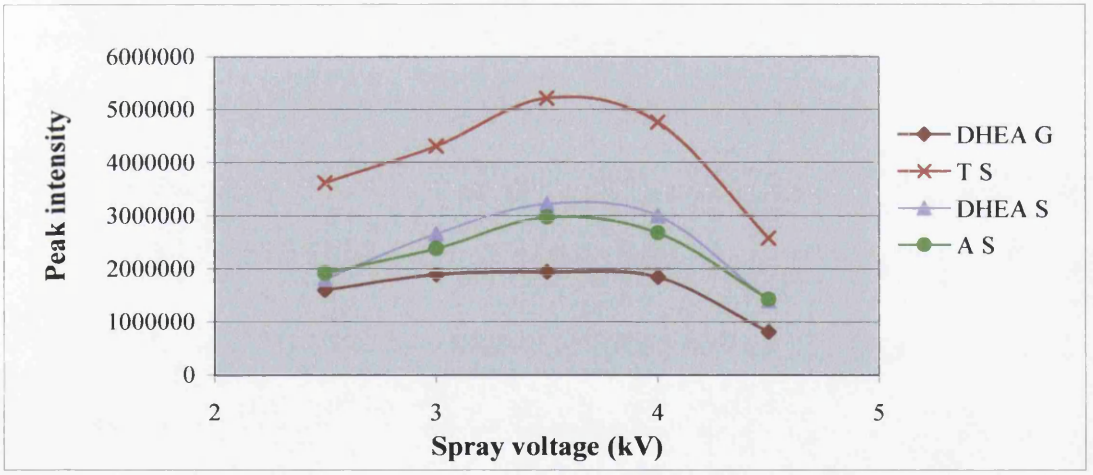

Finally the capillary temperature was varied between 170 and 250 °C. As shown in Figure 4.12 (g and h), each conjugate showed a characteristic response to increased capillary temperature. Diol G, DHEA G and A S exhibited a similar response when the

capillary temperature was changed, and gave an optimum signal with a capillary temperature of 200 °C. A G and T S gave an optimum signal at between 200 and 220°C, and this intensity tended to decrease sharply as the capillary temperature was increased.

(g)

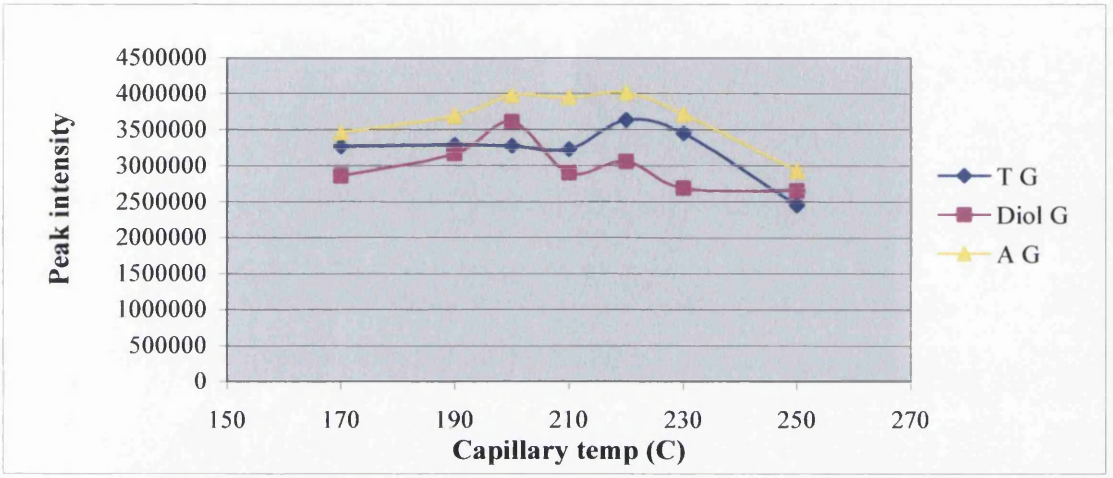

(h)

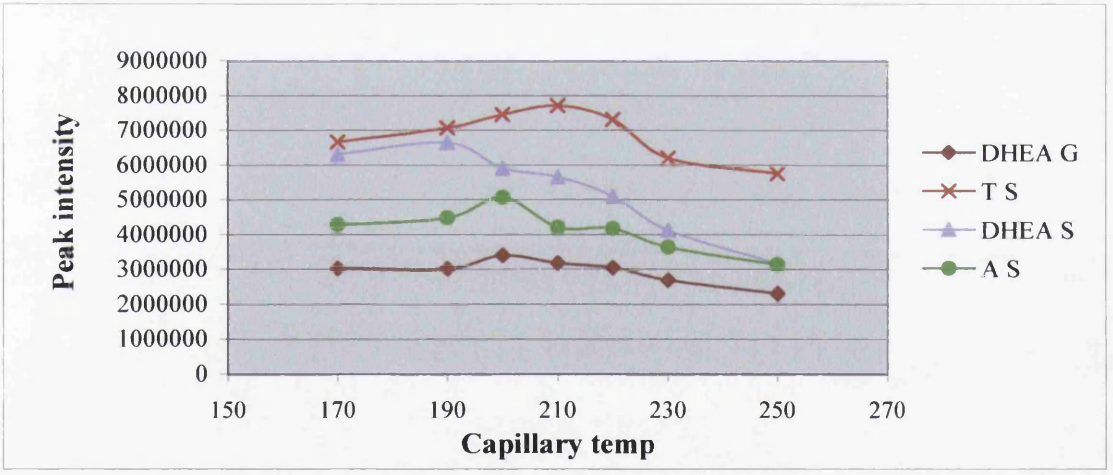

DHEA S on the other hand showed the best intensity at 190 °C, whereas T G exhibits a stable intensity between 170 and 210 °C, and a maximum intensity as the temperature increased to 220 °C, the signal decreasing as the temperature was increased further. Overall a capillary temperature of 200 °C gives an optimum intensity for four of the

seven steroid conjugates whilst having the least effect on the optimum signal of the other steroid conjugates, so this temperature was used for the further analysis.

4.4.2.4 Mass spectra of seven steroid conjugates by HPLC-MS

The ion distribution to TIC for each of steroid conjugates was summarized in Table 4.10. The major ions observed using the optimized conditions of HPLC-MS were the deprotonated molecule $[M-H]^-$, sodium formate adduct $[M-H+HCOONa]^-$, deprotonated dimer $[2M-H]^-$ and, for testosterone glucuronide, DHEA glucuronide and androsterone glucuronide, sodium adduct dimer $[2M-2H+Na]^-$. For steroid sulfates and 5α-androstan-3α, 17β-diol glucuronide, the desodium ion $[M-Na]^-$ was intense and accompanied by a formid adduct $[M+HCOO]^-$, the desodium dimer $[2M+H-2Na]^-$ and $[2M-Na]^-$. The intensity of the deprotonated molecule or desodiated ion far exceeds that of any of the other ions, and so the deprotonted or desodiated ions were selected as the most useful ions for quantitative analysis.

Table 4.10 Distributions of the major ions of the eight conjugated androgens (%TIC)

Ion	T G	DHEA G	Diol G	A G	T S	DHEA S	A S
$[M-H]^-$	67	67	_	71	_	_	_
$[M-H+HCOONa]^-$	8	9	_	8	_	_	_
$[2M-H]^-$	6	9	_	8	_	_	_
$[2M-2H+Na]^-$	2	2	_	2	_	_	_
$[M-Na]^-$	_	_	65	_	86	73	73
$[M+HCOO]^-$	_	_	7	_	2	7	5
$[2M+H-2Na]^-$	_	_	14	_	2	1	3
$[2M-Na]^-$	_	_	3	_	4	3	8

4.4.3 Limits of detection

Five steroid conjugates were tested for the different scan modes (Full scan, SIM and SRM) to screen for the most sensitive detection method. Table 4.11 shows the limits of detection of these steroid conjugates by different scan mode, and, in the majority of cases, the sensitivity of detection in SIM mode is about ten times greater than that in full scan mode, and two times higher than in SRM mode. Therefore, the SIM mode was used for further quantitative analyses.

Table 4.11 Limits of detection of five steroid conjugates in different scan modes

Steroid conjugate	Full scan (pg)	SIM (pg)	SRM (pg)
Testosterone glucuronide	500 (m/z 463)	50 (m/z 463)	100 (m/z 463→445)
5α-Androstan-3α, 17β-diol glucuronide	500 (m/z 467)	50 (m/z 467)	100 (m/z 467→449)
Androsterone glucuronide	500 (m/z 465)	50 (m/z 465)	100 (m/z 465→447)
Testosterone sulfate	250 (m/z 367)	25 (m/z 367)	50 (m/z 367→352)
Androsterone sulfate	250 (m/z 369)	25 (m/z 369)	_

4.4.4 Quantitative LC-MS for androgenic steroid conjugates

4.4.4.1 Analysis of variance of androgenic steroid conjugates

An ANOVA method was also used to analysis the variances for the five androgenic steroid conjugates, and results were summarized in Tables 4.12 and 4.13.

Table 4.12 Daily and overall mean (peak area) of the investigated steroid conjugates at three concentrations by repeated MS-SIM measurements

Steroid conjugate	Concentra-tion (pg/μl)	Mean (x E+5)	Concentrtra-tion (pg/μl)	Mean (x E+6)	Concentra-tion (pg/μl)	Mean (x E+7)
T G (m/z 463)	100	Day1 3.21	1000	Day1 2.97	5000	Day1 1.38
		Day2 3.58		Day2 3.03		Day2 1.53
		Day3 3.27		Day3 3.42		Day3 1.61
		Total 3.35		Total 3.14		Total 1.51
Diol G (m/z 467)	100	Day1 3.20	1000	Day1 2.85	5000	Day1 1.35
		Day2 3.70		Day2 3.13		Day2 1.53
		Day3 3.53		Day3 3.36		Day3 1.48
		Total 3.48		Total 3.11		Total 1.45
A G (m/z 465)	100	Day1 4.89	1000	Day1 4.26	5000	Day1 2.09
		Day2 5.60		Day2 4.55		Day2 2.34
		Day3 5.35		Day3 5.04		Day3 2.21
		Total 5.28		Total 4.62		Total 2.22
T G (m/z 367)	50	Day1 3.83	500	Day1 3.34	1000	Day1 1.67
		Day2 4.22		Day2 3.83		Day2 1.82
		Day3 3.62		Day3 3.95		Day3 1.87
		Total 3.89		Total 3.70		Total 1.79
A S (m/z 369)	50	Day1 3.52	500	Day1 3.18	1000	Day1 1.50
		Day2 3.52		Day2 3.54		Day2 1.66
		Day3 4.07		Day3 3.55		Day3 1.72
		Total 3.70		Total 3.42		Total 1.63

A one-tailed F-test was used to test the significant difference between intra-day and inter-day variance. All the calculated F values shown in Table 4.13 are smaller than the critical F value ($F_{critical}$ = 4.26, P = 0.05), therefore, we can conclude that there is no significant difference between intra-day and inter-day variance.

Table 4.13 Summary of ANOVA results for five androgenic steroid conjugates by repeated MS-SIM measurements

Steroid conjugate	Concentration (pg/μl)	Source of variation	Sum of squares	Degree of freedom	Mean square	F
T G (m/z 463)	100	Intra-day	5.74 E+9	9	6.38 E+8	2.51
		Inter-day	3.20 E+9	2	1.60 E+9	
	1000	Intra-day	1.58 E+12	9	1.75 E+11	1.35
		Inter-day	4.74 E+11	2	2.37 E+11	
	5000	Intra-day	1.25 E+13	9	1.39 E+12	3.95
		Inter-day	1.10 E+13	2	5.50 E+12	
Diol G (m/z 467)	100	Intra-day	1.53 E+10	9	1.70 E+9	1.53
		Inter-day	5.23 E+9	2	2.61 E+9	
	1000	Intra-day	9.40 E+11	9	1.04 E+11	2.47
		Inter-day	5.17 E+11	2	2.58 E+11	
	5000	Intra-day	1.98 E+13	9	2.20 E+12	1.64
		Inter-day	7.22 E+12	2	3.61 E+12	
A G (m/z 465)	100	Intra-day	1.56 E+10	9	1.74 E+9	2.99
		Inter-day	1.04 E+10	2	5.19 E+9	
	1000	Intra-day	2.49 E+12	9	2.77 E+11	2.27
		Inter-day	1.26 E+12	2	6.29 E+11	
	5000	Intra-day	1.57 E+13	9	1.75 E+12	3.58
		Inter-day	1.25 E+13	2	6.26 E+12	
T S (m/z 367)	50	Intra-day	9.81 E+9	9	1.09 E+9	3.39
		Inter-day	7.39 E+9	2	3.70 E+9	
	500	Intra-day	1.27E+12	9	1.41 E+11	2.96
		Inter-day	8.35 E+11	2	4.18 E+11	
	2500	Intra-day	2.07 E+13	9	2.30 E+12	1.87
		Inter-day	8.60 E+12	2	4.30 E+12	
A S (m/z 369)	50	Intra-day	2.28 E+10	9	2.53 E+9	1.56
		Inter-day	7.92 E+9	2	3.96 E+9	
	500	Intra-day	9.62 E+11	9	1.07 E+11	1.64
		Inter-day	3.50 E+11	2	1.75 E+11	
	2500	Intra-day	1.68 E+13	9	1.86 E+12	2.95
		Inter-day	1.10 E+13	2	5.49 E+12	

4.4.4.2 Precision and linearity

Precision in the measurements of the steroid conjugates was also studied by repeatedly injecting samples at three different concentrations (100 pg/μl, 1 ng/μl and 5 ng/μl for steroid glucuronides; 50, 500 pg/μl and 2.5 ng/μl for steroid sulfates) over three

days. The intra-day coefficient variances are between 6.0% and 13.6%, and the inter-day values range from 11.3% to 17.5%, whereas the total coefficient variances are from 7.2% to 14.3% (Table 4.14 a to e). It seemed that the precisions for steroid conjugates using the ESI source are not as good as those of free steroids with APCI source, this may be because the ESI source is more sensitive to interferences.

Responses to all the five steroid conjugates were found linear in the investigated range of concentrations (100 pg/μl to 10 ng/μl for steroid glucuronides and 50 pg/μl to 2.5 ng/μl for steroid sulfates). Correlation coefficients of linear regression are from 0,9997 up to 0.9999. Calibration curves and regression equation are presented in Figure 4.13 (a to e).

Table 4.14 (a) Precision in the measurements of testosterone glucuronide

Concentration (pg/μl)	Intra-day (%CV)	Inter-day (%CV)	Total (%CV)
100	7.5	11.9	8.5
1000	13.3	15.5	13.8
5000	7.8	15.6	13.8

Figure 4.13 (a) Calibration curve of testosterone glucuronide

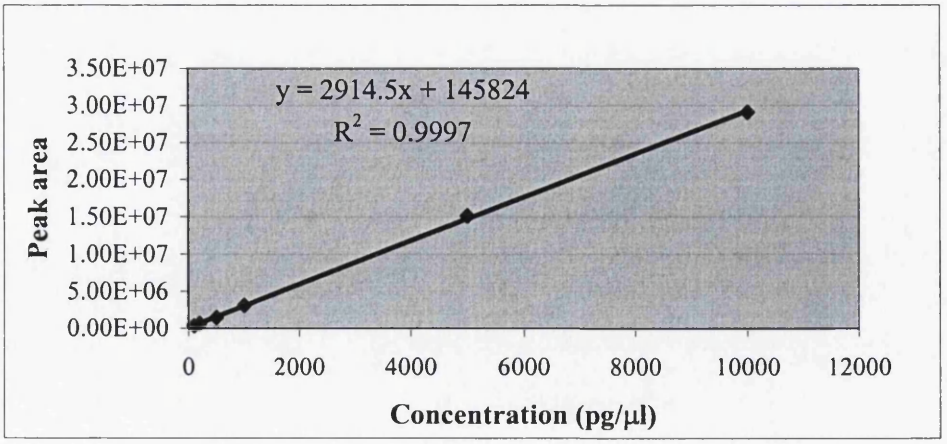

Table 4.14 (b) Precision in the measurements of 5α-androstan-3α, 17β-diol glucuronide

Concentration (pg/μl)	Intra-day (%CV)	Inter-day (%CV)	Total (%CV)
100	11.9	14.7	12.4
1000	10.4	16.3	11.7
5000	10.2	13.1	10.8

Figure 4.13 (b) Calibration curve of 5α-Androstan-3α, 17β-diol glucuronide

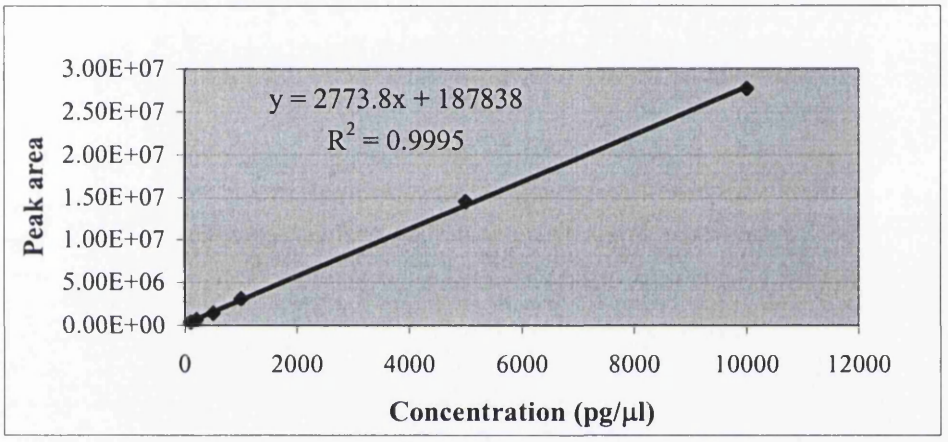

Table 4.14 (c) Precision in the measurements of androsterone glucuronide

Concentration (pg/μl)	Intra-day (%CV)	Inter-day (%CV)	Total (%CV)
100	7.9	13.6	9.2
1000	11.4	17.2	12.7
5000	6.0	11.3	7.2

Figure 4.13 (c) Calibration curve of androsterone glucuronide

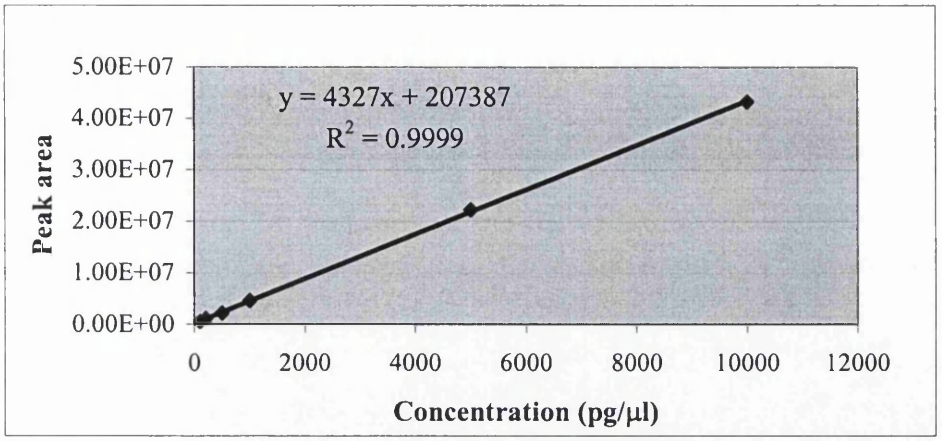

Table 4.14 (d) Precision in the measurements of testosterone sulfate

Concentration (pg/µl)	Intra-day (%CV)	Inter-day (%CV)	Total (%CV)
50	8.5	15.6	10.1
500	10.2	17.5	11.8
2500	8.5	11.6	9.1

Figure 4.13 (d) Calibration curve of testosterone sulfate

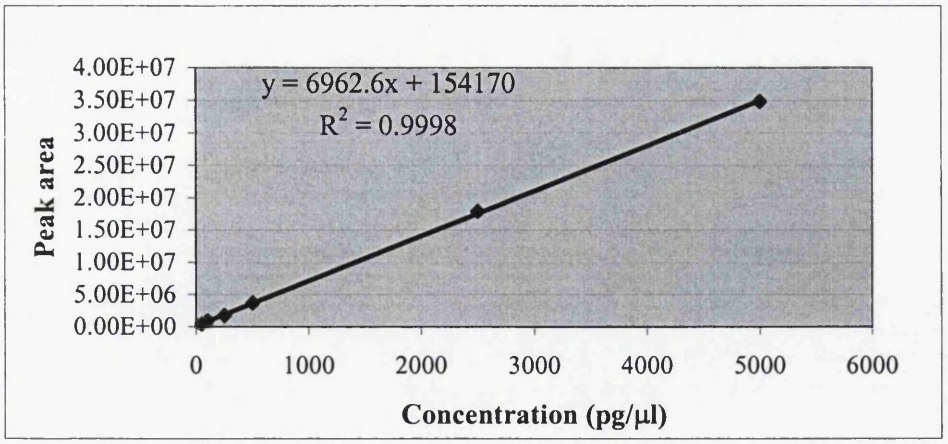

Table 4.14 (e) Precision in the measurements of androsterone sulfate

Concentration (pg/μl)	Intra-day (%CV)	Inter-day (%CV)	Total (%CV)
50	13.6	17.0	14.3
500	9.6	12.2	10.1
2500	8.4	14.4	9.8

Figure 4.13 (e) Calibration curve of androsterone sulfate

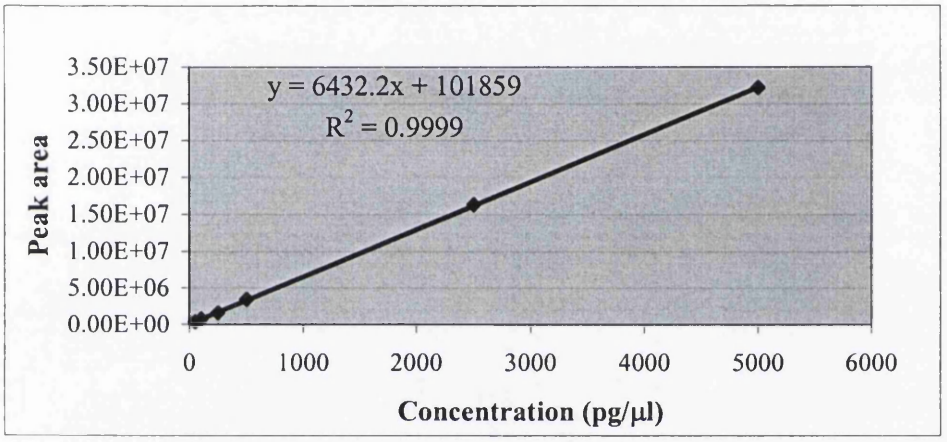

4.4.4.3 Limits of quantitation

Limits of quantitation of each steroid conjugate were also studied based on the regression lines of y on x from the calibration curves above, and the results were present in Table 4.15. The limits of quantitation of steroid glucuronides ranged from 89.4 to 139.6 pg, whilst lower values, from 60.2 to 55.6 pg, were obtained for steroid sulfates.

Table 4.15 Limits of quantitation of the steroid conjugates

Steroid conjugate	Limit of quantitation (pg)
Testosterone glucuronide	132.8
5α-Androstan-3α, 17β-diol glucuronide	139.6
Androsterone glucuronide	89.4
Testosterone sulfate	55.6
Androsterone sulfate	60.2

4.5 Conclusions

LC-MS methods were developed in the aim of quantitative analysis of some androgenic steroids and their glucuronide or sulfate conjugates in this chapter. C18 and C8 columns were compared to get the better separation for the androgenic steroids, and then a LC-APCI/MS method was used to successfully detect and identify testosterone from male and female plasma samples. In order to increase the sensitivity, APCI/MS parameters were optimized for a micro-bore column employing a lower flow rate to give the best intensities of their characterized peaks of these steroids. Limits of detection for different scan modes were determined and compared, and the more sensitive SIM mode was chosen for the simultaneous quantitative analysis of eight free steroids. An ANVOA method was used to estimate the variance. The precision and the linearity of quantitation for each compound were determined.

In the second part of this chapter, a LC-ESI/MS method was developed and the parameters of ESI/MS were optimized for the analysis the steroid conjugates. Following a similar procedure to the free steroids, the SIM scan mode was determined as the most appropriate mode for quantitative analysis of five steroid conjugates, and the precision,

linearity and the limit of quantitation were similarly evaluated for each of these conjugates.

The LC-MS technique discussed in this chapter has provided a reliable for the determination of steroids and their conjugates in the biological fluids. Moreover, it generates structural information at the same time of analysis, and it only detects ionizable components in the specified mass range, thus avoiding many interferences by choice of a mass range or "window" applicable to the compounds of interest, therefore, this technique is more specific compared to the other techniques such as RIA and HPLC itself. However, concentration steps may be need in the application of the clinical or biological analysis due to the extremely low concentration of many steroids of interest in biological fluids.

References

1. S. Akyuz, S. Pince, N. Hekin, *J. Clin. Pediatr. Dent.* 20 (1996) 219.
2. A. H. Yagnucci, E. Evans, *Am. J. Med.* 80 (1986) 83.
3. L. Ia. Farta, N.E. Kushlinskii, *Probl. Endokrinol. Mosk.* 32 (1986) 25.
4. G. Carpene, A. Vettoretti, F. Pedini, S. Rocco, F. Mantero, G. Opocher, *J. Chromatogr.* 553 (1991) 201.
5. C.H. Shackleton, *J. Steroid Biochem. Mol. Biol.* 45 (1993) 127.
6. C.H. Shackleton, H. Chuang, J. Kim, X. de la Torre, J. Segura, *Steroids* 62 (1997) 523.
7. R. Andrew, *Best Practice & Research Clinical Endocrinology and Metabolism*, 15 (2001) 1.
8. O. Nozaki, *J. Chromatogr. A* 935 (2001) 267.
9. K. Shimada, K. Mitamura, T. Higashi, *J. Chromatogr. A* 935 (2001) 141.
10. A. Marwah, P. Marwah, H. Lardy, *J. Chromatogr. A* 935 (2001) 279.
11. B.G. Wolthers, G.P.B. Kraan, *J. Chromatogr. A* 843 (1999) 247.
12. R. Gonzalo-Lumbreras, R. Izquierdo-Hornillos, *J. Chromatogr. B* 742 (2000) 1.
13. R. Gonzalo-Lumbreras, R. Izquierdo-Hornillos, *J. Chromatogr. B* 742 (2000) 47.
14. M.R.H. Baltes, J.G. Dubois, M. Hanocq, *J. Chromatogr. B* 706 (1998) 201.
15. A. Marwah, P. Marwah, H. Lardy, *J. Chromatogr. B* 721 (1999) 197.
16. R. Navajas, c. Imaz, D. Carreras, M. García, M. Pérez, C. Rodríguez, A.F. Rodríguez, R. Cortés, *J. Chromatogr. B* 673 (1995) 159.
17. F. Komatsu, M. Morioka, Y. Fujita *J. Mass Spectrom.* 30 (1995) 698.

18. R. Draisci, L. Giannetti, L. Lucentini, L. Palleschi, I. Purfficato, G. Moretti, J. *High Resol. Chromatogr.* 20 (1997) 421.

19. C.H.L. Shackleton, J.W. Honour, *Clin. Chim. Acta* 69 (1976) 267.

20. C.D. Pfaffenberger, E.C. Horning, *J. Chromatogr.* 112 (1975) 581.

21. C.H.L. Shackleton, *Clin. Chem.* 27 (1981) 509.

22. H.C.Curtis, J. Vollmin, M.J. Zagalak, M. Zachman, *J. Steroid Biochem.* 6 (1975) 677.

23. W. J.J. Leunissen, J.H.H. Thijssen, *J. Chromatogr.* 146 (1978) 365.

24. M. Nakajima, H. Wakabayashi, S. Yamato, K. Shimada, *Bunseki Kagaku* 45 (1996) 517.

25. M. Nakajima, S. Yamato, K. Shimada, *Biomed. Chromatogr.* 12 (1998) 211.

26. K. A. Bean, J. D. Henion, *J. Chromatogr. B* 690 (1997) 65.

27. D. J. Borts, L. D. Bowers, *J. Mass Spectrom.* 35 (2000) 50.

28. Q. Jia, M. Hong, Z. Pan, S. Orndorff, *J. Chromatogr.* B 750 (2001) 81.

29. J.T. Lin, E. Hefttmann, *J. Chromatogr.* 237 (1982) 215.

30. J. C. Miller and J. N. Miller, *Statistics for analytical chemistry, 2nd edition, Ellis Horwood Ltd., Chichester*, (1988) 116.

Chapter 5

Studies of Derivatization of Androgenic Steroids and their Conjugates by HPLC-MS

5.1 Introduction

As discussed in Chapter 4, LC-MS has become an important technique and been extensively studied by many researchers for androgenic steroid analysis. However, sensitivity is still a challenge for direct determination of most androgenic steroids in biological systems due to very low concentration of these compounds. Derivatization is a useful technique that can enhance the performance of analytes commonly used in GC or GC-MS, but still not widely applied in LC-MS.

In GC or GC-MS analysis, trimethylsiyl (TMS) and other alkysilyl ethers for hydroxy functions and the *O*-methyloxime (MO) for ketonic functions have been commonly used for derivatization agents. Kintz et al. determined DHEA [1] and testosterone (T) [2] in hair derivatized with silyl ether by GC-MS to confirm the physiological concentration range of these compounds. Using TMS ether derivatization and GC-MS, the concentrations of T, its glucuronide, androsterone and epitestosterone (ET) in blood spots were investigated by Peng et al. [3]. A method for determination of urinary DHEA and DHEAS using GC-MS was reported by Dehennin et al. [4] The DHEAS was extracted, hydrolyzed, and the liberated DHEA was derivatized to *tert*-butyldimethylsilyl ether and then analyzed by GC-MS with selected ion monitoring (SIM) to investigate the effect of a single dose of DHEA on the urinary androgen profile. Choi et al.[5] introduced pentafluorophenyldimethylsilyl (flophemesy)-TMS derivatives for simultaneous determination of eight steroids (AD, DHT, DHEA, T, A, ET, progesterone and pregneolone) in human hair, which was done with GC-MS using [$^2H_3$]T as internal standard (I.S.). The method involved alkaline digestion, liquid-liquid extraction and subsequent conversion to the flophemesyl-TMS ethers, which formed an intense molecular ion and minimized background noise so that a sensitive analysis was achieved

with SIM. The detection limits of the steroids varied in the range of 0.02 to 0.5 ng/g (S/N=3). Scherer et al. [6] reported a method for the determination of T in human hair by GC-MS using [$^2H_3$]T as I.S. They showed that the derivatization with heptafluorobutyric anhydride gave rise to high mass ions thus diminishing background noise, and that these derivatives had shorter retention times than those of MO-TMS ethers. The detection limit was 20 pg (S/N=3.4). Tagava et al. [7] presented a determination method for DHEAS and pregnenolone sulfate (PREGS) in serum of patients with hyperthyroidism and hypothyroidism using GC-SIM-MS after hydrolysis and derivatization with heptafluorobutyric anhydride.

Although conjugated metabolites have usually been analyzed by GC or GC-MS after enzymic or alkaline hydrolysis and derivatization, some methods not requiring deconjugation have been described. A simplified method for measurement of serum DHEA and DHEAS using GC-MS-MS in a single injection with selected reaction monitoring (SRM) was reported by Zemaitis and Kroboth [8] It appeared that at the elevated temperature of the GC injector port, a reproducible decomposition occurred in which the elements of sulfuric acid were removed and one of three isomers is formed with different location of double bonds in the steroid A- or B-ring. A method for simultaneous determination of nine urinary androgen glucuronides by high temperature GC-MS after derivatization to methyl ester-TMS ethers was reported by Choi et al. [9].

In recent years, derivatization technique has been applied to LC-MS, although it is still not widely used. Shackleton et al.[10] developed a method to derivatize nine testosterone fatty acid esters to Girard hydrozones, and the method was also applied to the measurement of testosterone fatty acid esters in the plasma of healthy volunteers after intramuscular adminstration of testosterone fatty acid esters using LC-ESI/MS/MS. Liu and co-workers[11] described a method to convert neutral oxosteroids into their oximes by

treatment with hydroxyl ammonium chloride in aqueous methanol. The fragmention pathways of these steroid oximes were studied by ESI/MS/MS, and the detection limits were found to be improved about 20 times relative to free steroids.

In this chapter, we have developed a derivatization method to improve the sensitivities of detection for the analysis of androgenic steroids and their conjugates by LC-ESI/MS/MS.

5.2 Experimental

5.2.1 Materials

HPLC grade methanol, acetonitrile, water and analytical grade ethanol were purchased from Fisher Scientific (Loughborough, Leicester, UK). Formic acid, acetic acid and most of the steroids were purchased from the Sigma-Aldrich Co. Ltd. (Poole, Dorset, UK), except 5β-androstan-17β-ol-3-one, Δ_4-androsten-17α-ol-3-one, Δ_4-androsten-17β-ol-3-one sulfate sodium salt and Δ_4-androsten-17α-ol-3-one glucuronide which were purchased from Steraloids INC (Newport RI, USA).

Hydrazide-TMPP reagent, (4-hydrazion-4-oxobutyl) [tris (2,4,6-trimethoxyphenyl)] phosphonium bromide was a kind gift from Glaxo Reseach and Development Ltd.

A LUNA $C_{18\ (2)}$ (100 × 2.0 mm, 3 μm) column and guard cartridge were purchased from Phenomenex (Cheshire, UK).

5.2.2 Derivatization

A hydrazide-TMPP reagent stock solution (1 mg/ml) was prepared by dissolving the solid reagent in ethanol-glacial acetic acid (9:1, v/v) using an ultrasonic bath. This solution is stable without significant decomposition at 20°C for at least one day. The steroid was dissolved in methanol as a stock solution (100 μg/ml), and 10 μl was added into 100 μl freshly prepared TMPP reagent solution; after briefly mixing in ultrasonic bath, the solution was allowed to react in a 60°C water bath for two hours.

5.2.3 HPLC parameters

The derivatized steroids were injected by an auto-sampler through the column into the mass spectrometer. The column temperature was maintained at 40°C, and the flow rate was 0.4ml/min with 5 μl volume injection. Gradient system (a) was used to study an individual derivatized steroid and (b) was used for the separation of derivatized steroid mixtures.

(a)

Time (min)	MeCN containing 0.1% formic acid (v/v %)	Water containing 0.1% formic acid (v/v %)
0	35	65
10	60	40
12	60	40

(b)

Time (min)	MeCN containing 0.1% formic acid (v/v %)	Water containing 0.1% formic acid (v/v %)
0	35	65
6	35	65
7	40	60
15	45	55
25	45	55

5.2.4 MS parameters

Mass spectrometric experiments were performed on a Finnigan LCQ ion trap mass spectrometer (San Jose, CA) equipped with X-callubar software. The ESI interface in positive mode was used for the analysis and the major parameters are listed as below:

MS parameter	HPLC Flow rate of 0.4ml/min
Sheath gas flow (arbitrary units)	80
Auxiliary gas flow (arbitrary units)	20
Spray voltage	4.5 kV
Capillary temperature	250°C
Capillary voltage	40 V
Tube lens offset	50 V

5.3 Derivatization of androgenic steroids

5.3.1 Structure of the derivatizing reagent

The structure of the derivatizing reagent, (4-hydrazion-4-oxobutyl) [tris (2,4,6-trimethoxyphenyl)] phosphonium bromide was shown in Figure 5.1.

Figure 5.1 Structure of hydrazide-TMPP reagent [12]

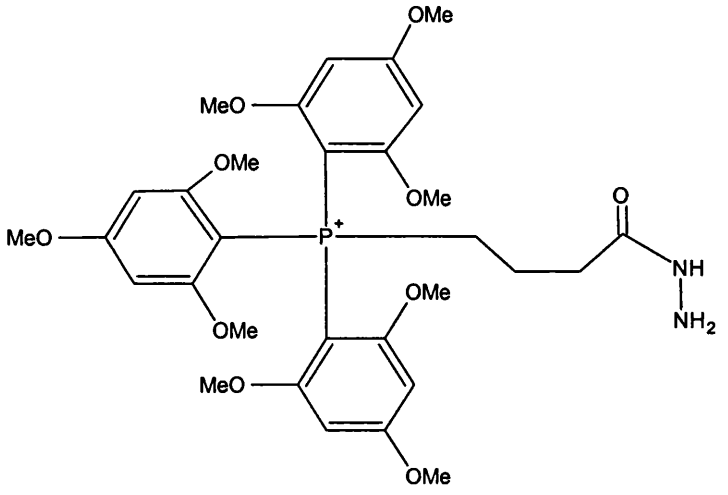

5.3.2 Reaction of hydrazide-TMPP reagent with androgenic steroids

As shown in Figure 5.2, steroid derivatives were formed by the reaction of the hydrazine group in the hydrazide-TMPP reagent with the keto group in the steroids [12]. The resulting positive charge introduced into the structures of the steroid derivative enhances their ionization efficiencies by ESI-MS.

Figure 5.2 Reaction of hydrazide-TMPP reagent with androgenic steroids

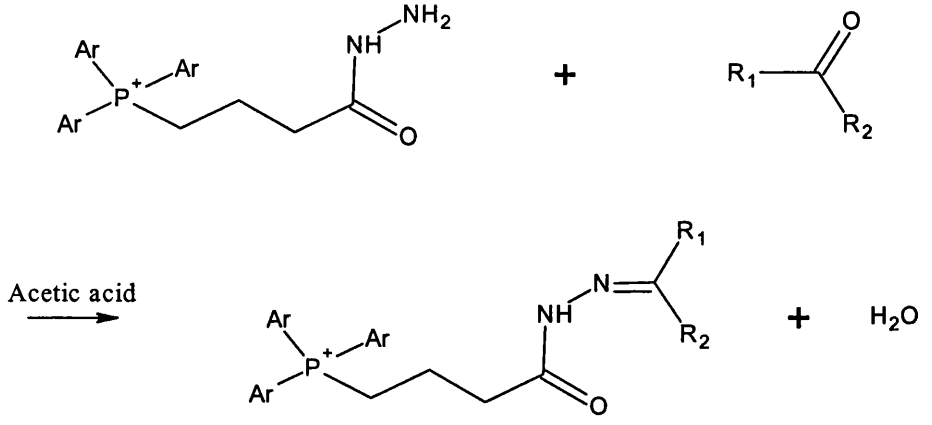

Ar = 2, 4, 6 - trimethoxyphenyl

5.3.3 Optimization of steroid derivatization reaction

5.3.3.1 Stability of hydrazide-TMPP reagent

The solid hydrazide-TMPP reagent was stored in a fridge and found to be stable for at least three months. However, when dissolved in ethanol-glacial acetic acid (9:1, v/v), the solution was found to have undergone about 50% degradation by the second day, a little further degradation by the third day, and no further degradation by the fourth

day. The reagent solution was therefore prepared fresh everyday for the derivatization experiments. Figure 5.3 shows the stability of the reagent solution detected by LC-MS for four days.

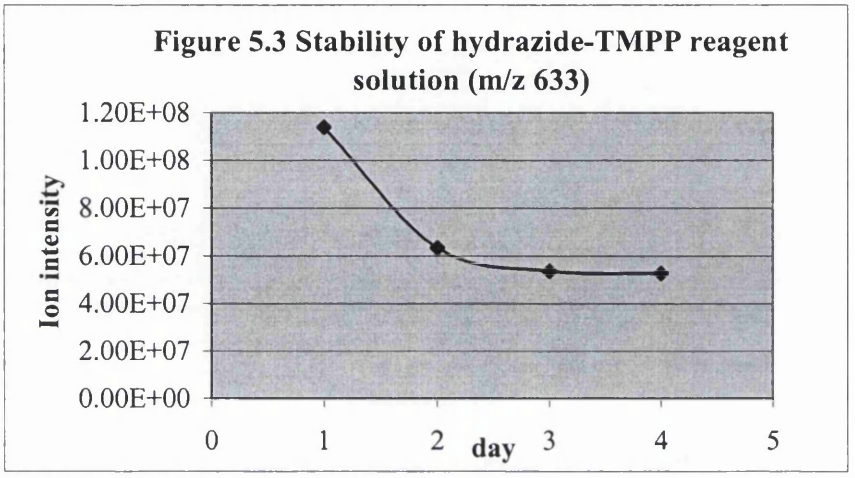

5.3.3.2 Optimization of the react conditions

To gain the maximum reaction of Hydrazide-TMPP reagent with the investigated steroids, at least 30-fold excess of the reagent was used for the reaction. The reaction conditions were optimized by a study of the effect of incubation temperature on yield. Samples were incubated at room temperature in sonic bath for 30 minutes, a water bath heated to 60 °C for 1 hour, 2 hours and 3 hours, and then further heated to 80 °C for 1 hour.

Figure 5.4 shows that the intensities of derivatization products are increased as the temperature increases, reaching maximum values after heating at 60 °C for 2 hours. In the case of testosterone, 5α-androstan-3, 17-dione, and dihydrotestosterone derivatives, heating for 3 hours at 60 °C caused the intensities to drop slowly, and to fall sharply for

DHEA and epitestosterone derivatives. When the temperature was increased to 80 °C, the intensities for all the test steroid derivatives decrease to the level observed at of room temperature.

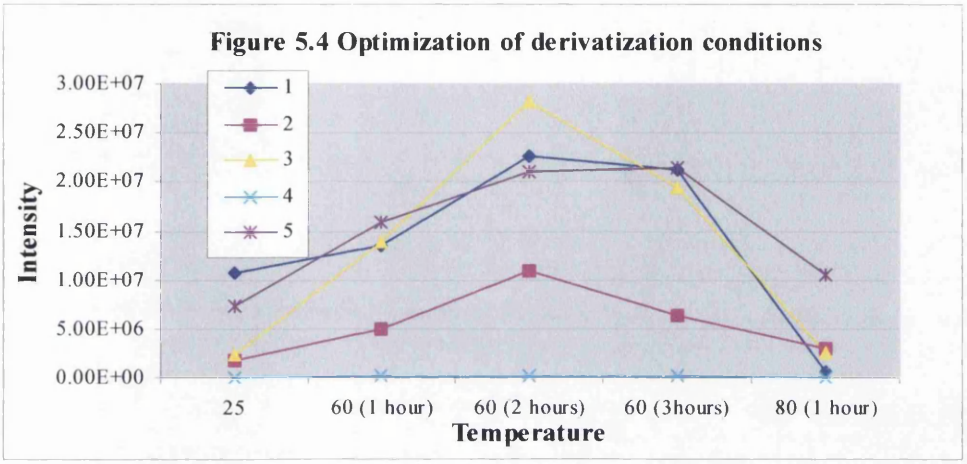

1. Testosterone; 2. Epitestosterone; 3. Dehydroisoandrosterone; 4. Dihydrotestoserone; 5. 5α-androstan-3, 17-dione

5.4 HPLC-MS of steroid derivatives

5.4.1 HPLC-MS of hydrazide-TMPP reagent

The hydrazide-TMPP reagent was eluted within two minutes. Figure 5.5 shows total ion chromatograph of the reagent and the corresponding mass spectrum. A very strong peak of $[M]^+$ (m/z 633) was observed, as well as the peak of $[M\text{-}NH_3]^+$ in a relative low abundance.

Figure 5.5 (a) Total ion chromatography of hydrazide-TMPP reagent (b) mass spectrum of hydrazide-TMPP reagent

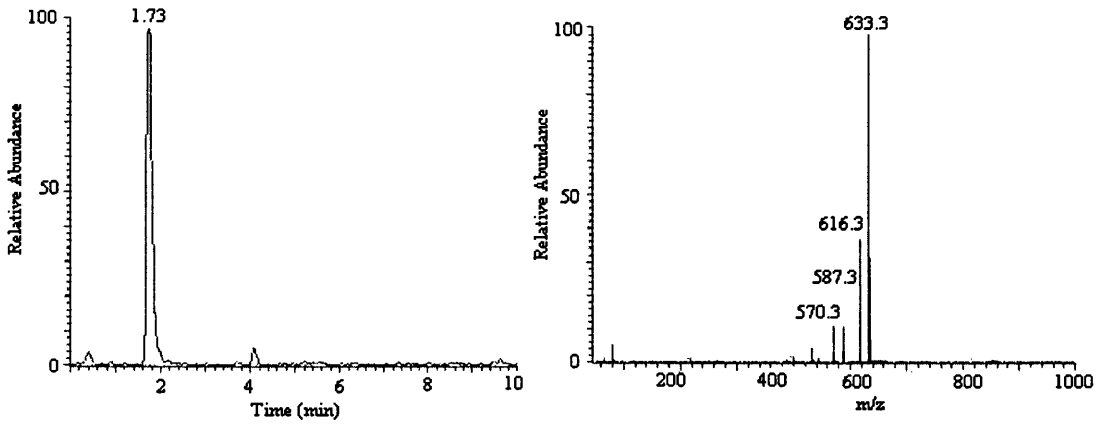

(a) (b)

5.4.2 HPLC-MS of derivatized steroids

5.4.2.1 Chromatography of steroid derivatives

Derivatization changed the chromatographic character of the investigated steroids, and the retention time of the derivatives was longer compared to the corresponding non-derivatized steroids. TMPP-derivatives of conjugated steroids were retained on the C18 column, which did not retain the non-derivatized conjugates. Retention times of the non-conjugated steroid derivatives fall between the steroid glucuronide derivatives which elute early and steroid sulfate derivatives that are considerably retained for all the investigated compounds. Table 5.1 presented the retention times of the TMPP-derivatives of some steroids and their conjugates.

Table 5.1 Retention times of TMPP derivatives of some steroids and their conjugates

Steroid derivatives	Retention time (min)	Steroid derivatives	Retention time (min)
Testosterone	11.63, 13.48	Dehydroisoandrosterone	12.44
Testosterone G*	5.24, 8.16	Dehydroisoandrosterone G	4.64
Testosterone S*	14.86, 16.60	Dehydroisoandrosterone S	16.06
Androsterone	16.41	Etiocholan-3α-ol-17-one	16.19
Androsterone G	11.07	Etiocholan-3α-ol-17-one G	10.98
Androsterone S	19.15	Etiocholan-3α-ol-17-one S	19.55

*G, glucuronide; S, sulfate. Experimental conditions are refer to 5.2.3 (a).

Only one peak was observed in the extracted ion current chromatogram for those of steroids without a Δ_4 bond after reaction of the keto-group with the TMPP reagent, but for those steroids of with a Δ_4 bond system e.g. testosterone, its conjugated derivatives and epitestosterone derivative (Table 5.1), there were two peaks observed, whilst three peaks were obtained for Δ_4-androsten-3, 17-dione and Δ_4-androstene-3, 11, 17-trione derivatives (Figure 5.7).

As the result of derivatization, two types of products could be formed: the keto-type hydrazone and the enol-type hydrazone. The keto-type may be dominant because it is much more stable than the enol-type, however, the Δ_4-double bond in the A-ring of testosterone and epitestosterone helps to stabilize the other two double bonds in the enol type hydrazone, and make it more competitive in the derivatized reaction. This also might explain two of the three peaks observed in the spectra of Δ_4-androsten-3, 17 dione and Δ_4-androstene-3, 11, 17-trione, whilst the third peak may be the 'ketone-tautomer' of the 17-one derivative. The conversion from ketone-type testosterone derivative to enol-type is presented in Figure 5.6. Another possibility is that there were two stereo-isomers (cis- or

trans-, Figure 5.2) formed after derivatization, and they were simply not separated for the steroid derivatives without Δ_4 bond.

Figure 5.6 Tautomerization of testosterone derivative

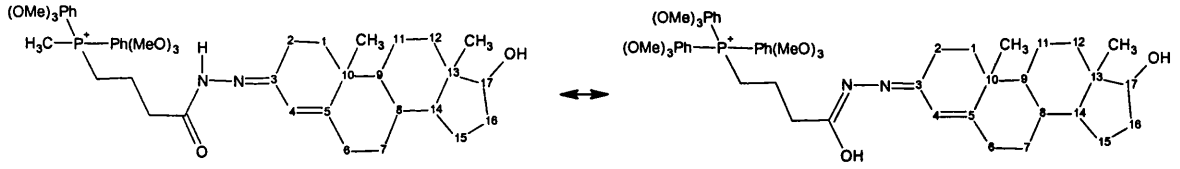

Ketone-type testosterone hydrazone Enol-type testosterone hydrazone

However, there is only one peak observed in the extracted ion current chromatograph of 5α-androstan-3, 17-dione derivative and 5α-androstan-3α-ol-11, 17-dione derivative, under various conditions of the HPLC solvent gradient. There are either two different compounds not to separated or only one compound resulted from the competition between 17-one and 3-one or 11-one. The latter is probably the case for 5α-androstan-3α-ol-11, 17-dione derivative, since there is much bigger steric hindrance at C11 than that at C17. The extracted ion current chromatogram of the TMPP-derivatives of selected steroids and steroid conjugates is present in Figure 5.7.

Figure 5.7 Extracted ion chromatogram of eight steroid TMPP-derivatives

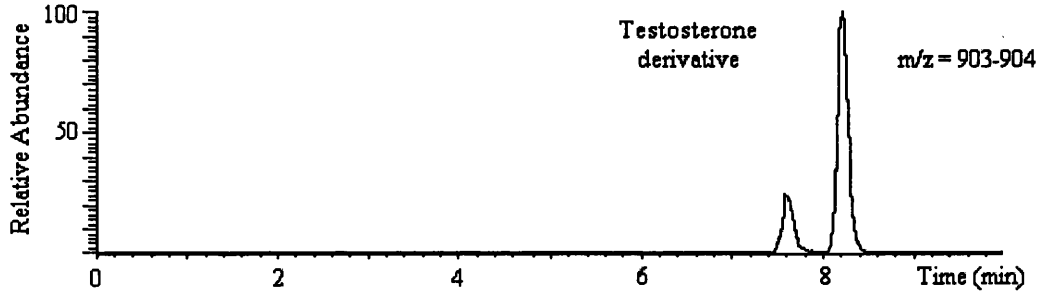

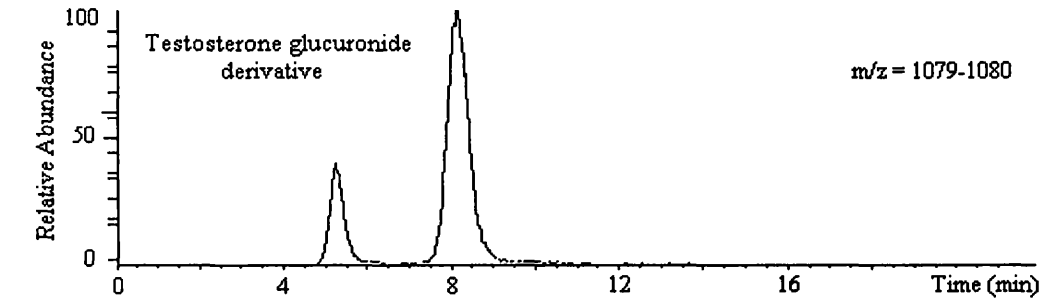
Testosterone glucuronide derivative
m/z = 1079-1080
Relative Abundance
Time (min)

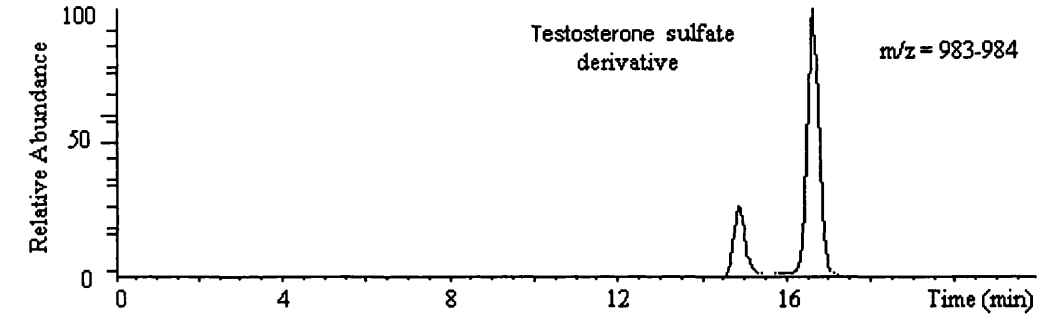
Testosterone sulfate derivative
m/z = 983-984
Relative Abundance
Time (min)

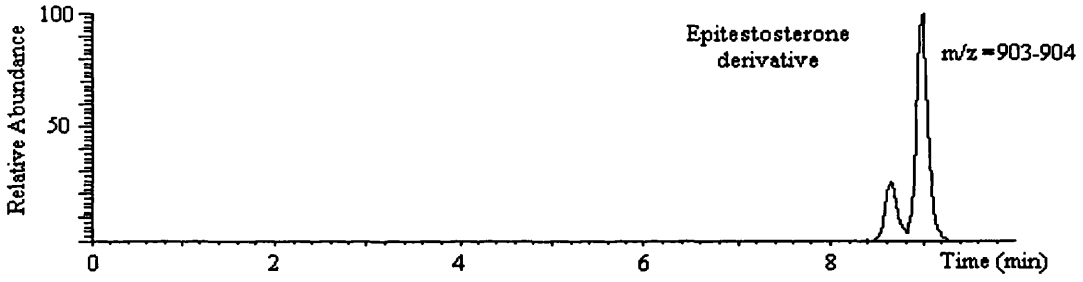
Epitestosterone derivative
m/z =903-904
Relative Abundance
Time (min)

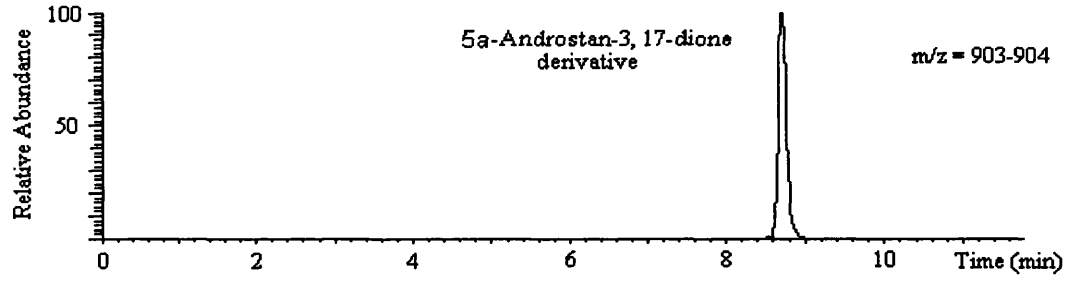
5a-Androstan-3, 17-dione derivative
m/z = 903-904
Relative Abundance
Time (min)

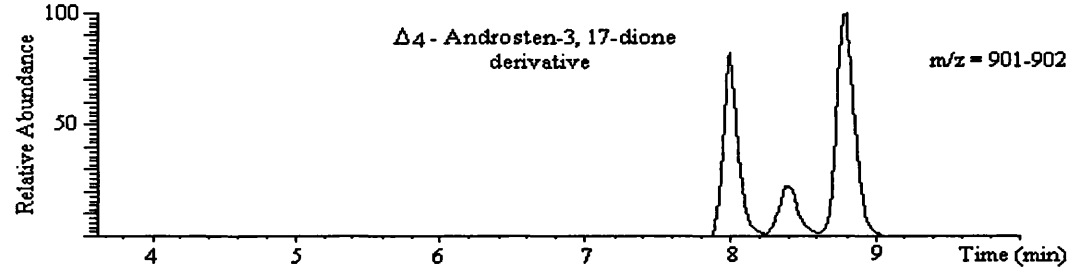
Δ4 - Androsten-3, 17-dione derivative
m/z = 901-902
Relative Abundance
Time (min)

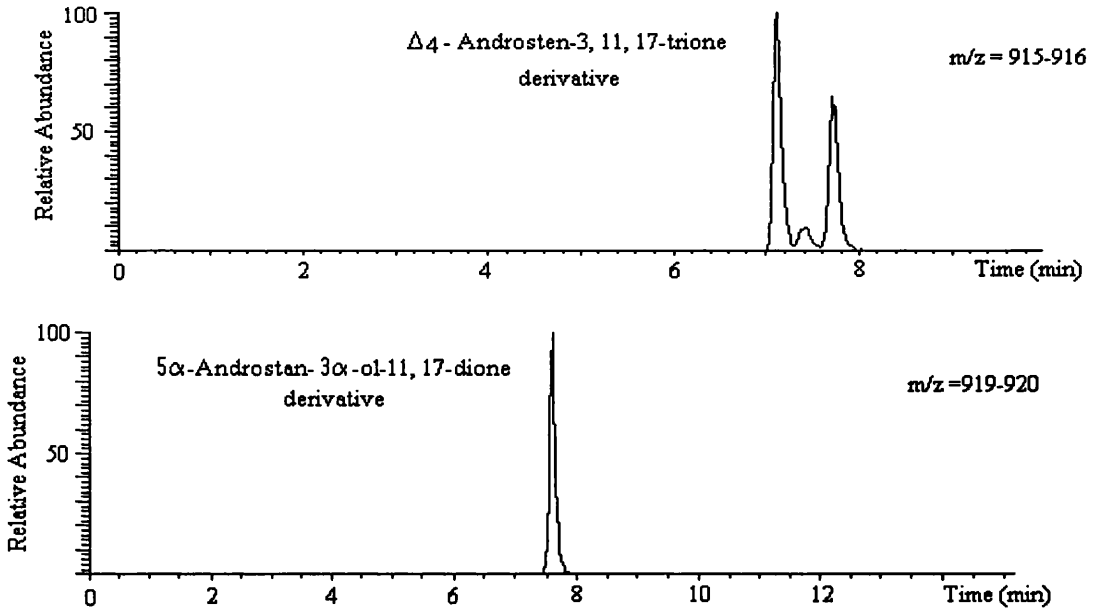

Note: sample was injected at 5 μl and at 1pg/μl for each of compound.

5.4.2.2 Mass spectra of steroid TMPP-derivatives

The steroid TMPP-derivatizes, in which the molecular ion of the parent steroid was increased by 615 mass units by the TMPP moiety, were investigated under ESI-MS condition due to the introduction of the positive charge in the derivatization reaction. For the TMPP-derivatives of non-conjugated steroids, M^+ was generally dominant in the spectrum of each of these compounds, with the exception of DHT and 5β-androstan-17β-ol-3-one, in the spectra of which the fragment ion at m/z 633 was the most intensive peak. There were also isotope peaks of $[M+1]^+$, $[M+2]^+$ and $[M+3]^+$ observed in each of these spectra. Significant peaks assigned to dehydration of the molecular ion were observed in the spectra of non-derivatized steroids without a 4-ene-3-one group (Chapter 3), but peaks due to loss of water were not observed the spectra of their TMPP-derivatives. It seemed that the spectra of DHT and 5β-androstan-17β-ol-3-one contained

more fragments than their 17-one isomers. The major ions of the derivative of each non-conjuated steroid are presented in Table 5.2.

Table 5.2 Major ions of TMPP-derivatives of non-conjugated steroids by ESI-MS

Steroid	M^+	$[M+1]^+$	$[M+2]^+$	$[M-176]^+$	m/z 633	m/z 616	m/z 587	m/z 570
Dehydroisoandroste-rone (DHEA)	903.6 (100)	904.6 (47)	905.6 (13)	_	_	_	_	_
5α-Androstan-3, 17-dione	903.6 (100)	904.6 (44)	905.6 (14)	_	_	_	_	_
Etiocholan-3β-ol-17-one	905.6 (100)	906.6 (49)	907.6 (15)	_	_	_	_	_
5α-Androstan-3β-ol-17-one	905.6 (100)	906.6 (46)	907.6 (15)	_	_	_	_	_
Androsterone	905.6 (100)	906.6 (43)	907.6 (14)	_	_	_	_	_
Etiocholan-3α-ol-17-one	905.6 (100)	906.6 (44)	907.6 (15)	_	_	_	_	_
5α-Androstan-17β-ol-3-one (DHT)	905.6 (65)	906.6 (31)	907.6 (8)	_	633.4 (100)	616.4 (33)	587.4 (9)	570.3 (11)
5β-Androstan-17β-ol-3-one	905.6 (30)	906.6 (14)		729.4 (60)	633.4 (100)	616.4 (33)	587.4 (13)	570.3 (6)
5α-Androstan-3β-ol-16-one	905.6 (100)	906.6 (47)	907.6 (15)	_	_	_	_	_
5α-Androstan-3α-ol-11, 17-dione	919.6 (100)	920.6 (44)	921.6 (14)	_	_	_	_	_
5α-Androstan-3α, 11β-diol-17-one	921.6 (100)	922.6 (48)	923.6 (14)	_	_	_	_	_

For the derivatives of steroid glucuronides, M^+ was the most intense peak in the spectrum of each compound which was also increased by 615 mass units relative to the original steroid, whereas, for the derivatives of steroid sulfates, $[M+H-Na]^+$ was the dominant peak in each case, although a molecular ion (M^+) was also observed in low

relative abundance. The major ions of the TMPP-derivatives of each conjugated steroid are presented in Table 5.3.

Table 5.3 Major ions of TMPP-derivatives of conjugated steroids by ESI-MS

Steroid Derivative	M^+	$[M+1]^+$	$[M+2]^+$	$[M+H-Na]^+$	$[M+H-Na+1]^+$	$[M+H-Na+2]^+$	m/z 887
DHEA G	1079.3 (100)	1080.3 (45)	1081.3 (16)	_	_	_	_
DHEA S	1005.3 (7)	_	_	983.3 (100)	984.3 (40)	985.3 (16)	_
Androsterone G	1081.4 (100)	1082.4 (51)	1083.4 (17)	_	_	_	_
Androsterone S	1007.3 (9)	_	_	985.3 (100)	986.3 (40)	987.3 (15)	887.5 (17)
Etiocholan-3α-ol-17-one G	1081.4 (100)	1082.4 (51)	1083.4 (15)	_	_	_	_
Etiocholan-3α-ol-17-one S	1007.3 (20)	_	_	985.3 (100)	986.3 (46)	987.3 (15)	887.5 (87)

DHEA, dehydroisoandrosterone; G, glucuronide; S, sulfate

TMPP-derivatives of steroids without a Δ_4-bond

The peak intensities in the extracted current chromatograms observed with 17-one derivatives were much higher than those from 3-oxo derivatives for keto-steroids. For example, the peak intensities of DHT and 5β-Androstan-17β-ol-3-one derivatives are more than 50 times lower that those of their 17- or 16-one isomers. Therefore, the keto-group at D ring may be more reactive than the keto-group at the A ring for the derivatization reaction. However, there seems an exception when Δ_4-double bond is present at A ring, because very intense peaks were observed for testosterone and epitestosterone derivatives (Table 5.6). For the 17-one steroids, there was little difference

in signal strengths between either the 5α- and 5β- isomer, or the 3α-ol and 3β-ol isomers (Table 5.4). As to the two dione-steroids, only one peak observed in their spectra, but the peak intensities are higher than those steroid derivatives containing only one oxo group. The peak intensities in the extracted current chromatogram for DHT and its isomers at m/z of 905 are listed in table 5.4.

Table 5.4 Peak intensities of TMPP-derivatives of eleven oxo-steroids

Steroid	Concentration of react steroid (μg/ml)	m/z	Peak intensity
*5α-Androstan-17β-ol-3-one (DHT)	10.0	905.6	1.01×10^6
*5β-Androstan-17β-ol-3-one	10.0	905.6	5.19×10^5
5α-Androstan-3β-ol-17-one	1.0	905.6	4.80×10^6
5α-Androstan-3α-ol-17-one	1.0	905.6	7.95×10^6
5β-Androstan-3α-ol-17-one	1.0	905.6	7.95×10^6
5β-Androstan-3β-ol-17-one	1.0	905.6	5.31×10^6
5α-Androstan-3β-ol-16-one	1.0	905.6	6.28×10^6
Δ_5-Androstan-3β-ol-17-one	1.0	903.6	5.25×10^6
5α-Androstan-3α, 11β-diol-17-one	1.0	921.6	3.95×10^6
5α-Androstan-3, 17-dione	1.0	903.6	1.12×10^7
5α-Androstan-3α-ol-11, 17-dione	1.0	919.6	2.22×10^7

Note: sample was injected at 5 μl.

TMPP-derivatives of 4-ene-3-oxo steroids

There were two peaks observed in the total ion chromatogram for testosterone, its conjugated derivatives and epitestosterone derivative, three peaks observed for Δ_4-androsten-3, 17-dione derivative and four for the derivative of Δ_4-androstene-3, 11, 17-trione. The ions showed in the mass spectrum of each are presented in Table 5.5.

Table 5.5 m/z Values and relative abundance (%) of major ions of TMPP-derivatives of 4-ene-3-oxo steroids by ESI-MS

Steroid	Peak No.	RT (min)	M^+	$[M+1]^+$	$[M+2]^+$	$[(M+615)/2]^+$ or $[(M+2*615)/3]^+$	$[M+H-Na]^+$	$[M+H-Na+1]^+$	$[M+H-Na+2]^+$
T	1	7.50	903.6 (100)	904.6 (47)	905.6 (14)	–	–	–	–
	2	8.32	903.6 (100)	904.6 (47)	905.6 (14)	–	–	–	–
T G	1	5.24	1079.5 (100)	1080.5 (47)	1081.5 (16)	–	–	–	–
	2	8.16	1079.5 (100)	1080.5 (47)	1081.5 (15)	–	–	–	–
T S	1	14.86	1005.3 (8)	–	–	–	983.3 (100)	984.3 (44)	985.3 (16)
	2	16.60	1005.3 (8)	–	–	–	983.3 (100)	984.3 (44)	985.3 (15)
ET	1	9.00	903.6 (100)	904.6 (47)	905.6 (14)	–	–	–	–
	2	9.42	903.6 (100)	904.6 (44)	905.6 (14)	–	–	–	–
Δ_4-	1	7.55	901.6 (100)	902.6 (45)	903.6 (14)	–	–	–	–
Dione	2	8.10	901.6 (85)	902.6 (42)	903.6 (12)	758.9 (100)	–	–	–
	3	8.61	901.6 (100)	902.6 (43)	903.6 (15)	–	–	–	–
Δ_4-	1	7.11	915.5 (100)	916.5 (41)	917.5 (14)	–	–	–	–
Trione	2	7.40	915.5 (100)	916.5 (54)	917.5 (17)	–	–	–	–
	3	7.58	915.5 (41)	916.5 (20)	917.5 (8)	715.4 (100)	–	–	–
						765.6 (13)			
	4	7.72	915.5 (100)	916.5 (47)	917.5 (15)	765.8 (42)			

T, tesosterone; T G, testosterone glucuronide; T S, testosterone sulfate; ET, epitestosterone; Δ_4-Dione, Δ_4-Androsten-3, 17-dione; Δ_4-Trione, Δ_4-Androstene-3, 11, 17-trione.

The spectra of the two peaks were in each case extremely similar for the derivatives of testosterone, its conjugates and epitestosterone. There was only slight difference in abundance of their isotope peaks. However, absolute peak intensities of the peaks are quite different for each of these derivatives as in Table 5.6. For the derivatives of testosterone, its conjugates and epitestosterone, the intensities of later eluting peak are about ×2 - ×4 higher than those of the first. The later eluting peak may therefore be the enol-type product of the derivatization reaction, because the three conjugated double bonds make it more stable than the keto-type product, therefore favouring its formation in the reaction.

There were three peaks observed for Δ_4-androsten-3, 17-dione derivative in its total ion chromatogram. The spectra of peak one and peak three are very similar, only slight differences in the isotope peaks of m/z 901.6, but peak two showed a very different spectrum that contained a very intense peak at m/z 758.9, corresponding to a doubly charged ion derived from the bi-TMPP derivative. It therefore appear that when the Δ_4-double bond is present, both the 3- and 17-oxo group can be derivatized, whereas, there was no corresponding ion was observed in the spectra of 5α-androstan-3, 17-dione and 11-ketoandrosterone derivatives, which lack the Δ_4-double bond. Thus there were only mono-TMPP derivatives produced in the di-oxo steroids without Δ_4-double bond in ring A. In a similar pattern, four peaks were obtained in the total ion chromatogram of the Δ_4-androstene-3, 11, 17-trione derivative. The first two peaks showed very similar spectra, with a molecular ion of m/z 915.5 dominant. In peak three, however, the most intense ion in the spectrum was observed at m/z 715.4, corresponding to a triply-charged ion derived from the tri-TMPP derivative, and this peak was accompanied by a much weaker but significant ion of m/z 765.8, corresponding to a doubly-charged ion derived for a di-

substituted TMPP-derivative. The m/z 765.8 ion was also present and dominant in the spectrum of peak four, probably due to the incomplete HPLC separation of di- and tri-substituted TMPP-derivatives. The peak intensities of these observed ions were presented in Table 5.6.

Table 5.6 Comparison of the peak intensities of the TMPP-derivatives of 4-ene-3-oxo steroids

Steroid	m/z	Peak 1	m/z	Peak 2	m/z	Peak 3	m/z	Peak 4
Testosterone	903.6	2.22×10^6	903.6	9.14×10^6	_	_	_	
Epitestosterone	903.6	2.01×10^6	903.6	7.85×10^6	_	_	_	
Testosterone G	1079.5	6.53×10^6	1079.5	1.64×10^7	_	_	_	
Testosterone S	983.3	8.23×10^6	983.3	3.15×10^7	_	_	_	
Δ_4-Androsten-3,	901.6	8.81×10^6	758.9	1.24×10^6	901.6	1.10×10^7	_	
17-dione			901.6	2.46×10^6				
Δ_4-androstene-3,	915.5	6.91×10^6	915.5	6.89×10^5	715.4	9.01×10^5	765.8	1.36×10^6
11, 17-trione							915.5	3.87×10^6

For Δ_4-androsten-3, 17-dione, the intensity of m/z 901.6 in peak three is a little stronger than that in peak one, and more than four times that in peak two. Both the ion of m/z 901.6 and 758.9 are present in the spectra of peak two, but the intensity of m/z 758.9 is about as half as that of m/z 901.6, therefore, the mono-TMPP derivative is the major product in the derivatization reaction. As to Δ_4-androstene-3, 11, 17-trione, the derivatization yields a more complicated mixture of product, with both the bi-TMPP (m/z 715.4) and tri-TMPP (m/z 765.8) derivatives, as well as the mono-TMPP product (m/z 915.5) observed. The intensity of m/z 915.5 in peak one is the strongest one in all four peaks, and it is almost ten times to the one in peak two. Although ion at m/z 715.4 was observed in peak three, it is very weak, about ten times lower in abundance than those of m/z 915.5 and m/z 765.8 in peak four. Therefore, the mono-TMPP and tri-TMPP derivatives are major products in the reaction.

5.4.3 HPLC-MS/MS of steroid derivatives

5.4.3.1 CID spectra of TMP- derivatives of steroids without a Δ_4-bond

Non-conjugated steroids

A fragment ion of m/z 859 was observed in the CID spectra derived from the molecular ion of DHT and all of its isomers, which corresponded to loss of nitrogen and water ($[M-N_2-H_2O]^+$). The fragment ions from the fission of the TMPP group were observed in quite high abundances at m/z 616, 600, 570 and 533 (Figure 5.5 b). These fragments were very similar for all the 17-one and 16-one isomers, with the fragment ion at m/z 533 dominant in the spectra of these compounds, whereas the spectra of the 3-one isomers were dominated by the peak at m/z of 600. A further difference was apparent between 17-one and 3-one isomers: whilst in the spectra of 3-one isomers, m/z 889, corresponding to loss of oxygen, was present relatively low abundances, no such an ion was detected in the spectra of the 17-one isomers. Some typical spectra of these steroids are present in Figure 5.8.1-2, and the proposed of the identity fragment ions and their abundances are listed in the Table 5.7.

Figure 5.8.1 CID of DHT derivative

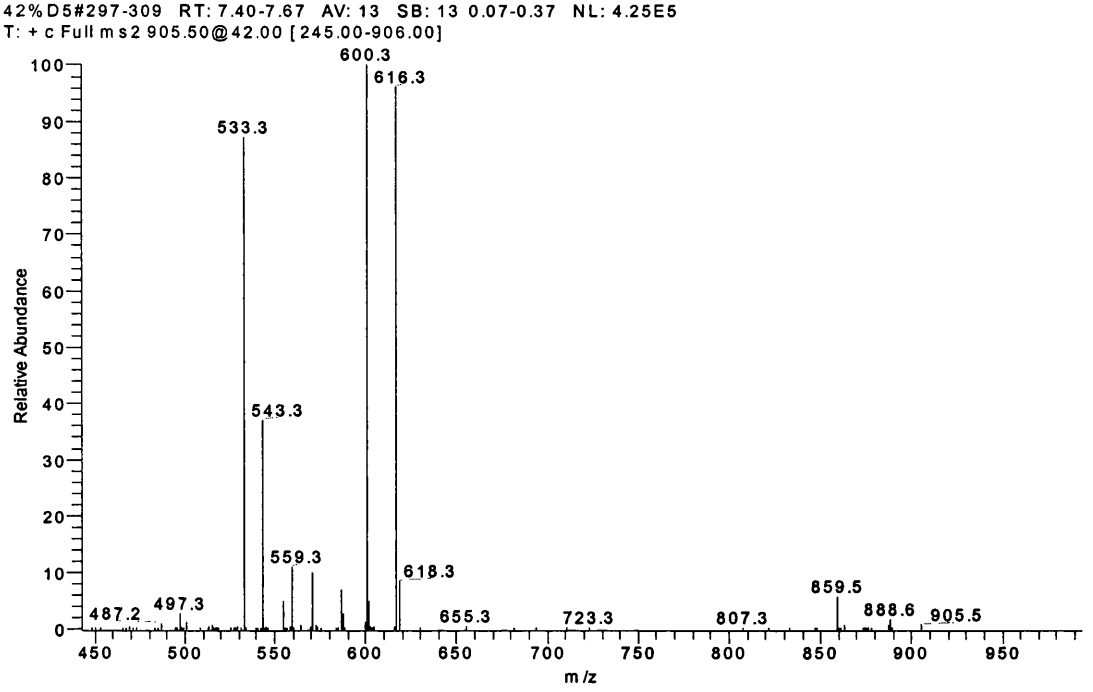

Figure 5.8.2 CID of androsterone derivative

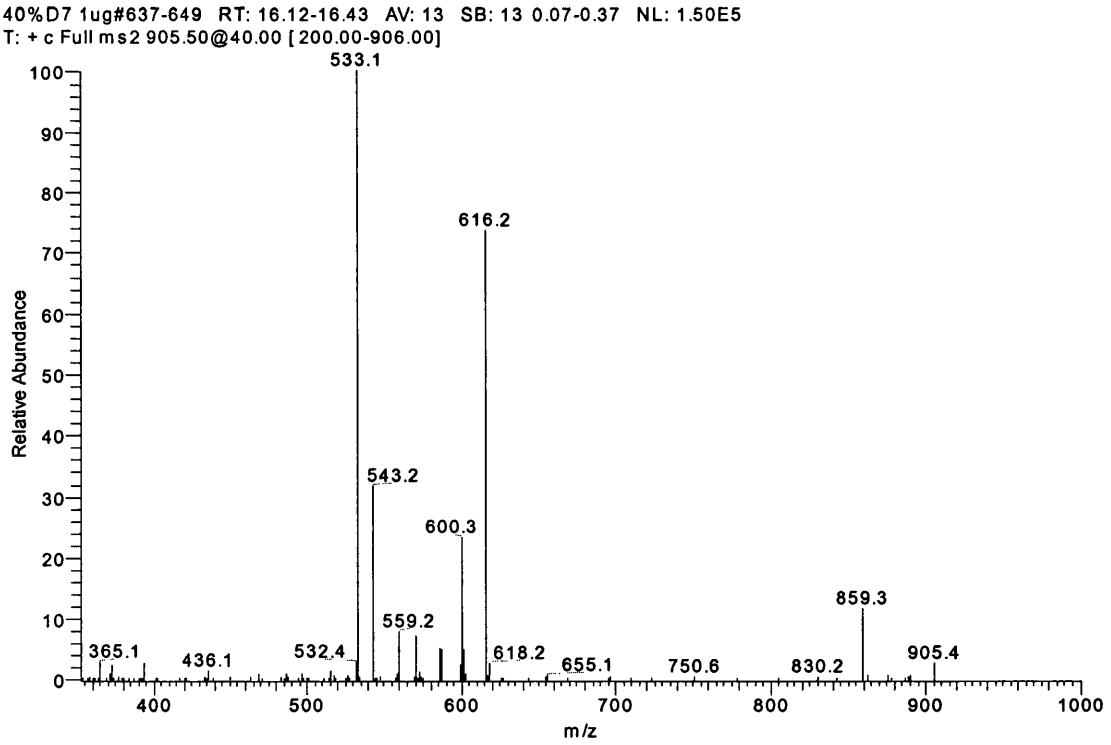

The CID spectra of the TMPP-derivatives of 5α-Androstan-3, 17-dione (Figure 5.9.1) and of DHEA (Figure 5.9.2) contained a similar set of fragments characteristic of the TMPP group; m/z 533 was dominant in both spectra. Fragment ions assigning from Wolff-Kishner reaction (m/z 857) were also present, and the spectrum of DHEA, contained a fragment ion at m/z 873, representing loss of 30 mass units from the parent ion.

Figure 5.9.1 CID of 5α-androstan-3, 17-dione derivative

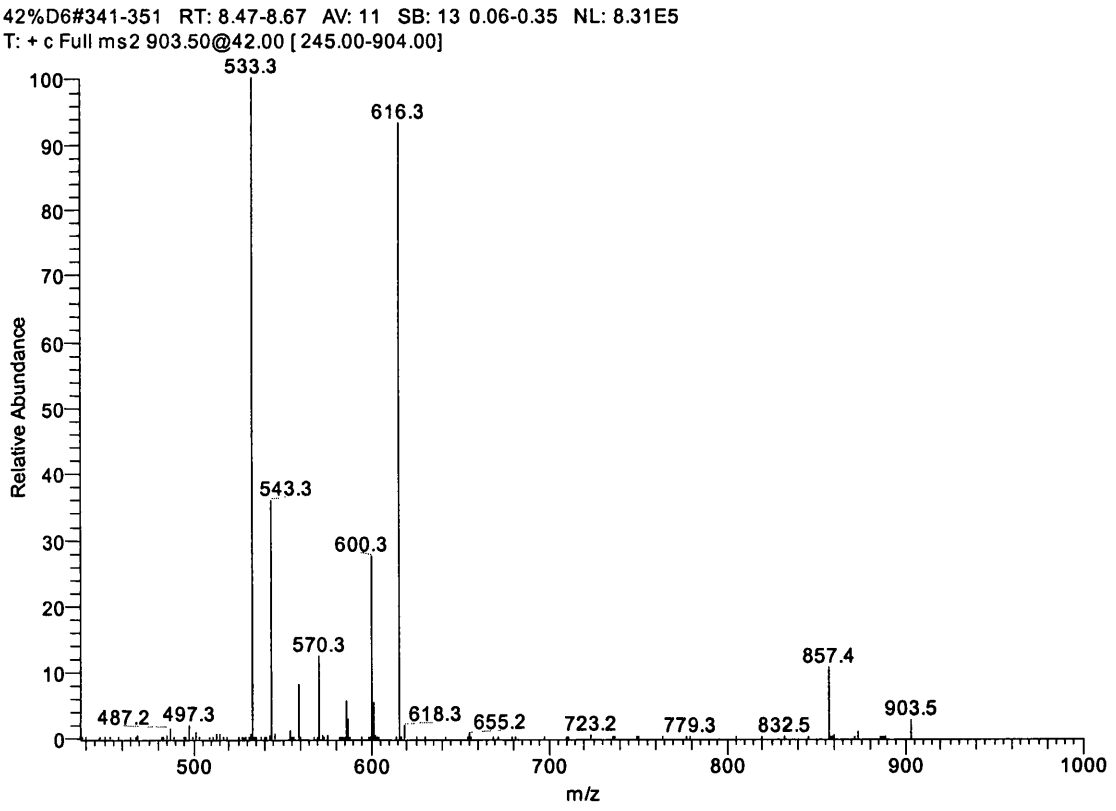

Figure 5.9.2 CID of DHEA derivative

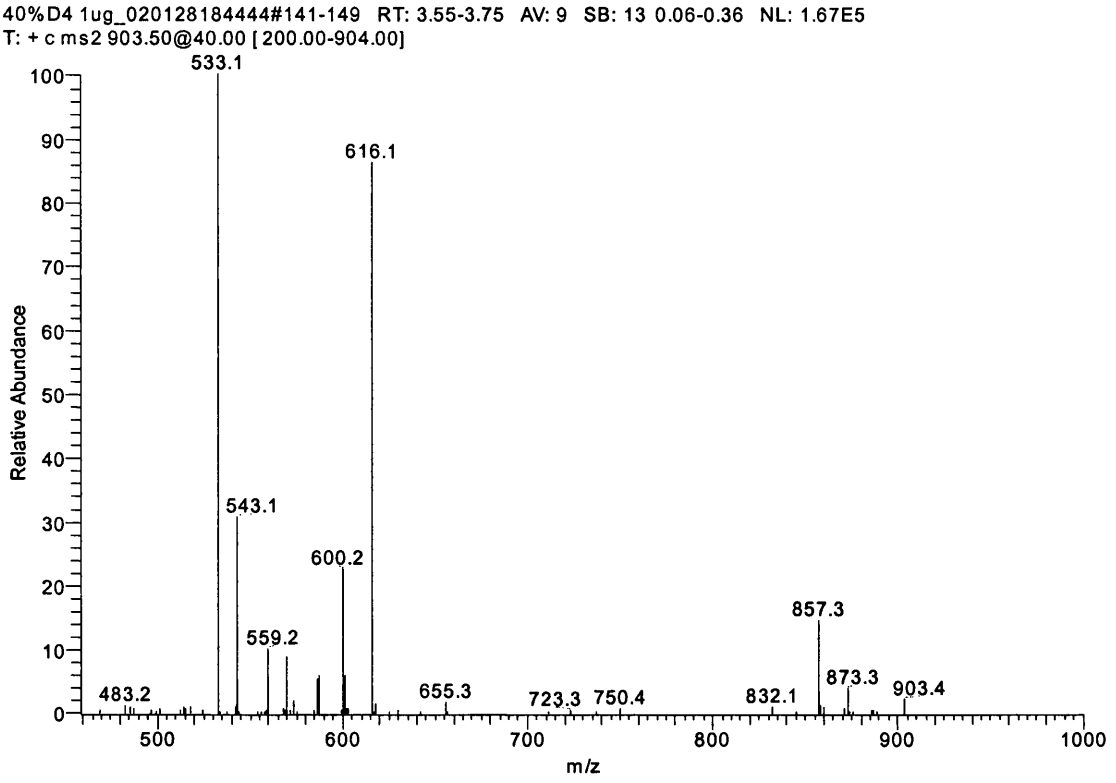

It seems that the mechanism of the fragmentation of the 11β-hydroxyandrosterone derivative (Figure 5.10.1) is as the same as the 17-one isomers of DHT (Figure 5.8.1), because the CID spectrum of the former was very similar to the latter, indicating that the second hydroxy group does not cause any difference in the fragmentation pathway. However, in the case of 11-ketoandrosterone (Figure 5.10.2) the spectrum is different, the abundance of m/z 616 being enhanced relative to 5α-Androstan-3, 17-dione and DHEA in its CID spectrum, probably suggesting that the additional keto-group at the C11 of the structure modifies the fragmentation process of the 11-ketoandrosterone derivative.

Figure 5.10.1 CID of 11β-hydroxyandrosterone derivative

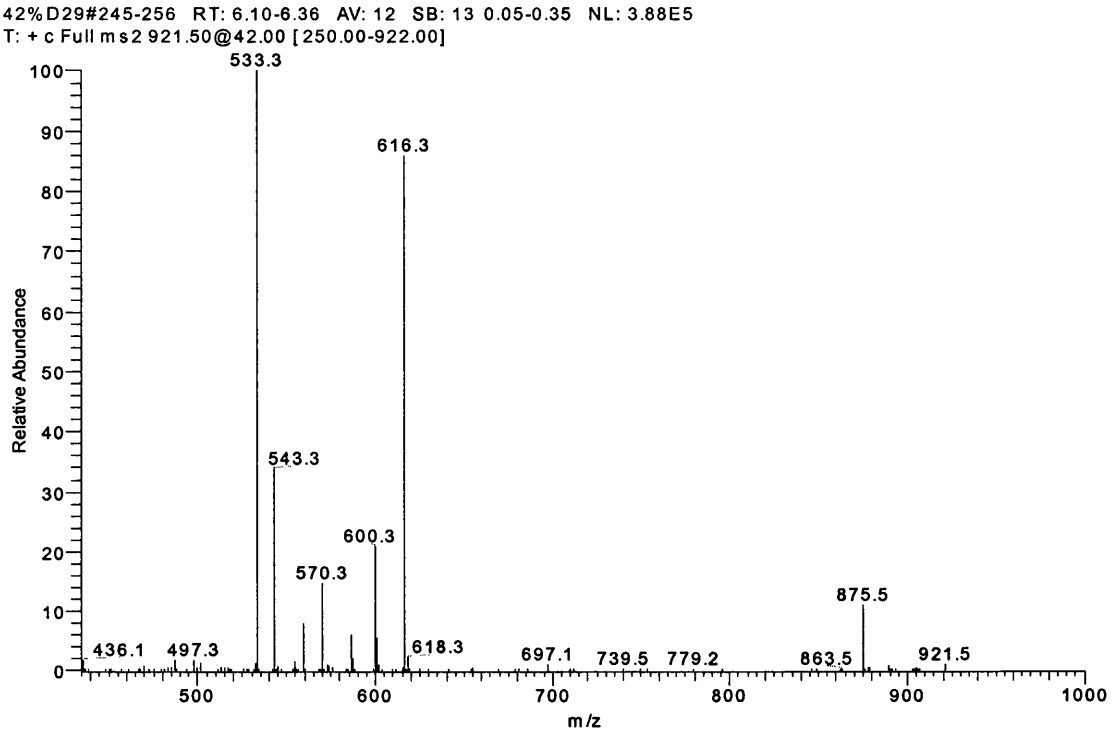

Figure 5.10.2 11-Ketoandrosterone derivative

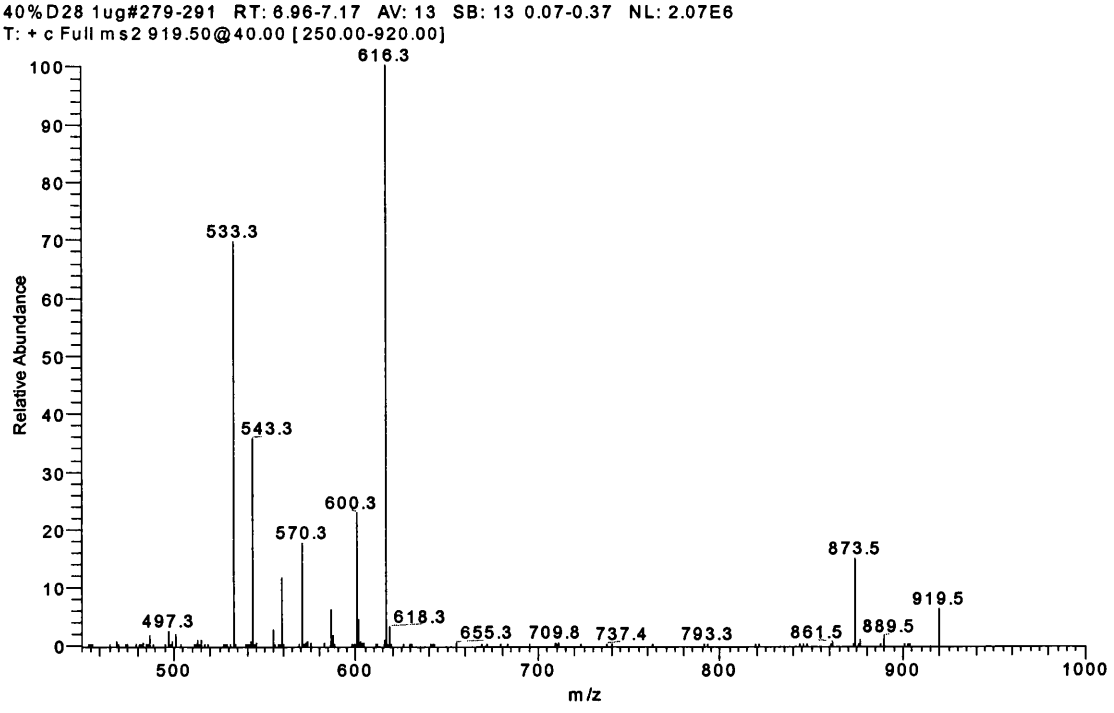

Table 5.7 CID of the TMPP-derivatives of eleven non-conjugated steroids without a Δ_4-bond system

Steroid	Parent ion	Collision energy (%)	Product ions m/z (relative abundance %)
1	905	40	859 (11), 616 (78), 600 (21), 586(7), 570 (7), 559 (11), 543 (28), 533 (100)
2	905	42	859 (12), 616 (83), 600 (26), 586(5), 570 (13), 559 (8), 543 (30), 533 (100)
3	905	42	859 (14), 616 (94), 600 (24), 586(5), 570 (14), 559 (7), 543 (36), 533 (100)
4	905	40	859 (11), 616 (79), 600 (22), 586(6), 570 (7), 559 (8), 543 (32), 533 (100)
5	905	42	889 (2), 859 (6), 616 (95), 600 (100), 586(7), 570 (10), 559 (11), 543 (37), 533 (87)
6	905	42	889 (5), 859 (5), 616 (95), 600 (100), 586(7), 570 (9), 559 (13), 543 (44), 533 (80)
7	905	42	859 (12), 616 (62), 600 (21), 586(3), 570 (9), 559 (16), 543 (24), 533 (100)
8	903	42	857 (11), 616 (93), 600 (27), 586(6), 570 (12), 559 (9), 543 (36), 533 (100)
9	919	40	873 (15), 616 (100), 600 (23), 570 (18), 559 (11), 543 (35), 533 (69)
10	921	42	875 (11), 616 (86), 600 (21), 586(6), 570 (15), 559 (8), 543 (34), 533 (100)
11	903	40	873 (4), 857 (15), 616 (87), 600 (24), 586 (5), 570 (8), 559 (10), 543 (32), 533 (100)

1. Etiocholan-3β-ol-17-one, 2. Etiocholan-3α-ol-17-one, 3. 5α-Androstan-3β-ol-17-one, 4. Androsterone, 5. DHT, 6. 5β-Androstan-17β-ol-3-one, 7. 5α-Androstan-3β-ol-16-one, 8. α-Androstan-3, 17-dione, 9. 11-ketoandrosterone, 10. 11β-hydroxyandrosterone, 11. DHEA

Conjugated derivatives

The CID spectra of the TMPP-derivatives of the conjugated steroids were quite simple compared to those of the free steroids. It seemed that the steroid glucuronide derivatives were more likely to lose the glucuronide moiety rather than TMPP moiety, because $[M\text{-}Glu]^+$ was dominant in the CID spectra of all the conjugated steroid derivatives investigated. For the androsterone glucuronide derivative (Figure 5.11.1), the most intense ion was at m/z 905, and there were further fragment peaks at m/z 533, 543, and 616 observed in the CID spectrum at relatively strong abundance, originating from the TMPP moiety. The $[M\text{-}H_2O]^+$ (m/z 1063) and $[M\text{-}H_2O\text{-}N_2]^+$ (m/z 1035) ions were also observed in this spectrum, as well as peaks at m/z 975 and 947 in relatively low abundances. The CID spectrum of its 5β-H isomer (Figure 5.11.2) was much simpler, the spectrum containing no fragment ions other than that at m/z 905, as was also the case for

the DHEA glucuronide derivative (Figure 5.11.3). The proposed identity of fragment ions of these compounds and their abundances are listed in the Table 5.8.

Figure 5.11.1 CID of androsterone glucuronide derivative

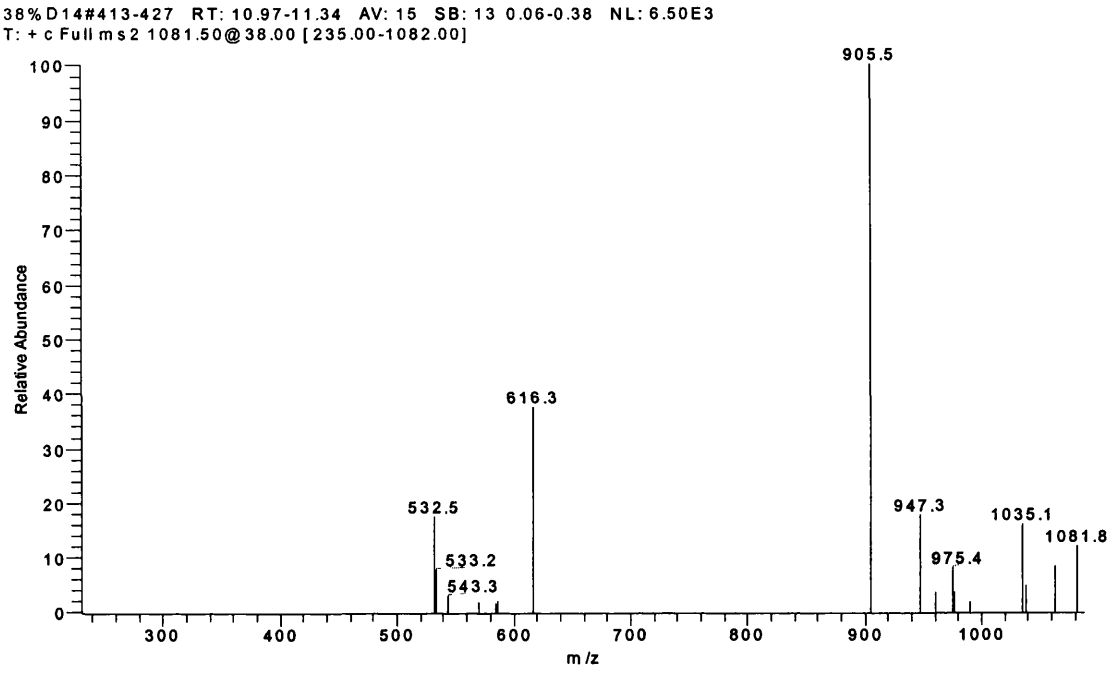

Figure 5.11.2 CID of etiocholan-3α-ol-17-one glucuronide derivative

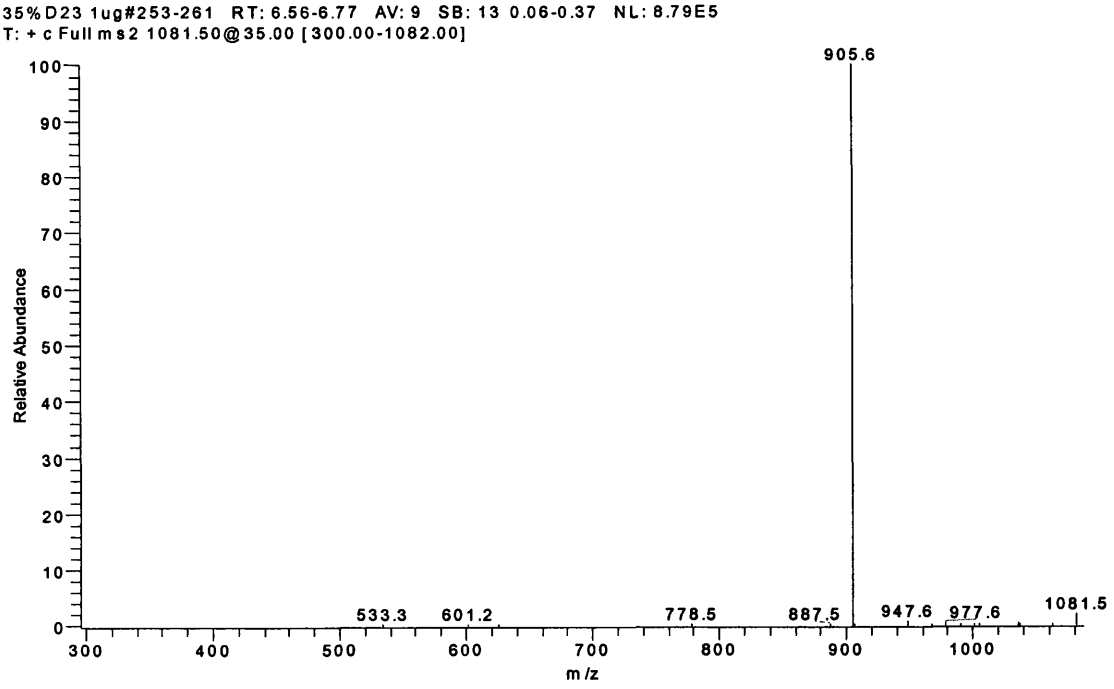

Figure 5.11.3 CID of DHEA glucuronide derivative

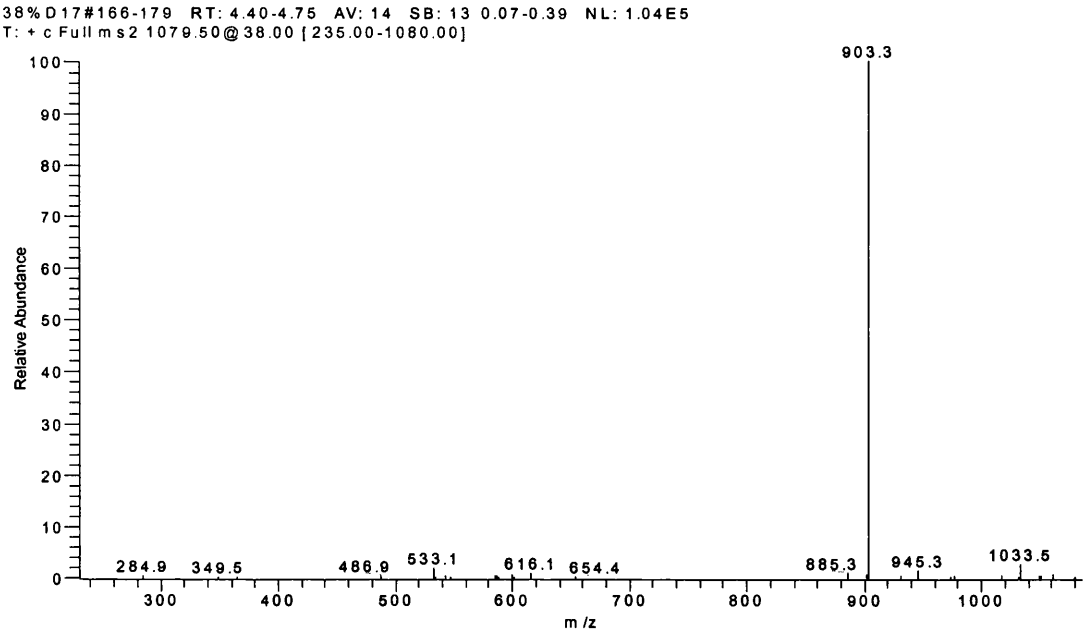

The CID spectra for the steroid sulfate derivatives (except testosterone sulfate derivative) could not be determined by collision cell fragments due to their low efficiency of fragmentation, and therefore, the source skimmer was used to obtain their CID spectra. Fragment ion at m/z 903 was observed in a low intensity, corresponding to loss of sulfate sodium moiety ($-SO_3Na$) and fragment ion at m/z 885, corresponding to further loss of water, was the most intense peak in the source CID spectrum of DHEA sulfate derivative (Figure 5.12.1). No fragment ions assigning from cleavage of the TMPP structure was observed, in contrast to the spectra of free steroid TMPP-derivatives, and this might be explained by the strong negative charge in the sulfate group, which make the whole structure more stable. A significant fragment at m/z 181 was also observed in the spectra, but its origin is not clear. Very similar spectra were observed for the TMPP-derivatives of androsterone sulfate (Figure 5.12.2) and eticholan-3α-ol-17-one sulfate (Figure 5.12.3), but the relative intensities of the peaks at m/z 905 and 181 were much lower for the latter.

Figure 5.12.1 CID of DHEA sulfate derivative

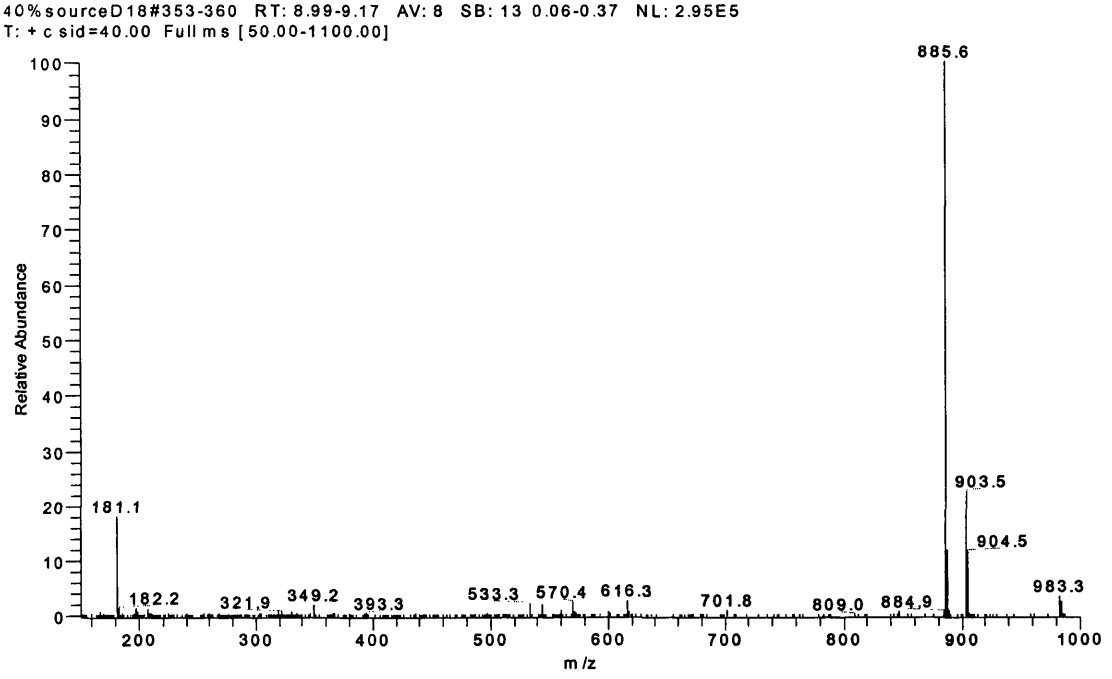

Figure 5.12.2 CID of androsterone sulfate derivative

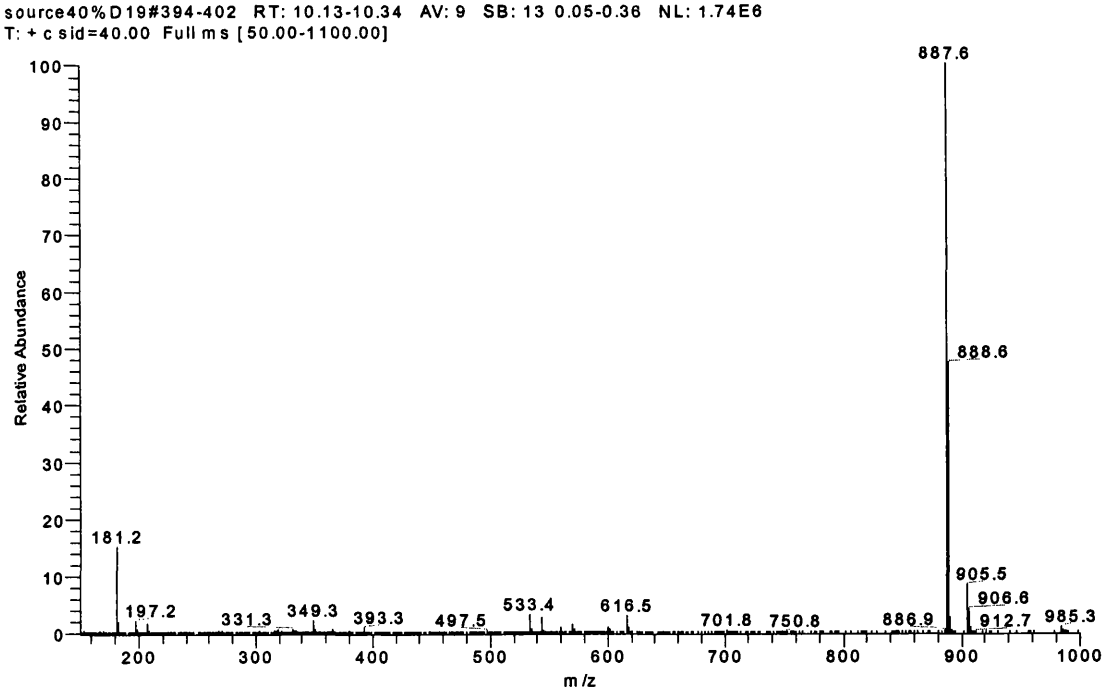

Figure 5.12.3 CID of etiocholan-3α-ol-17-one sulfate derivative

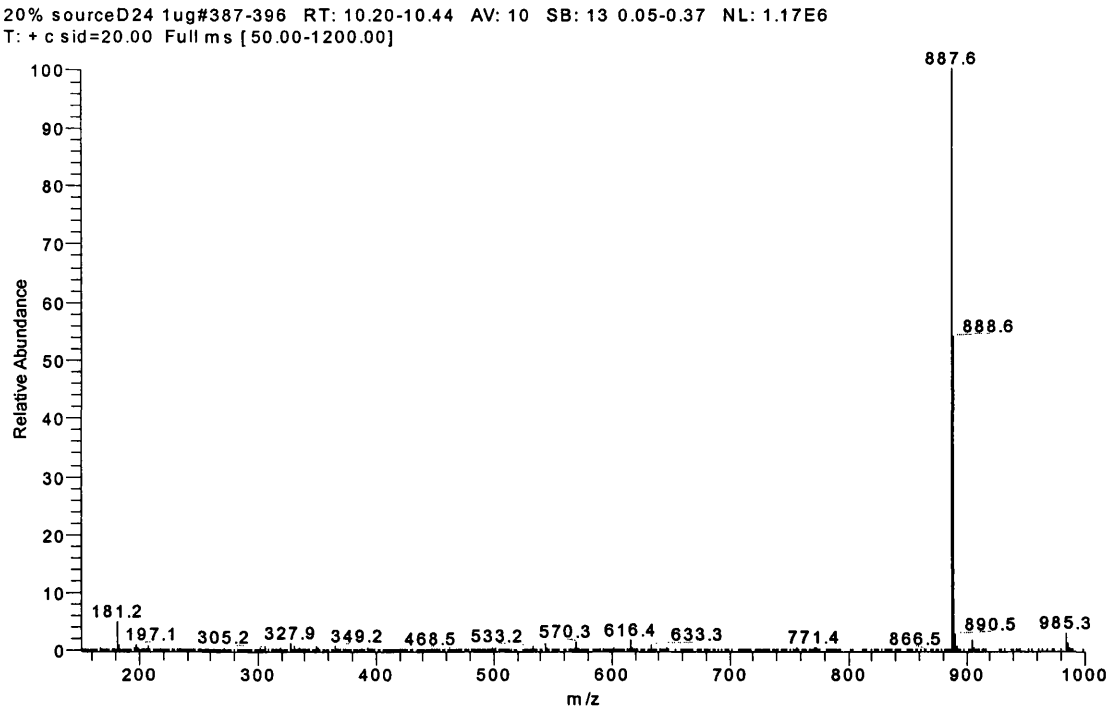

Table 5.8 CID spectra of TMPP-derivatives of conjugated steroids lacking a Δ_4-bond system

steroid	Parent ion	Collision energy (%)	Product ions m/z (relative abundance%)
A G	1081	40	1063 (10), 1035 (24), 975 (7), 947 (16), 905 (100), 616 (40), 533 (9)
DHEA G	1079	35	1033 (3), 903 (100)
DHEA S*	983	40	903 (23), 885 (100), 181 (18)
A S*	985	40	905 (8), 887 (100), 181 (15)
E G	1081	35	905 (100)
E S*	985	20	905 (2), 887 (100), 181 (6)

*Spectrum was obtained by source CID.

A G, androsterone glucuronide; DHEA G, dehydroisoandrosterone glucuronide;

DHEA S, dehydroisoandrosterone androsterone A S; androsterone sulfate;

E G, Etiocholan-3α-ol-17-one glucuronide; E S, Etiocholan-3α-ol-17-one sulfate

5.4.3.2 CID spectra of TMPP-derivatives of the steroids with a Δ_4-bond system

Non-conjugated steroids

Differentiation of testosterone from its 17α-OH isomer epitestosteone could not be achieved from the CID spectra of their TMPP-derivatives, because they gave not only the same fragments but also similar abundances of those fragments. Their spectra essentially contained a fragment ion at m/z 857, the product from Wolff-Kishner reduction, and also a series of fragment ion peaks from the TMPP group (m/z 616, 601, 600, 570, 543, 533, 371). As reported above, there were two peaks observed in the total ion chromatographs for testosterone and epitestosterone derivatives. The CID spectra of these two peaks were also very similar, however, the slight differences of the ratio of relative abundance of m/z 600 and its isotope peak m/z 601 between these two peaks (Table 5.9) may indicate some differences of their steric structures. Typical CID spectra of TMPP-derivatives of steroids with a Δ_4-bond are show in Figure 5.13, 5.14.1-2, 5.15.1-2 and 5.16.1-2, and details of these spectra are summarized in Table 5.9.

Figure 5.13 CID of testosterone derivative

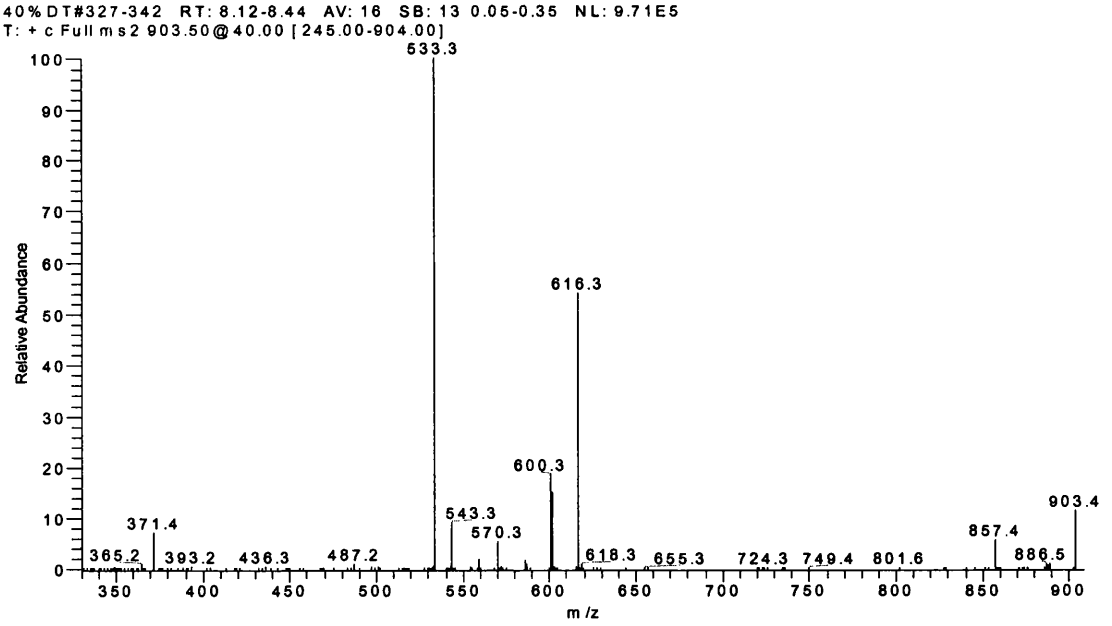

The CID spectra of Δ_4-androsten-3, 17-dione derivative generated from a parent ion of m/z 901 were also investigated (Figure 5.14.1-2). Of the three peaks previously observed in total ion chromatograph, the CID spectrum of peak one was quite different from those of peaks two and three. A fragment ion at m/z 616 was dominant in the spectrum of peak one, whilst m/z 533 was dominated in the spectra of peaks two and three. Moreover, fragments of m/z 369 was observed in the spectra of peak two and three, but no such an ion found in the spectrum of peak one. Comparing the CID spectra of peaks two and three of the Δ_4-androsten-3, 17-dione derivative with that of the testosterone derivative, it seems the pattern of their dissociation is similar, so peaks two and three may be correspond to the 3-oxo product formed during the derivatization of Δ_4-androsten-3, 17-dione, that may also undergo structure tautomerization in a similar manner to testosterone. A CID spectrum of the bi-derivative product (m/z 759) was not available due to insufficient abundance.

Figure 5.14.1 CID of Δ_4-androsten-3, 17-dione derivative (peak1)

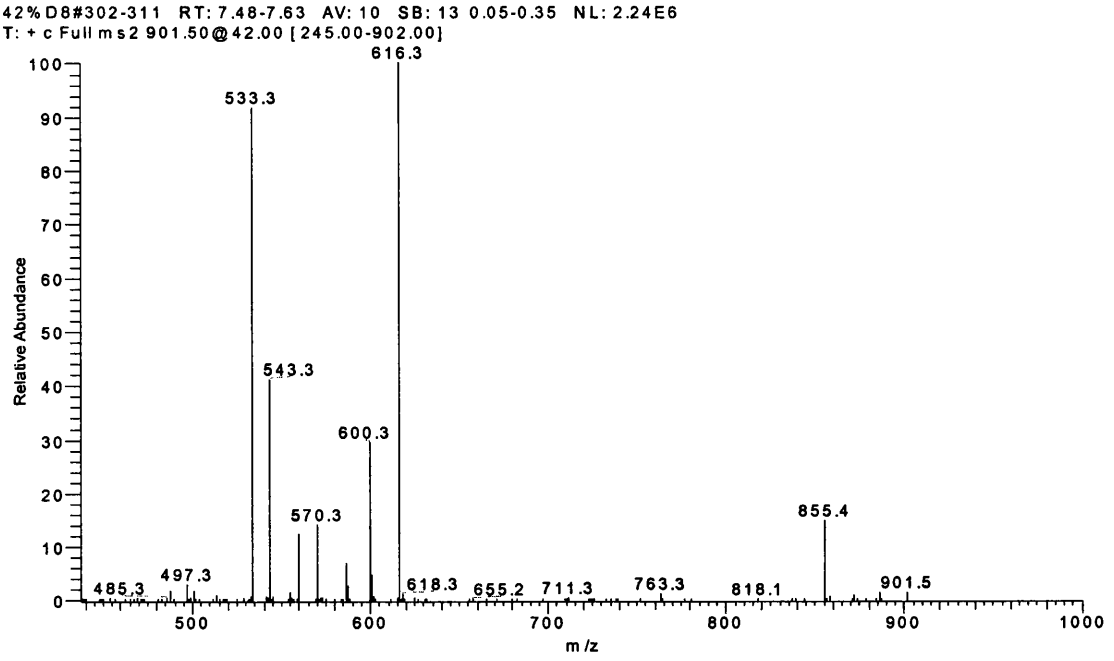

Figure 5.14.2 CID of Δ_4-androsten-3, 17-dione derivative (peak2)

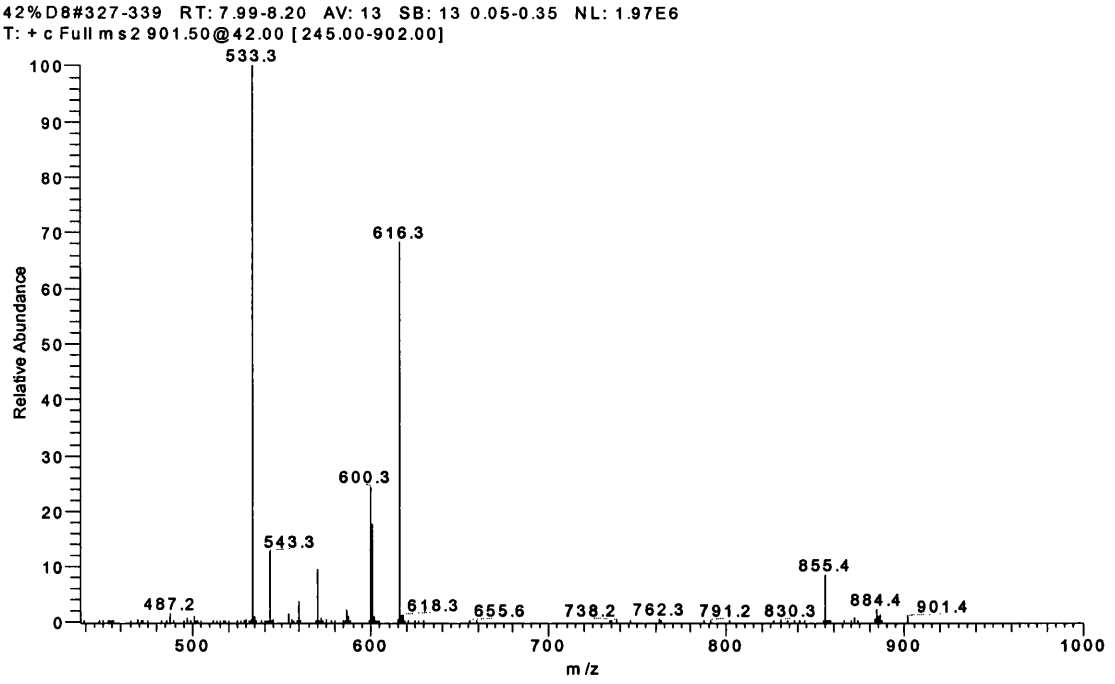

The pattern of dissociation observed for Δ_4-androstene-3, 11, 17-trione from patent ion at m/z 915 was very similar to Δ_4-androsten-3, 17-dione. The CID spectrum of peak one was also different from those of peaks two and four. In the former m/z 616 was dominant, but m/z 533 was most intense in the latter. In addition, there was a peak at m/z 383 observed in the latter CID spectra but not observed in the former. The CID spectra of bi- and tri-derivatives were also not achieved as the result of their sensitivities. The CID spectra of Δ_4-androstene-3, 11, 17-trione TMPP derivative from peak 2 and peak 4 are shown in Figure 5.15.1-2.

Figure 5.15.1 CID of Δ_4-androstene-3, 11, 17-trione derivative (peak1)

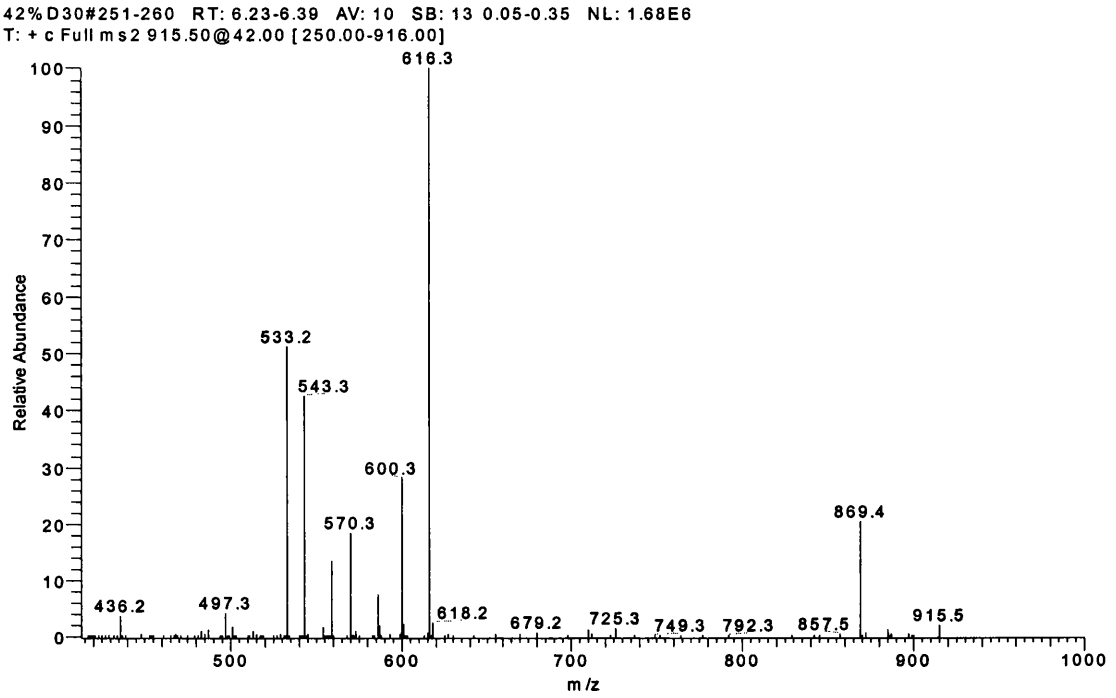

Figure 5.15.2 CID of Δ_4-androstene-3, 11, 17-trione derivative (peak2)

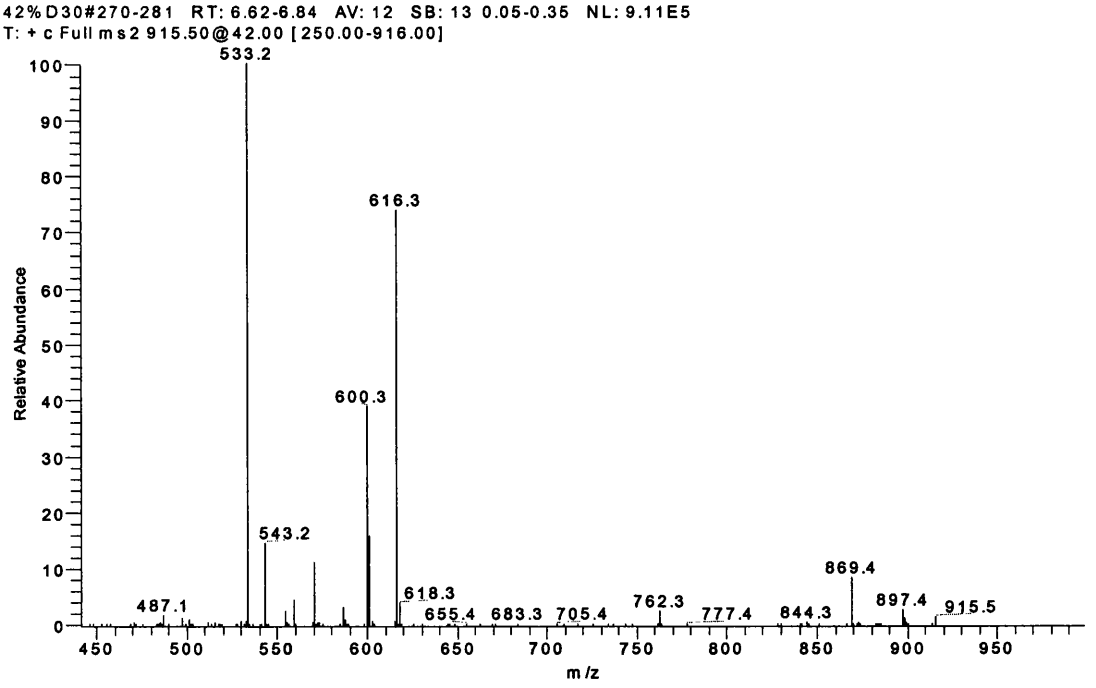

Conjugated steroids

CID spectra of conjugated testosterone derivatives were quite simple, only m/z of 903 was observed in the spectrum of testosterone glucuronide (Figure 5.16.1), corresponding to the loss of glucuronide moiety. Whilst besides m/z 903, there was only a peak of low abundance at m/z 885 in the spectrum of testosterone sulfate (Figure 5.16.2), corresponding to the further loss of water. There was no difference observed between peaks one and two for either of these two conjugated derivatives.

Figure 5.16.1 CID of testosterone glucuronide derivatve

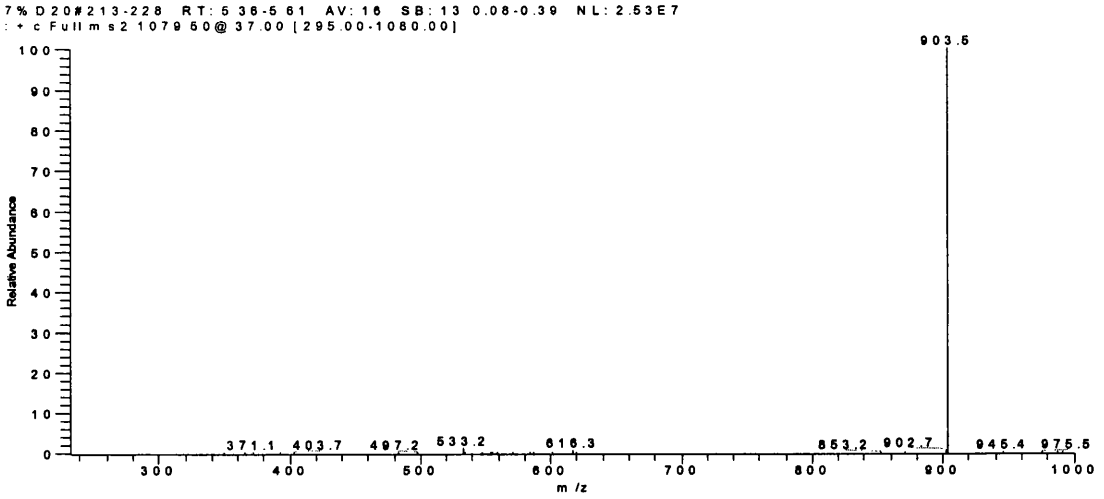

Figure 5.16.1 CID of testosterone sulfate derivative

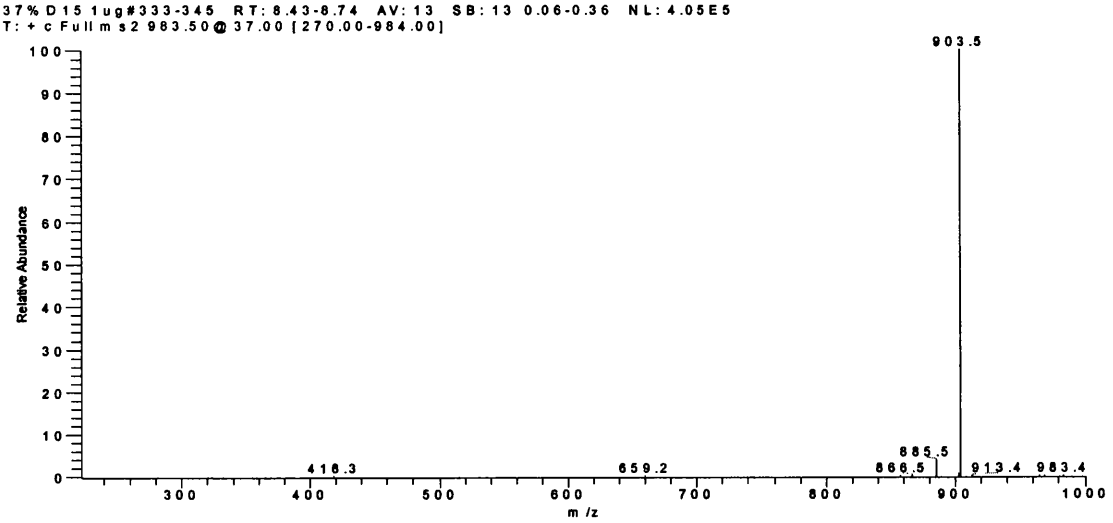

Table 5.9 ESI-MS/MS of derivatized androgenic steroids

Steroid	Parent ion	Collision energy (%)	Product ions m/z (relative abundance)
T	903 (peak 1)	40	857 (5), 616 (54), 601 (15), 600 (18), 570 (6), 543 (8), 533 (100), 371 (7)
	903 (peak2)	40	857 (6), 616 (54), 601 (15), 600 (19), 570 (5), 543 (9), 533 (100), 371 (7)
ET	903 (peak1)	40	857 (6), 616 (54), 601 (14), 600 (19), 570 (6), 543 (7), 533 (100), 371 (7)
	903 (peak2)	40	857 (6), 616 (51), 601 (15), 600 (16), 570 (6), 543 (7), 533 (100), 371 (7)
Δ_4-Dione	901(peak 1)	42	855 (15), 616 (100), 601 (5), 600 (29), 570 (14), 559 (12), 543 (41), 533 (92)
	901 (peak 2)	42	855 (8), 616 (68), 601 (17), 600 (24), 570 (9), 559 (4), 543 (12), 533 (100), 369 (6)
	901 (peak 3)	42	855 (8), 616 (66), 601 (15), 600 (24), 570 (9), 559 (3), 543 (10), 533 (100), 369 (6)
Δ_4-Trione	915 (peak 1)	42	869 (20), 616 (100), 601 (2), 600 (27), 586 (7), 570 (18), 559 (13), 543 (42), 533 (50)
	915 (peak 2)	42	869 (8), 616 (74), 601 (16), 600 (40), 586 (3), 570 (11), 559 (5), 543 (15), 533 (100), 383 (5)
	915 (peak 4)	42	869 (8), 616 (69), 601 (18), 600 (42), 586 (3), 570 (10), 559 (4), 543 (11), 533 (100), 383 (6)
T G	1079 (peak1)	37	903 (100)
	1079 (peak2)	37	903 (100)
T S	983 (peak 1)	37	903 (100), 885 (4)
	983 (peak 2)	37	903 (100), 885 (5)

*Spectrum was achieved by source CID.

T, testosterone; ET, epitestosterone; Δ_4 - Dione, Δ_4-androstene-3, 17-dione;

Δ_4 - Trione, Δ_4-androstene-3, 11, 17-trione; T G, testosterone glucuronide; T S, testosterone sulfalte.

5.4.4 Limits of detection

Limits of detection for steroids with the ESI source were significantly improved by derivatization (Figure 5.17). Although structural information could be obtained by ESI-MS for the steroids investigated, the sensitivities obtained were disappointing. Comparing steroids with their TMPP-derivatives in full scan mode, the minimum level at which most of free non-conjugated steroids were detectable was 10 ng, and only the 4-ene-3-one steroids could be detected at 1ng. However, the sensitivities for steroid conjugates were much better than the non-conjugated steroids by negative ESI-MS. The detection limits were 500 pg for the steroid glucuronides and 250 pg for the sulfates (Refer to chapter 4, table 4.11). In contrast, the detection limits for most of the TMPP-derivatives of conjugated and non-conjugated steroids were no more than 20 pg,

significant exception however included dihydrotestosterone and 5β-androstan-17β-ol-3-one derivatives for which the detection limit was 1 ng. Formation of the TMPP-derivatives generally increased sensitivities 50 to 100 times for non-conjugated steroids and more than 20 times for conjugated steroids. Even compared to the APCI source, which is more sensitive for most of non-conjugated steroids, derivatization also provides a substantial improvement (Refer to chapter 4, table 4.5). Therefore, derivatization method should benefit the analysis of some of these compounds in biological fluids, in which the concentrations are very low.

Figure 5.17 Comparison of limits detection between non-derivatized and derivatized steroids in full scan mode

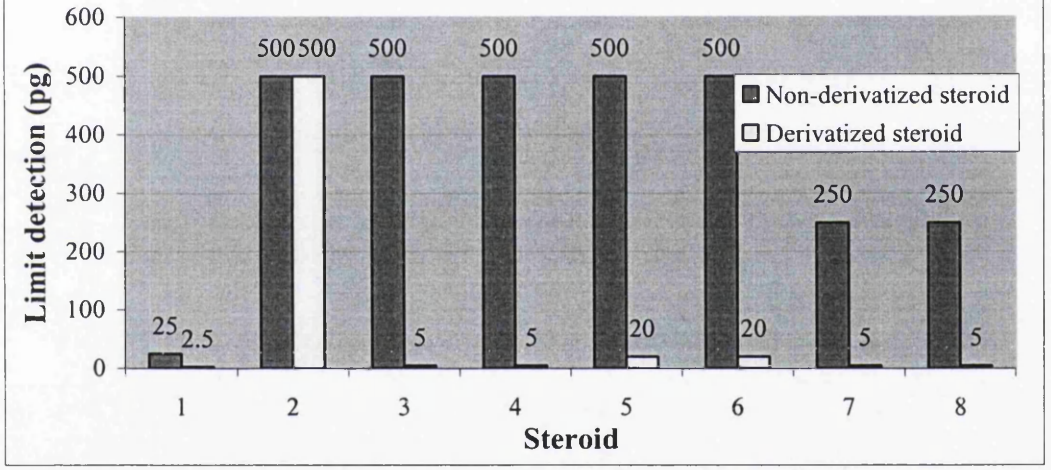

1. Testosterone (m/z 289/903); 2. Dihydrotestosterone m/z 291/905); 3. Dehydroisoandrosterone (m/z 271/903); 4. Androsterone (m/z 273/905); 5. Dehydroisoandrosterone glucuronide (m/z 463/1079); 6. Androsterone glucuronide (m/z 465/1081); 7. Dehydroisoandrosterone sulfate (m/z 367/983); 8. Androsterone sulfate (m/z 369/985).

The limits of detection were also studied by the different scan modes for the steroid derivatives. Androsterone, etiocholan-3β-ol-17one, dehydroepiandrosterone, dehydroepiandrosterone glucuronide and androsterone glucuronide were used for comparisons, and the results are summarized in Table 5.10.

Table 5.10 Limits of detection of TMPP-derivatives of some steroids by full scan, SIM and SRM mode of MS (S/N≥ 3)

Steroid derivative	Full scan (pg)	SIM (pg)	SRM (pg)
Androsterone	10 (m/z 903)	10 (m/z 905)	2 (m/z 905 → 533)
Etiocholan-3β-ol-17one	10 (m/z 905)	10 (m/z 905)	2 (m/z 905 → 533)
DHEA	10 (m/z 903)	10 (m/z 903)	2 (m/z 903 → 533)
DHEA glucuronide	20 (m/z 1079)	20 (m/z 1079)	5 (m/z 1079→ 903)
Androsterone glucuronide	20 (m/z 1081)	20 (m/z 1081)	5 (m/z 1081→ 905)

The comparisons in Table 5.10 show that SRM is about four to five times more sensitive than full scan and SIM mode. Moreover, SRM is less prone to chemical noise than full scan and more specific than SIM mode, as it monitors only selected transitions from parent ions to daughter ions. As the objective of this work is to detect a very low concentration of androgenic steroids in biological fluids, the SRM mode would benefit this purpose.

5.5 Quantitative LC-MS for androgenic steroid derivatives

5.5.1 Separation of 5 steroid derivatives by HPLC-MS

A gradient system (Section 5.2.3) was applied for the separation of the TMPP-derivatives of five androgenic steroids at a flow rate of 0.4 ml/min. The five compounds were totally separated by micro-bore C_{18} column, and the conjugated derivatives were eluted faster than the unconjugated derivatives. The total ion chromatograph and the extracted ion chromatograph of each compound by SRM mode of MS were showed in Figure 5.18.

Figure 5.18 Total ion chromatograph and extracted ion chromatograph of five steroid derivatives

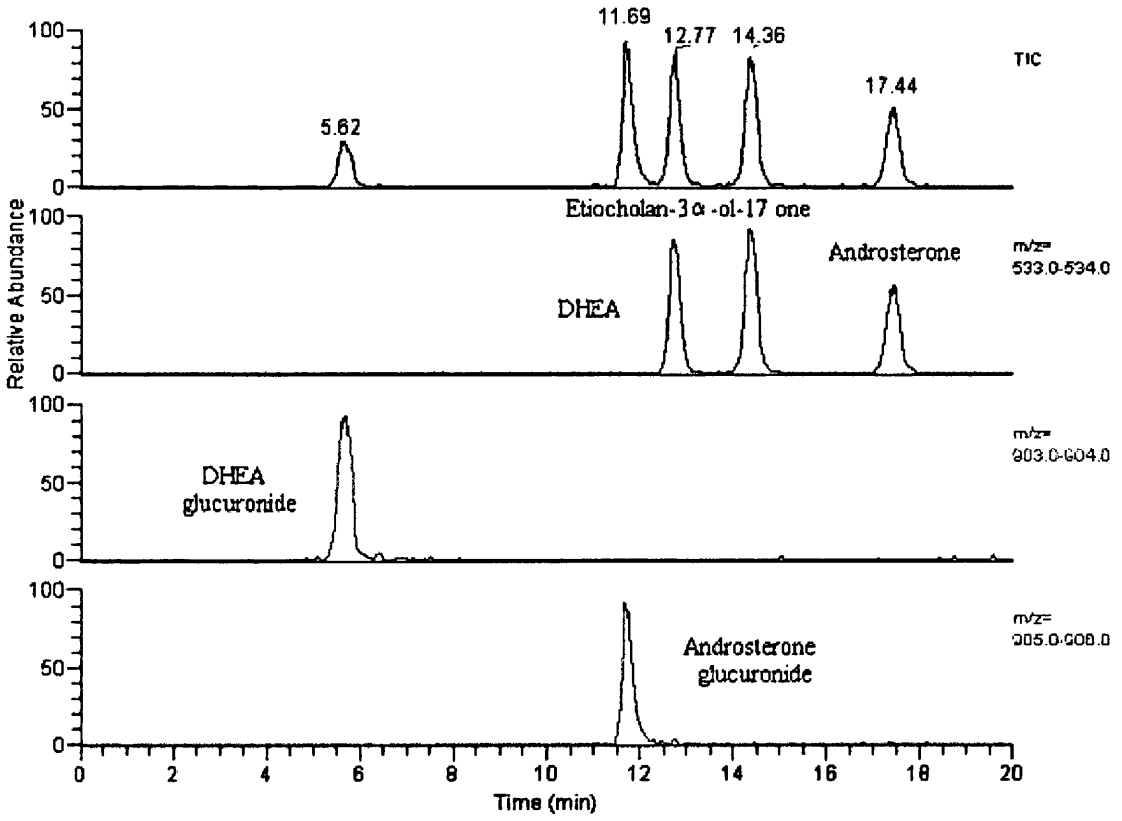

Note: sample was injected at 5 μl and at 1 ng/μl of each compound.

5.5.2 Analysis of variance of androgenic steroid derivatives

An ANOVA method was used to analyses the variances for the androgenic steroid derivatives, and the results were summarized in table 5.11 and 5.12.

A one-tailed F-test was used to test the significant difference between intra-day and inter-day variance. All the calculated F values shown in Table 5.12 are smaller than the critical F value ($F_{critical}$ = 5.14, P = 0.05), therefore, we can conclude that there is no significant difference between intra-day and inter-day variance.

Table 5.11 Daily and overall mean (peak area) of steroid TMPP-derivatives at three concentrations by repeated MS-SRM measurements

Steroid	Concentration (pg/μl)	Mean (peak area)	Concentration (pg/μl)	Mean (peak area)	Concentration (pg/μl)	Mean (peak area)
Etiocholan-3β-ol-17 one (m/z 905)	5	Day1 8.94 E+4	50	Day1 1.43 E+6	200	Day1 4.47 E+6
		Day2 1.15 E+5		Day2 1.26 E+6		Day2 4.97 E+6
		Day3 1.02 E+5		Day3 1.12 E+6		Day3 4.76 E+6
		Total 1.02 E+5		Total 1.27 E+6		Total 4.73 E+6
Androsterone (m/z 905)	5	Day1 7.78 E+4	50	Day1 6.87 E+5	200	Day1 2.77 E+6
		Day2 8.90 E+4		Day2 7.84 E+5		Day2 3.18 E+6
		Day3 8.17 E+4		Day3 7.48 E+5		Day3 3.32 E+6
		Total 8.28 E+4		Total 7.40 E+6		Total 1.45 E+7
DHEA (m/z 903)	5	Day1 1.34 E+5	50	Day1 8.97 E+5	200	Day1 3.55 E+6
		Day2 9.96 E+4		Day2 1.09 E+6		Day2 3.96 E+6
		Day3 1.24 E+5		Day3 1.19 E+6		Day3 3.62 E+6
		Total 1.19 E+5		Total 1.06 E+6		Total 3.71 E+6
DHEA glucuronide (m/z 1079)	5	Day1 7.64 E+4	50	Day1 1.02 E+6	200	Day1 4.92 E+6
		Day2 6.55 E+4		Day2 1.15 E+6		Day2 5.66 E+6
		Day3 7.35 E+4		Day3 1.13 E+6		Day3 5.47 E+6
		Total 7.18 E+4		Total 1.10 E+6		Total 5.35 E+6
Androsterone glucuromide (m/z 1081)	5	Day1 2.22 E+5	50	Day1 1.36 E+6	200	Day1 5.31 E+6
		Day2 1.76 E+5		Day2 1.46 E+6		Day2 5.99 E+6
		Day3 1.81 E+5		Day3 1.23 E+6		Day3 5.10 E+6
		Total 1.93 E+5		Total 1.35 E+6		Total 5.47 E+6

Table 5.12 Summary of ANOVA results for steroid TMPP-derivatives by repeated MS-SRM measurements

Steroid	Concentration (pg/μl)	Source of variation	Sum of squares	Degree of freedom	Mean square	F
Etiocholan-3β-ol-17 one (m/z 905)	5	Intra-day	2.08 E+9	6	3.47 E+8	1.36
		Inter-day	9.48 E+8	2	4.74 E+8	
	50	Intra-day	4.66 E+11	6	7.76 E+10	0.95
		Inter-day	1.48 E+11	2	7.40 E+10	
	200	Intra-day	8.09 E+11	6	1.35 E+11	1.40
		Inter-day	3.78 E+11	2	1.89 E+11	
Androsterone (m/z 905)	5	Intra-day	9.18 E+8	6	1.52 E+8	0.63
		Inter-day	1.92 E+8	2	9.60 E+7	
	50	Intra-day	6.17 E+10	6	1.03 E+10	0.70
		Inter-day	1.44 E+10	2	7.21 E+9	
	200	Intra-day	5.59 E+11	6	9.32 E+11	1.64
		Inter-day	4.79 E+11	2	2.40 E+11	
DHEA (m/z 903)	5	Intra-day	2.46 E+9	6	4.10 E+8	2.25
		Inter-day	1.84 E+9	2	9.22 E+8	
	50	Intra-day	1.25 E+11	6	2.08 E+10	3.27
		Inter-day	1.36 E+11	2	6.80 E+10	
	200	Intra-day	8.91 E+11	6	1.48 E+11	0.94
		Inter-day	2.80 E+11	2	1.40 E+11	
DHEA glucuronide (m/z 1079)	5	Intra-day	2.05 E+8	6	3.42 E+7	2.83
		Inter-day	1.93 E+8	2	9.67 E+7	
	50	Intra-day	5.95 E+10	6	9.92 E+9	1.58
		Inter-day	3.14 E+10	2	1.57 E+10	
	200	Intra-day	1.58 E+12	6	2.63 E+11	1.70
		Inter-day	8.97 E+11	2	4.49 E+11	
Androsterone glucuronide (m/z 1081)	5	Intra-day	4.98 E+9	6	8.30 E+8	2.25
		Inter-day	3.74 E+9	2	1.87 E+9	
	50	Intra-day	2.92 E+11	6	4.87 E+10	0.79
		Inter-day	7.73 E+10	2	3.86 E+10	
	200	Intra-day	1.99 E+12	6	3.31 E+11	1.99
		Inter-day	1.32 E+12	2	6.60 E+11	

5.5.3. Precision and linearity

Precision in the measurements of the steroid derivatives was also studied by repeatedly injecting samples at three different concentrations (5 pg/μl, 50 pg/μl and 200

pg/μl for steroid derivatives) over three days. The intra-day coefficient variances are between 7.8% and 21.9%, and the inter-day values range from 9.2% to 25.4%, whereas the total coefficient of variances are from 8.1% to 21.8% (Table 5.13 a to e).

All the five steroid derivatives were found to give a linear response in the investigated range of concentrations (5 to 200 pg/μl). Correlation coefficients of linear regression are from 0.9997 up to 0.9999. Calibration curves and regression equation are presented in Figure 5.19 (a to e).

Table 5.13 (a) Precision of Etiocholan-3β-ol-17 one TMPP-derivative

Concentration (pg/μl)	Intra-day (%CV)	Inter-day (%CV)	Total (%CV)
5	18.3	21.3	19.1
50	21.9	21.4	21.8
200	7.8	9.2	8.1

Figure 5.19 (a) Linearity of etiocholan-3β-ol-17 one TMPP-derivative

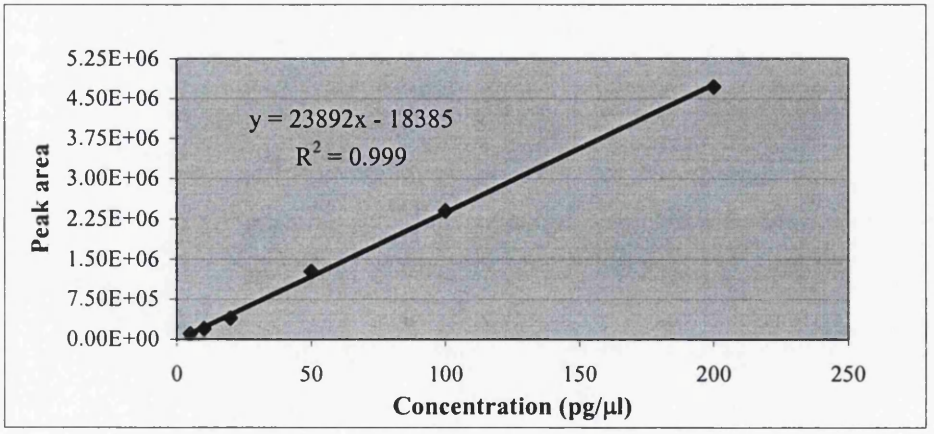

Table 5.13 (b) Precision of androsterone TMPP-derivative

Concentration (pg/µl)	Intra-day (%CV)	Inter-day (%CV)	Total (%CV)
5	14.9	11.8	14.2
50	13.7	11.5	13.2
200	9.9	15.8	11.7

Figure 5.19 (b) Linearity of androsterone TMPP-derivative

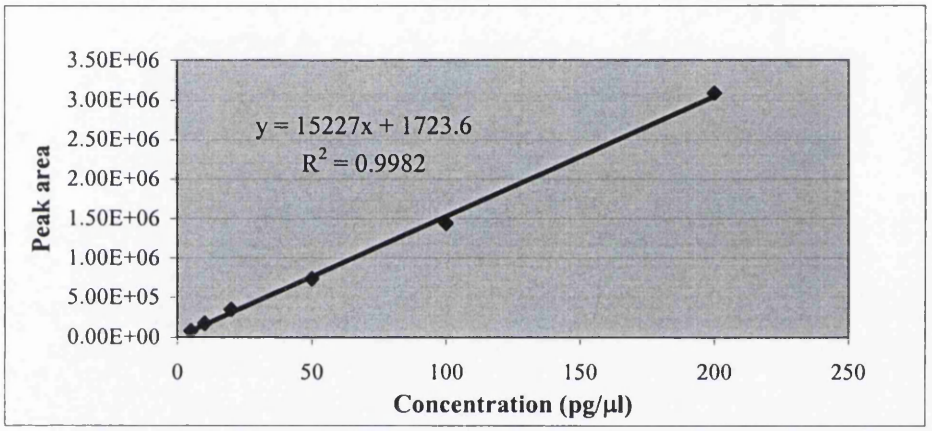

Table 5.13 (c) Precision of DHEA TMPP-derivative

Concentration (pg/µl)	Intra-day (%CV)	Inter-day (%CV)	Total (%CV)
5	17.0	25.5	19.5
50	13.6	24.6	17.0
200	10.4	10.1	10.3

Figure 5.19 (c) Linearity of DHEA TMPP-derivative

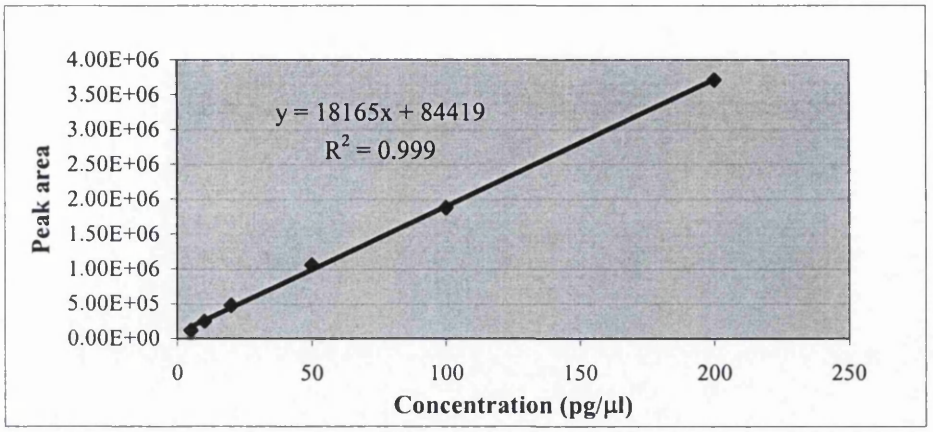

Table 5.13 (d) Precision of DHEA glucuronide TMPP-derivative

Concentration (pg/µl)	Intra-day (%CV)	Inter-day (%CV)	Total (%CV)
5	8.1	13.7	9.8
50	9.1	11.4	9.7
200	9.6	12.5	10.4

Figure 5.19 (d) Linearity of DHEA glucuronide TMPP-derivative

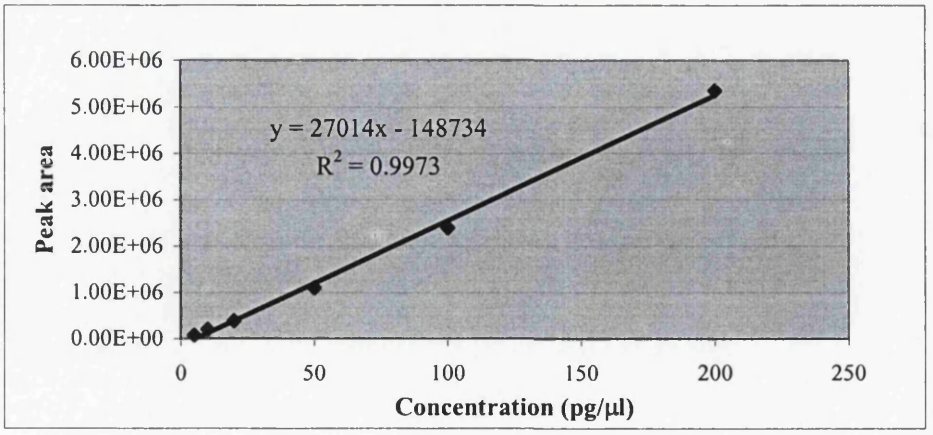

Table 5.13 (e) Precision of androsterone glucuronide TMPP-derivative

Concentration (pg/μl)	Intra-day (%CV)	Inter-day (%CV)	Total (%CV)
5	14.9	22.4	17.9
50	16.3	14.6	15.9
200	10.5	14.9	11.8

Figure 5.19 (e) Linearity of androsterone glucuronide TMPP-derivative

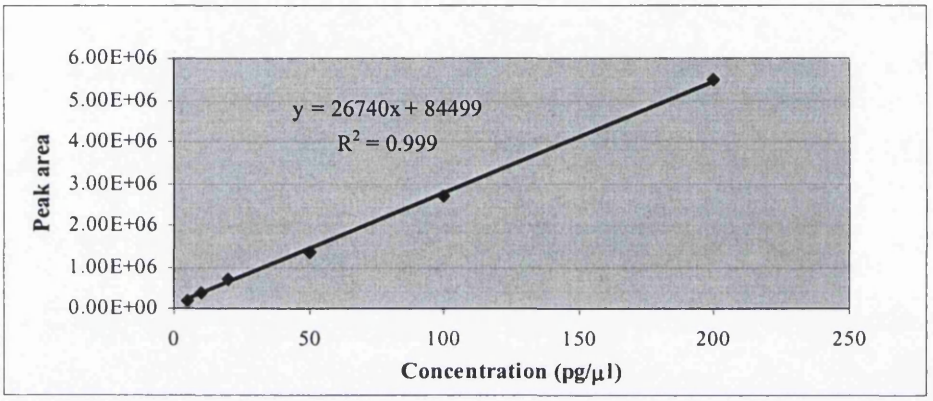

5.5.4 Limits of quantitation

Limits of quantitation of each steroid derivative were also studied based on the regression lines of y on x from the previously calibration curves, and the results were present in Table 5.14.

Table 5.14 Limits of quantitation of five steroid derivative

Steroid derivative	Limit of quantitation (pg)
Etiocholan-3β-ol-17 one	16.2
Androsterone	25.4
DHEA	21.3
DHEA glucuronide	14.3
Androsterone glucuronide	14.5

5.6 Conclusions

In this chapter, a derivatization method was developed in the aim of increasing the sensitivities and quantitation for detection of the investigated androgenic steroids and their conjugates. The derivatization of steroids interest was carefully studied and optimized by different conditions to get maximum reaction yields, and then a LC-ESI/MS method was used to detect these product derivatives on line, with no need of sample pretreatment. The chromatographic characteristics of these derivatives were studied, and they were found to have longer retention time compared to the non-derivatized steroids. There was more than one peak observed in the total ion chromatographs of 4-ene-3-oxo steroid derivatives, and the possible reasons were considered. The full scan and CID mass spectra were also studied for each individual steroid derivative and different scan modes were compared to choose the most sensitive mode for quantitative analysis.

A second gradient system was set up to get baseline separation of the TMPP-derivatives of five steroids interest, and an ANVOA method was used to estimate the intra-day and inter-day variance for simultaneous quantitation of these five compounds. The precision, linearity and limit of quantitation were also measured for each of these compounds. Results showed that the derivatization method significantly improved the sensitivity of most investigated steroids and the method could possibly be applied for steroid residue analysis in biological fluids. However, internal standard may need to decrease variability during the experiments. Further work is required including optimization of the derivatized reaction to improve the activity of 3-oxo cholestane-steroids, and separation of other steroid derivatives due to the similarities of their mass

spectra after derivatization. Because of time limitation this direction could not be further pursued, but it is clearly a promising direction for future studies.

References

1. P. Kintz, V. Cirimele, B. Ludes, *J. Anal. Toxicol.* 23 (1999) 424.
2. P. Kintz, V. Cirimele, T. Jeanneau, B. Ludes, *J. Anal. Toxicol.* 23(1999) 352.
3. S. H. Peng, J. Segura, M. Farré, X. *de la Torre. Clin. Chem.* 46(2002) 347
4. L.Dehennin, M. Ferry, P. Lafarge, G. Pérès, J.-P. Lafarge, *Steroids* 63 (1998) 80.
5. M. H. Choi, B.C. Chung, *Analyst* 124 (1999) 1297.
6. C. Scherer, U. Wachter, S.A. Wudy, *Analyst* 123 (1998) 2661.
7. N. Tagawa, J. Tamanaka, A. Fujianmi, Y. Kobayashi, T. Takano, S. Fukta, K. Kuma, H. Tada, N. *Amin, Clin. Chem.* 46 (2000) 523.
8. M. A. Zemaitis, P.D. Kroboth, *J. Chromatogr. B* 716 (1998) 19.
9. M.H. Choi, K.R. Kim, B.C. Chung, Steroids 65 (2000) 54.
10. C.H.L. Shackleton, H. Chuang, J. Kim, X. de la Torre, *J. Segura, Steroids* 62 (1997) 523.
11. S. Liu, J. Sjövall W.J. Griffiths, *Rapid Commun. Mass Spectrom.* 14 (2000) 390.
12. W. J. Leavens, S. J. Lane, R. M. Carr, A. M. Lockie, I. Waterhouse, *Rapid Commun. Mass Spectrom.* 16 (2002) 433.

Appendices

Appendix 1. 5β-Dihydrotestosterone: MS^2 of ion m/z 273; collision energy 28%

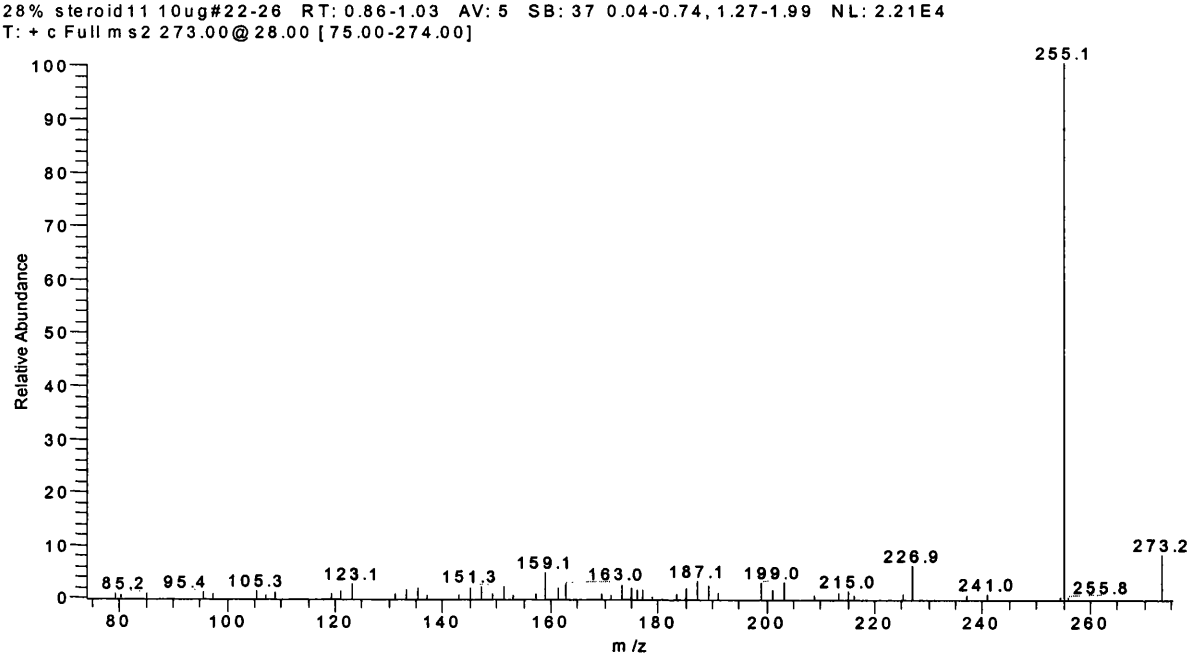

Appendix 2. Etiocholan-3β-ol-17-one: MS^2 of ion m/z 273; collision energy 28%

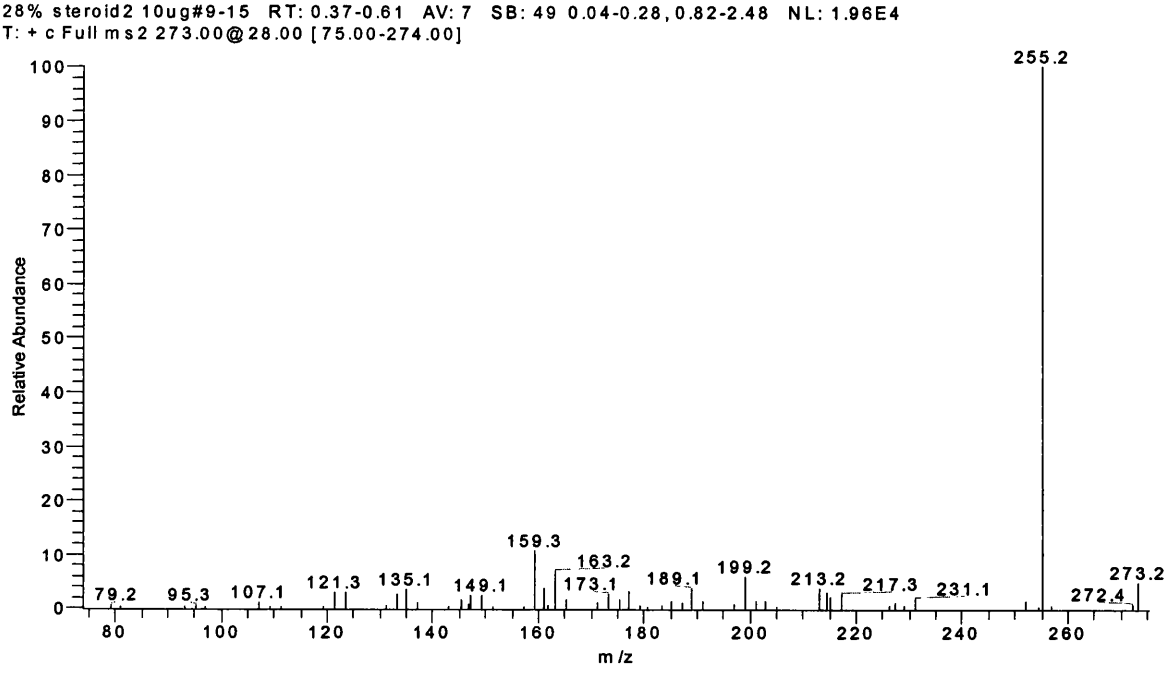

Appendix 3. Etiocholan-3α-ol-17-one: MS^2 of ion m/z 273; collision energy 28%

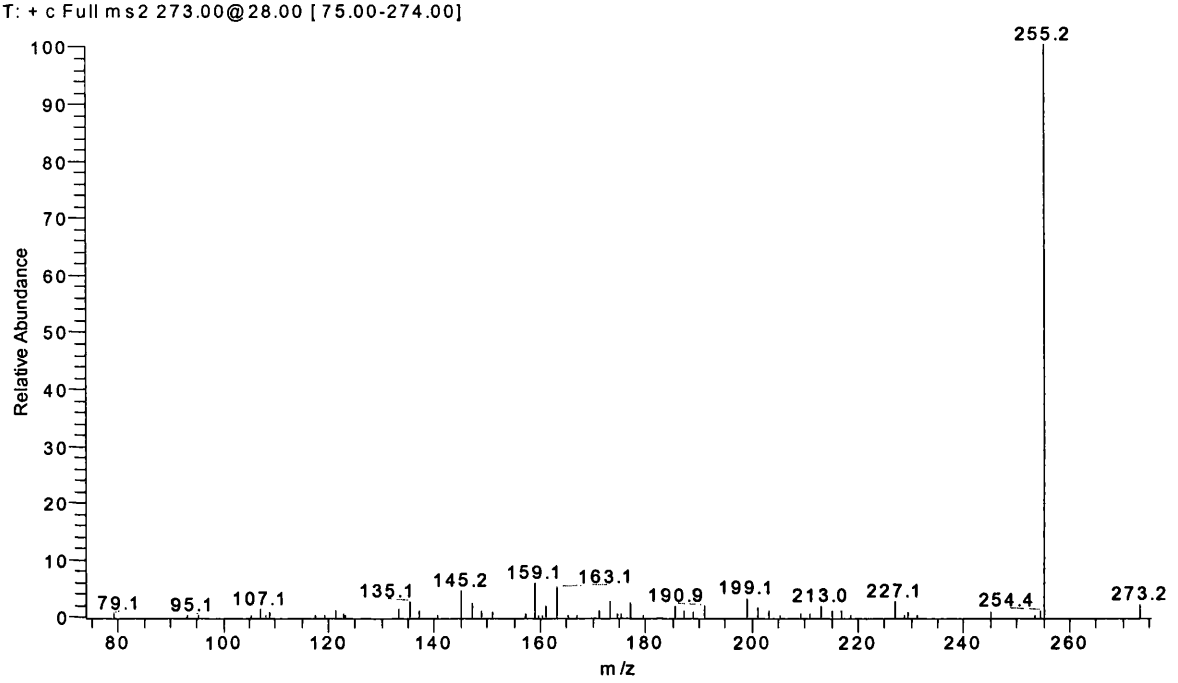

Appendix 4. Epiandrosterone: MS^2 of ion m/z 273; collision energy 28%

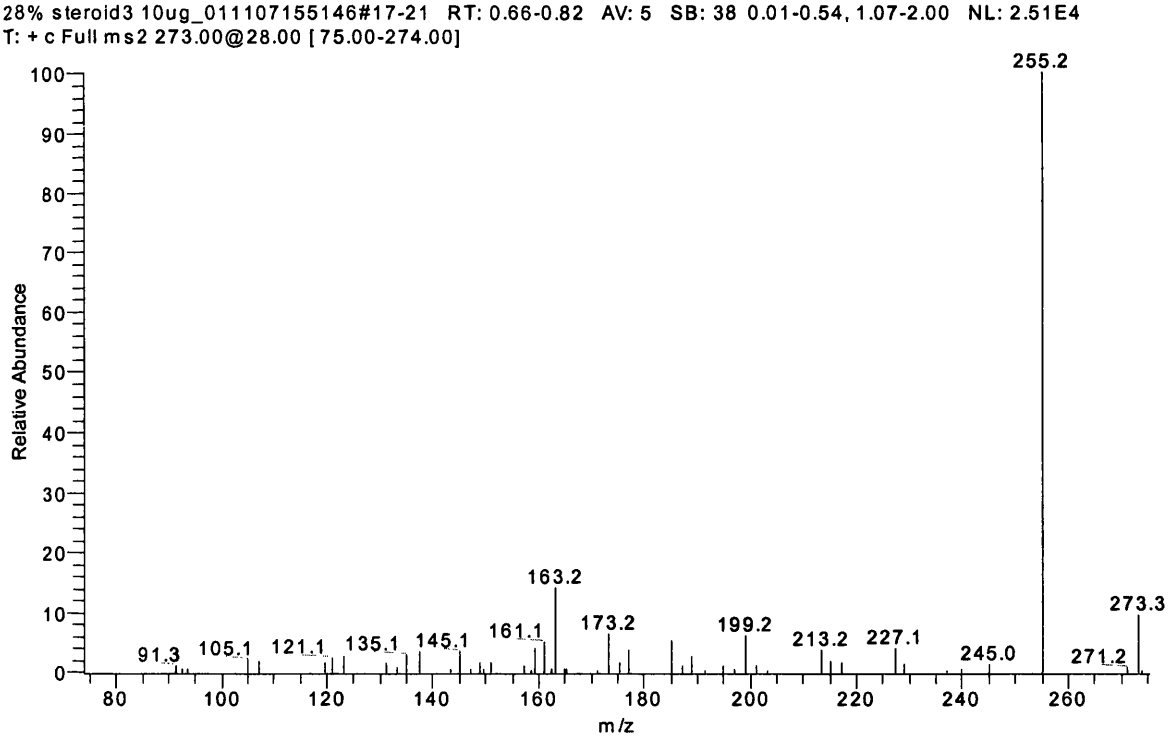

Appendix 5. Androsterone: MS^2 of ion m/z 273; collision energy 28%

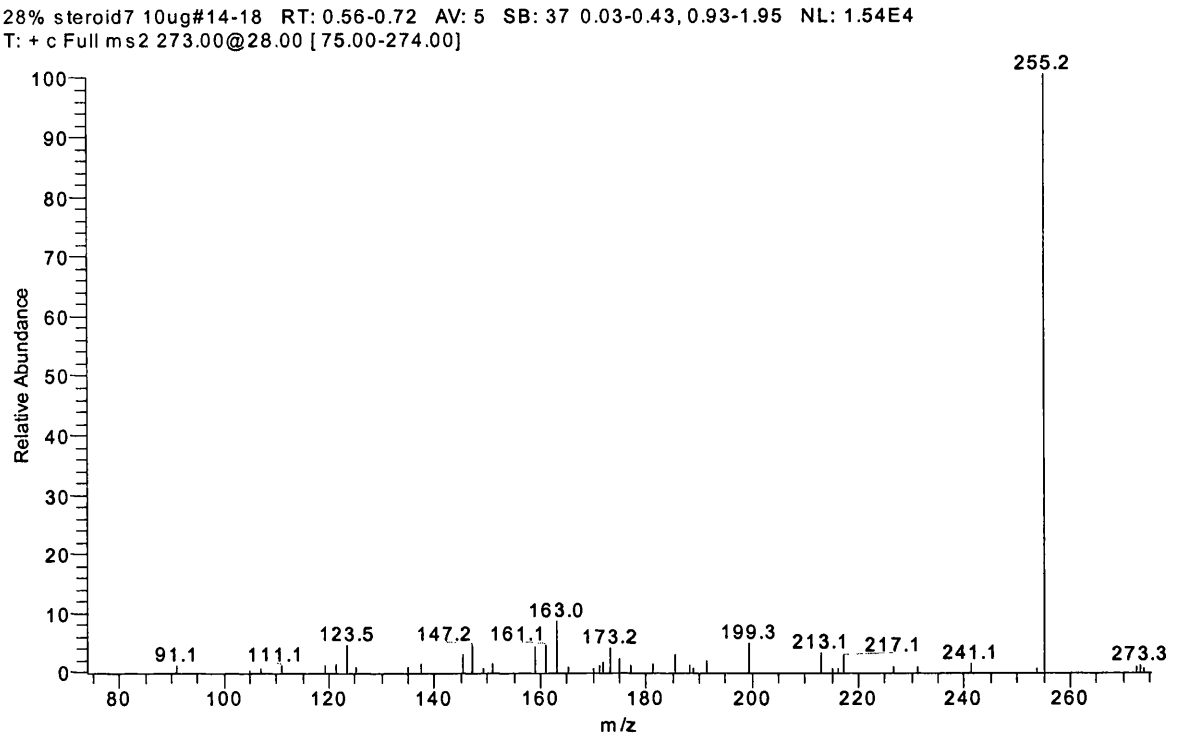

Appendix 6. 5β-Dihydrotestosterone: MS^2 of ion m/z 255; collision energy 30%

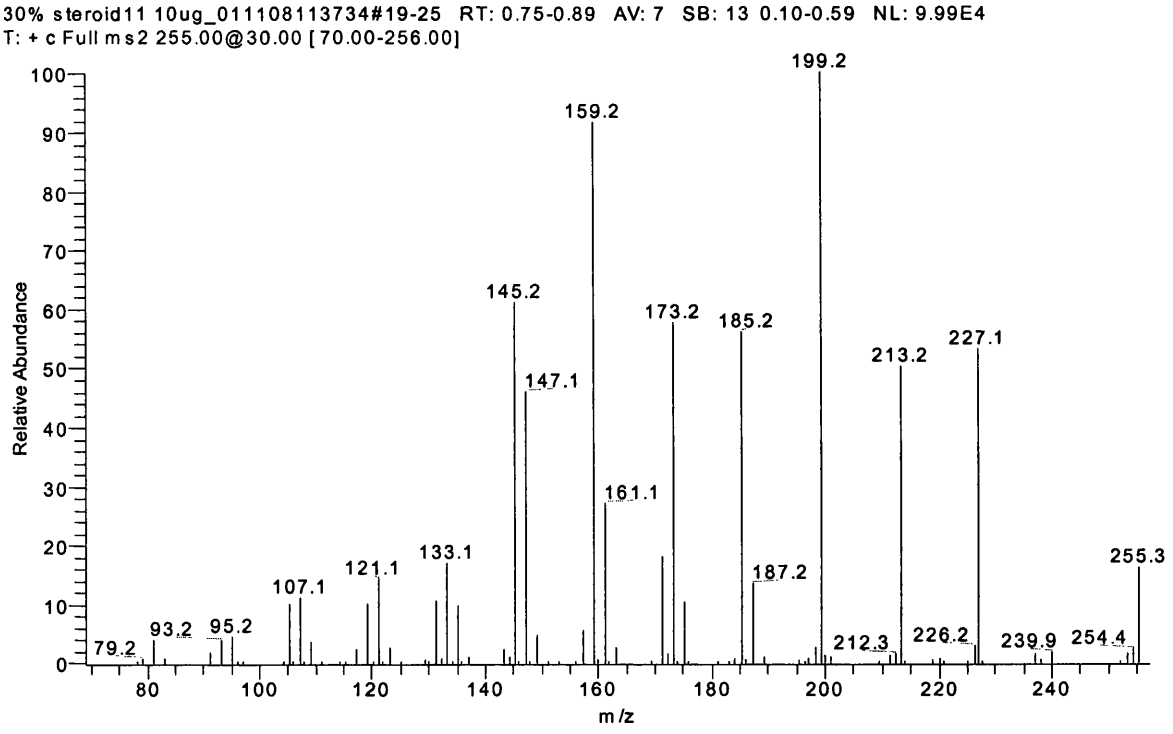

Appendix 7. Etiocholan-3β-ol-17-one: MS^2 of ion m/z 255; collision energy 30%

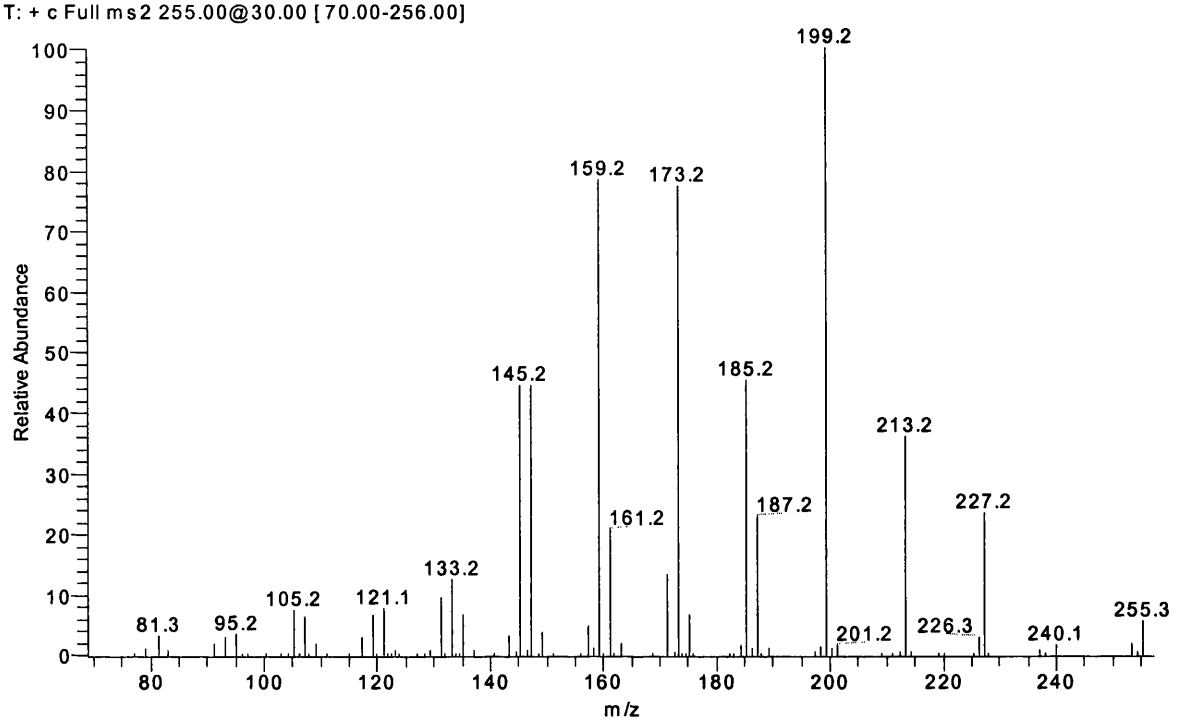

Appendix 8. Etiocholan-3α-ol-17-one: MS^2 of ion m/z 255; collision energy 30%

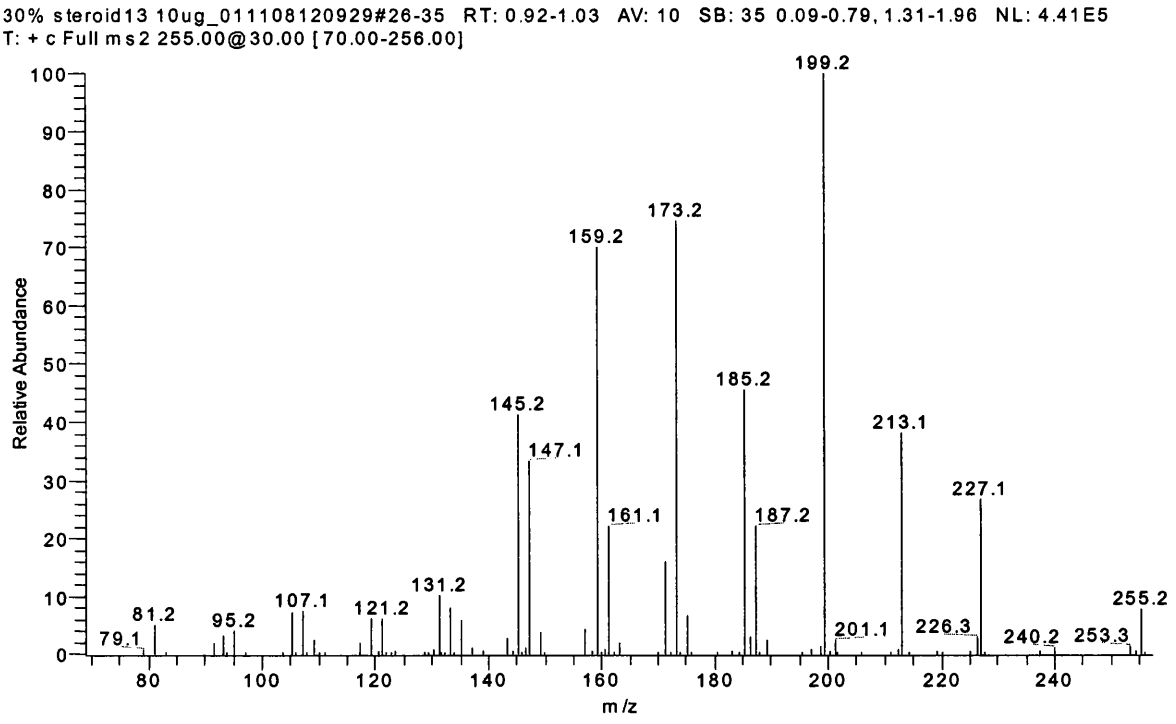

Appendix 9. Epiandrosterone: MS^2 of ion m/z 255; collision energy 30%

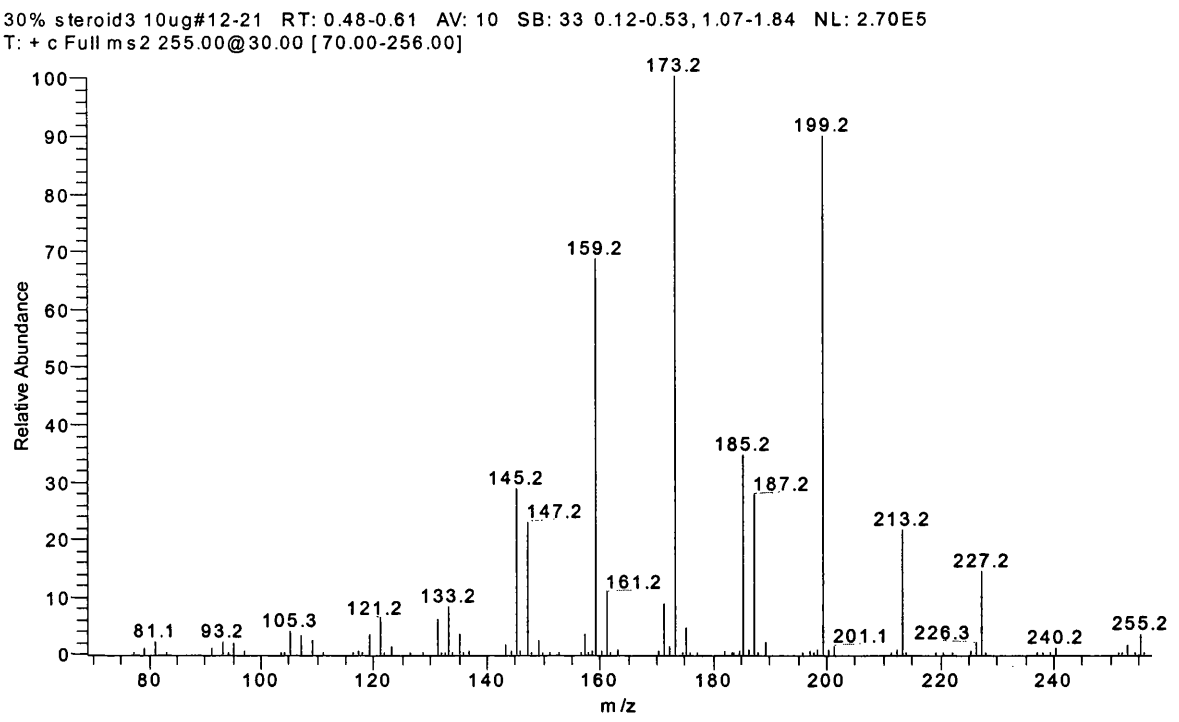

Appendix 10. Androsterone: MS^2 of ion m/z 255; collision energy 30%

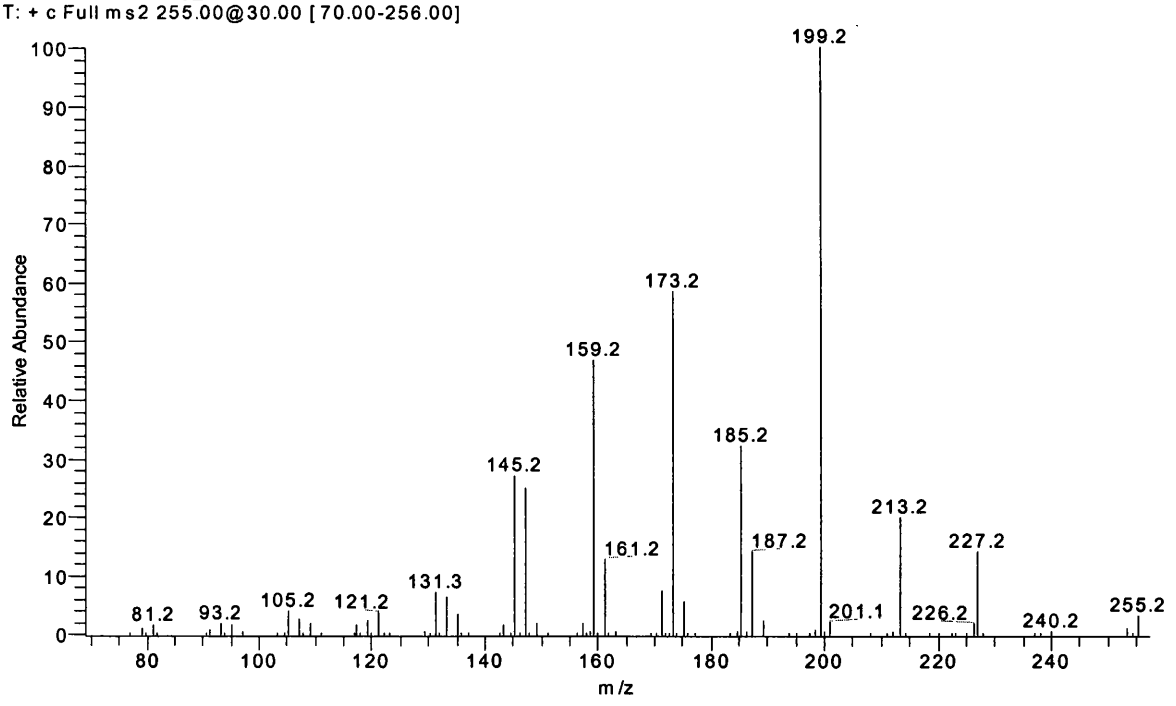

Appendix 11. 11-Ketoandrosterone: MS^2 of ion m/z 287; collision energy 30%

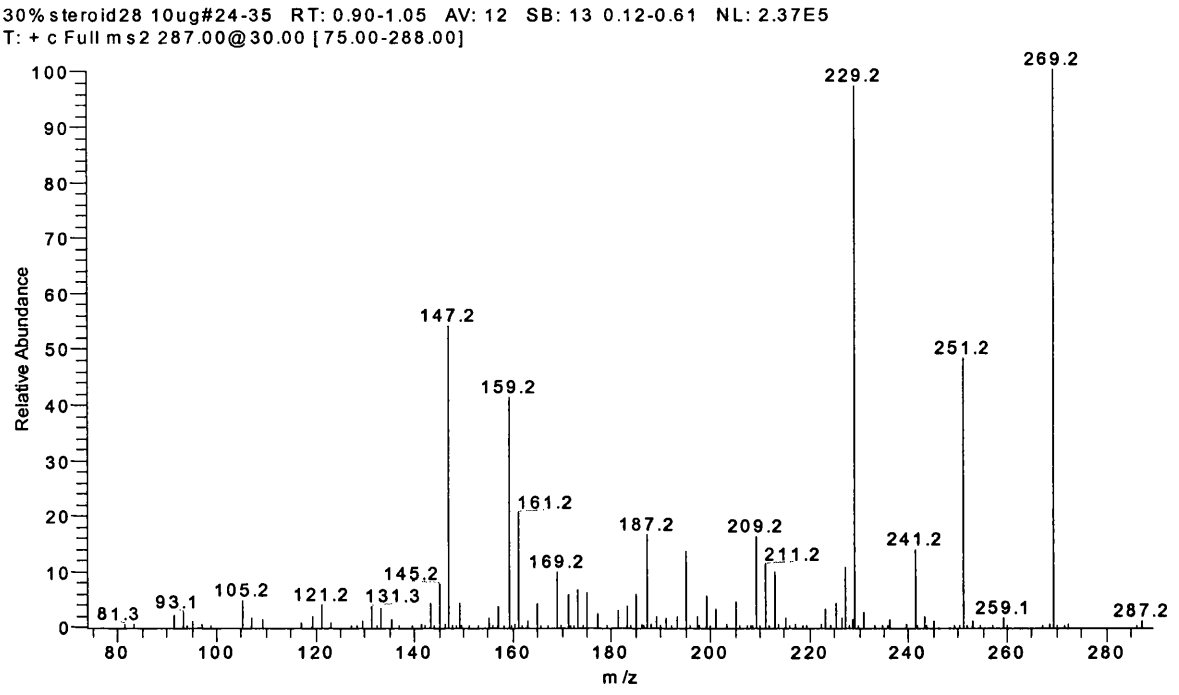

Appendix 12. 11-Ketoandrosterone: MS^2 of ion m/z 269; collision energy 30%

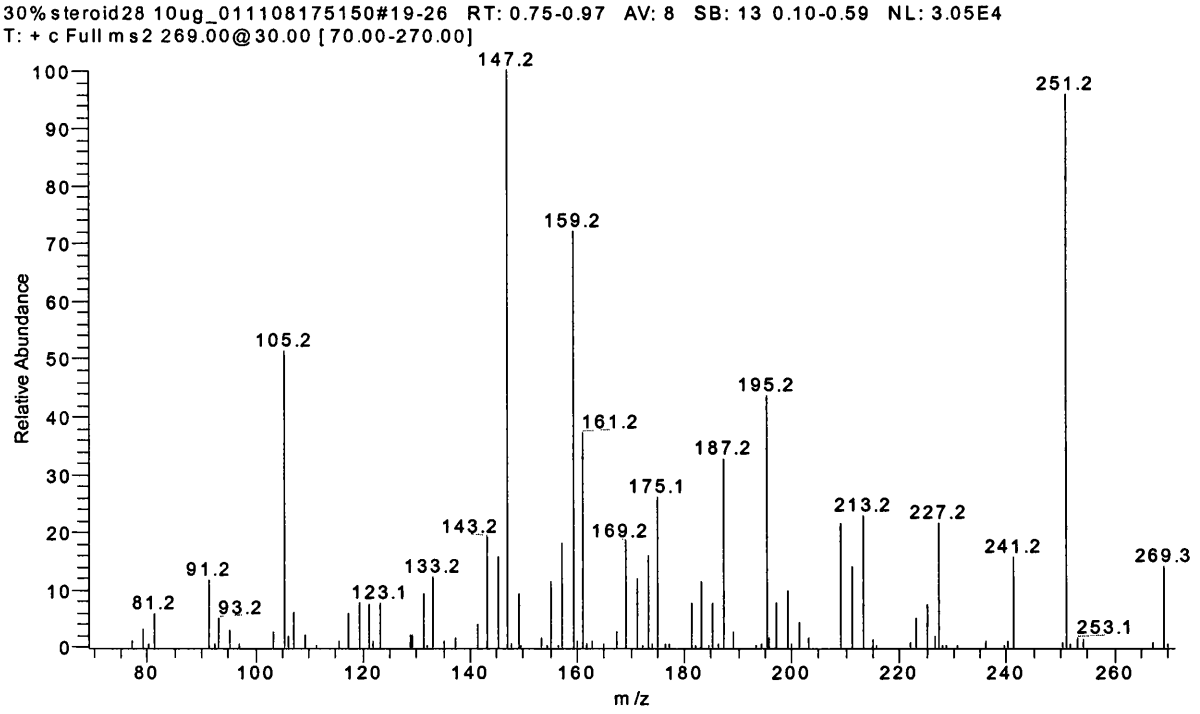

Appendix 13. 11β-Hydroxyandrosterone: MS2 of ion m/z 271; collision energy 30%

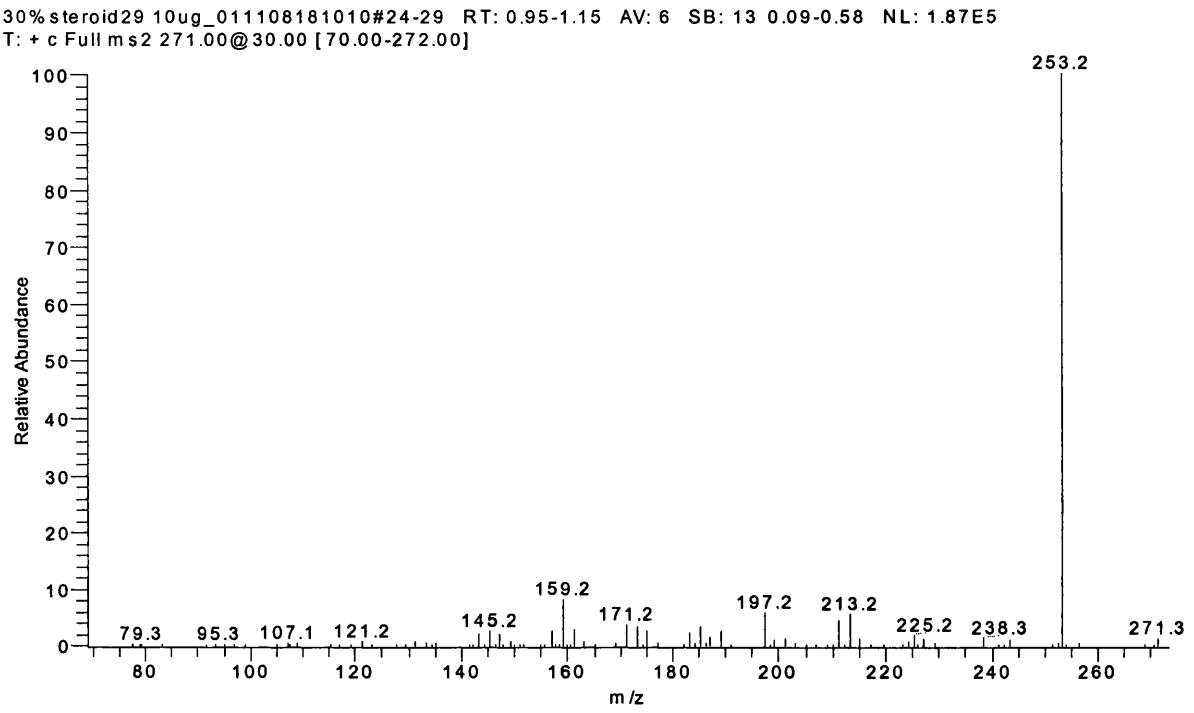

Appendix 14. 11β-Hydroxyandrosterone: MS^2 of ion m/z 253; collision energy 30%

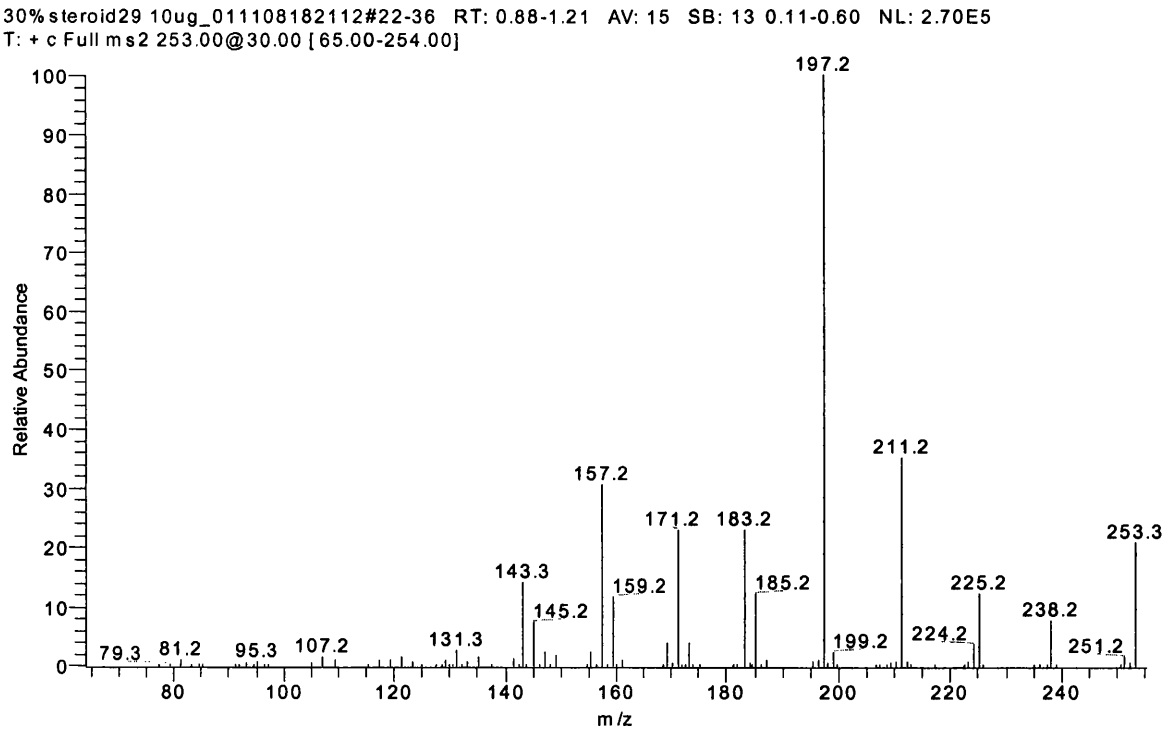

Appendix 15. 5α-Androstan-3, 17-dione: MS^2 of ion m/z 271; collision energy 32%

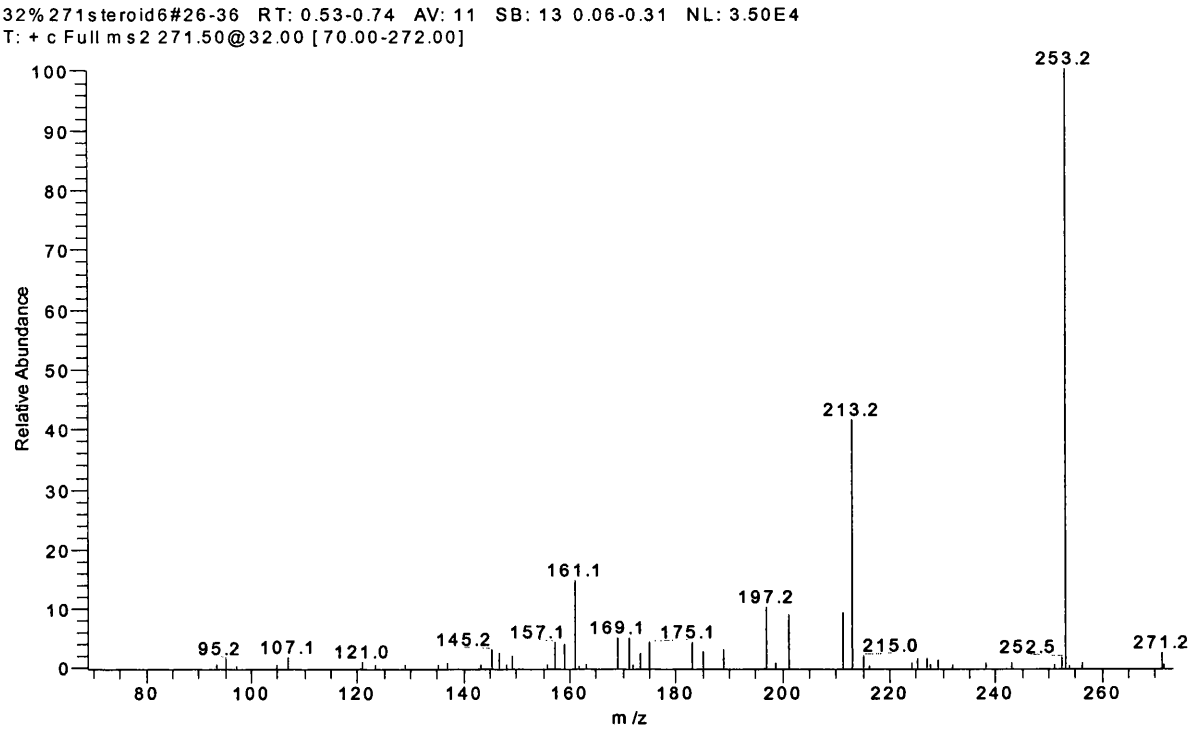

Appendix 16. 5α-Androstan-3, 17-dione: MS^2 of ion m/z 253; collision energy 35%

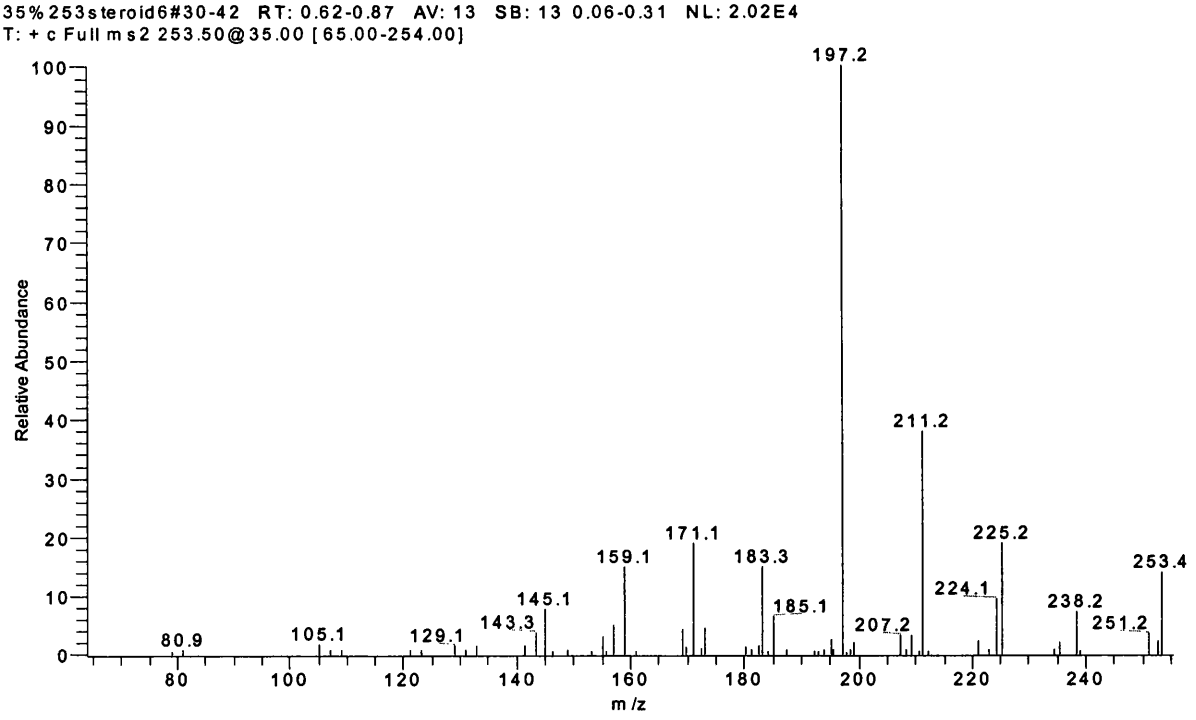

Appendix 17. Androstanediol: MS^2 of ion m/z 257; collision energy 33%

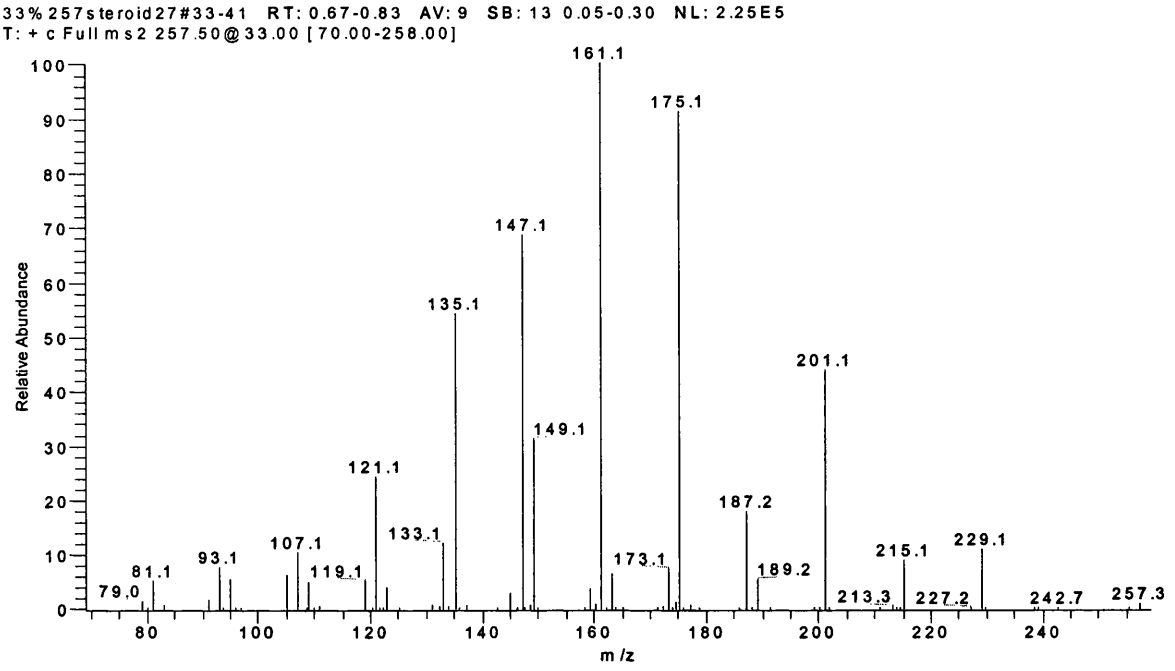

Appendix 18. Δ_5-Androstene-3β, 17β-diol: MS^2 of ion m/z 273; collision energy 32%

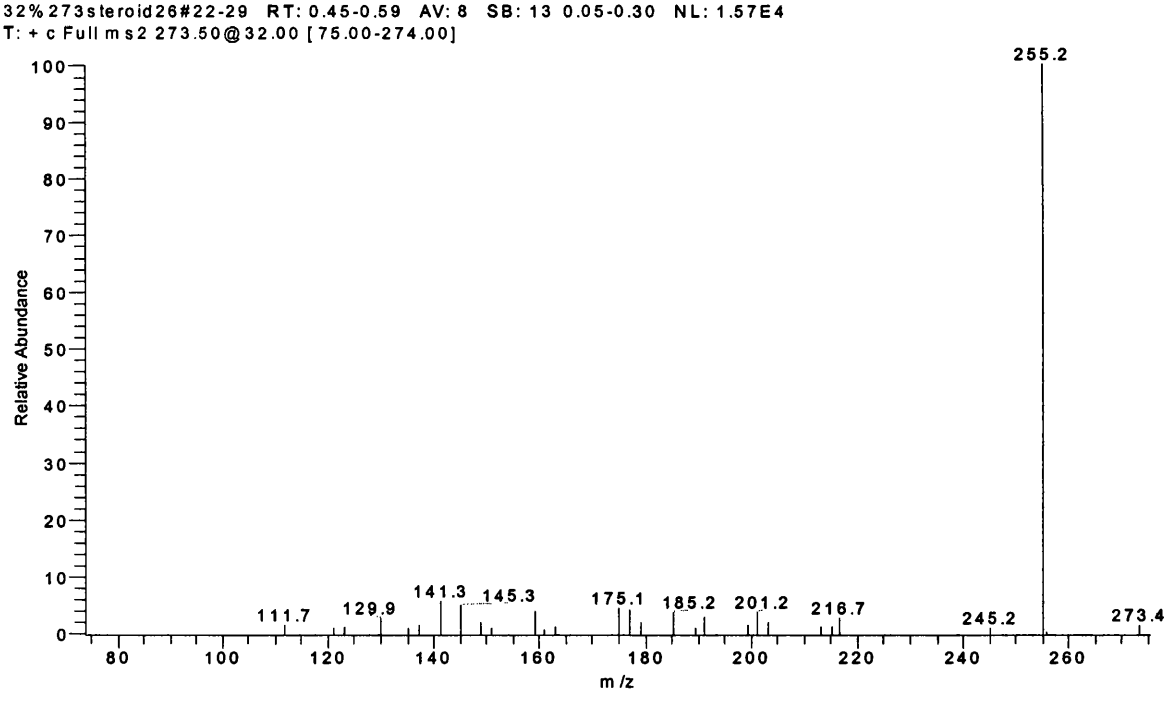

Appendix 19. Androstene-3β, 17β-diol: MS^2 of ion m/z 255; collision energy 34%

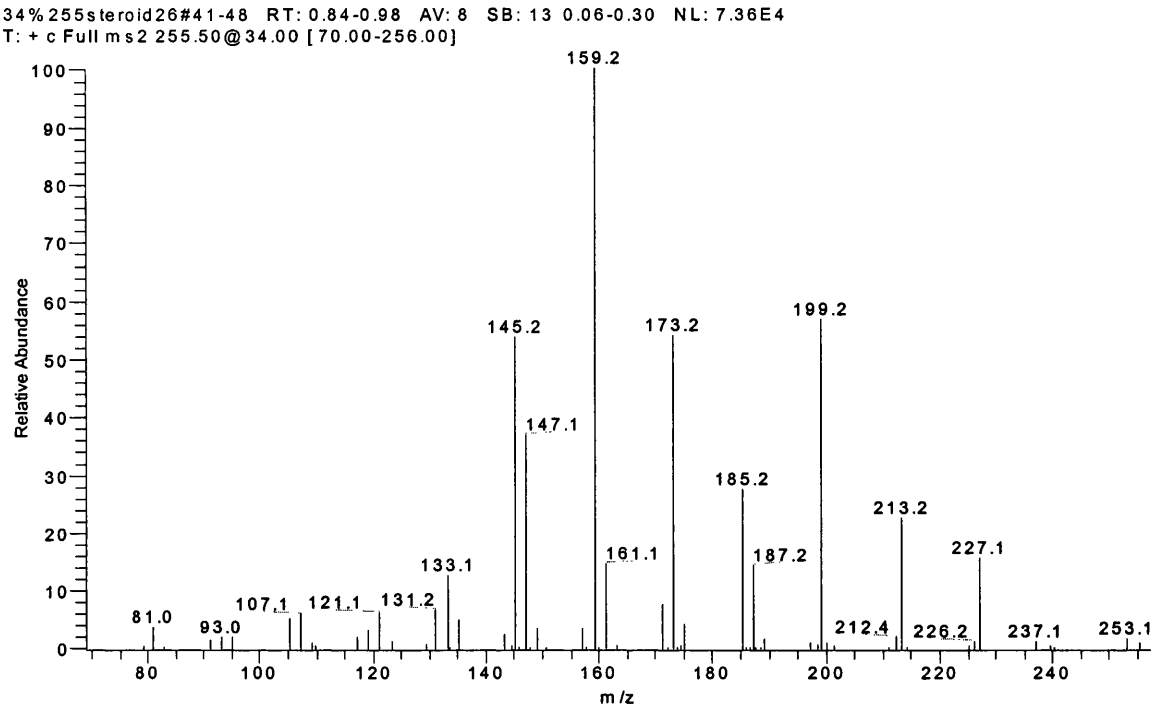

Appendix 20. DHEA glucuronide: MS^2 of $[2M-2H+3Na]^+$ (m/z 995); collision energy 32%

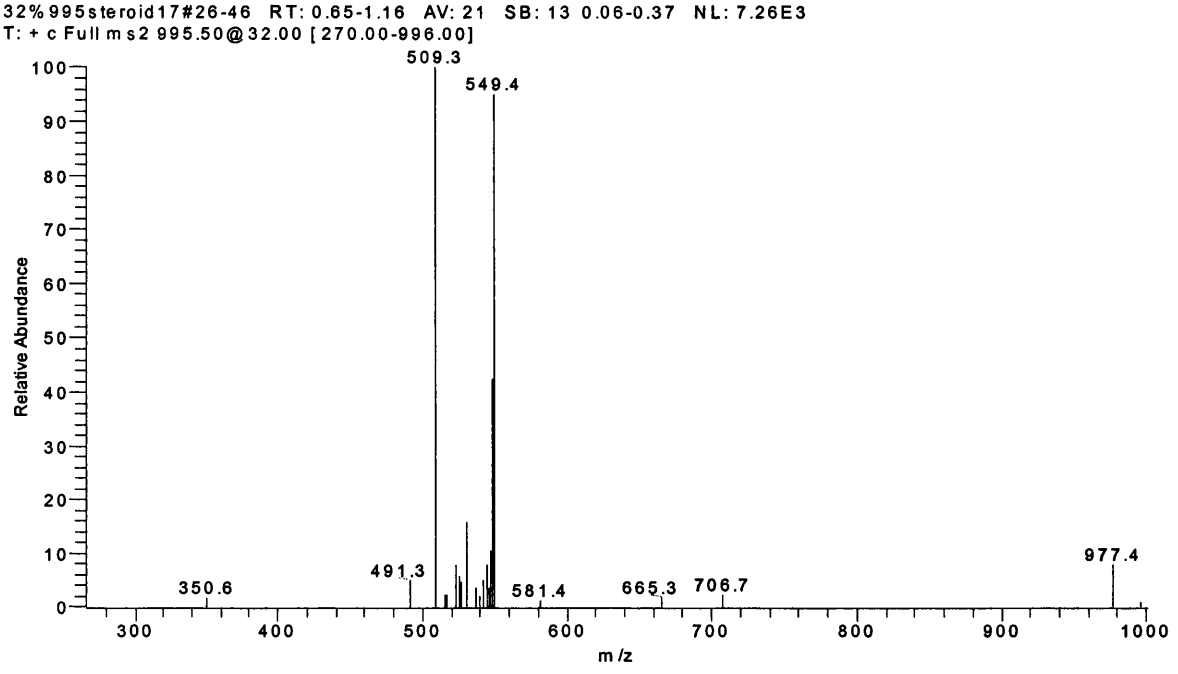

Appendix 21. Etiocholan-3α-ol-17-one glucuronide: MS^2 of $[2M-2H+3Na]^+$ (m/z 999); collision energy 32%

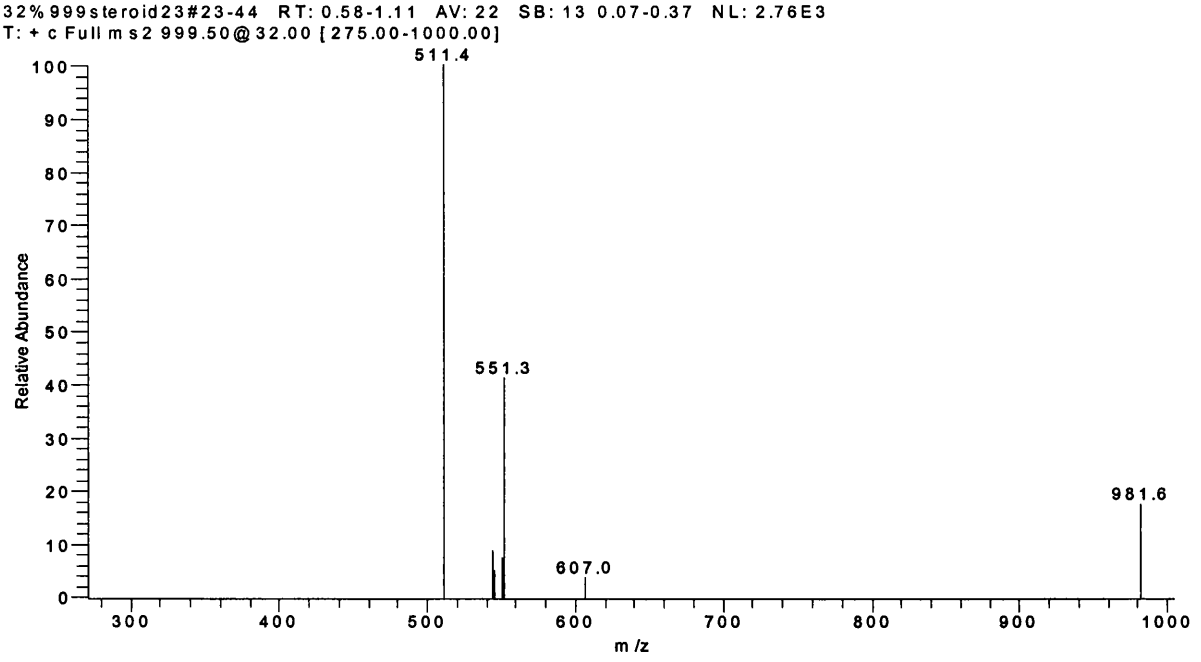

Appendix 22. Androsterone glucuronide: MS^2 of $[M-H+2Na]^+$ (m/z 511); collision energy 34%

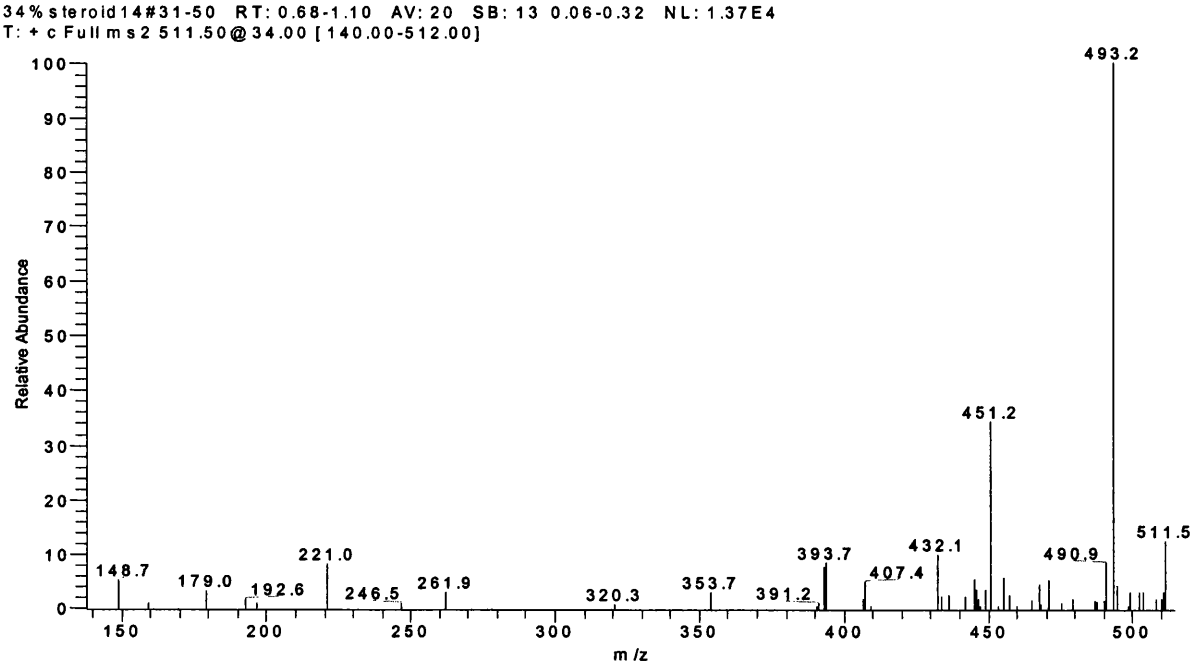

Appendix 23. DHEA glucuronide: MS^2 of $[M-H+2Na]^+$ (m/z 509); collision energy 35%

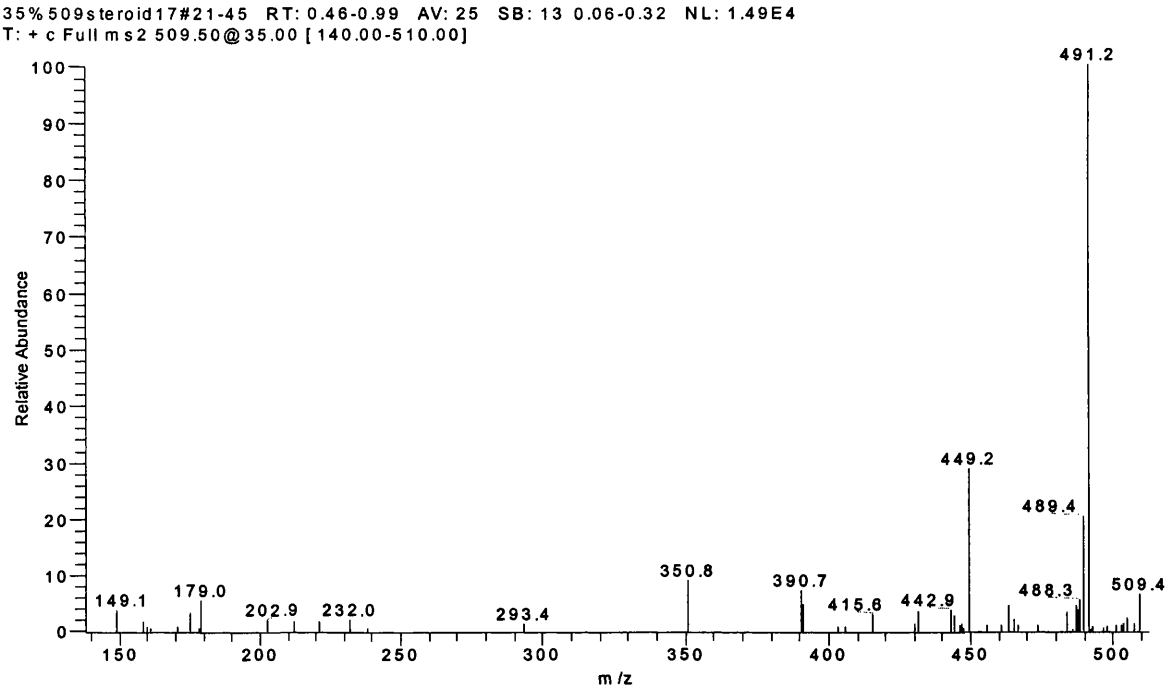

Appendix 24. Etiocholan-3α-ol-17-one glucuronide: MS^2 of $[M-H+2Na]^+$ (m/z 511); collision energy 35%

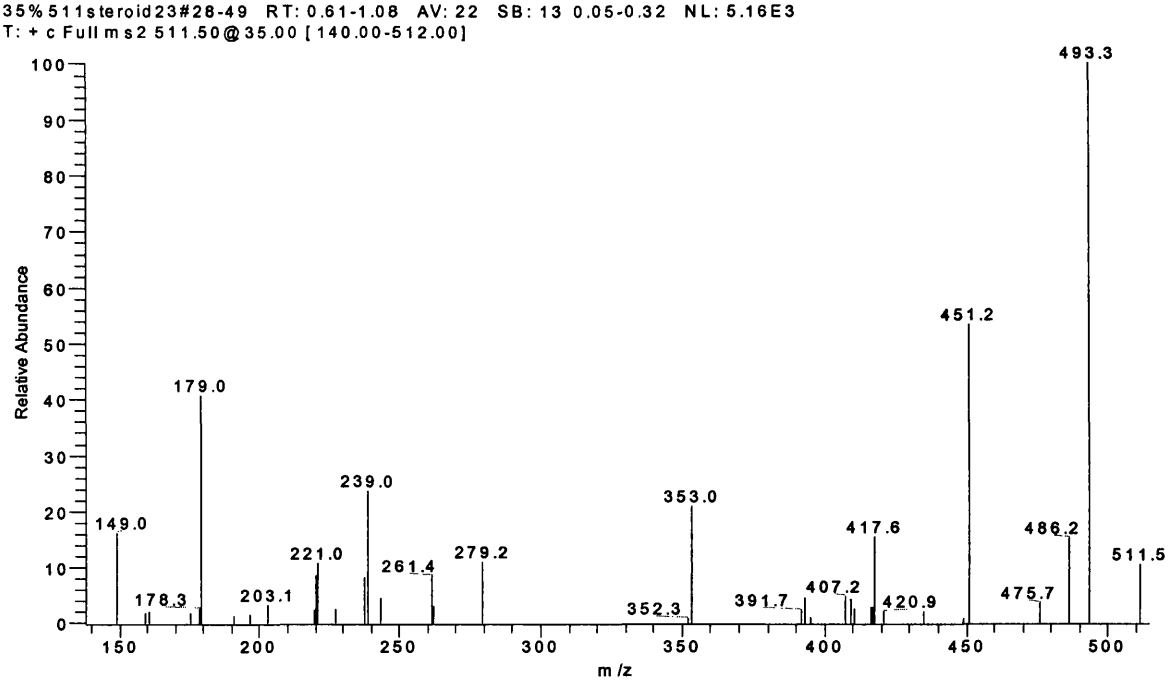

Appendix 25. Testosterone glucuronide: MS^2 of $[M+Na]^+$ (m/z 487); collision energy 27%

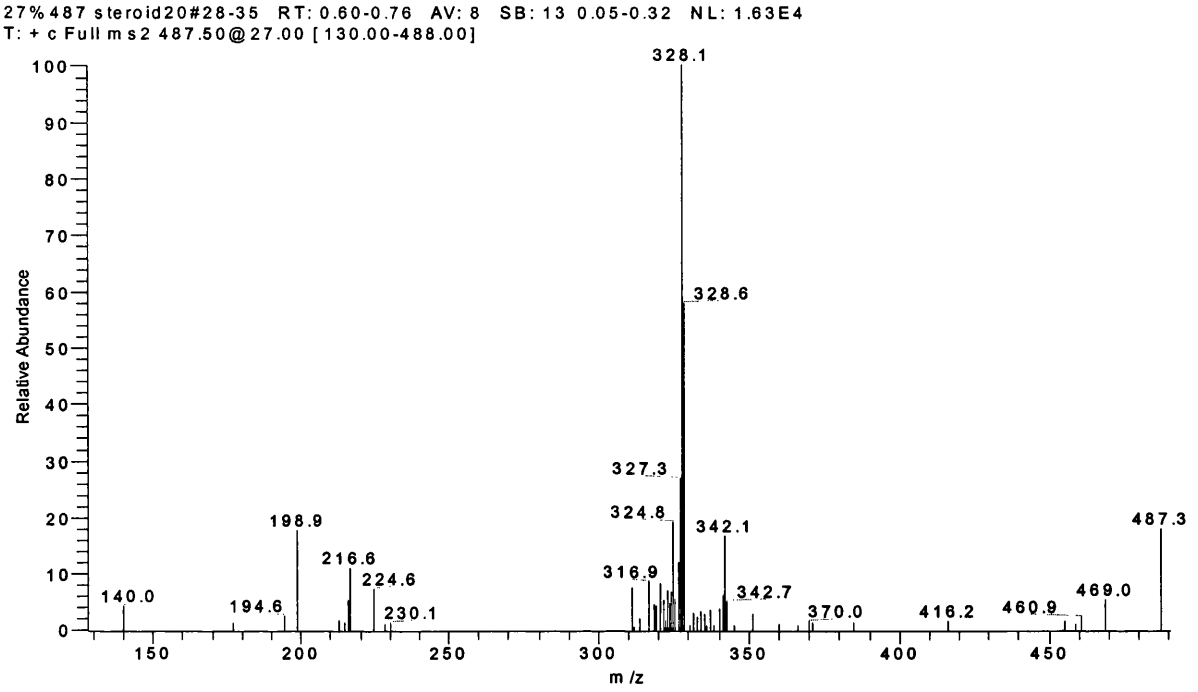

Appendix 26. Androsterone glucuronide: MS^2 of $[M+Na]^+$ (m/z 489); collision energy 25%

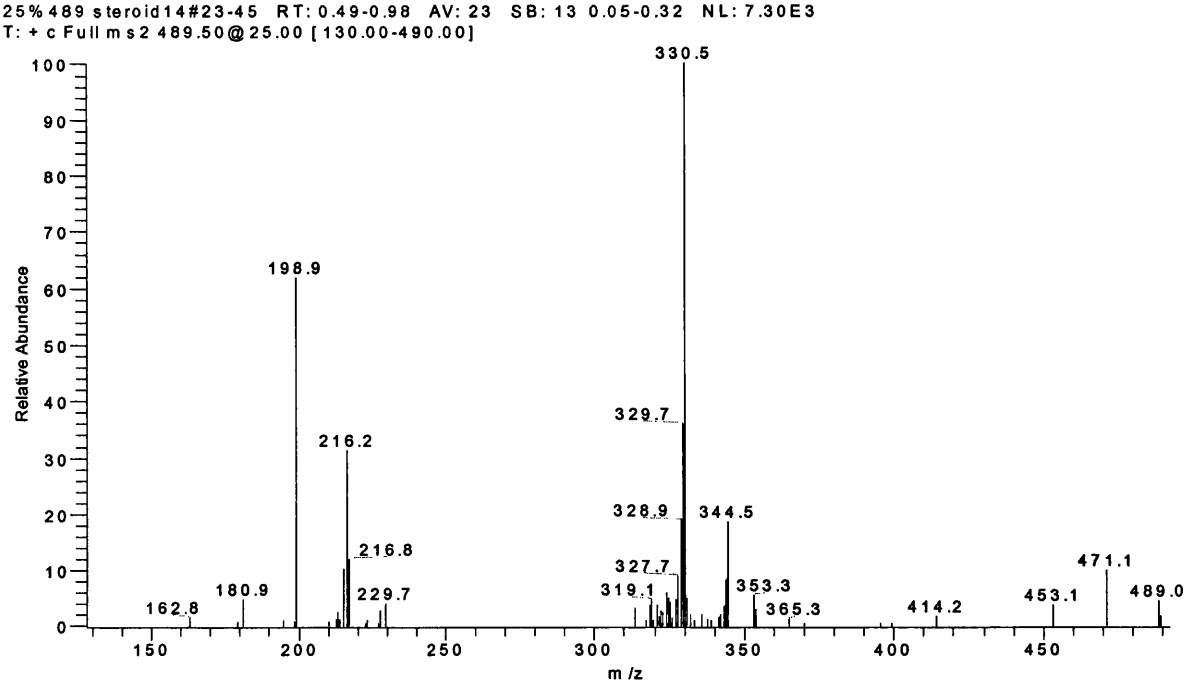

Appendix 27. Etiocholan-3α-ol-17-one glucuronide: MS^2 of $[M+Na]^+$ (m/z 489); collision energy 25%

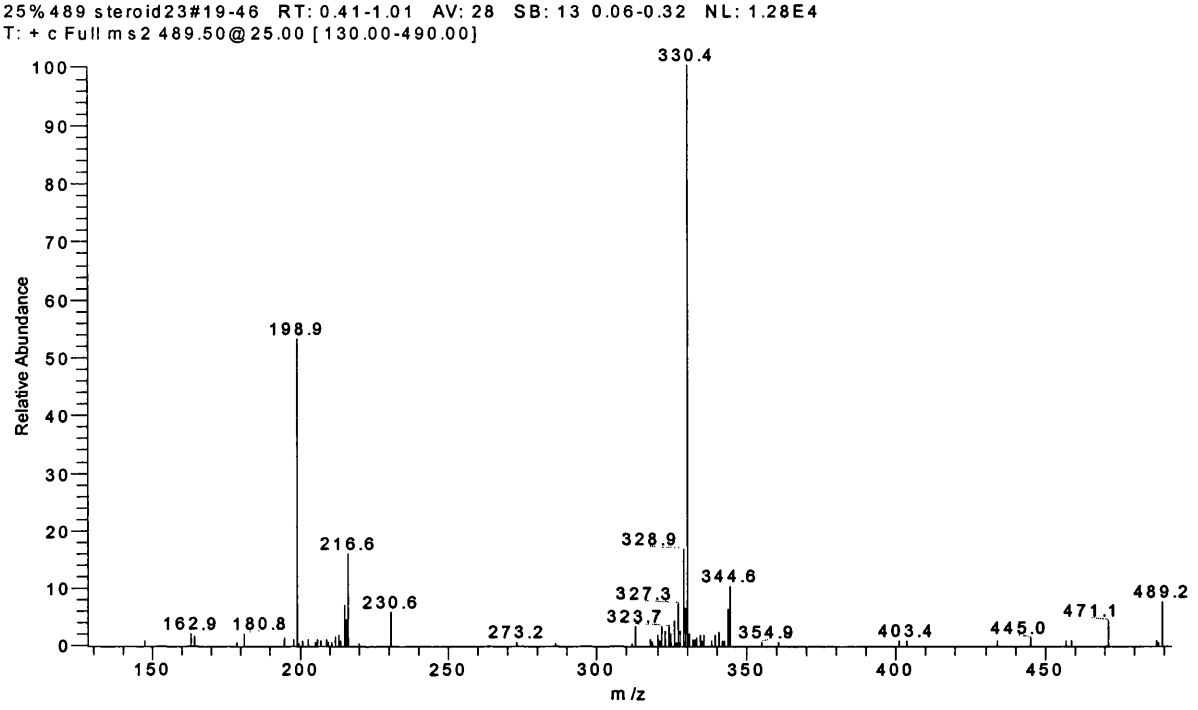

Appendix 28. DHEA glucuronide: MS^2 of $[M+Na]^+$ (m/z 487); collision energy 27%

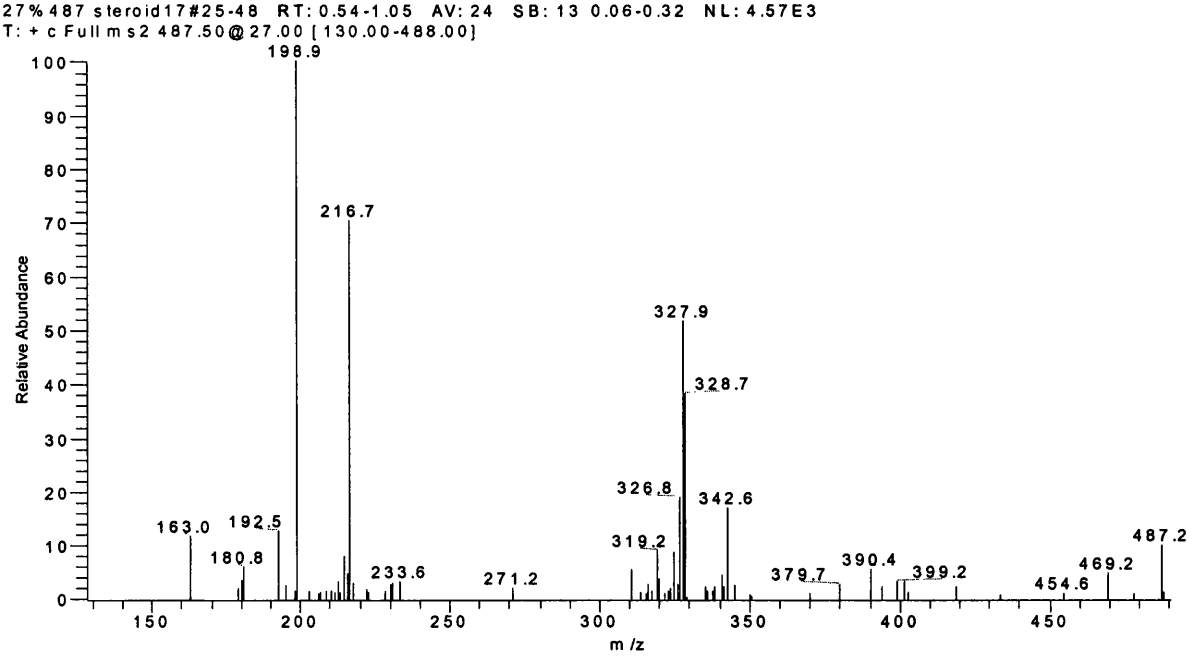

Appendix 29. 5β-Androstane-11, 17-dione-3α-ol glucuronide: MS^2 of $[MH]^+$ (m/z 503); collision energy 25%

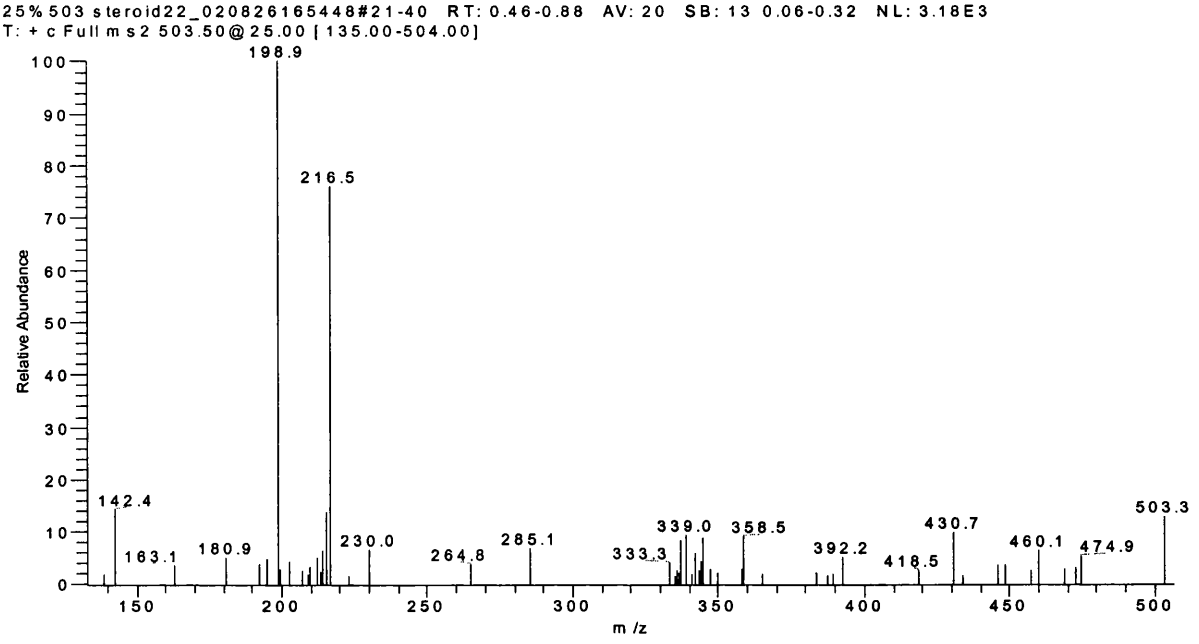

Appendix 30. 5α-Androstan-3α, 17β-diol glucuronide: MS^2 of $[MH]^+$ (m/z 491); collision energy 27%

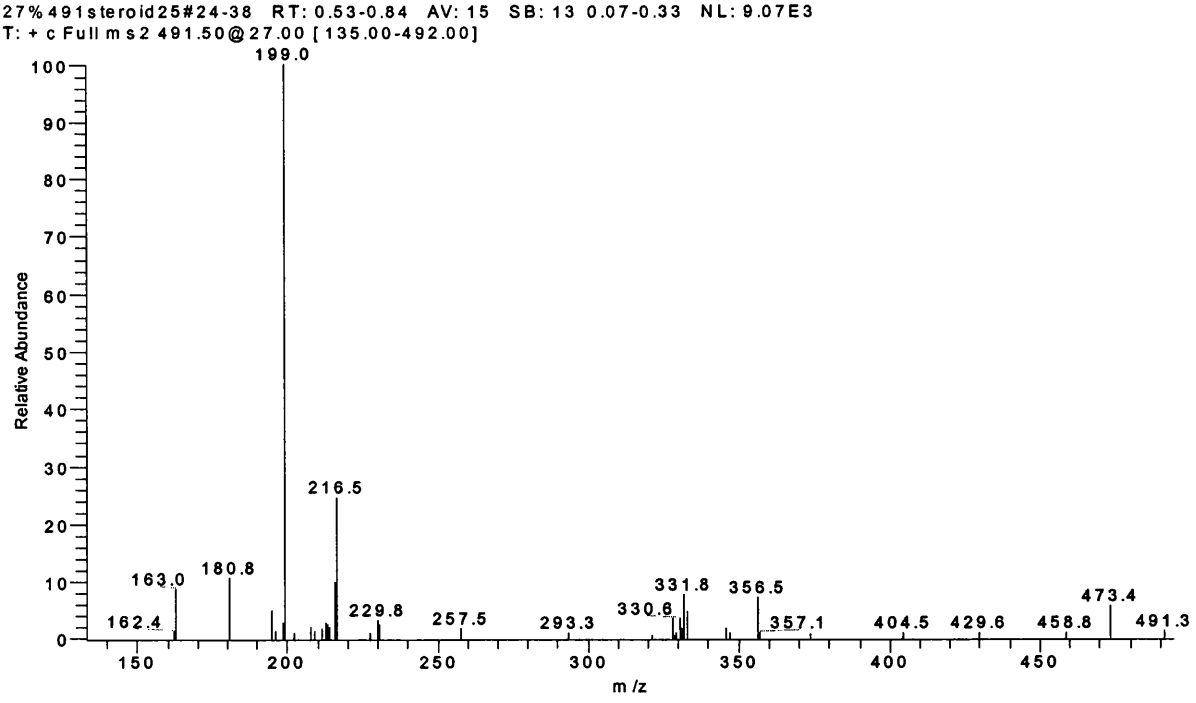

Appendix 31. Testosterone glucuronide: MS^2 of $[2M+Na-2H]^-$ (m/z 949); collision energy 31%

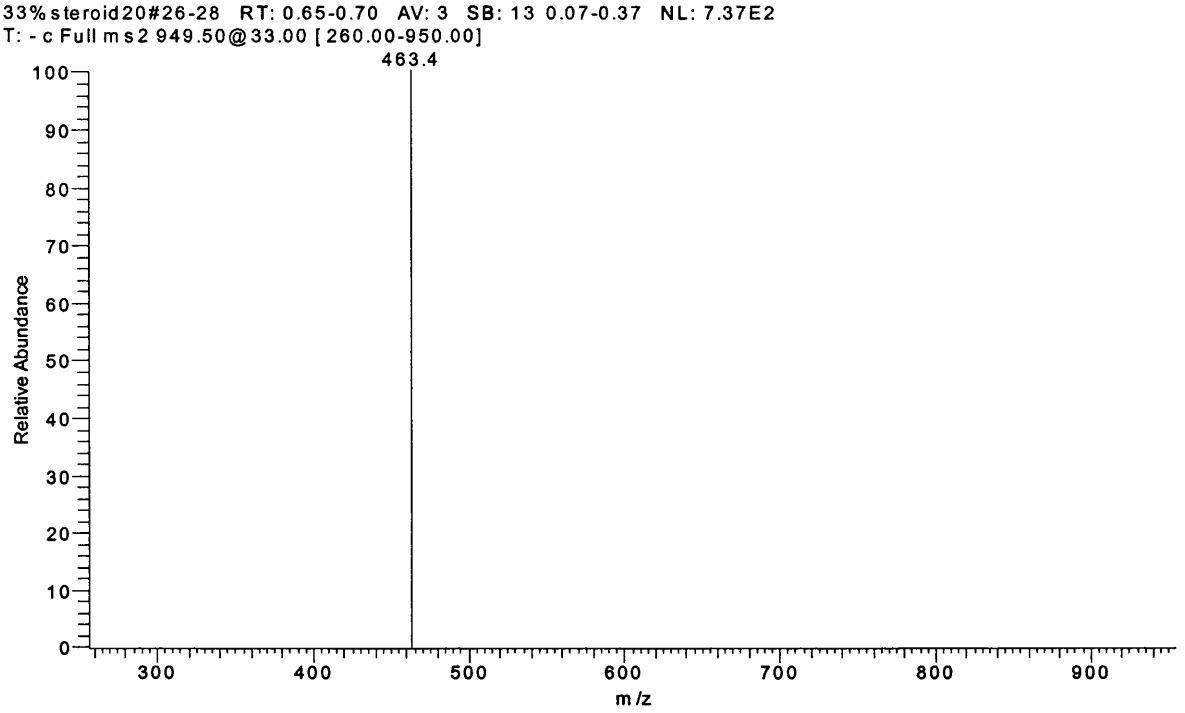

Appendix 32. Androsterone glucuronide: MS^2 of $[2M+Na-2H]^-$ (m/z 953); collision energy 32%

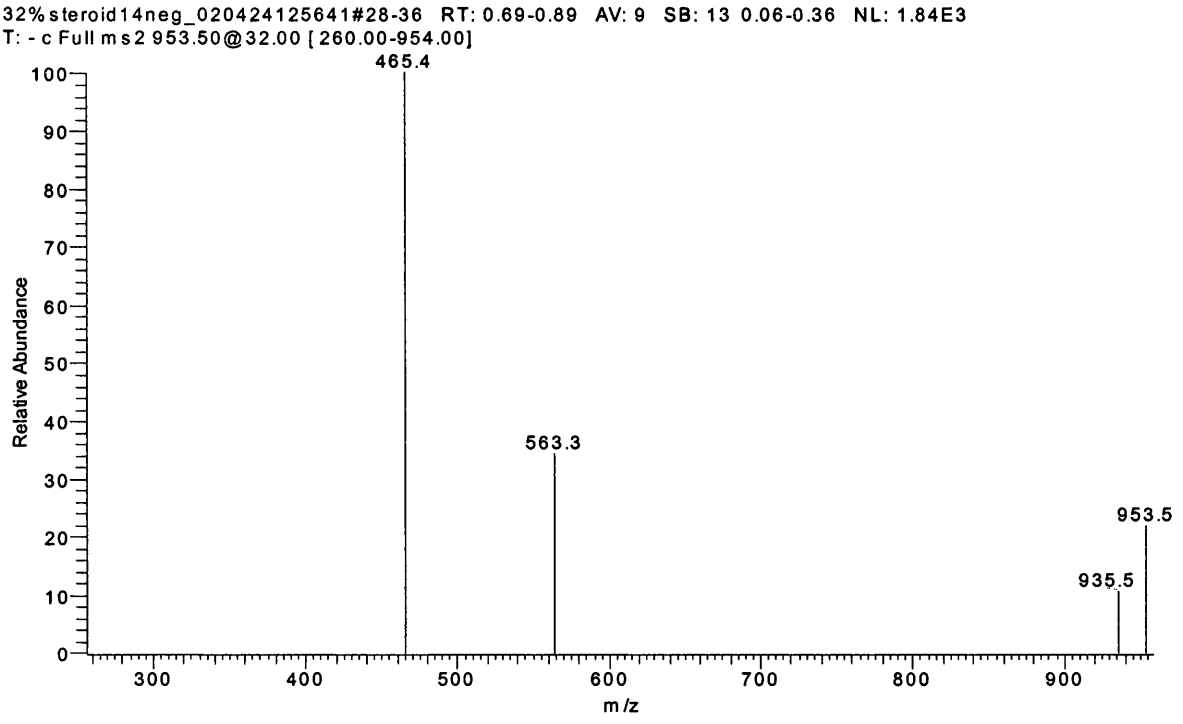

Appendix 33. Etiocholan-3α-ol-17-one glucuronide: MS^2 of $[2M+Na-2H]^-$ (m/z 953); collision energy 31%

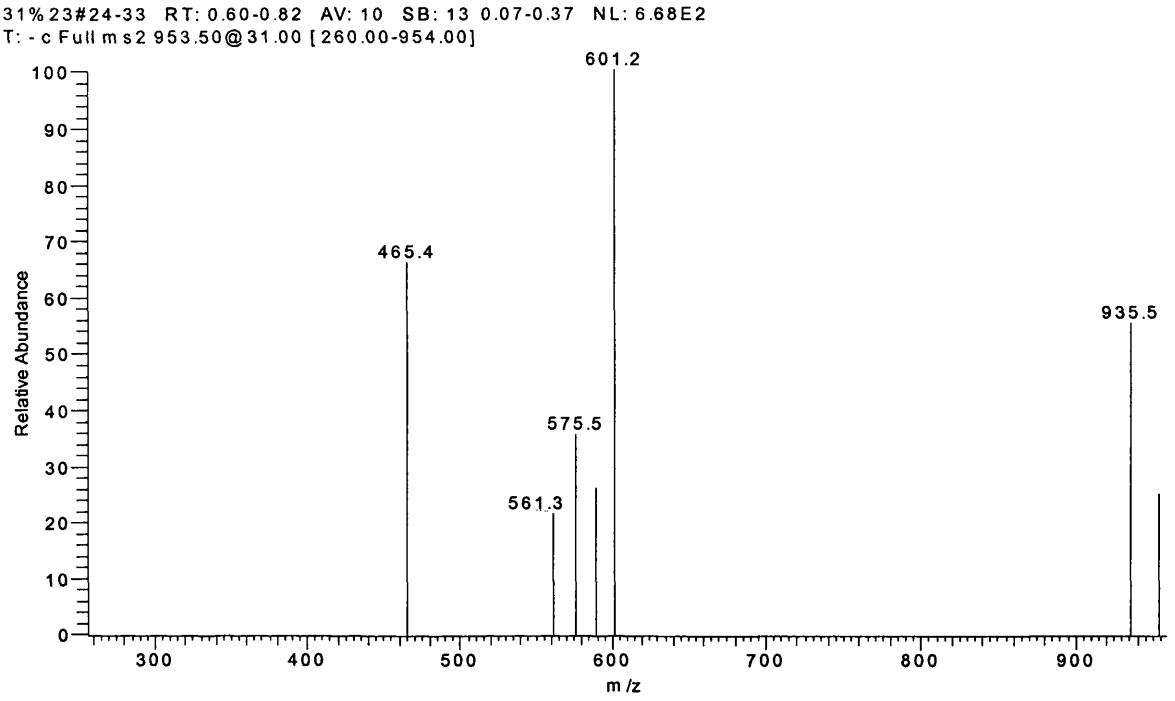

Appendix 34. DHEA glucuronide: MS^2 of $[2M+Na-2H]^-$ (m/z 949); collision energy 32%

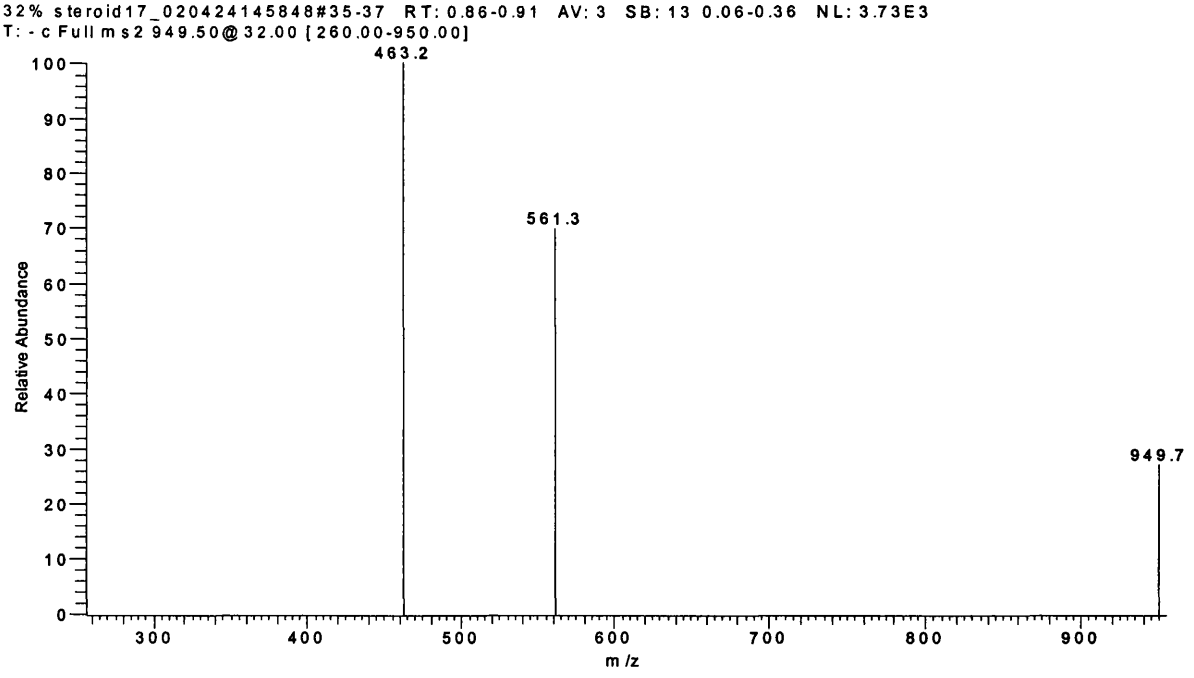

Appendix 35. 5β-Androstane-11, 17-dione-3α-ol glucuronide sodium salt: MS^2 of $[2M-Na]^-$ (m/z 981); collision energy 31%

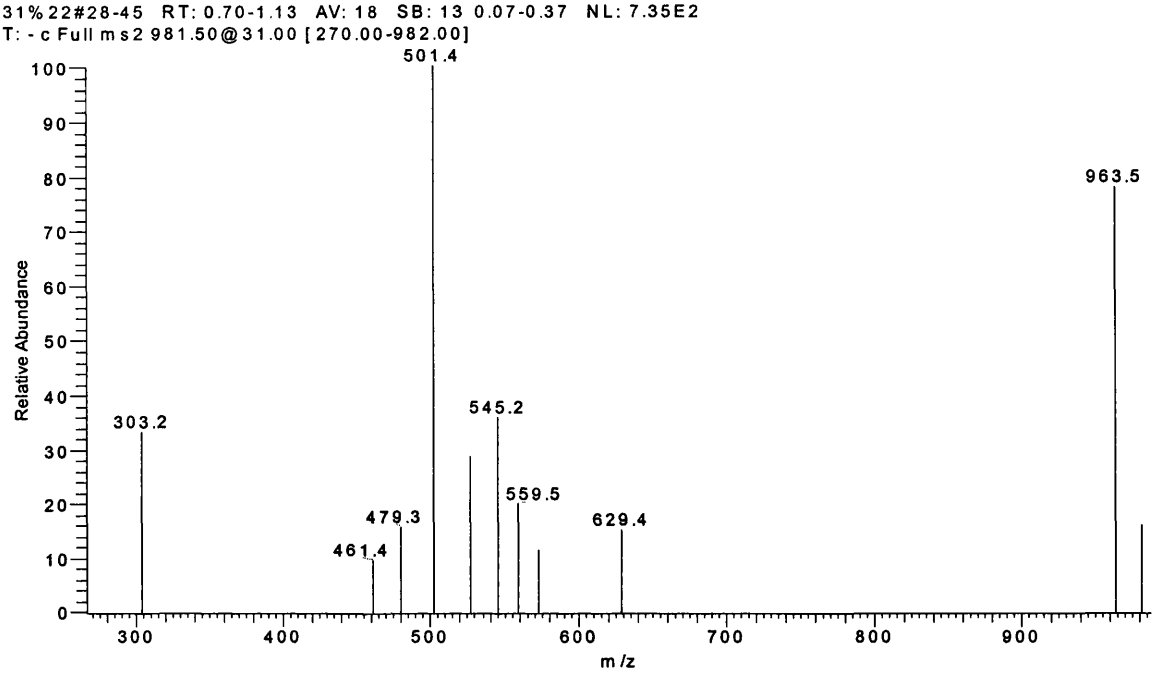

Appendix 36. 5α-Androstan-3α, 17β-diol glucuronide: MS^2 of $[2M-H]^-$ (m/z 957); collision energy 32%

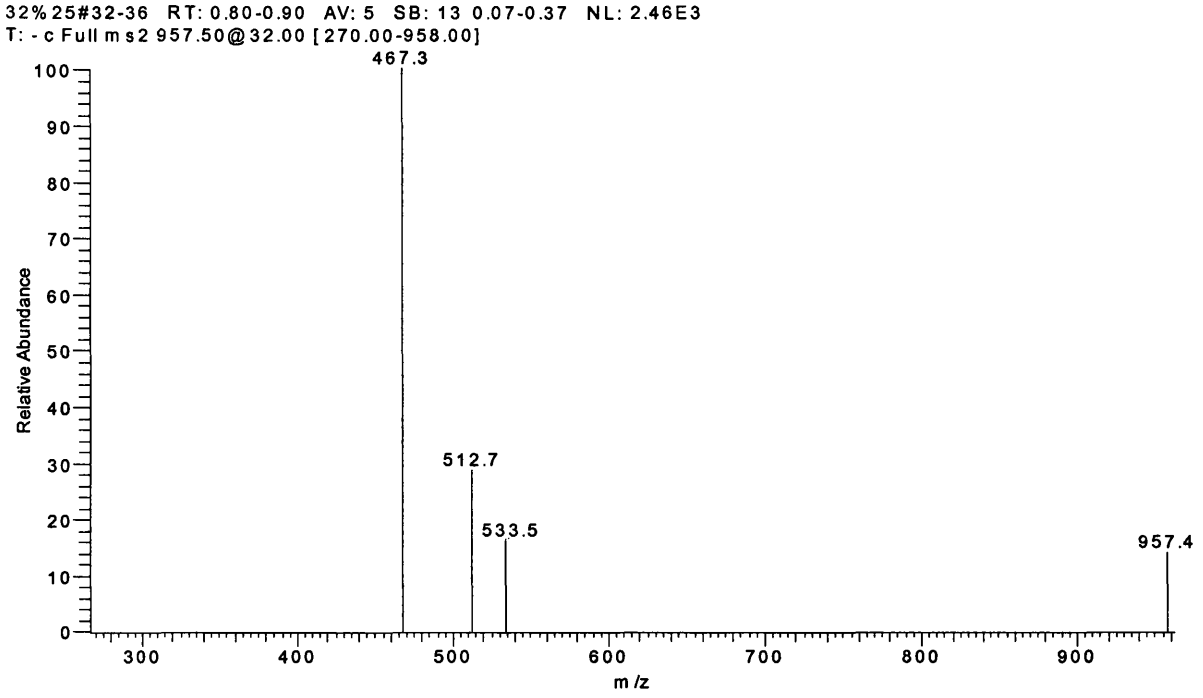

Appendix 37. 5β-Androstane-11, 17-dione-3α-ol glucuronide: MS^2 of $[M-Na]^-$ (m/z 479); collision energy 32%

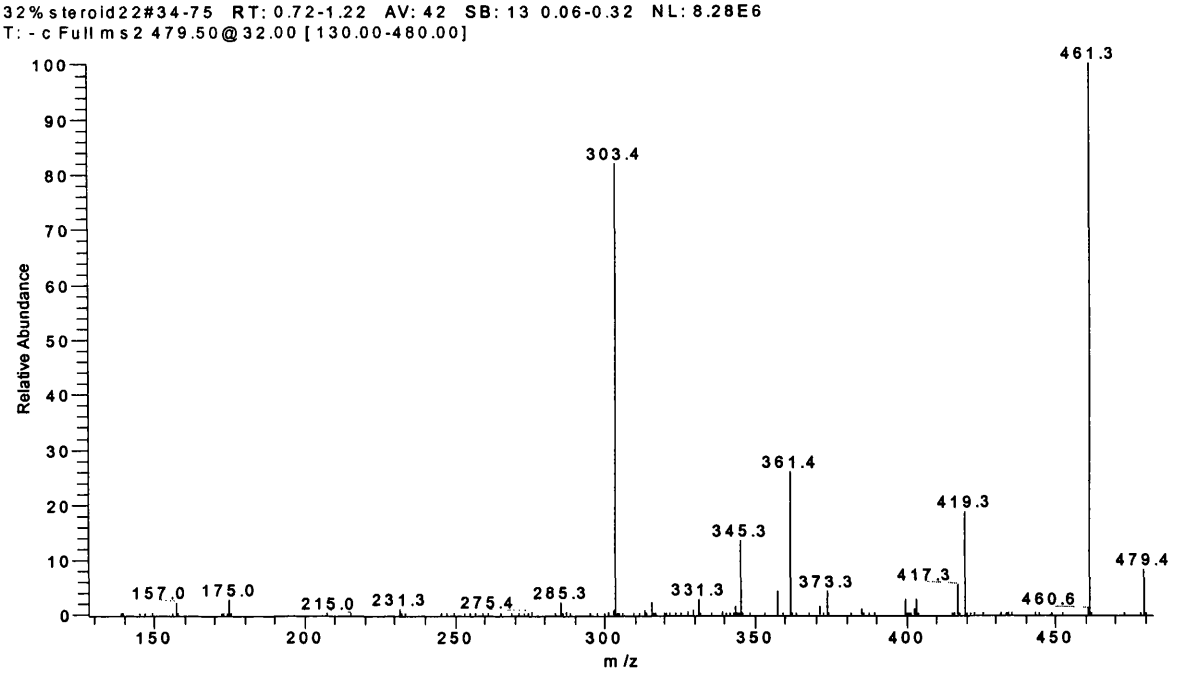

Appendix 38. 5α-Androstan-3α, 17β-diol glucuronide: MS^2 of $[M-Na]^-$ (m/z 467); collision energy 33%